STATISTICAL ENERGY ANALYSIS OF ENGINEERING STRUCTURES

A Thesis Submitted for the Degree of Doctor of Philosophy

by

Andrew John Keane

Department of Mechanical Engineering,
Brunel University,
Uxbridge, UB8 3PH,
United Kingdom.

March 1988

to my wife

Abstract

This thesis examines the fundamental equations of the branch of linear oscillatory dynamics known as Statistical Energy Analysis (SEA). The investigation described is limited to the study of two, point coupled multi-modal sub-systems which form the basis for most of the accepted theory in this field. Particular attention is paid to the development of exact classical solutions against which simplified approaches can be compared. These comparisons reveal deficiencies in the usual formulations of SEA in three areas, viz., for heavy damping, strong coupling between sub-systems and for systems with non-uniform natural frequency distributions. These areas are studied using axially vibrating rod models which clarify much of the analysis without significant loss of generality. The principal example studied is based on part of the structure of a modern warship. It illustrates the simplifications inherent in the models adopted here but also reveals the improvements that can be made over traditional SEA techniques.

The problem of heavy damping is partially overcome by adopting revised equations for the various loss factors used in SEA. These are shown to be valid provided that the damping remains proportional so that inter-modal coupling is not induced by the damping mechanism. Strong coupling is catered for by the use of a correction factor based on the limiting case of infinite coupling strength, for which classical solutions may be obtained. This correction factor is used in conjunction with a new, theoretically based measure of the transition between weakly and strongly coupled behaviour. Finally, to explore the effects of non-uniform natural frequency distributions, systems with geometrically periodic and near-periodic parameters are studied. This important class of structures are common in engineering design and do not posses the uniform modal statistics commonly assumed in SEA. The theory of periodic structures is used in this area to derive more sophisticated statistical models that overcome some of these limitations.

Table of Contents

CHAPTER 1

Introduction

1.1. Statistical Energy Analysis (SEA)

Analysing the dynamical behaviour of engineering structures is a difficult task. Nonetheless, such analysis is of great importance when designing the artefacts of modern technology, whether it concerns the motions of fighter aircraft or the frequency response of a domestic loudspeaker. For most practical purposes, problems in dynamics can be categorised as rigid-body dynamics or distortional dynamics. Within the field of distortional dynamics the study of vibrations holds a central place. It is to this study that the current work is addressed.

Vibrations are associated with the interchange of energy between its kinetic and potential forms. That is, motions occur that are of an oscillatory nature and the most important characteristic of such motions is the frequency at which this energy interchange takes place. The study of vibrations has yielded an enormous literature but perhaps the most famous treatise is that by Rayleigh[1] which may be said to define *the* classical approach to the study of vibrations.

The application of classical vibration theory to real problems in engineering is never simple or wholly satisfying. Difficulties arise for a number of reasons; not least among these are the problems involved in solving the resulting differential equations or, indeed, in providing an adequate model in the first place. These may be compounded by the lack of a detailed description during the early stages of design, or by the inaccuracies inherent in manufacture or construction (leading to the study of statistical models). However, some progress can be made.

If the system to be analysed is simple enough, classical techniques may suffice. For example, using such methods it is usually possible to predict the behaviour of musical instruments, especially those using taut strings, such as the violin or piano. Even so, problems may still arise; e.g., the

description of how an instrument is played will be rather complex, especially if it is to reflect differences in the skills of musicians. When it comes to predicting whether the blades of a gas turbine will vibrate badly at high rotational speeds and gas flows, the problems will be even more difficult.

In general, all vibration analysis has some common threads running through it; central to these is the concept of a natural frequency or mode. This idea, which is only really justified in systems which obey linear differential equations with well behaved damping, leads to the technique of modal analysis. Using modal analysis, all the dynamical responses of a system can be characterised by the weighted sum of the responses in each mode. However, one must first find the modes, a not insignificant task.

Because of the necessity of knowing the natural modes of a system before proceeding with further analysis, many techniques have evolved to find them, see, for example, Bishop, Gladwell and Michaelson[2] or Bishop and Johnson[3]. Passing over the few simple cases where classical theories are adequate, the most popular methods in use today appear to be those collectively known as finite elements or F.E., see Meirovitch[4] or Zienkiewicz[5].

The F.E. technique, which is basically a discretization procedure, works well provided that the model used is sufficiently detailed for the natural frequencies being studied (and such detail may be unavailable at the earliest stages of design). However, classical approaches teach that all structures, even the most simple, have an infinite variety of natural modes, with corresponding natural frequencies covering the entire frequency spectrum. This inevitably leads to the conclusion that F.E. will be best suited to the study of low-frequency responses, covering perhaps no more than the first twenty or thirty modes.

Beyond these first few modes F.E. frequently misbehaves. Two underlying problems are the cause; first the models used to predict the responses become increasingly complex and difficult to handle (numerically as well as physically), and secondly the models used become so complex that questions arise as to the consequences of small changes in modelling. If a small change may have a large effect among the higher modes (and it may well), worries arise concerning the faithfulness with which

the responses of the final product will follow those of the design. It is not that the results given by F.E. at high frequencies are necessarily wrong, rather that deterministic calculations at high frequencies are too sensitive to minor changes in a design. This kind of problem explains why two sister ships which have entirely similar responses at the lowest frequencies have ever larger discrepancies at higher frequencies. Clearly, although similar, no two engineering products can be identical.

The fact that engineering manufacture inevitably involves small deviations from item to item leads inexorably into the study of statistics. If it is no longer possible to predict the exact behaviour of every loudspeaker coming off a production line, perhaps it is possible to predict the *average* performance. Statistical Energy Analysis (SEA) addresses this problem. In short, it aims to deal with problems where uncertainties in manufacture, or even the lack of detailed knowledge at an early stage of design, prevent the use of deterministic approaches, and statistical measures are acceptable instead. In this respect it differs from more traditional random vibration methods, in that it is the underlying structure, and not necessarily the excitation, that is considered random. In fact the principal random variables are taken to be the natural frequencies of the system under study. One problem that arises when considering such average behaviour concerns the case of systems with unusual properties. These may give extreme responses under certain conditions, which can only be predicted by deterministic methods. Such extremes may be critically important in engineering design, and in these cases SEA (or any other statistical approach) may give mathematically correct but misleading answers. The users of such techniques must be wary of these limitations.

Apart from dealing with problems where the structures are not well defined, SEA additionally allows for the study of interactions occurring between a number of coupled sub-systems, such as the wings and fuselage of an aircraft, or the decks and bulkheads of a ship. Figure 1.1 illustrates a cross-section taken through a typical modern aircraft that contains some sensitive item of equipment, such as a computer. Figure 1.2 shows one possible SEA model of this problem. Here the individual sub-systems (engines, wings, fuselage and computer) have been reduced to reservoirs of vibrational energy, and the subsequent analysis is involved with the various time-averaged energy flows between the

components (indicated by Π and arrows in the figure) and the vibration levels within them (indicated by the energy variables E and associated mode counts N). Notice that all the sub-systems are excited and dissipate energy and that, additionally, energy flows from the engines to the fuselage either through the wings or directly through the air (which has not been modelled as a separate sub-system here).

The fact that SEA can deal with the behaviour of such imprecisely defined, coupled structures interacting at medium to high frequencies makes it potentially very powerful. However, it has not been without its critics, and the aim of the present work is to attempt to understand some of the defects of SEA and, where possible, to offer improvements.

1.2. A Brief Historical Survey

The earliest references to Statistical Energy Analysis appear to be those by Lyon and Maidanik[6] and Smith[7], which discuss independent calculations carried out in England and the United States at about the same time. Both these works address the problem of energy flow between lightly coupled linear oscillators and lead on to the analogy between flows of vibrational energy between such oscillators, and those of thermal energy between coupled objects at differing temperatures.

Following these early works, a number of references appeared in which improvements and generalizations of the underlying theories were discussed[8, 9, 10, 11, 12, 13, 14]. The most relevant of these are those by Ungar[9] and Lyon and Scharton[12], which deal with coupling, and by Scharton and Lyon[11], which deals with multiple systems. The birth of SEA is reviewed by Lyon[15] in a paper which has the revealing title 'What Good is Statistical Energy Analysis, Anyway?'. In this, the author accepts that by this stage in its development (some eight years later), SEA had received a good deal of attention from workers in academic and government institutions both in the United States and England but had *'not been adopted by the staff engineer or designer'*.

Nonetheless, both theoretical and practical studies in the area of SEA continued apace, so that when writing his major text book on the subject some five years later, Lyon[16] was able to extend the

bibliography of the earlier review from 38 to 137 items, of which over 90 are concerned with theoretical developments.

Another review was produced at about this time by Fahy[17] in which a critical evaluation of some of the underlying assumptions of SEA is carried out. Fahy[17] concludes by noting that SEA *'has unfortunately been abused by people who attempt to apply it without understanding its basis and its limitations'*. The lack of simple tests that can establish whether or not SEA is applicable to a given problem would seem to be one of the major problems which limits uptake of the technique.

More recently, SEA has been considered from the standpoint of diffusive transport theory and reviewed by Hodges and Woodhouse[18]. As well as discussing transport theories these writers examine the consequences for SEA of using the approach to examine *geometrically periodic* structures. Such structures are commonly encountered in engineering design. The literature of periodic vibrations theory has been well reviewed in a recent paper by SenGupta[19].

It would be fruitless to attempt to reproduce the excellent bibliographies given in these various reviews but, for the purposes of the current work, a few key relevant papers may be highlighted. Foremost amongst these are two by Davies[20,21] which set out an exact method for calculating the energy flow between a pair of point coupled multi-modal systems, allowing for direct comparison between SEA and classical analysis. The work of Remington and Manning[22] and that of Keane and Price[23] also discuss such comparisons.

Concerning the problem of varying coupling strengths between sub-systems are works by Ungar[9], Chandiramani[24], Smith[25], and Keane and Price[26]. These writers discuss various measures of coupling strength, and that by Keane and Price[26] illustrates the sudden breakdown that occurs in SEA models at high coupling strengths. It goes on to propose corrections that may be applied in such cases.

The whole field of periodic systems is enormous, but Brillouin's monograph on the subject[27] is extremely useful, as are the text books of Ziman[28,29]. The motions of purely periodic mono-coupled structures are analysed from the wave approach by Mead[30,31] and using transfer matrices by Lin[32] and

Faulkner and Hong[33]. Lin[32] discusses the concepts of near-periodic systems where some kind of disorder is present, see also Mead and Lee[34]. Disorder is, of course, fundamental to the application of periodic theory to SEA where it is an underlying assumption. These various methods are recapitulated and extended for near-periodic structures by Keane and Price[35].

1.3. The Present Investigation

Having briefly examined the literature on SEA, a great many comments could be made; among these are:-

(1) The method holds out the prospect of a very powerful approach to vibrations analysis in an area where other techniques are, at best, of limited use.

(2) Given the prospects already outlined, SEA seems to be remarkably little used by practising engineers, seeming to have fallen into disrepute, if ever accepted in the first place.

(3) Nowhere are the underlying assumptions inherent in SEA spelt out, and their consequences discussed, in an easily accessible fashion.

(4) The treatment of statistical topics within SEA appears very haphazard and only cursorily discussed.

These points may be unconnected, but certainly a fundamental study of SEA, paying particular attention to assumptions and statistics seems worthwhile. The present work attempts to address this matter.

To quantify the impact of any of the assumptions made within SEA requires a standard for comparison. Such standards are difficult to formulate, but if attention is restricted to the study of a pair of linear sub-systems with well behaved damping, connected at a single point, one may be found, see Davies[21]. Clearly, this is a much reduced problem when compared with that of many interacting sub-systems with possibly complex coupling, but valuable insights can still be gained. The whole of the present investigation is addressed to the study of this reduced problem.

Having established a standard for comparison, all the assumptions required to recover the accepted results of SEA may be introduced and their effects studied. Some weighting may then be given to the various ideas used, allowing a judgement as to whether SEA is likely to be of use in any given case. Also, the areas of SEA that most require improvement may be identified. Of course, any improvements may be difficult to make, especially when reverting to more complex problems, but at least a rational basis for decisions can be established.

The ideas of Davies[21] are extended in the present work to allow derivations for all the parameters of interest in an SEA study of two interacting sub-systems. This permits a deterministic calculation to be performed, provided the natural frequencies and mode shapes of the interacting sub-systems are available. By nominating random parameters and relevant probability density functions, it is then possible to carry out multi-dimensional integrations to establish exactly the average values described by SEA. Direct comparisons may then be made. Moreover, since this work is carried out in the frequency domain, it reveals how SEA performs frequency by frequency.

Since the restrictions of this approach concern only the requirements of well behaved damping and point coupling, it is used for two SEA studies; first, that of a pair of axially vibrating rods and secondly an idealised model of part of a ship. Both of these cases are dealt with in terms of axial, rather than transverse vibration, since single-point coupling is required. Nonetheless worthwhile results are obtained. The first case demonstrates the importance of coupling strength and also of the statistical descriptions employed. It also shows that details of the forcing functions and damping strength are less important, although improved results for describing damping mechanisms are obtained. This study leads to suggestions for further improvements to the usual SEA formulations, which are then applied to the more complex structure of the ship.

The first of these suggestions concerns the effects of strong coupling between two sub-systems, when they tend to behave as a single entity. Analysis of this problem leads to a new approximating function which is exactly correct at the extremes of coupling strength and well behaved in between. This new approximation is shown to give very good results in the simple case of the coupled rods and

also, under some circumstances, for the ship structure model.

The ship model exhibits geometrically periodic characteristics, being a 'plated and stiffened' steel structure. This characteristic naturally leads into a study of the vibrations of periodic and near-periodic systems. A major novelty of the present work is that the results from this study are used to provide more sophisticated statistical models for use in SEA. In particular, knowledge of the likely positions of natural frequency 'pass' and 'stop' bands is used to yield enhanced probability density functions for the natural frequencies. This results in worthwhile improvements in the predictions of SEA.

The problems of predicting mode shapes, especially at the coupling point, are discussed throughout this work; no simple methods for dealing with them can be offered. However, the effects of modal coherence are shown to be of secondary importance, compared with those of accuracy, in modelling natural frequencies and establishing coupling strength. Nonetheless, further theoretical studies of coupling mechanisms would seem to be warranted.

1.4. Outline of Thesis

In Chapter 2 the principal results of SEA are described and the analogy to heat flow introduced. The terms used in SEA are defined and their physical meanings outlined. The concepts of long term means and ensemble averages are introduced and the requirements for probability density functions mentioned. The cases where the original formulation of SEA is exactly correct are noted. The assumptions inherent in SEA are tabulated and a brief critique of these presented.

In Chapter 3 the frequency-domain work of Davies[21] for two point coupled sub-systems is introduced and extended to provide all the quantities of interest. These are related to the relevant SEA parameters. The simplifications of point and so called 'rain on the roof' forcing are discussed and expressions for receptances formed. Probabilistic measures are then introduced, and this leads into the use of multi-dimensional integrals to establish expected values. The idea of the summation band width is elaborated on. These various results are used as the starting point to recover the principal results of

SEA detailed in Chapter 2, showing more clearly the implications of the various assumptions noted at its end.

In Chapter 4, a simple example problem is described that has been studied elsewhere. It is used to study deterministically the two kinds of forcing function described in Chapter 3, which are shown to give similar results. They also reveal that the precise details of damping are of little importance in SEA, provided that it remains light. When it is heavy, more elaborate formulations are used, and these require only that the damping remains proportional. The effects of coupling strength are seen to be dominant above certain levels, and the calculation of these levels is discussed. The effects of mode shape coherence are shown to give rise to certain distortions in the results. It is noted that such distortions are difficult to predict.

In Chapter 5, statistical measures are adopted for the two rod model and some of the limitations of such models discussed. Exact solutions for the energy flow parameters are derived for the limiting case of infinite coupling strength, and the problem of high coupling strength is then examined in some detail. This leads to an improved measure of coupling strength, which, together with results for infinitely strong and weak coupling strength, is used to propose a new approximate correction factor. This factor is applied to the example and significant improvements are obtained in the results at high coupling strengths.

In Chapter 6, the use of statistical models is investigated further and their relationships to deterministic analyses discussed. This leads to proposals for approximate probability density functions to model natural frequencies. The possible ways of introducing these non-uniform probability density functions into SEA are outlined and likely problems noted. The difficulties inherent in applying a similar approach to mode shapes are discussed.

In Chapter 7, the theories underlying the vibrations of purely periodic structures are examined paying particular regard to the likely consequences for SEA. The central position of geometrically periodic design in modern structures is mentioned. The classical results of periodic theory are re-

capitulated using wave, transfer matrix and receptance theories. These theories are applied to a periodic rod model which is also analysed using finite element techniques, which are shown to give similar results.

The effects of deviations from pure periodicity are discussed in Chapter 8. These effects are studied first for a single isolated discontinuity; next when parameters are randomized throughout the structure and finally a combination of these. This work is used to establish a method for predicting the probability density functions for natural frequencies, based on 'pass' and 'stop' bands. The difficulties of predicting mode shapes in periodic structures are shown to be at least as great as for simpler structures and the likely consequences again mentioned.

In Chapter 9, the ship hull/bulkhead interaction problem is introduced and a simplified model constructed. Periodic theory is applied to this model to generate 'pass' and 'stop' band information. The model is then randomized and monte-carlo techniques used to derive the actual probability density functions for an ensemble of models. These are compared with those based on the 'pass' and 'stop' bands. SEA is applied to this problem and the exact energy flows calculated for a variety of coupling strengths using multi-dimensional integrals; these are contrasted with the traditional SEA approach. The methods outlined in Chapter 6 are then used to introduce approximate probability density functions into the SEA model at various coupling strengths, both with and without the coupling strength correction. The results arising from these revised methods are discussed.

In Chapter 10, the work is re-capitulated and the main concepts introduced are highlighted, in particular the modelling of heavy proportional damping, the strong coupling correction and the use of non-uniform natural frequency probability density functions. It is concluded that the modified methods provide worthwhile improvements. Areas for further work are outlined.

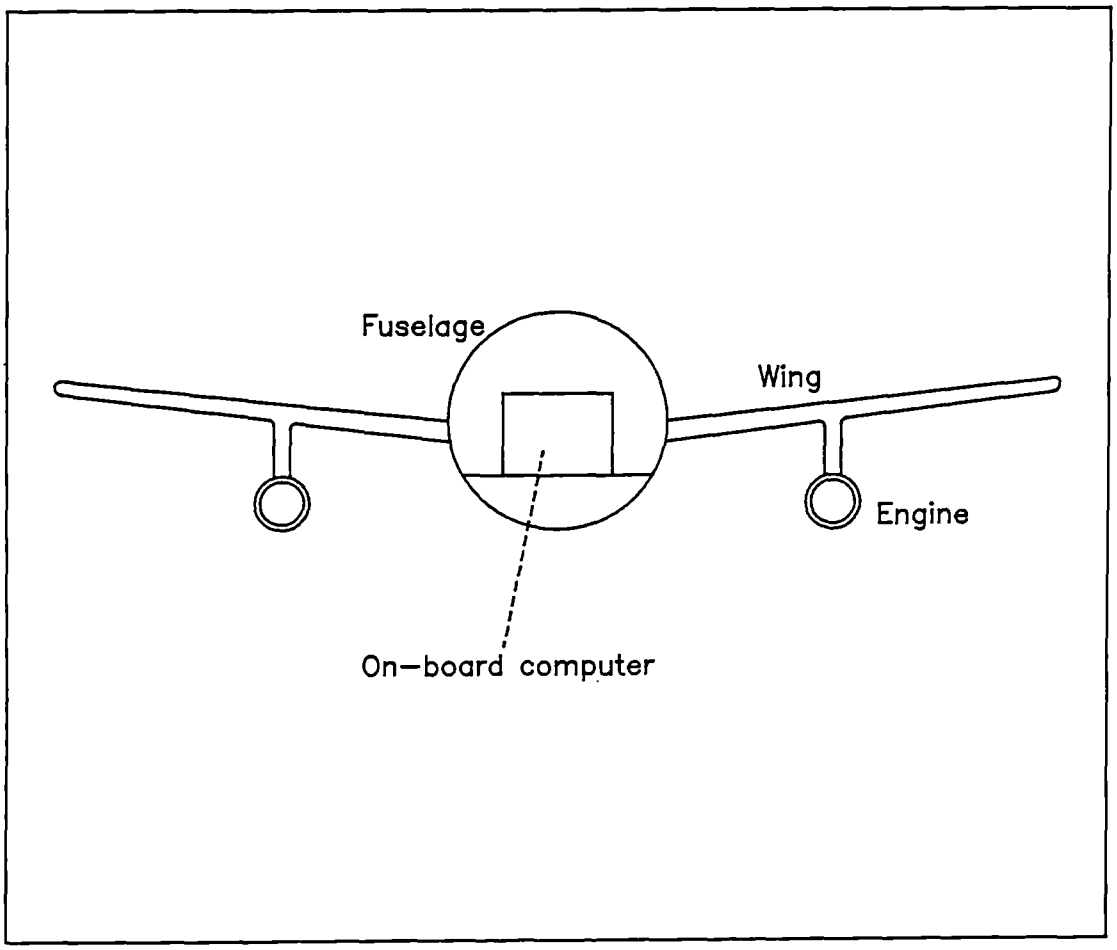

Figure 1.1 - Cross section of an aircraft, showing engines, wings, fuselage and an on-board computer system.

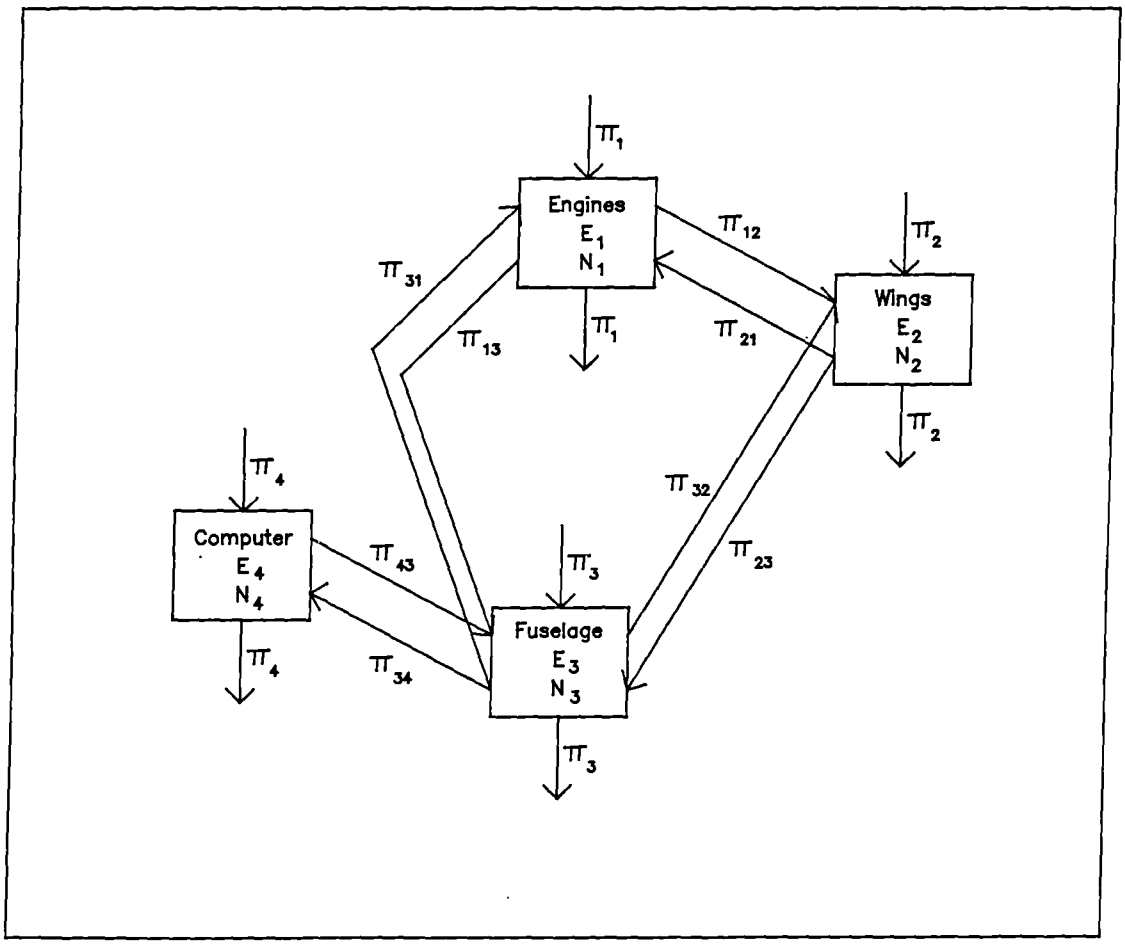

Figure 1.2 - SEA model of the problem illustrated in Figure 1.1.

CHAPTER 2

Statistical Analysis - A Brief Review

2.1. The Principal Ideas of Statistical Energy Analysis

Statistical energy analysis is concerned with calculation of the average energy levels and flows associated with the interactions of numerous sub-systems. However, most of the ideas of SEA are derived from the study of just two sub-systems, and these are then generalised for more complex cases. Consider Figure 2.1 which shows two, as yet unspecified, sub-systems and where the arrows again indicate flows of energy. Either sub-system may be driven, both dissipate energy through internal viscous damping and there is a conservative interchange of energy between them. They also possess certain kinetic and potential energy levels. These parameters may be considered as long-term time averages and under such circumstances the law of conservation of energy requires

$$<\Pi_{1_{DISS}}> = <\Pi_{1_{IN}}> - <\Pi_{12}> \tag{2.1}$$

and

$$<\Pi_{2_{DISS}}> = <\Pi_{1_{IN}}> + <\Pi_{12}> \tag{2.2}$$

(where angle brackets <> indicate long-term time averages and Π a flow of energy). This system forms the most primitive SEA model and, at its simplest, each sub-system may consist of a single, viscously damped, linear oscillator (as used in the earliest studies of SEA)[6,7]. A number of comments may be made about this model which reveal some of the prospects and difficulties inherent in SEA. First there is a clear similarity between this vibrational model and the heat flow between connected masses (or reservoirs). In the thermal sense the energy flows arise because of the interactions of vibrating molecules and the average parameters of interest are then temperatures. All that is required to make the analogy complete is that the amount of energy flowing should be proportional to the relevant potential differences. Assuming that such a condition holds, it is possible to construct simultaneous equa-

tions linking the energy flows and levels, for example

$$<\Pi_{12}> = K_1(<E_1> - K_2<E_2>) \tag{2.3}$$

$$<\Pi_{1_{DISS}}> = K_{1_{DISS}}<E_1> \tag{2.4}$$

$$<\Pi_{2_{DISS}}> = K_{2_{DISS}}<E_2> \tag{2.5}$$

then

$$<\Pi_{1_{IN}}> - (K_1 + K_{1_{DISS}})<E_1> + K_1K_2<E_2> = 0 \tag{2.6}$$

and

$$<\Pi_{2_{IN}}> - (K_1K_2 + K_{2_{DISS}})<E_2> + K_1<E_1> = 0 \tag{2.7}$$

(The exact forms of the various K constants used here are derived in subsequent sections.) Knowledge of the amount of energy flowing into the sub-systems enables a complete solution for all the unknown energy levels and flows here. Given such a solution, many other parameters of interest may be calculated (e.g., average stresses or displacements). The central idea is that energy flow be proportional to energy level differences in some way. It is precisely this idea that gave birth to SEA, and it is the form and assumptions under which it is correct, that are of interest here.

The next feature which deserves comment about this model concerns the mechanism by which energy flows between the sub-systems. This has not yet been specified, other than to say that it is conservative. This restriction avoids losses in the coupling and is in contrast to the sub-systems themselves where damping losses are a prerequisite that ensures finite amplitudes of vibration under all circumstances. This factor may limit the way in which a problem is broken down into sub-systems, since any features responsible for large dissipations of energy must lie wholly within a sub-system.

The final point to make about this simple model is its use of long-term averages, which are adopted so that steady, as opposed to transient, flow theories can be applied. This again imposes limits on the utility of SEA, but greatly simplifies the approach.

This brief discussion reveals that, despite restrictions, SEA may still be applied to quite a wide range of vibration problems. Although this first model uses only two sub-systems, its similarity to ther-

mal models holds out the possibility of dealing with flows of energy between complex arrangements of many sub-systems (such as those mentioned in Chapter 1 and illustrated in Figures 1.1 and 1.2). However, before attempting to generalise the theory, the postulate that energy flow is proportional to energy level difference, which is the principal result of SEA, must be substantiated. If this is possible so is a great deal more and if not SEA would appear to suffer from a fatal flaw.

Of course, nothing in vibrations analysis is so clear cut and it will transpire that the energy flow proportionality is exactly correct in some circumstances, a good approximation in others, and completely wide of the mark in yet others. As has already been mentioned, the beginnings of SEA were concerned with the behaviour of two linear, viscously damped, coupled oscillators and it is perhaps worth recapitulating that analysis.

2.2. Two Coupled, Linear Oscillators

The earliest reference to Statistical Energy Analysis begins by discussing the energy flow between two coupled, linear oscillators[6]. The reference considers the case when inertia, stiffness and viscous coupling are all present, which considerably complicates the analysis and so, since most subsequent work does not require all of these, here only the case of stiffness coupling is presented.

Figure 2.1 is still applicable to this problem, illustrating and defining the various energy flows. For the specific case of interest here, Figure 2.2 shows the various sub-system parameters. It is clear that the equations of motion describing this problem are

$$m_1\ddot{y}_1(t)+c_1\dot{y}_1(t)+(k_1+k_c)y_1(t) = F_1(t)+k_c y_2(t) \tag{2.8}$$

and

$$m_2\ddot{y}_2(t)+c_2\dot{y}_2(t)+(k_2+k_c)y_2(t) = F_2(t)+k_c y_1(t) \tag{2.9}$$

where $F_1(t)$ and $F_2(t)$ are two, time-varying forcing functions. In the subsequent analysis long term time averages of the various parameters will be formed (again indicated by angle brackets <>) and a number of identities used. Such identities are discussed in most standard texts on random vibration theory, see for example Newland[36]. Specifically, if $F_1(t)$ and $F_2(t)$ are both statistically independent,

stationary white noise, then the various derived processes (y_1, $\dot{y}_1$ etc.), are also stationary and the following relationships hold

$$\langle F_1(t)y_1\rangle = 0 \qquad \langle y_1\dot{y}_1\rangle = 0 \tag{2.10}$$

$$\langle F_1(t)y_2\rangle = 0 \qquad \langle y_2\dot{y}_2\rangle = 0$$

$$\langle F_2(t)y_1\rangle = 0 \qquad \langle \dot{y}_1\ddot{y}_1\rangle = 0$$

$$\langle F_2(t)y_2\rangle = 0 \qquad \langle \dot{y}_2\ddot{y}_2\rangle = 0$$

$$\langle \ddot{y}_1 y_1\rangle = -\langle \dot{y}_1^2\rangle \qquad \langle \ddot{y}_2 y_2\rangle = -\langle \dot{y}_2^2\rangle$$

$$\langle \ddot{y}_1 \dot{y}_2\rangle = -\langle \dot{y}_1 \ddot{y}_2\rangle \qquad \langle y_1 \dot{y}_2\rangle = -\langle \dot{y}_1 y_2\rangle$$

$$\langle \ddot{y}_1 y_2\rangle = -\langle \dot{y}_1 \dot{y}_2\rangle \qquad \langle y_1 \ddot{y}_2\rangle = -\langle \dot{y}_1 \dot{y}_2\rangle$$

If the coupling between the sub-systems does not involve any inertia terms, which is the case here, additionally

$$\langle F_1(t)\dot{y}_2\rangle = 0 = \langle F_2(t)\dot{y}_1\rangle \tag{2.11,12}$$

To calculate the energy flowing at any instant requires that the product of force and velocity at the point of application be formed. Therefore the various average energy flows are calculated from

$$\langle \Pi_{1_{IN}}\rangle = \langle F_1(t)\dot{y}_1\rangle \qquad \langle \Pi_{2_{IN}}\rangle = \langle F_2(t)\dot{y}_2\rangle \tag{2.13,14}$$

$$\langle \Pi_{1_{DISS}}\rangle = c_1\langle \dot{y}_1^2\rangle \qquad \langle \Pi_{2_{DISS}}\rangle = c_2\langle \dot{y}_2^2\rangle \tag{2.15,16}$$

$$\langle \Pi_{12}\rangle = k_c\langle y_1\dot{y}_2\rangle \qquad \langle \Pi_{21}\rangle = k_c\langle \dot{y}_1 y_2\rangle \tag{2.17,18}$$

Application of the identities to the last of these shows that $\langle \Pi_{12}\rangle = -\langle \Pi_{21}\rangle$, as expected for this conservatively coupled problem.

Following the original analysis of Lyon and Maidanik[6], the equations of motion are multiplied by y_1, $\dot{y}_1$, y_2 and $\dot{y}_2$ in turn, averages being taken in each case. Using the identities already outlined, this allows the following matrix equation to be formed

$$\begin{bmatrix} c_1 & 0 & 0 & 0 & 0 & 0 & k_c & 0 \\ 0 & c_2 & 0 & 0 & 0 & 0 & -k_c & 0 \\ 0 & 0 & 0 & 0 & 0 & c_1 & (k_1+k_c) & m_1 \\ 0 & 0 & 0 & 0 & 0 & c_2 & -(k_2+k_c) & -m_2 \\ -m_1 & 0 & (k_1+k_c) & 0 & -k_c & 0 & 0 & 0 \\ 0 & -m_2 & 0 & (k_2+k_c) & -k_c & 0 & 0 & 0 \\ 0 & 0 & 0 & -k_c & (k_1+k_c) & -m_1 & -c_1 & 0 \\ 0 & 0 & -k_c & 0 & (k_2+k_c) & -m_2 & c_2 & 0 \end{bmatrix} \tag{2.19}$$

$$\cdot \begin{Bmatrix} <\dot{y}_1^2> \\ <\dot{y}_2^2> \\ <y_1^2> \\ <y_2^2> \\ <y_1 y_2> \\ <\dot{y}_1 \dot{y}_2> \\ <y_1 \dot{y}_2> \\ <\ddot{y}_1 \dot{y}_2> \end{Bmatrix} = \begin{Bmatrix} <F_1 \dot{y}_1> \\ <F_2 \dot{y}_2> \\ 0 \\ 0 \\ 0 \\ 0 \\ 0 \\ 0 \end{Bmatrix}$$

This equation may be solved to gain expressions for the various quantities $<\dot{y}_1^2>$, etc., in terms of the system parameters and the input powers ($\Pi_{1_{IN}} = F_1(t)\dot{y}_1$ and $\Pi_{2_{IN}} = F_2(t)\dot{y}_2$).

Notice that the term $<\dot{y}_1^2>$ defines both the average energy dissipated by sub-system 1 and the average kinetic energy of the sub-system; also $<y_1^2>$ defines the average potential energy of sub-system 1. Similar remarks apply to sub-system 2, and additionally $<y_1\dot{y}_2>$ defines the average energy flow between the sub-systems. This matrix equation also contains a statement of the law of conservation of energy, since rows one and two of the matrix system of equations are

$$c_1<\dot{y}_1^2>+k_c<y_1\dot{y}_2> = <F_1(t)\dot{y}_1> \tag{2.20}$$

and

$$c_2<\dot{y}_2^2>-k_c<y_1\dot{y}_2> = <F_2(t)\dot{y}_2> \tag{2.21}$$

or

$$<\Pi_{1_{DISS}}>+<\Pi_{12}> = <\Pi_{1_{IN}}> \tag{2.22}$$

and

$$<\Pi_{2_{DISS}}>-<\Pi_{12}> = <\Pi_{2_{IN}}> \tag{2.23}$$

It additionally encapsulates the relationship between the average potential and kinetic energies of the sub-systems as rows five and six, viz.

$$-m_1<\dot{y}_1^2>+(k_1+k_c)<y_1^2>-k_c<y_1y_2> = 0 \tag{2.24}$$

and

$$-m_2<\dot{y}_2^2>+(k_2+k_c)<y_2^2>-k_c<y_1y_2> = 0 \tag{2.25}$$

In terms of energies these become

$$-<KE_1>+<PE_1> = 2k_c<y_1y_2> = -<KE_2>+<PE_2> \tag{2.26}$$

i.e., if there is no coupling at all ($k_c = 0$) the average potential and kinetic energies of the individual sub-systems are equal (which is well known) and, under all circumstances, the difference between these energies is the same for both sub-systems.

In their original paper Lyon and Maidanik[6] solve the matrix equation (2.19) under the assumption that the coupling is light ($k_c \ll k_1, k_2$), keeping only terms linear in k_c to obtain

$$<y_1\dot{y}_2> = \frac{k_c^2\left[\frac{c_1}{m_1}+\frac{c_2}{m_2}\right]\left[\frac{m_1}{c_1}<F_1\dot{y}_1>-\frac{m_2}{c_2}<F_2\dot{y}_2>\right]}{\left[\frac{k_1+k_c}{m_1}-\frac{k_2+k_c}{m_2}\right]^2+\left[\frac{c_1}{m_1}+\frac{c_2}{m_2}\right]\left[\frac{c_1\{k_2+k_c\}+c_2\{k_1+k_c\}}{m_1m_2}\right]} \tag{2.27}$$

which indicates that under these assumptions the energy flowing between the sub-systems is

$$<\Pi_{12}> = h_{12}\left[\frac{m_1}{c_1}<\Pi_{1_{IN}}>-\frac{m_2}{c_2}<\Pi_{2_{IN}}>\right] \tag{2.28}$$

where

$$h_{12} = \frac{k_c^2\left[\frac{c_1}{m_1}+\frac{c_2}{m_2}\right]}{\left[\frac{k_1+k_c}{m_1}-\frac{k_2+k_c}{m_2}\right]^2+\left[\frac{c_1}{m_1}+\frac{c_2}{m_2}\right]\left[\frac{c_1\{k_2+k_c\}+c_2\{k_1+k_c\}}{m_1m_2}\right]} \tag{2.29}$$

Now under the assumption of light coupling, all the power injected into a sub-system by its driving term is dissipated within that sub-system to a first approximation, so that for sub-system 1

$$<\Pi_{1_{IN}}> \approx <\Pi_{1_{DISS}}> = c_1<\dot{y}_1^2> = \frac{2c_1}{m_1}<KE_1> \tag{2.30}$$

and similarly for sub-system 2. Additionally, under the assumption of light coupling

$$<KE_1> = <PE_1> \quad , \quad <KE_2> = <PE_2> \tag{2.31,32}$$

so that finally the desired result

$$<\Pi_{12}> = h_{12}(<KE_1> + <PE_1> - <KE_2> - <PE_2>) \tag{2.33}$$

is achieved. This result depends only on the coupling being light and the forcing functions being independent, stationary white noise. The requirement that the coupling between sub-systems be light forms a major topic for discussion in Chapter 5 of the current work, whilst the use of independent stationary white forcing functions is not addressed further, save to note that under certain circumstances the requirement for spectrally flat forces may be relaxed, see Lyon[16]. The *spatial* variation of such forces is discussed in later chapters.

In the original reference[6] it is shown that this result holds for the more complex forms of linear coupling provided they are conservative. If the coupling mechanism gives rise to dissipation of energy the energy flow between the sub-systems also depends on the total energy levels of the sub-systems and not just their differences (also $<\Pi_{12}> \neq <\Pi_{21}>$ of course).

Having established the desired result, its applicability to more complex problems must be investigated. However, before continuing, it is worth noting that this analysis primarily shows the relationships between $<\Pi_{12}>$, $<\Pi_{1_{IN}}>$ and $<\Pi_{2_{IN}}>$. The use of potential and kinetic energies is a subsequent manipulation, and indeed the inclusion of potential energy is rather artificial. This is fortunate because the definition of potential energy involves the decision as to whether the coupling spring should be included or not. It is valid to use either approach, that is

$$<PE> = k<y^2>/2 \tag{2.34}$$

or

$$<PE> = (k+k_c)<y^2>/2 \tag{2.35}$$

The first is an 'uncoupled' definition and the second a 'blocked' one. They have different natural fre-

quencies as well, these being $\omega_1 = \sqrt{\frac{k_1}{m_1}}$ or $\sqrt{\frac{k_1+k_c}{m_1}}$ etc. This definition of blocked natural frequency can be used to simplify further the expression for the constant of proportionality, giving

$$h_{12} = \frac{k_c^2\left[\frac{c_1}{m_1}+\frac{c_2}{m_2}\right]}{\left[\omega_1^2-\omega_2^2\right]^2+\left[\frac{c_1}{m_1}+\frac{c_2}{m_2}\right]\left[\frac{c_1\omega_2^2}{m_1}+\frac{c_2\omega_1^2}{m_2}\right]} \tag{2.36}$$

These two lines of reasoning can cause confusion, but the previous analysis shows that such matters are peripheral to the main ideas discussed. When dealing with more complex problems this point reappears.

2.3. Multi-Modal Sub-Systems

Thus far the sub-systems considered have contained only a single oscillator, with an associated single natural frequency. Before the energy flow proportionality result is of any use in engineering problems, this restriction must be relaxed and multi-modal sub-systems considered. The additional assumptions that are necessary to preserve the results of the previous section for this wider class of problems (along which those already mentioned concerning coupling strength) lie at the heart of the present study.

SEA deals with multi-modal systems on the assumption that individual modes within one sub-system interact with those of another without mutual interference. Therefore if the 'average' interaction between any two modes can be established, all that is required to find the total interaction between two sub-systems is knowledge of the total number of modes involved, a simple product of this number and the interaction being formed. The assessment of the number of modes to include in these calculations is open to much debate. Usually consideration is given to whether certain classes of modes exchange energy at all (i.e., twisting and transverse modes of connected structures), and then to the so called 'modal density', which is the number of modes per unit of frequency. This density is multiplied by an 'averaging' bandwidth (with limits ω_u and ω_l and therefore width $\omega_u-\omega_l$), outside of which modes do not make a contribution sufficient for their inclusion to be justified, giving a mode count N. Whether or

not a mode actually contributes to the energy flow between coupled sub-systems depends primarily on its natural frequency, and to a lesser extent on its mode shape in the vicinity of the coupling and driving points. Therefore it is natural to consider how the proportionality constant, h_{12}, varies with these parameters. The usual approach of SEA is to assume that mode shapes do not, on average, affect the flow of energy between sub-systems, and therefore they are omitted from the following analysis. The natural frequencies are dealt with in rather more detail.

If the natural frequencies of the average modes, ω_1 and ω_2, are considered to be random variables with some specified two-dimensional probability density function, $f_{\omega_1\omega_2}$, then the average or expected value of h_{12} (indicated by $E[]$) is calculated from

$$E[h_{12}] = \int_{-\infty}^{\infty}\int_{-\infty}^{\infty} f_{\omega_1\omega_2}(u,v)h_{12}(u,v)\mathrm{d}u\mathrm{d}v \tag{2.37}$$

where u and v are suitable dummy variables of integration. The most commonly used definition for the density function, and that adopted by Lyon[16], is a constant applying over the range of frequencies defined by the averaging bandwidth ($\omega_u - \omega_l$), i.e., all frequencies between these given limits are equally likely to be natural frequencies. The previous integration is then performed under the assumption that the bandwidth is narrow compared with its centre frequency and also that the damping constants are small compared with the bandwidth, i.e.

$$\omega, \omega_1, \omega_2 \gg \omega_u - \omega_l \gg c_1, c_2 \tag{2.38}$$

Given these restrictions, Lyon[16] shows that

$$E[h_{12}] = \frac{\pi k_c^2}{2\omega^2 m_1 m_2 (\omega_u - \omega_l)} \tag{2.39}$$

where ω is the centre frequency of the averaging bandwidth. Therefore if there are N_1 modes interacting from sub-system 1, the energy flowing between all these modes and the 'average' mode of sub-system 2 is N_1 times as great, so that the total flow from all the modes of sub-system 1 to those of sub-system 2 is $N_1 N_2$ times that between the 'average' pair, giving

$$<\Pi_{12_{TOTAL}}> = N_1 N_2 E[h_{12}](<E_1> - <E_2>) \tag{2.40}$$

where $<E_1>$ and $<E_2>$ are the total (kinetic plus potential) energies of one individual (the average)

mode of the respective sub-systems. It is the assumption of mutual independence that allows the separation of the proportionality constant h_{12} and the modal energies E_1 and E_2 when carrying out this averaging process.

Now if the forcing functions are ergodic, as has already been assumed, so also are the derived energy levels and flows in this linear system, permitting the time averages to be replaced by averages across the modes, i.e.

$$E[\Pi_{12_{TOTAL}}] = N_1 N_2 E[h_{12}](E[E_1]-E[E_2]) \tag{2.41}$$

However $E[E_1]$ and $E[E_2]$ are the energies of the average modes, so that if the sub-systems contain N_1 and N_2 interacting modes, respectively, the total energy within a sub-system is N times as great, i.e.

$$E[E_{1_{TOTAL}}] = N_1 E[E_1] \quad , \quad E[E_{2_{TOTAL}}] = N_2 E[E_2] \tag{2.42,43}$$

Finally, substituting these results into equation (2.41) gives

$$E[\Pi_{12_{TOTAL}}] = N_2 E[h_{12}] \left[E[E_{1_{TOTAL}}] - \frac{N_1}{N_2} E[E_{2_{TOTAL}}] \right] \tag{2.44}$$

which is usually written as

$$E[\Pi_{12_{TOTAL}}] = \omega \eta_{12} \left[E[E_{1_{TOTAL}}] - \frac{N_1}{N_2} E[E_{2_{TOTAL}}] \right] \tag{2.45}$$

where η_{12}, the so called 'coupling loss factor', is defined here by

$$\eta_{12} = \frac{\pi k_c^2 N_2}{2\omega^3 m_1 m_2 (\omega_u - \omega_l)} \tag{2.46}$$

This equation is commonly cited as being the fundamental result of SEA; it has not been achieved without making a number of sweeping assumptions.

Notice that the various K constants of section 2.1 are related to these results as follows:-

$$K_1 = \omega \eta_{12} \tag{2.47}$$

$$K_2 = \frac{N_1}{N_2} \tag{2.48}$$

$$K_{1_{DISS}} = 2c_1 \tag{2.49}$$

$$K_{2_{DISS}} = 2c_2 \tag{2.50}$$

where the relevant energy levels are then defined as twice the kinetic energies.

2.4. Limitations and Inherent Assumptions of Statistical Energy Analysis

In the previous sections the original steps of SEA have been recapitulated so that the underlying ideas may be set in context. More recent studies have increased understanding of the technique, and have shown that energy flow proportionality is exactly correct for the case of two oscillators for *arbitrary* conservative, linear coupling. This has also been shown for the case of many identical oscillators with *identical* arbitrary conservative, linear coupling, see Lyon and Scharton[11] and Woodhouse[37]. These results for single-oscillator sub-systems hold out the promise that results for multi-modal sub-systems may be acceptably accurate. The case of point coupling between two such multi-modal sub-systems is analysed in some detail in the following chapters. However, before commencing these investigations, it is worth tabulating the various assumptions made thus far :-

(i) Sub-systems and coupling mechanisms are assumed linear.

(ii) Only statistically independent, stationary driving forces are applied to the sub-systems (i.e. ergodic forcing).

(iii) The driving forces have flat spectra compared with the frequency responses of the sub-systems.

(iv) The coupling between sub-systems is conservative and weak (weak coupling may be relaxed in some cases of the single-oscillator results).

(v) Proportional damping exists so that modal analysis generates uncoupled principal co-ordinates within each sub-system.

(vi) Modes are statistically independent within sub-systems which implies that the modal components of the driving forces should all be directly proportional to the overall driving force levels (so that all modes are equally excited by the driving forces).

(vii) Mode shapes of the uncoupled sub-systems in the vicinity of the coupling and driving points do not, on balance, affect the average energy flows.

(viii) Natural frequencies are uniformly distributed within given frequency limits.

(ix) The frequency limits containing the natural frequencies give a narrow bandwidth compared with the frequencies themselves.

(x) The damping is light compared with the frequency bandwidth.

In addition, it is clear that the more modes that interact in a given situation, the more useful will be the relevant averages, decreasing the deviations from the mean. Therefore another often stated requirement is for many interacting modes, i.e. high modal densities.

Of these assumptions, (i), (v) and (x) are usually applicable to engineering structures although the presence of either fluid actions or vibration absorbers may cause problems. Assumptions (ii), (iii) and (vi) indicate that SEA will be most useful in situations where forcing arises because of turbulent flow noise or complex machinery vibrations, whilst assumption (iv) implies that natural divisions between portions of the overall system will be useful in defining sub-systems. The remaining assumptions, and also the need for many interacting modes, require knowledge of the particular problem under investigation before their effects can be judged.

Given all these points, some idea may be formed as to whether SEA will be a useful technique in any set of circumstances. However, it is much easier to point to a particular failing of SEA in any given case than to propose alternatives. This fact alone may underly the recent resurgence of interest in SEA after a fallow period.

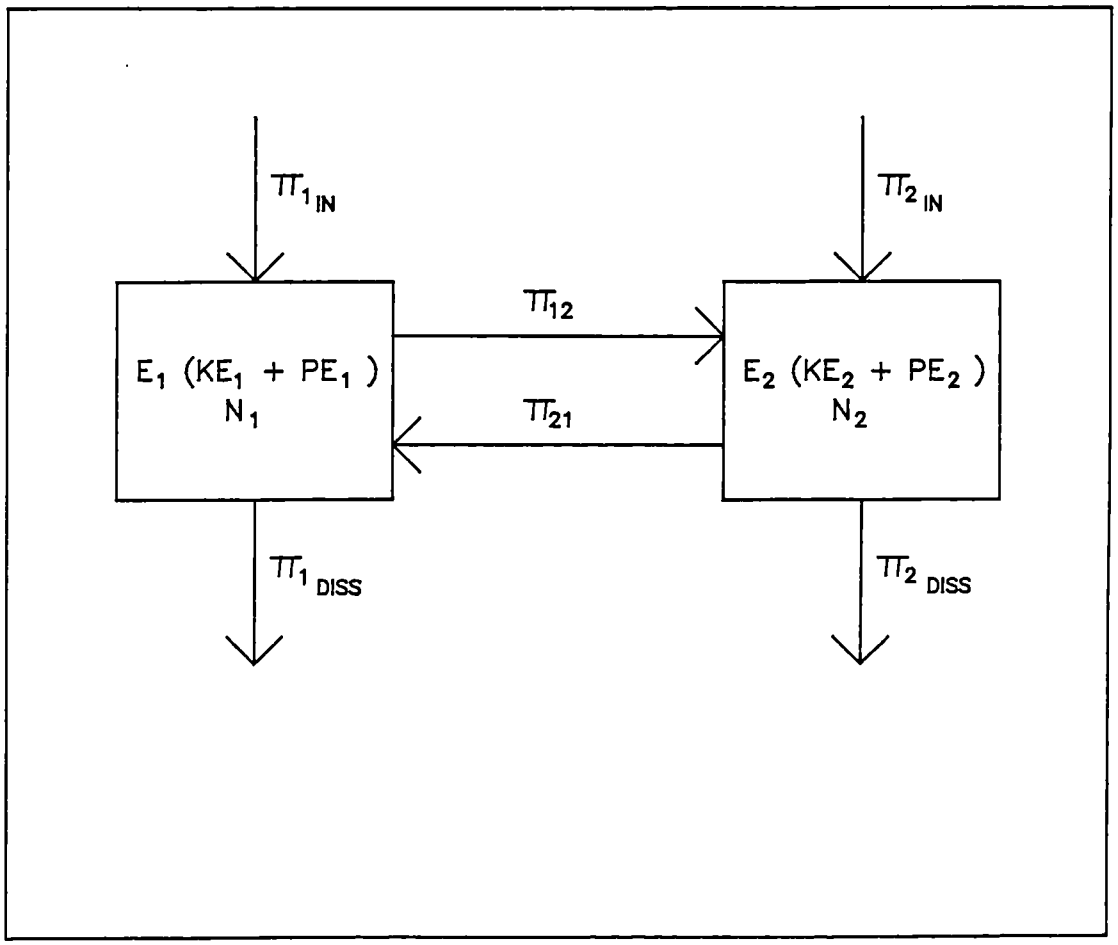

Figure 2.1 - SEA model of two interacting sub-systems.

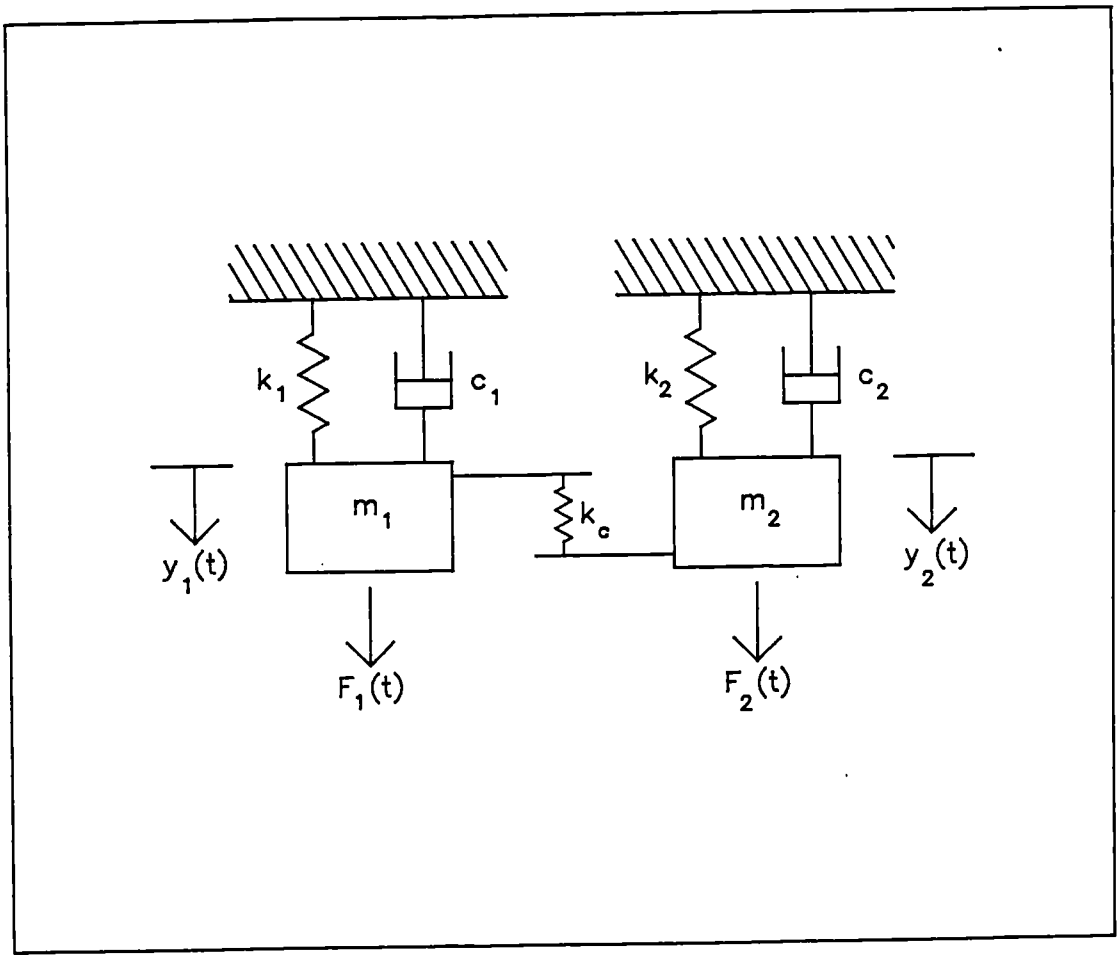

Figure 2.2 - A pair of coupled simple oscillators.

CHAPTER 3

Point Coupling of Two Systems

3.1. General Theory for Two Coupled Sub-Systems

The aim of this chapter is to derive exact expressions describing the energy flows between two point coupled, multi-modal systems. To begin with consider again Figure 2.1 and now define $H_{11}(\omega)$ as the direct receptance of sub-system 1 and $H_{12}(\omega)$ as the cross-receptance between sub-systems 1 and 2. These receptances govern the flow of energy into and out of sub-system 1 when *coupled* to sub-system 2. Also define $S_{F_1F_1}(\omega)$ as the spectral density of the driving force on sub-system 1 (which may include spatial variations). All of these functions are assumed to vary with the frequency of interest ω, with similar quantities applying to sub-system 2, but with the subscripts interchanged. Also here $E[]$ is taken to indicate an average across an *ensemble* of similar *systems* as opposed to modes within *one* system. Clearly, for linear systems and independent stationary driving forces

$$E[\Pi_{1_{IN}}(\omega)] = E[H_{11}(\omega)]S_{F_1F_1}(\omega) \tag{3.1}$$

and

$$E[\Pi_{1_{DISS}}(\omega)] = c_1 E[E_1(\omega)] \tag{3.2}$$

where the energy level $E_1(\omega)$ is taken to be twice the kinetic energy and it is assumed that the damping constant c_1 is known deterministically. (This assumption is not absolutely necessary, but is a reasonable approximation and considerably simplifies the algebra. For similar reasons it will also be assumed that sub-system total masses are fixed.) Additionally, if the coupling mechanism is conservative

$$E[\Pi_{12}(\omega)] = E[\Pi_{1_{IN}}(\omega)] - E[\Pi_{1_{DISS}}(\omega)] \tag{3.3}$$

and

$$E[\Pi_{12}(\omega)] = -E[\Pi_{21}(\omega)] \tag{3.4}$$

Of course, similar results hold for sub-system 2 but with the subscripts 1 and 2 interchanged.

By using these equations it may be shown that if the general form of the energy flow proportionality result, equation (2.3), i.e.

$$E[\Pi_{12}(\omega)] = K_1(E[E_1]-K_2E[E_2]) \tag{3.5}$$

is to hold, then it follows that

$$E[\Pi_{12}(\omega)] = E[H_{12}(\omega)]S_{F_1F_1}(\omega)-E[H_{21}(w)]S_{F_2F_2}(\omega) \tag{3.6}$$

Rearrangement of these equations results in the following definitions for the constants K_1 and K_2

$$K_1 = \frac{c_1E[H_{12}(\omega)]}{E[H_{11}(\omega)]\left[1-\frac{E[H_{12}(\omega)]}{E[H_{11}(\omega)]}-\frac{E[H_{21}(\omega)]}{E[H_{22}(\omega)]}\right]} \tag{3.7}$$

$$K_2 = \frac{c_2E[H_{11}(\omega)]E[H_{21}(\omega)]}{c_1E[H_{22}(\omega)]E[H_{12}(\omega)]} \tag{3.8}$$

Since all the receptances are rapidly varying functions of frequency, it is not surprising that K_1 and K_2 are also frequency dependent, despite the averaging process. Notice that these equations deal in energy flows at a particular frequency ω. If the total flow of energy across a range of frequencies is desired, these ensemble average values must be integrated across that range. The values of the constants K_1 and K_2 are then found by applying the previous equations with the *integrated* receptances (as opposed to integrating the expressions for K_1 and K_2 directly). Equations (3.1-3.4,3.6) are analogous to equations (1) to (4) derived by Smith[25]. However, he proceeded by making various implicit assumptions which were stated to hold with 'considerable generality'. Here the assumptions are made explicitly and their effects explored in greater detail.

By determining under what conditions equation (3.6) holds for K_1 and K_2 to be dependent *only* on the sub-system parameters, the range of validity of the proportionality result can be established. This allows relationships between these new definitions of K_1 and K_2 and those of the previous chapter to be ascertained. The cases of two arbitrarily coupled and many similarly coupled oscillators have been mentioned and the results noted to be valid, provided the driving forces on all the oscillators considered are statistically independent. It appears that this is still true when considering two multi-modal sub-systems for certain kinds of driving forces, even when the two sub-system parameters differ

considerably, for all coupling strengths, at least in the case of point coupling.

To show that the main SEA result holds for point spring coupling, the exact deterministic equations relating the energy flows between two multi-modal systems are derived following the methods of Davies[20,21]. This allows the equations for the ensemble averages of the energy flows to be formed in terms of the probability density functions (PDFs) of the sub-system parameters. These expressions have the particular forms that show the various mean receptances to be functions *only* of the sub-system parameters in *all* such cases, proving the desired result. This leads to a method for calculating exactly the various receptances as functions of frequency, and hence the constants K_1 and K_2 in the energy flow equations (2.3,3.5), with arbitrary coupling strength and mode counts. Under certain conditions, complex algebraic expressions for these functions are obtained and their connections with the coupling loss factor and mode count ratio established. These formulations allow criteria to be placed on the mode counts and coupling strength of any given problem for the more simple results of the previous chapter to be valid.

3.2. Exact Deterministic Energy Flow Equations

Using the assumptions of the previous section, Davies[21] studied the case of two multi-modal sub-systems coupled by a linear spring. Figure 2.1 still depicts this problem, but now it is emphasized that the coupling is at a single point and the mode shapes at the point of coupling become important. The coupled differential equations of motion describing this class of problem are

$$\{\Lambda_1+r_1(x_1)\mathrm{d}/\mathrm{d}t+\rho_1(x_1)\mathrm{d}^2/\mathrm{d}t^2\}y_1(x_1,t)=P_1(x_1,t), \tag{3.9}$$

$$\{\Lambda_2+r_2(x_2)\mathrm{d}/\mathrm{d}t+\rho_2(x_2)\mathrm{d}^2/\mathrm{d}t^2\}y_2(x_2,t)=P_2(x_2,t) \tag{3.10}$$

where Λ_1 is a linear spatial differential operator on sub-system 1, $r_1(x_1)$ is the damping constant of sub-system 1, $\rho_1(x_1)$ is the mass density per unit length of sub-system 1, and $P_1(x_1,t)$ is a forcing function on sub-system 1 which may be a function of $y_2(x_2,t)$; similarly for sub-system 2, but with the subscripts reversed, 2 for 1. Both the damping and mass densities are allowed to vary with the positions within the sub-systems x_1, x_2, subject to assumption (v) of Chapter 2 which requires that

$$r_1(x_1) = c_1\rho_1(x_1) \tag{3.11}$$

and

$$r_2(x_2) = c_2\rho_2(x_2) \tag{3.12}$$

i.e., proportional damping within the sub-systems. The forcing functions P are assumed to contain the coupling forces resulting from the connection between the two sub-systems. If this is a point spring coupling at $x_1 = a_1$ and $x_2 = a_2$ with a spring of strength k_c, the forcing function becomes

$$P_1(x_1,t) = F_1(x_1,t) + k_c\{y_2(a_2,t) - y_1(a_1,t)\}\delta(x_1 - a_1) \tag{3.13}$$

where $F_1(x_1,t)$ is the external driving force on sub-system 1 which may vary with position as well as time, and similarly for sub-system two, but with the subscripts altered. This problem is classically solved by using modal analysis. An expansion in the eigenfunctions of the uncoupled ($k_c = 0$) sub-systems $\psi_i(x_1)$ and $\psi_r(x_2)$ is made, and this produces equations of the form

$$\{\Lambda_1 - \rho_1(x_1)\omega_i^2\}\psi_i(x_1) = 0 \tag{3.14}$$

where the ω_i are the natural frequencies of the modes of system 1. These eigenfunctions may be normalized so that

$$\int \psi_i(x_1)\psi_j(x_1)\rho_1(x_1)dx_1 = m_1\delta_{ij} \tag{3.15}$$

Equations (3.9-3.15) hold for any pair of point spring coupled sub-systems whose uncoupled mode shapes and frequencies are known and where assumptions (i)-(iv) of the previous chapter are valid.

This problem was examined in the frequency domain[21] and the previous standard results used to derive exact expressions governing the flow of energy between the coupled sub-systems. The energy flow from sub-system 1 to 2, was shown to be

$$\Pi_{12}(\omega) = \frac{\omega^2 k_c^2 c_2}{m_1^2 m_2 |\Delta|^2} \sum_{r=1}^{\infty} \left[\frac{\psi_r^2(a_2)}{|\phi_r|^2} \right] \sum_{i=1}^{\infty}\sum_{j=1}^{\infty} \left[\mathrm{Re}\{S_{ij}(\omega)\} \frac{\psi_i(a_1)\psi_j(a_1)\mathrm{Re}\{\phi_i\phi_j^*\}}{|\phi_i|^2|\phi_j|^2} \right] \tag{3.16}$$

$$- \frac{\omega^2 k_c^2 c_1}{m_1 m_2^2 |\Delta|^2} \sum_{i=1}^{\infty} \left[\frac{\psi_i^2(a_1)}{|\phi_i|^2} \right] \sum_{r=1}^{\infty}\sum_{s=1}^{\infty} \left[\mathrm{Re}\{S_{rs}(\omega)\} \frac{\psi_r(a_2)\psi_s(a_2)\mathrm{Re}\{\phi_r\phi_s^*\}}{|\phi_r|^2|\phi_s|^2} \right]$$

Here $\psi_i(a_1)$ is taken to be the mode shape at the coupling point of the ith mode of sub-system 1, $S_{ij}(\omega)$ is the cross-spectral density of the *modal* force components on modes i and j on sub-system 1; similarly for sub-system 2 with modes r and s. Re{} denotes a real part and * a complex conjugate. Δ and

ϕ are given by

$$\Delta = 1 + (k_c/m_1)\sum_{i=1}^{\infty}(\psi_i^2(a_1)/\phi_i) + (k_c/m_2)\sum_{r=1}^{\infty}(\psi_r^2(a_2)/\phi_r) \tag{3.17}$$

$$\phi_i = \omega_i^2 - \omega^2 + \sqrt{-1}\, c_1\omega \tag{3.18}$$

$$\phi_r = \omega_r^2 - \omega^2 + \sqrt{-1}\, c_2\omega \tag{3.19}$$

Note that in theory all these summations should be carried out over an infinite number of modes. However, modes with natural frequencies distant from the frequency of interest contribute only slightly and may therefore be omitted. This leads to a method for fixing the mode counts N_1 and N_2 of equations (2.46) and (2.48), barring modal densities that rise without limit, so that the summations converge.

This work is repeated in Appendix A and extended to derive relationships for the energy flowing into the sub-systems from the driving forces, the energy dissipated by internal damping and the energy levels of the sub-systems. The energies flowing into the sub-systems from the external driving forces are shown to be given by the expression

$$\Pi_{1_{IN}}(\omega) = \frac{\omega^2 c_1}{m_1}\sum_{i=1}^{\infty}\frac{S_{ii}(\omega)}{|\phi_i|^2} + \frac{\omega k_c}{m_1^2}\mathrm{Im}\left\{\sum_{i=1}^{\infty}\sum_{j=1}^{\infty}\frac{S_{ij}(\omega)\psi_i(a_1)\psi_j(a_1)}{\phi_i\phi_j\Delta}\right\} \tag{3.20}$$

where again the result for sub-system 2 is obtained by interchanging the subscripts. Note that the input has two distinct parts. The first deals with the external driving forces in the absence of coupling, whilst the second describes the changes due to the coupling forces. Given these frequency dependent equations and the relevant modal information, it is possible to calculate all the energy parameters of interest for any suitable problem.

Upon comparing equations (3.16) and (3.20) with equations (3.1) and (3.6) respectively, it is apparent that the desired proportionality result holds only if the the modal forcing spectra ($S_{ij}(\omega)$, etc.) can be taken outside of the various summations of equations (3.16) and (3.20). Now $S_{ij}(\omega)$ is related to the *sub-system* forcing spectrum $S_{F_1F_1}(\omega,x_i,x_j)$ (which describes the relationship between the driving force at various positions on the sub-system) by

$$\iint S_{F_1F_1}(\omega,x_i,x_j)\psi_i(x_i)\psi_j(x_j)dx_i dx_j = S_{ij}(\omega) \tag{3.21}$$

Any forcing function where the frequency variations are the same for all modes of a sub-system allows a separation between the spatial and frequency variables here, and so satisfies the previous requirement. Additionally, modal incoherence of the driving function, or point driving, allows further simplifications where the double summations can be collapsed to single summations or their products. Specifically, point driving at $x_i = b_1 = x_j$ is described by

$$S_{F_1F_1}(\omega,x_i,x_j) = S_{F_1F_1}(\omega)\delta(x_i-b_1)\delta(x_j-b_1)(\rho_1/m_1)^2 \tag{3.22}$$

(Note that here $S_{F_1F_1}(\omega)$ just describes the frequency content of the forces and this is independent of the position. Also, the factor ρ_1/m_1 is included to maintain dimensional homogeneity). Substitution of this expression into equation (3.21) results in

$$S_{ij}(\omega) = S_{F_1F_1}(\omega)\psi_i(b_1)\psi_j(b_1) \tag{3.23}$$

where now $\psi_i(b_1)$ is the mode shape at the *driving* point, as opposed to that at the *coupling* point $\psi_i(a_1)$. Under these circumstances equations (3.16) and (3.20) describing the energy flows may be simplified to give

$$\Pi_{12}(\omega) = (\omega^2 k_c^2 c_2/m_1^2 m_2 |\Delta|^2) S_{F_1F_1}(\omega) \sum_{r=1}^{\infty} (\psi_r{}^2(a_2)/|\phi_r|^2) \left| \sum_{i=1}^{\infty} (\psi_i(b_1)\psi_i(a_1)/\phi_i) \right|^2 \tag{3.24}$$

$$- (\omega^2 k_c^2 c_1/m_1 m_2^2 |\Delta|^2) S_{F_2F_2}(\omega) \sum_{i=1}^{\infty} (\psi_i^2(a_1)/|\phi_i|^2) \left| \sum_{r=1}^{\infty} (\psi_r(b_2)\psi_r(a_2)/\phi_r) \right|^2$$

and

$$\Pi_{1_{INV}}(\omega) = (\omega^2 c_1 S_{F_1F_1}(\omega)/m_1) \sum_{i=1}^{\infty} (1/|\phi_i|^2) \tag{3.25}$$

$$+ (\omega k_c S_{F_1F_1}(\omega)/m_1^2) \mathrm{Im} \left\{ \frac{1}{\Delta} \left[\sum_{i=1}^{\infty} \psi_i(b_1)\psi_i(a_1)/\phi_i \right]^2 \right\}$$

Modally incoherent or 'rain on the roof' forcing implies that

$$\iint S_{F_1F_1}(\omega,x_i,x_j)\psi_i(x_i)\psi_j(x_j)dx_i dx_j = S_{ij}(\omega)\delta_{ij} \tag{3.26}$$

This result has been discussed more fully elsewhere[38], from which it is noted that for equation (3.26) to hold requires

$$S_{F_1F_1}(\omega,x_i,x_j) = S_{F_1F_1}(\omega)\delta(x_i-x_j)(\rho_1/m_1)^2 \tag{3.27}$$

which provides one definition for a 'rain on the roof' driving function. Notice also that, if ρ_1 is a function of position, this implies further restrictions on this kind of forcing, requiring that areas of high density receive greater energy input than those of low density. Upon adopting this assumption of modal incoherence, equations (3.16) and (3.20) describing the energy flows may be simplified to give

$$\Pi_{12}(\omega) = (\omega^2 k_c^2 c_2/m_1^2 m_2 |\Delta|^2) S_{F_1F_1}(\omega) \sum_{r=1}^{\infty} (\psi_r^2(a_2)/|\phi_r|^2) \sum_{i=1}^{\infty} (\psi_i^2(a_1)/|\phi_i|^2) \tag{3.28}$$

$$-(\omega^2 k_c^2 c_1/m_1 m_2^2 |\Delta|^2) S_{F_2F_2}(\omega) \sum_{i=1}^{\infty} (\psi_i^2(a_1)/|\phi_i|^2) \sum_{r=1}^{\infty} (\psi_r^2(a_2)/|\phi_r|^2),$$

and

$$\Pi_{1_{IN}}(\omega) = (\omega^2 c_1 S_{F_1F_1}(\omega)/m_1) \sum_{i=1}^{\infty} (1/|\phi_i|^2) \tag{3.29}$$

$$+ (\omega k_c S_{F_1F_1}(\omega)/m_1^2) \mathrm{Im} \left\{ \sum_{i=1}^{\infty} (\psi_i^2(a_1)/\phi_i^2 \Delta) \right\}$$

Comparison of these various results with equations (3.1) and (3.6) allows algebraic expressions for the sub-system input and cross-receptances to be given in terms of the modal expansions. That is, for point driving,

$$H_{11}(\omega) = (\omega^2 c_1(\omega)/m_1) \sum_{i=1}^{\infty} (1/|\phi_i|^2) + (\omega k_c/m_1^2) \mathrm{Im} \left\{ \frac{1}{\Delta} \left[\sum_{i=1}^{\infty} \psi_i(b_1)\psi_i(a_1)/\phi_i \right]^2 \right\} \tag{3.30}$$

$$H_{12}(\omega) = (\omega^2 k_c^2 c_2/m_1^2 m_2 |\Delta|^2) \sum_{r=1}^{\infty} (\psi_r^2(a_2)/|\phi_r|^2) \left| \sum_{i=1}^{\infty} (\psi_i(b_1)\psi_i(a_1)/\phi_i) \right|^2 \tag{3.31}$$

and for modally incoherent driving,

$$H_{11}(\omega) = (\omega^2 c_1(\omega)/m_1) \sum_{i=1}^{\infty} (1/|\phi_i|^2) + (\omega k_c/m_1^2) \mathrm{Im} \left\{ \sum_{i=1}^{\infty} (\psi_i^2(a_1)/\phi_i^2 \Delta) \right\} \tag{3.32}$$

$$H_{12}(\omega) = (\omega^2 k_c^2 c_2/m_1^2 m_2 |\Delta|^2) \sum_{r=1}^{\infty} (\psi_r^2(a_2)/|\phi_r|^2) \sum_{i=1}^{\infty} (\psi_i^2(a_1)/|\phi_i|^2) \tag{3.33}$$

These definitions form the deterministic results on which any statistical calculations may be based.

To reiterate, when two multi-modal, point spring coupled sub-systems are excited by either point or 'rain on the roof' type forces, then energy flow proportionality holds *whatever* the values of the cou-

pling strength or other sub-system parameters. Consequently, strong coupling, or differing sub-systems does cause equation (3.5) to break down; it simply results in definitions for the proportionality constants which are more complex than those of equations (2.46-2.48). Since they are the more generally used of the two, 'rain on the roof' type forces will be adopted for most of the subsequent analysis; however, to illustrate the differences, which will be shown to be relatively unimportant, point driving will also be applied to the first example considered. Also, for clarity, most of the subsequent analysis will be directed towards the receptances rather than the proportionality constants, since the latter are just a further algebraic manipulation.

3.3. Exact Statistical Energy Flow Equations

To establish the exact forms of the receptances and constants K_1 and K_2, a statistical description of the problem must be adopted. Deterministic knowledge of the sub-systems is relinquished, and probabilistic characteristics ascribed to them instead. The resulting equations are then expressed in terms of ensemble averages. That is, any particular pair of sub-systems is taken to be a typical member of an infinite set of possible systems and the results are averages taken over the infinite ensemble. This is not the same as taking an average in the frequency domain, which involves integrating with respect to ω rather than ω_i, ω_r. (However, because the variations of ϕ_i with ω and ω_i, etc., are not greatly different, similar results are obtained when the coupling is weak and the damping light.) With this ensemble averaging approach, equations (3.32) and (3.33) become

$$E[H_{11}(\omega)] = (\omega^2 c_1(\omega)/m_1)E\left[\sum_{i=1}^{\infty}(1/|\phi_i|^2)\right] \tag{3.34}$$

$$+ (\omega/m_1^2)E\left[k_c\mathrm{Im}\left\{\sum_{i=1}^{\infty}(\psi_i{}^2(a_1)/\phi_i{}^2\Delta)\right\}\right]$$

$$E[H_{12}(\omega)] = (\omega^2 c_2/m_1^2 m_2)E\left[k_c^2/|\Delta|^2)\sum_{r=1}^{\infty}(\psi_r{}^2(a_2)/|\phi_r|^2)\sum_{i=1}^{\infty}(\psi_i{}^2(a_1)/|\phi_i|^2)\right] \tag{3.35}$$

where both equations are complicated functions of frequency since Δ, ϕ_i and ϕ_r are all frequency dependent.

By inserting these results into equations (3.7) and (3.8), the exact statistical expressions for the systems are derived. However, it must be realised that to make use of equations (3.34) and (3.35) requires probability density functions (PDFs) for each probabilistically modelled term, so that the expected values or averages may be calculated. Given suitable PDFs, all that is required, in theory, to arrive at the mean value is that a multi-dimensional integral be carried out involving the relevant functions combined with the chosen PDFs. Unfortunately the required integrals are of the form

$$E[H_{11}(\omega)] = \int\!\!\int \cdots \int_{-\infty}^{\infty} \int\!\!\int \left[\frac{\omega^2 c_1}{m_1} \sum_{i=1}^{N_1} \left[1/|\phi_i|^2 \right] + \frac{\omega k_c}{m_1^2} \mathrm{Im} \left\{ \sum_{i=1}^{N_2} \left[\psi_i{}^2 (a_1)/\phi_i^2 \Delta \right] \right\} \right] \tag{3.36}$$

$$\times f(k_c, \psi_{i=1}, \cdots, \psi_{i=N_1}, \psi_{r=1}, \cdots, \psi_{r=N_2}, \omega_{i=1}, \cdots, \omega_{i=N_1}, \omega_{r=1}, \cdots, \omega_{r=N_2})$$

$$\times dk_c d\psi_{i=1} \cdots d\psi_{i=N_1} d\psi_{r=1} \cdots d\psi_{r=N_2} d\omega_{i=1} \cdots d\omega_{i=N_1} d\omega_{r=1} \cdots d\omega_{r=N_2}$$

where

$$f(k_c, \psi_{i=1}, \cdots, \psi_{i=N_1}, \psi_{r=1}, \cdots, \psi_{r=N_2}, \omega_{i=1}, \cdots, \omega_{i=N_1}, \omega_{r=1}, \cdots, \omega_{r=N_2})$$

is some unspecified multi-dimensional PDF and N_1 and N_2 are chosen such that the summations have converged.

These may be evaluated using standard monte-carlo integration techniques, but they are of course, very time consuming to deal with, even with increasingly powerful computers, and therefore additional simplifications are usually sought.

3.4. Recovery of Traditional Statistical Energy Analysis Results

The results of the previous section may be simplified and the traditional results of SEA described in Chapter 2 recovered by adopting, in turn, the various assumptions noted there. Assuming that the coupling strength and location are known deterministically allows these terms to be dropped from the relevant PDFs. Further, the infinite summations are truncated by defining the bandwidth surrounding the frequency of interest ω which fixes N_1 and N_2, the numbers of modes contributing to energy flows at that frequency. The choice of the upper and lower limits of this bandwidth, ω_u and ω_l, is somewhat arbitrary, but it may be made by noting that it is convenient to take them equidistant from the fre-

quency of interest ω, and also that they should be chosen so that modes with natural frequencies at these limits do not significantly affect the response at the centre frequency. This requires information about the sub-system damping factors and the number of interacting modes. In practice, it is the modal densities (i.e., the ratios of the numbers of interacting modes to the separation between ω_u and ω_l) that are normally specified for a problem, based either on calculation or experiment. This implies that during energy flow calculations at a number of frequencies of interest, ω_u and ω_l will change, with only their separation from the central frequency being held constant. Therefore although the number of interacting modes is fixed (upon assuming constant modal densities) the particular modes actually contributing will change. Moreover, modal summations require integer numbers of modes to be considered, while the products of modal densities and bandwidth in general give rise to non-integers. These facts indicate an inconsistent statistical model, but it suffices if the fundamental information available for a sub-system is the modal density rather than a knowledge of individual modal behaviour. These points are illustrated in the examples discussed later. However, it must be emphasized that correct modelling may require systems with low modal density to be analysed on the assumption that modes well separated from the frequency of interest *do* contribute significantly to the results. This is particularly awkward in lightly damped systems and throws doubt on the usual SEA assumption of narrow bandwidths in such cases.

This approach leaves the equations for $E[H_{11}(\omega)]$, etc., dependent only on the natural frequencies and mode shapes of the interacting modes. The mode shape parameters ψ^2 are discarded from these relationships by noting that averaging across many modes and averaging across various positions within a *single* mode are basically similar processes (a kind of ergodicity). Moreover, the average of the square of the mode shape across the positions within the sub-system is identically unity in systems with uniform mass density because of the normalization scheme adopted earlier in equation (3.15). This assumption works well provided that the various mode shapes of the uncoupled sub-systems do not exhibit any spatial coherence at the points of interest (i.e. the values of the mode shapes at the points of interest are suitably random when considering all the relevant modes). In practice, this

assumption may well be invalid since couplings and sources of energy usually occur at the boundaries of sub-systems where coherence does exist, a problem which is discussed later.

The assumption concerning natural frequencies lies at the very heart of SEA. If these are all uniformly probable within a given range, the previous integral relationship may be greatly simplified since the PDF term for each frequency is like that of Figure 3.1, being a constant within the range of interest and zero outside it. Combining this idea with the previous assumptions causes the integral equations to be reduced to

$$E[H_{11}(\omega)] = \int\!\!\int \cdots \int_{\omega_l}^{\omega_u} \int\!\!\int \left[\frac{\omega^2 c_1}{m_1} \sum_{i=1}^{N_1} \left[1/|\phi_i|^2 \right] \right. \tag{3.37}$$

$$\left. + \frac{\omega k_c}{m_1^2} \mathrm{Im} \left\{ \sum_{i=1}^{N_1} \left[1/\phi_i^2 \Delta \right] \right\} \right] \frac{d\omega_{i=1} \cdots d\omega_{i=N_1} d\omega_{r=1} \cdots d\omega_{r=N_2}}{(\omega_u - \omega_l)^{N_1+N_2}}$$

and

$$E[H_{12}(\omega)] = \int\!\!\int \cdots \int_{\omega_l}^{\omega_u} \int\!\!\int \left[\frac{\omega^2 k_c^2 c_2}{m_1^2 m_2 |\Delta|^2} \sum_{i=1}^{N_1} \left[1/|\phi_i|^2 \right] \sum_{r=1}^{N_2} \left[1/|\phi_r|^2 \right] \right] \tag{3.38}$$

$$\frac{d\omega_{i=1} \cdots d\omega_{i=N_1} d\omega_{r=1} \cdots d\omega_{r=N_2}}{(\omega_u - \omega_l)^{N_1+N_2}}$$

Notice that the reduced limits of integration are possible here because at these limits the contribution of the integrand is negligibly small, this requirement being the reason for their choice. However, even these integrals are difficult to handle, primarily because of the presence of Δ in the denominator of the integrands, which is a function of the natural frequencies of both sub-systems. Complete discussion of this problem is deferred to Chapter 5, where it is shown that under certain circumstances the problem may be overcome; the assumption of weak coupling removes it completely, however, because then Δ is unity. Making this assumption the previous multiple integrals collapse to the products of many simple integrals, each of which is of identical form for each sub-system so that

$$E[H_{11}(\omega)] = \frac{\omega^2 c_1 N_1}{m_1(\omega_u - \omega_l)} \int_{\omega_l}^{\omega_u} \frac{d\omega_i}{|\phi_i^2|^2} = \frac{\omega^2 N_1 c_1}{m_1} E\left[1/|\phi_i|^2 \right] \tag{3.39}$$

and

$$E[H_{12}(\omega)] = \frac{\omega^2 k_c^2 c_2 N_1 N_2}{m_1^2 m_2 (\omega_u - \omega_l)^2} \int_{\omega_l}^{\omega_u} \frac{d\omega_i}{|\phi_i|^2} \int_{\omega_l}^{\omega_u} \frac{d\omega_r}{|\phi_r|^2} \tag{3.40}$$

$$= \frac{\omega^2 k_c^2 c_2 N_1 N_2}{m_1^2 m_2} E\left[1/|\phi_i|^2\right] E\left[1/|\phi_r|^2\right]$$

Note that the second summation in the previous expression for $E[H_{11}(\omega)]$ has also been dropped because k_c is assumed small. These integrals are rather tedious, but may be determined analytically, see Appendix B (note also that it is with this greatly simplified form that integrating with respect to ω is similar to using ω_i, ω_r, given light damping). The assumption of weak coupling also allows the expression for K_1, equation (3.7) to be simplified to

$$K_1 = \frac{c_1 E[H_{12}(\omega)]}{E[H_{11}(\omega)]} \tag{3.41}$$

so that a combination of the previous results gives

$$K_1 = \frac{k_c^2 c_1 N_2}{m_1 m_2} E\left[1/|\phi_i|^2\right] \tag{3.42}$$

$$K_2 = \frac{c_1 N_1 E\left[1/|\phi_i|^2\right]}{c_2 N_2 E\left[1/|\phi_r|^2\right]} \tag{3.43}$$

This pair of equations together with equation (3.5) give exact statistical energy flow results in the limit when the coupling is vanishingly weak; moreover, they do not require restrictions to be placed either on the damping strengths of the sub-systems or the width of the frequency band containing the interacting modes. (Note however that modes lying outside the bandwidth must not affect the receptance equations (3.34) and (3.35).)

When additionally the approximations for light damping and narrow frequency bands are made, the integrals simplify so that

$$E\left[1/|\phi_i|^2\right] = \frac{\pi}{2\omega^2 c_1 (\omega_u - \omega_l)} \tag{3.44}$$

$$E\left[1/|\phi_r|^2\right] = \frac{\pi}{2\omega^2 c_2 (\omega_u - \omega_l)} \tag{3.45}$$

(see again Appendix B) and these allow the following simpler forms for the various receptances to be

derived

$$E[H_{11}(\omega)] = \frac{\pi N_1}{2m_1(\omega_u - \omega_l)} \tag{3.46}$$

$$E[H_{12}(\omega)] = \frac{\pi^2 k_c^2 N_1 N_2}{4\omega^2 c_1 m_1^2 m_2 (\omega_u - \omega_l)^2} \tag{3.47}$$

$$E[H_{22}(\omega)] = \frac{\pi N_2}{2m_2(\omega_u - \omega_l)} \tag{3.48}$$

$$E[H_{21}(\omega)] = \frac{\pi^2 k_c^2 N_1 N_2}{4\omega^2 c_2 m_1 m_2^2 (\omega_u - \omega_l)^2} \tag{3.49}$$

Finally, substituting these results into the equations for K_1 and K_2, equations (3.41) and (3.8), the results given at the end of the previous chapter are recovered.

It should be noted that the results derived in this chapter have been based on uncoupled natural frequencies, whilst those of the previous are based on blocked frequencies; however, under the assumption of weak coupling, these definitions converge.

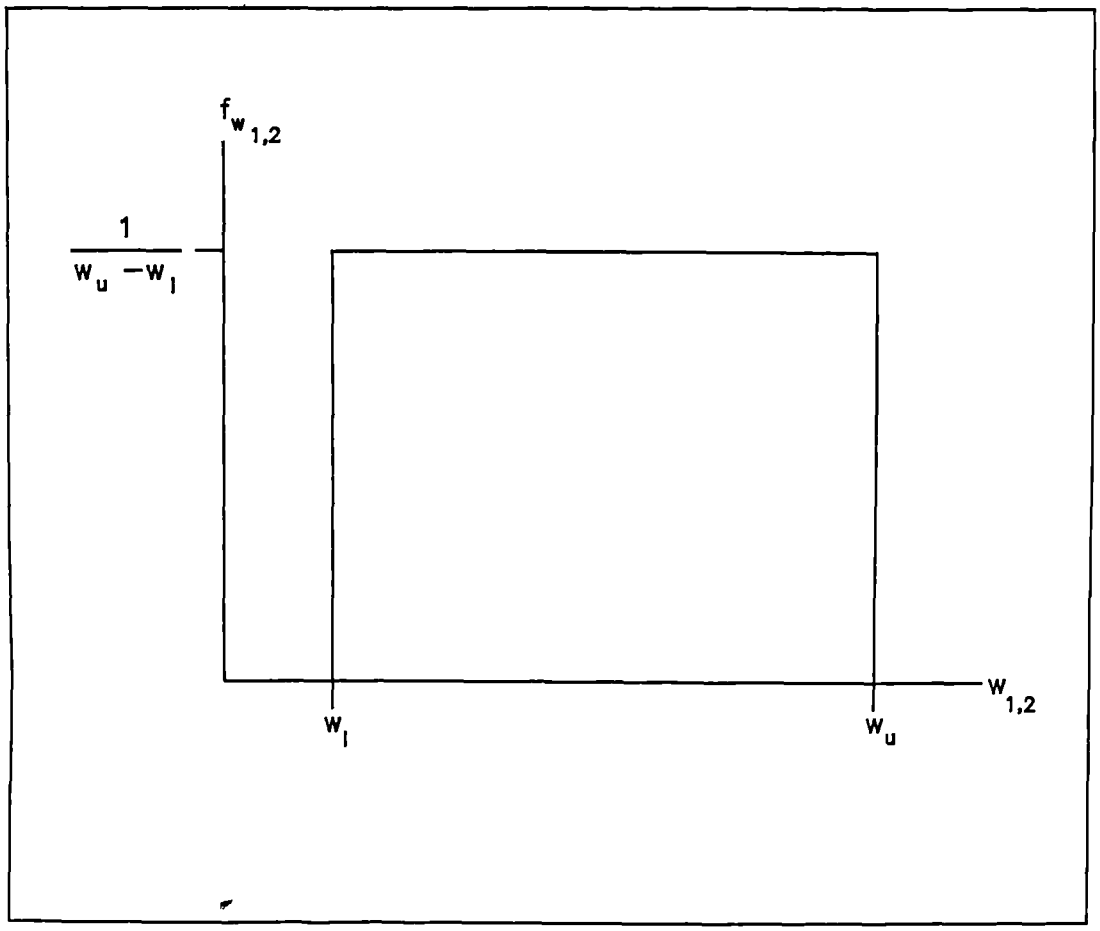

Figure 3.1 - A simple probability density function for random natural frequencies ω_1 or ω_2.

CHAPTER 4

Deterministic Analysis of a Simple Example

4.1. The Example

To enable the results of the previous chapter to be set in context, the cross-receptance, $H_{12}(\omega)$ of a simple example will be studied. Consider two axially vibrating free-free rods coupled at some point by a linear spring, illustrated in Figure 4.1. Such a system has been examined previously[22, 23, 26] and the parameter values used will be adopted here to aid comparison, see Table 4.1. In all cases only rod 1 will be forced, so that the energy flow from rod 1 to 2 is directly proportional to $H_{12}(\omega)$.

This model will be used to illustrate a number of features, using various combinations of forcing position and type, damping strength and type and coupling position and strength. These different cases are detailed in Table 4.2 and each arrangement will be discussed in turn. (Notice that when comparing differing damping types, the parameters detailed in the table have been chosen to give rise to directly comparable responses, i.e., the same level of damping compared with critical damping at resonance in each case).

All the variations in this chapter will be discussed using deterministic as opposed to probabilistic models, since this clarifies the various effects being studied. The application of random parameters, which involve changes from those of Table 4.1, will be reserved to the next chapter.

PARAMETERS USED IN THE EXAMPLES OF CHAPTER 4			
Parameter	Sub-system 1	Sub-system 2	Units
Mass density per unit length (ρ)	4.156	4.156	kg/m
Length (l)	5.182	4.328	m
Rigidity (AE)	17.85	17.85	MN

Table 4.1

LOAD CASES USED IN THE EXAMPLES OF CHAPTER 4								
Case No.	Force Type	Forcing Position	Damping Type	Damping Strength		Coupling Position		Coupling Strength
		x_1, m		c_1	c_2	x_1, m	x_2, m	N/m
1	Point	0.0	Point	0.4788	0.4788	0.1776	0.7042	861.4
2	Point	0.0	Prop'nal	88.95	106.49	0.1776	0.7042	861.4
3	Point	0.0	Point	0.4788	0.4788	0.0	0.0	861.4
4	Point	0.0	Prop'nal	88.95	106.49	0.0	0.0	861.4
5	Point	0.3738	Point	0.4788	0.4788	0.1776	0.7042	861.4
6	Point	0.3738	Prop'nal	88.95	106.49	0.1776	0.7042	861.4
7	Point	0.0	Point	4.788	4.788	0.1776	0.7042	861.4
8	Point	0.0	Prop'nal	889.5	1064.9	0.1776	0.7042	861.4
9	Point	0.0	Point	4.788	4.788	0.0	0.0	861.4
10	Point	0.0	Prop'nal	889.5	1064.9	0.0	0.0	861.4
11	Point	0.3738	Point	4.788	4.788	0.1776	0.7042	861.4
12	Point	0.3738	Prop'nal	889.5	1064.9	0.1776	0.7042	861.4
13	Dist'd	n/a	Prop'nal	88.95	106.49	0.1776	0.7042	861.4
14	Dist'd	n/a	Prop'nal	88.95	106.49	0.1776	0.7042	various

Table 4.2 - Notice that when the damping is proportional the constants c_1 and c_2 are for the constants in the equations of motion and have units of s^{-1}, whilst when it is applied at specific points the constants refer to the rates of the viscous dashpots and have units of Ns/m.

4.2. Point Forcing. Variations in Damping

Take first the situation where rod 1 is forced at a single point and consider two different models of damping. The damping is applied either by supporting the free ends of the rods in viscous dashpots (cases 1, 3, 5, 7, 9 and 11 of Table 4.2) or alternatively by an unspecified distributed form that results in proportional damping which obeys equations (3.11, 3.12) and therefore gives uncoupled principal modes (cases 2, 4, 6, 8, 10, and 12 of Table 4.2). The first of these damping models is simple to visualize, but does not meet the underlying requirements of modal analysis; the damping gives rise to coupling between all the modes of the individual sub-systems. Conversely, proportional damping is more complex from a physical standpoint but results in simplified equations of motion. Nonetheless, it is possible to conceive of a proportional damping scheme for sub-systems with uniform mass density, as here. The more complex the model being studied becomes, the more difficult to support is this assumption, especially for heavy damping.

When point, end damping is applied to the coupled rods of Figure 4.1 a Green's function may be constructed which relates excitation and response at any two interior positions, see Remington and Manning[22]. This function allows complete solutions to be formed for all the parameters of interest, see Appendix C. Equation (C.14) of the Appendix gives an expression for $\Pi_{12}(\omega)$ for this model ($\Pi_{12}(\omega) = H_{12}(\omega)$ if only sub-system 1 is forced and $S_{F_1F_1}(\omega)$ is unity) and this involves very few inherent assumptions, since no appeal to modal analysis has been made, rather the equations of motion have been solved directly.

To apply the modal summation results of the previous chapter for the case of proportional damping requires details of various modal parameters (frequencies and shapes, see Bishop and Johnson[3]) and also the number of modes contributing to the energy flows, N_1 and N_2, and therefore the summation bandwidth, $\omega_u - \omega_l$.

Figure 4.2 shows the effect of varying this bandwidth (and therefore the ranges of the summations) on the results of the deterministic cross-receptance calculation, $H_{12}(\omega)$, equation (3.31), at a fixed centre frequency of 5000 rad/s (796 Hz). The jumps that occur in this function arise when the increasing bandwidth reaches the point where an extra mode must be included in the summations for one or the other of the coupled sub-systems, incrementing the mode counts N_1 or N_2. These jumps in the curve indicate the effect of changes in the mode counts on the various calculations, illustrating the importance of a consistent approach in their choice. This curve settles to a limiting value because of the presence of constant modal density. The bandwidth of 8796 rad/s (1.4 kHz) used subsequently and shown dotted on the figure results in N_1 and N_2 being six and seven, respectively. It may be seen that this value is reasonable as the curve has sensibly settled by this point, although slight discontinuities will still be seen in the following example. Note that the maximum bandwidth that may be used at any given centre frequency is just twice that frequency if the usual analysis is to hold (i.e., if the band is to be evenly distributed); also it must be limited to the range of frequencies over which the SEA model of uniform modal density is valid.

If the level of damping is light, the Green's function and modal summation models tend to converge, especially for problems with well separated, undamped natural frequencies, because then the inter-modal coupling terms in the point damping model rapidly vanish (cases 1, 3 and 5 of Table 4.2). It is fortunate that most of the structures of interest to vibration engineers are lightly damped and therefore well behaved in this respect. The presence of fluid actions (i.e., fuel in tanks, or water surrounding a ship) gives rise to an important class of exceptions to this rule, but these lie outside the scope of the present work.

Taking first the case of light damping and interior coupling, Figure 4.3 shows the variation of $H_{12}(\omega)$ calculated using the Green's function and modal summation approaches (cases 1 and 2 of Table 4.2 respectively) i.e., comparing equations (C.14) and (3.31). The point damping curve is the same as that given as Figure 2 of Remington and Manning's paper[22]. The proportional damping result differs little from this, indicating that both the changed damping model and truncations of the infinite summations inherent in the modal summation approach have had very little effect. Those differences that do occur arise midway between the peaks in the function, when the frequency concerned is most distant from the natural frequencies of either sub-system. This is as expected, since it is between natural frequencies that any cross-coupling terms have most effect. Clearly, the total energy flow across a range of frequencies, which is found by integrating these curves with respect to ω, would be sensibly identical. Moving the coupling point to the ends of the rods (cases 3 and 4 of Table 4.2) or moving the driving point to the interior of rod 1 (cases 5 and 6 of Table 4.2) modifies the curves for $H_{12}(\omega)$ because of the effects of mode shape coherence at the free ends of the rods, see Figures 4.4 and 4.5 respectively. However the similarities between the two models remain.

The regions of the modal summation $H_{12}(\omega)$ curve indicated by the numbers 1 and 2 in Figure 4.5 highlight abrupt changes in the function. Those indicated by the number 1 in the figure occur because the summation bandwidth chosen here is not quite wide enough to ensure converged summations under these circumstances; increasing it removes these steps, see Figure 4.6, for example. This figure also reveals that the change indicated by the number 2 in Figure 4.5 is a characteristic of the

model being studied rather than the method adopted.

The effects of mode shape coherence, either at the coupling or driving points, are remarkably difficult to predict; traditional SEA ignores them completely. However, it is clear that such effects result in changes of magnitude rather than in behaviour, c.f. Figures 4.3 to 4.5, perhaps justifying the SEA approach. This is most readily acceptable in problems with uniform mass densities and very many modes where the mode shapes tend to show little coherence. However, if a sub-system has a particularly dense region, it is simple to see that the resulting mode shapes in this region will trail off with increasing frequency. If this area is coincident either with the position of loading or coupling, this fall off will give rise to a significant bias in the resulting frequency responses; such problems are discussed further in later chapters.

Turning next to the case of heavy damping, Figures 4.7 to 4.9 are equivalent to Figures 4.3 to 4.5, respectively, but with ten times greater damping levels (i.e., cases 7-12 of Table 4.2). Under these circumstances the response contributed by any given natural mode is much reduced and the total additionally contains significant contributions from adjacent modes; the modes are said to overlap (of course increased modal densities assist this phenomenon). Here the difference between the two damping models is clearly seen, indicating that modal analysis, which ignores coupling between modes due to damping, would be inappropriate if point damping were actually present. Under such circumstances, it would not be surprising if SEA gave misleading, results since it is so heavily dependent on the modal approach. Notice that this does *not* imply that SEA cannot be used in cases of heavy damping, merely that the combination of heavy damping and modal cross-coupling should be avoided. If a proportional damping model were still applicable to a heavily damped system, SEA could be used; however, as is shown in Appendix B, the simple integration results for the receptances and therefore the K constants of the main SEA equation given by Lyon[16] are no longer appropriate and the more complex forms given in the appendix should be used instead. One *advantage* of heavily damped systems is that extremes of response are much less likely at any given frequency, which indicates that the ensemble average results of SEA would be more reliable in these cases because the statistics would show much

reduced deviations from their means, see Keane and Price[23].

These various results indicate that a proportional damping model, and therefore modal analysis, may be used to study the behaviour of a wide class of point coupled multi-modal problems, subject only to the restriction that cases involving heavy damping should not contain significant inter-modal cross-coupling via the damping mechanism. Additionally, the presence of heavy damping indicates that although SEA *may* still be valid in such cases and indeed have improved statistics, the various constants in the energy flow expressions will differ from those appertaining to light damping.

For simplicity, all subsequent analysis in the current work will be restricted to cases of light proportional damping.

4.3. Light, Proportional Damping. Variations in Forcing

Assuming that the damping of the sub-systems is light and proportional, next consider the effects of adopting modally incoherent ('rain on the roof') as opposed to point forcing. That is, compare the results from equations (3.31) and (3.33). Figure 4.10 illustrates $H_{12}(\omega)$ under these circumstances and also includes the results for point forcing and light proportional damping from Figures 4.3-4.5 (i.e., cases 13,2,4 and 6 from Table 4.2, respectively). All four curves show the same trends, peaking at the natural frequencies of both sub-systems, as expected. The effects of modal coherence on the point driving curves reveal themselves, as before, in changes of amplitude along the curves. However, the behaviour between natural frequencies takes one of two forms, falling virtually to zero or merely showing a marked dip. The 'rain on the roof' forcing curve always gives dips at these frequencies, whilst the point forcing curves can take either form.

These various differences can be explained by considering the underlying equations (3.31) and (3.33) and noting that, for the damping model used here, at most two terms dominate the various summations in the equations, reducing to only one at a natural frequency. Additionally, the summations over sub-system 2 are the same for both forcing models, which is to be expected since sub-system 2 is not affected by changes in the forcing on sub-systems 1. Neglecting all but the two modes of sub-

system 1 lying on either side of the frequency of interest, equations (3.31) and (3.33) become, respectively

$$H_{12}(\omega) = \left[\frac{\psi_i^2(b_1)\psi_i^2(a_1)}{|\phi_i|^2} + \frac{\psi_j^2(b_1)\psi_j^2(a_1)}{|\phi_j|^2} \right. \tag{4.1}$$

$$\left. + \psi_i(b_1)\psi_i(a_1)\psi_j(b_1)\psi_j(a_1) \left[\frac{1}{\phi_i \phi_j^*} + \frac{1}{\phi_i^* \phi_j} \right] \right]$$

$$\times \left[\frac{\omega^2 k_c^2 c_2}{m_1^2 m_2 |\Delta|^2} \sum_{r=1}^{N_2} \psi_r^2(a_2)/|\phi_r|^2 \right]$$

and

$$H_{12}(\omega) = \left[\frac{\psi_i^2(a_1)}{|\phi_i|^2} + \frac{\psi_j^2(a_1)}{|\phi_j|^2} \right] \times \left[\frac{\omega^2 k_c^2 c_2}{m_1^2 m_2 |\Delta|^2} \sum_{r=1}^{N_2} \psi_r^2(a_2)/|\phi_r|^2 \right] \tag{4.2}$$

If ω is almost adjacent to *one* of these natural frequencies, these further simplify to

$$H_{12}(\omega) = \frac{\psi_i^2(b_1)\psi_i^2(a_1)}{|\phi_i|^2} \left[\frac{\omega^2 k_c^2 c_2}{m_1^2 m_2 |\Delta|^2} \sum_{r=1}^{N_2} \psi_r^2(a_2)/|\phi_r|^2 \right] \tag{4.3}$$

and

$$H_{12}(\omega) = \frac{\psi_i^2(a_1)}{|\phi_i|^2} \left[\frac{\omega^2 k_c^2 c_2}{m_1^2 m_2 |\Delta|^2} \sum_{r=1}^{N_2} \psi_r^2(a_2)/|\phi_r|^2 \right] \tag{4.4}$$

These four equations show that *at* the natural frequencies of the forced sub-system, the values of $H_{12}(\omega)$ for the point forcing model are scaled by the square of the modal amplitude for the relevant mode at the *driving* point. Midway between the natural frequencies of the driven sub-system (and therefore possibly *at* the natural frequencies of the undriven sub-system) the differences between the preceding pairs of equations are at their greatest, containing effects from both modal coherence at the driving point and modal cross-couping. When the modal functions at the driving point are of opposite signs equation (4.1) is much reduced, but equation (4.2) is unaffected. It is this phenomenon that causes the cross-receptance curves to tend to zero and this always occurs with end-point driving, sometimes with interior point driving and is not relevant to 'rain on the roof' driving, see also Skudrzyk[39].

The presence of the mode shape at the coupling point in all these equations indicates that modal coherence at this point will have significant effects, a subject discussed later; here attention is focused

instead on the driving model. Since *all* the modes of axially vibrating free-free rods show the same mode shape amplitudes at their ends ($\sqrt{2}$), *all* the peaks occurring at the natural frequencies of rod 1 for the *end* driven curve are exactly twice those for the modally incoherent force curve when the same coupling point is used (i.e., cases 2 and 13 of Table 4.2). It is clear that a distinct shift occurs at all frequencies between these two models, resulting in doubled energy flows. The more complex behaviour of the modes shapes within the sub-systems is much harder to predict, but does not rule out such biases across certain ranges of frequencies. Indeed, if the driving point were coincident with the node of a particular mode, such that $\psi_i(b_1) = 0$, the relevant peak in the curve of $H_{12}(\omega)$ would disappear altogether. These various shifts and omissions are not possible with the modally incoherent force model, which reflects *all* modes of the driven sub-system, and supports its use in SEA where precise details of the forcing will usually not be known. Because of the difficulties of dealing with modal coherence, particularly at the coupling point, these problems arise again in later chapters. The use of modally incoherent *forces* will be adopted for all subsequent analysis.

4.4. Light Proportional Damping. Incoherent Forcing. Variations in Coupling Strength

To conclude this deterministic examination of the two rod model, consider finally the effect of varying the coupling strength k_c at a fixed frequency of interest, case 14 of Table 4.2. Figure 4.11 illustrates the variation of $H_{12}(\omega)$ under these circumstances at a frequency of 5000 rad/s (796 Hz, a value that corresponds to a natural frequency of one sub-system, but none of the other).

The figure shows quite clearly the two regimes of 'weak' and 'strong' coupling. Whilst the coupling remains 'weak' the cross-receptance, and therefore the energy flow through the coupling, rises with the square of the coupling strength; when it is 'strong' the cross-receptance is unaffected by further increases in coupling strength and 'equi-partition' of energy is said to hold. Notice that simple SEA *is* valid for the case of equi-partition of energy when, although the cross-receptances are in error, the equivalence of energy levels causes the net energy flows predicted to be zero, i.e., correctly predicted, but for the wrong reasons! Also shown on Figure 4.11 is the parameter $|\Delta|$ which occurs in

the denominator of the expressions for $H_{12}(\omega)$. Since it is the presence of k_c in the expression for Δ which cancels with that in the numerator of the equations for $H_{12}(\omega)$ at high coupling strengths, it is not surprising that $|\Delta|$ is a good indicator of the coupling strength, a point which has been made elsewhere[40].

Since simple SEA is strictly valid only for the case of weak coupling, when considering more than two differing sub-systems, such measures of coupling strength are very useful; however, it will be shown in subsequent chapters that $|\Delta|$ is not the only possible measure and that an alternative may be formulated that is more appropriate to the underlying mathematics. Nonetheless, it is clear that the coupling strength between any two sub-systems must be classified before SEA can be applied, if the usual formulations are to hold. If the coupling is found to be strong, as is often the case with engineering structures, the normal SEA approach to the problem is to group the two sub-systems together as a single multi-modal sub-system whose combined modes and natural frequencies must then be found. This may be rather difficult in practice and is certainly a limitation on the utility of the method. By using a more sophisticated formulation this limitation can sometimes be overcome, as discussed in the next chapter.

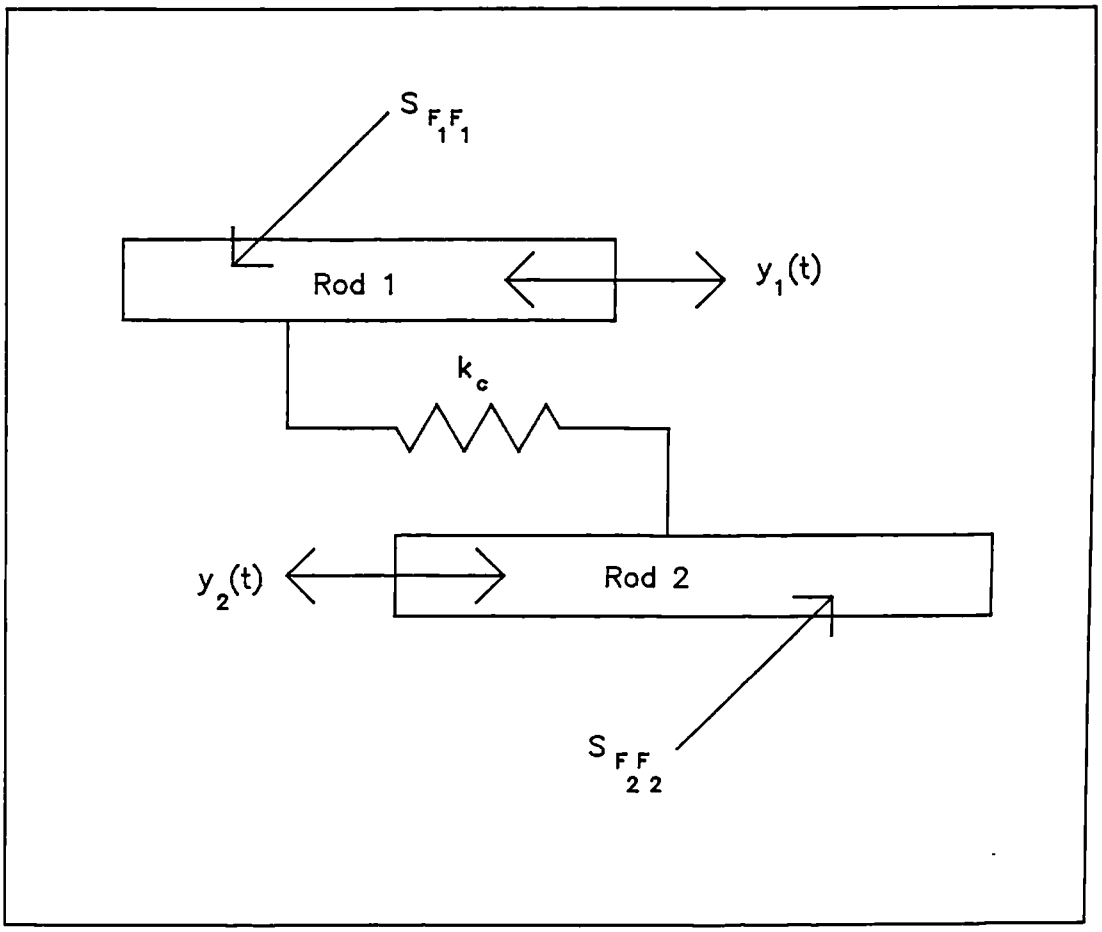

Figure 4.1 - Two, point spring coupled, axially vibrating rods.

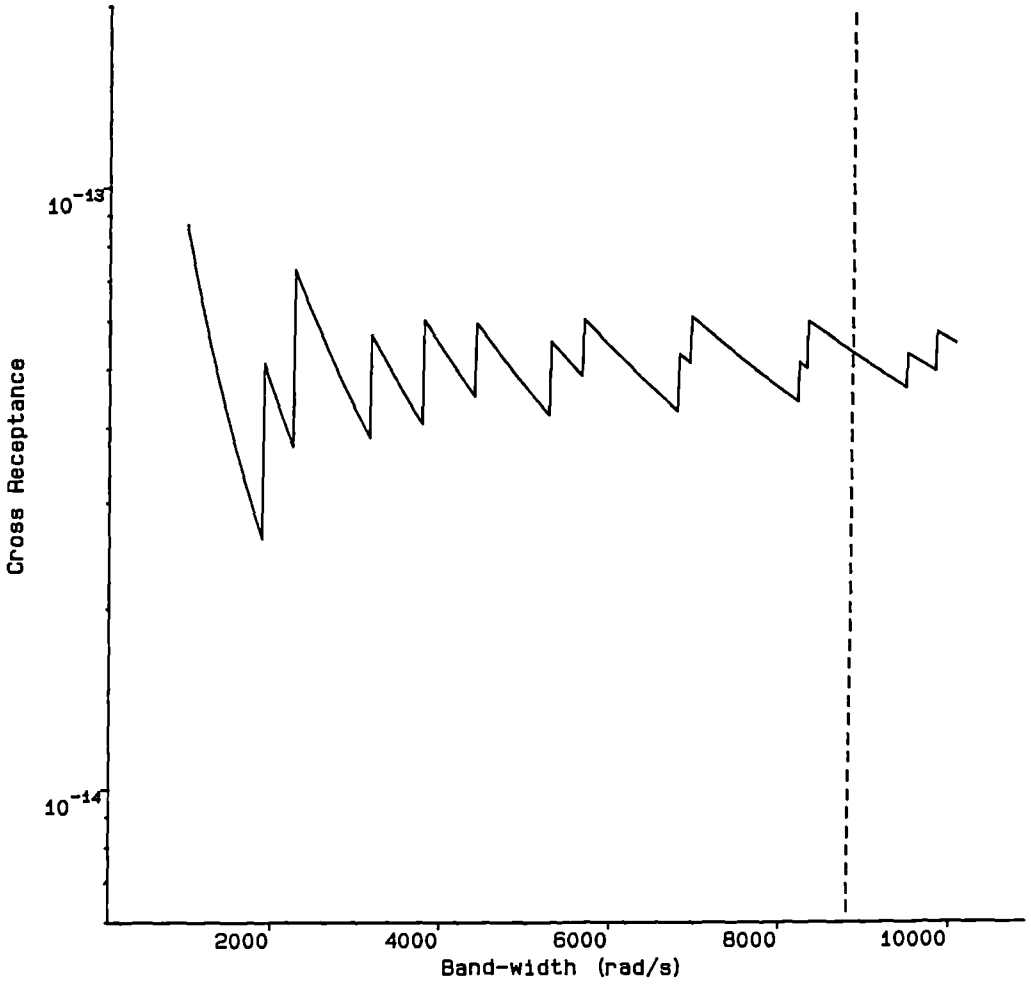

Figure 4.2 - Variation of H_{12} with summation bandwidth $\omega_u - \omega_l$. The bandwidth of 8796 rad/s (1.4 kHz) used in the example is shown dotted.

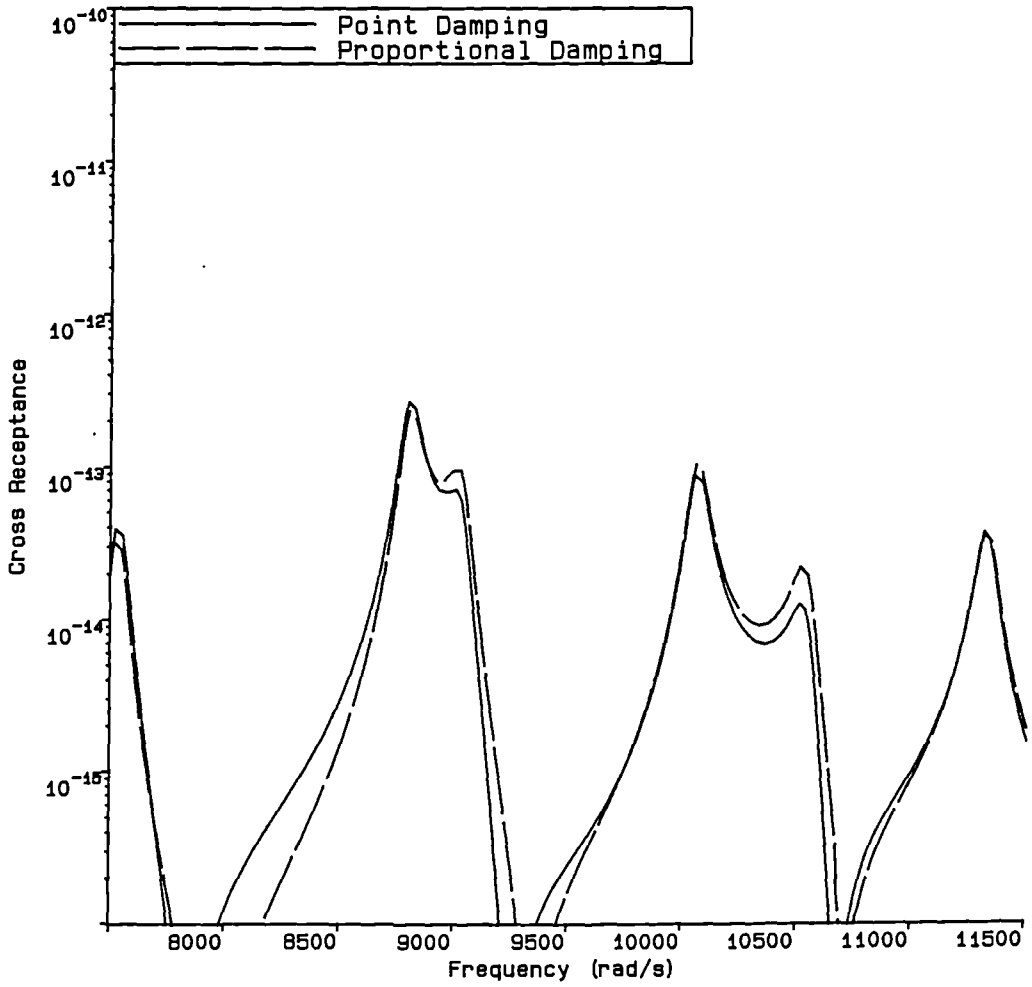

Figure 4.3 - Variation of H_{12} with frequency ω for cases 1 and 2 of Table 4.2.

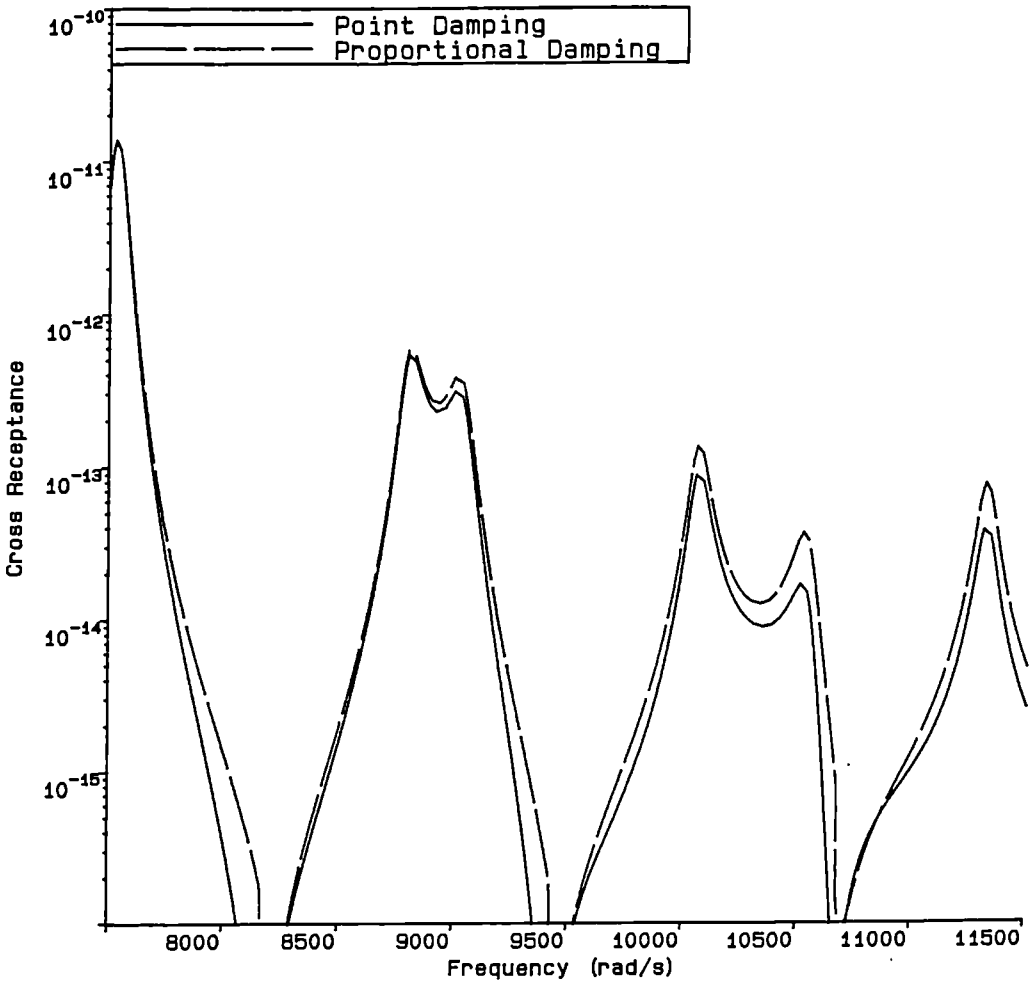

Figure 4.4 - Variation of H_{12} with frequency ω for cases 3 and 4 of Table 4.2.

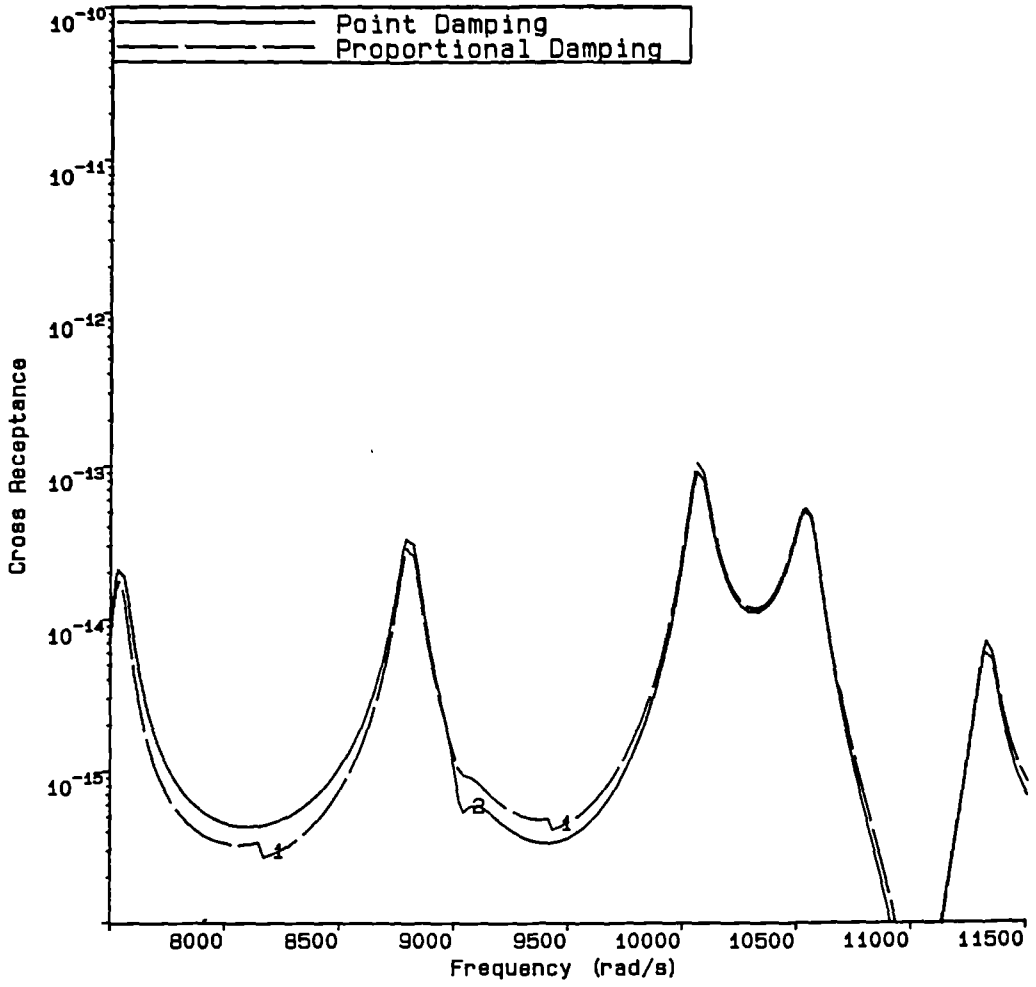

Figure 4.5 - Variation of H_{12} with frequency ω for cases 5 and 6 of Table 4.2. The regions of the curves marked 1 and 2 are discussed in the text.

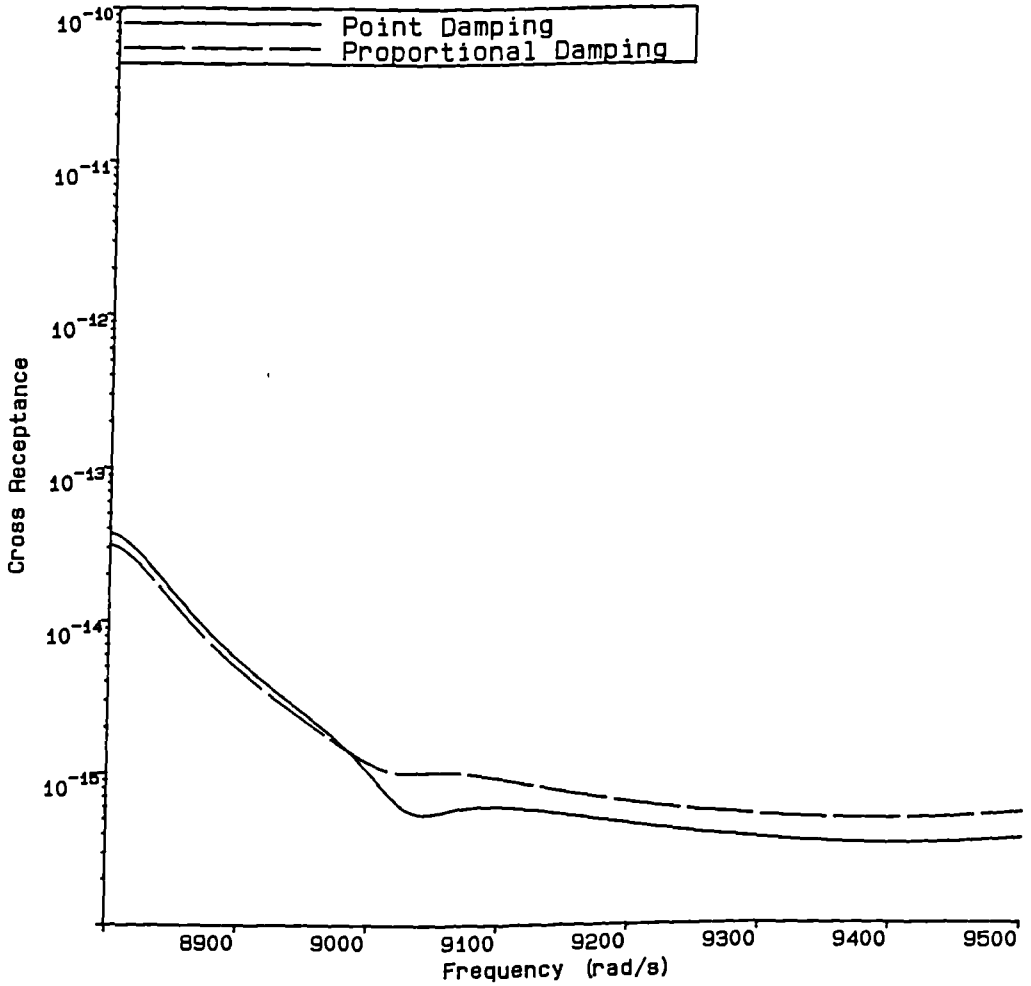

Figure 4.6 - Detail of the variation of H_{12} with frequency ω for cases 5 and 6 of Table 4.2, but with increased summation bandwidth $\omega_u - \omega_l$.

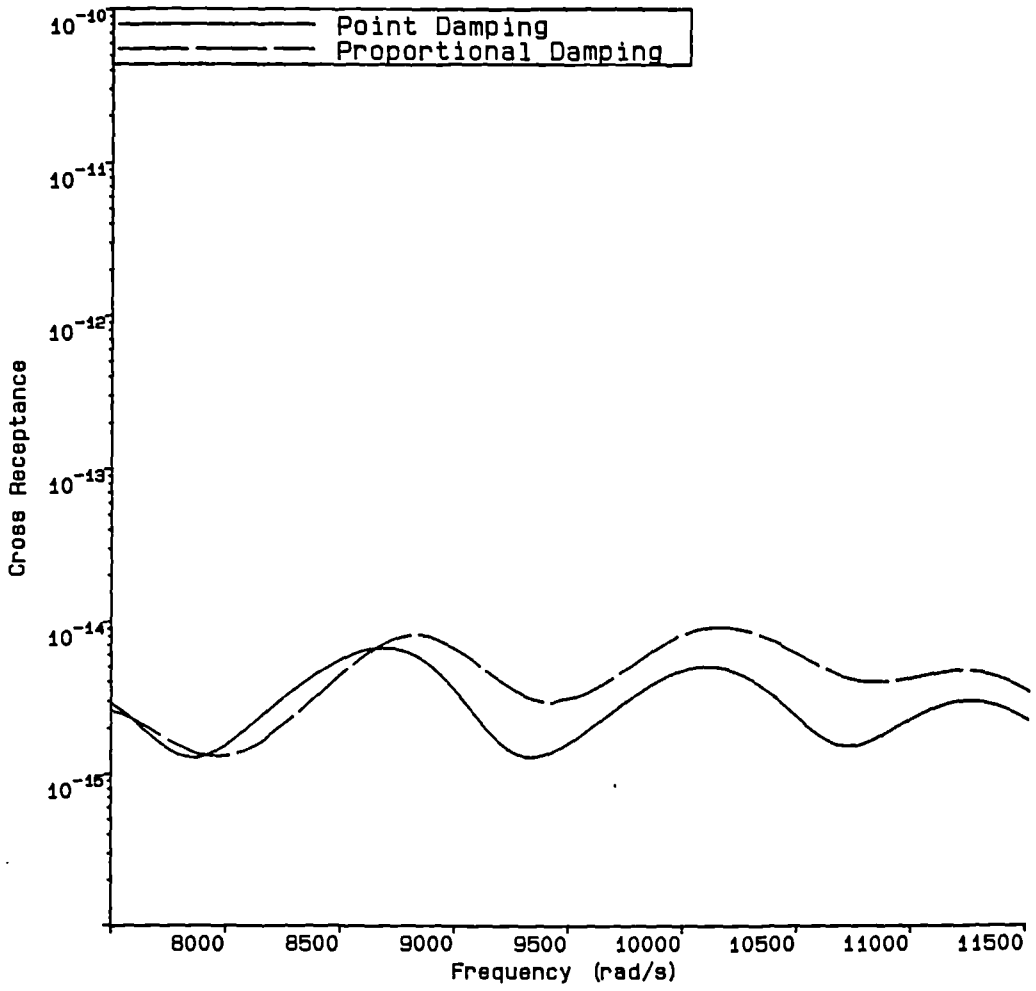

Figure 4.7 - Variation of H_{12} with frequency ω for cases 7 and 8 of Table 4.2.

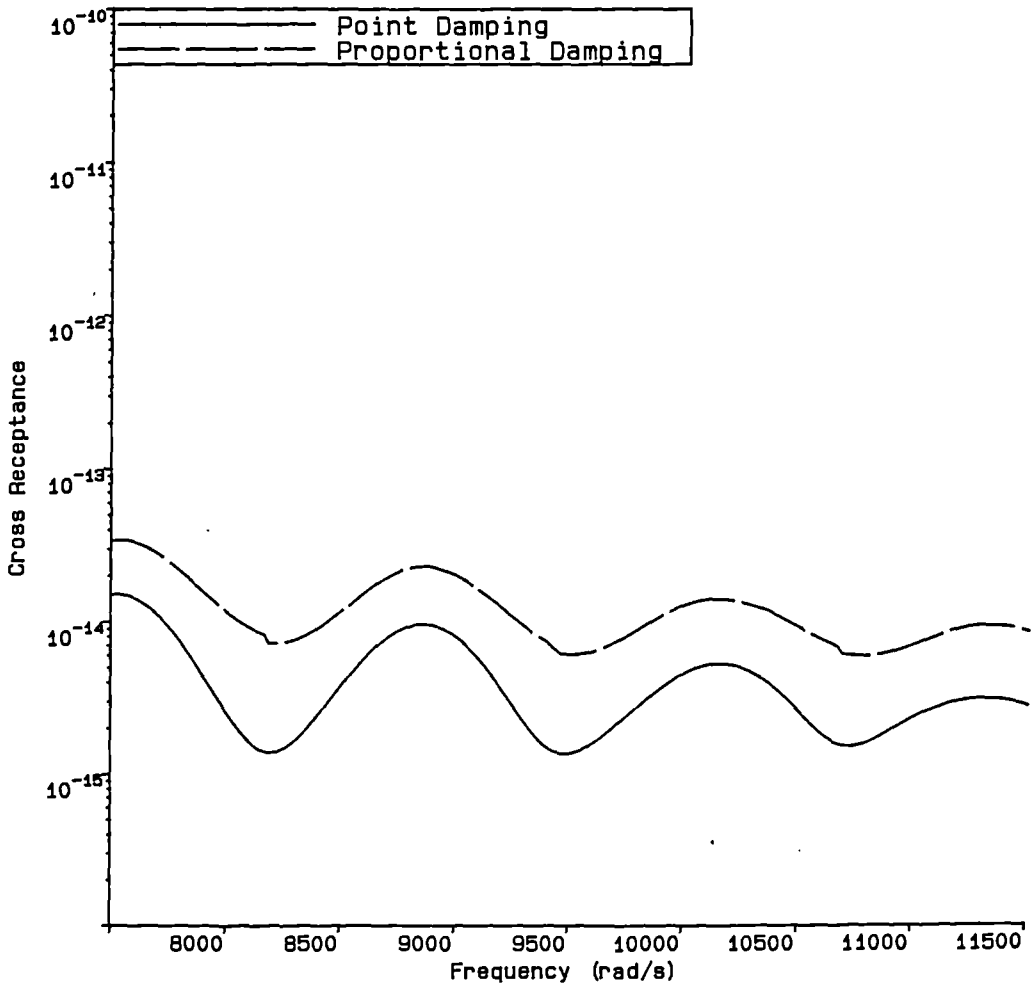

Figure 4.8 - Variation of H_{12} with frequency ω for cases 9 and 10 of Table 4.2.

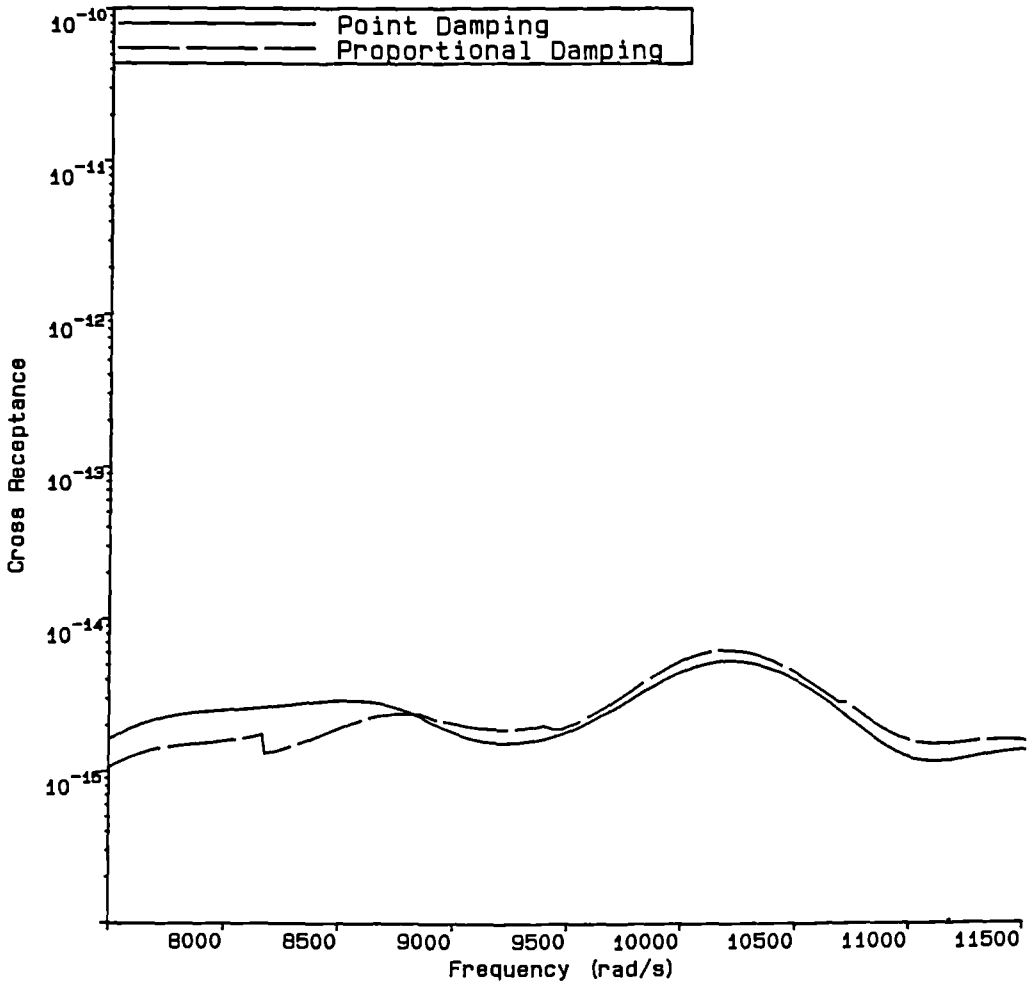

Figure 4.9 - Variation of H_{12} with frequency ω for cases 11 and 12 of Table 4.2.

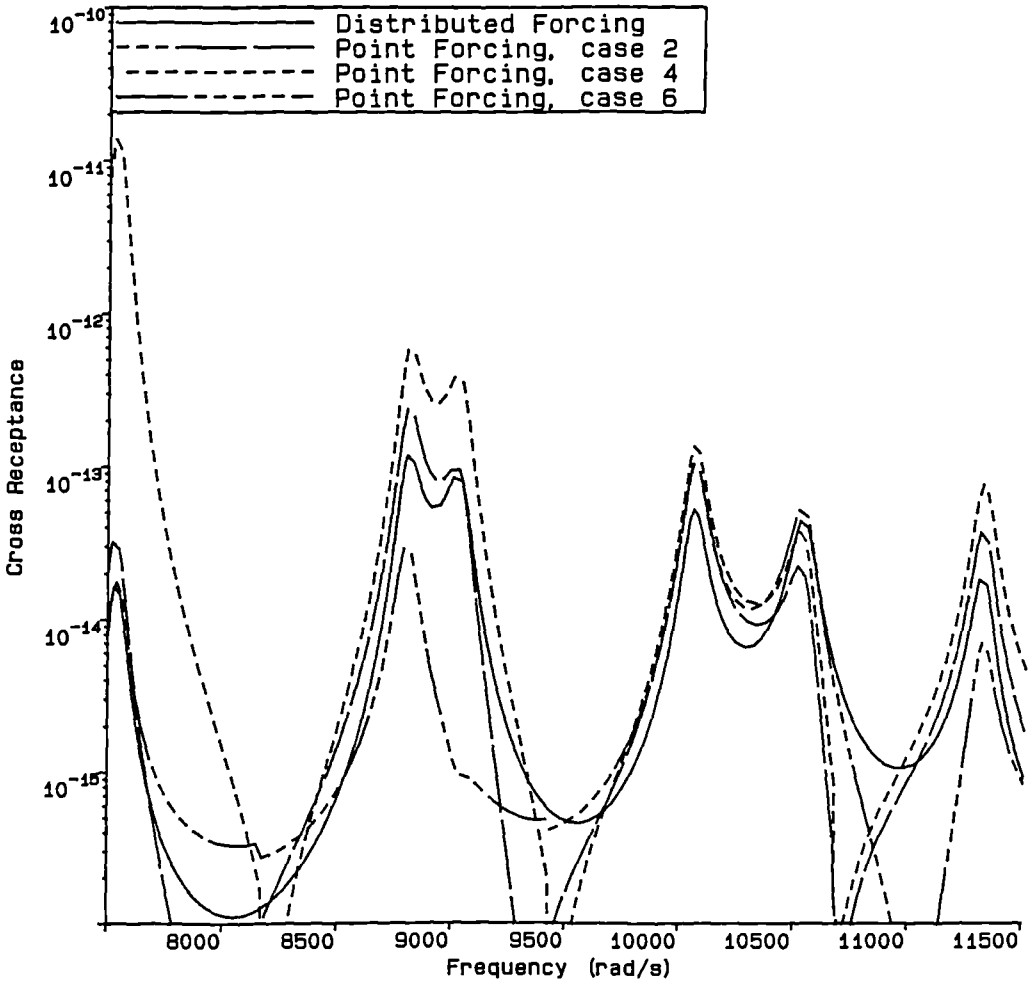

Figure 4.10 - Variation of H_{12} with frequency ω for cases 13, 2, 4 and 6 of Table 4.2.

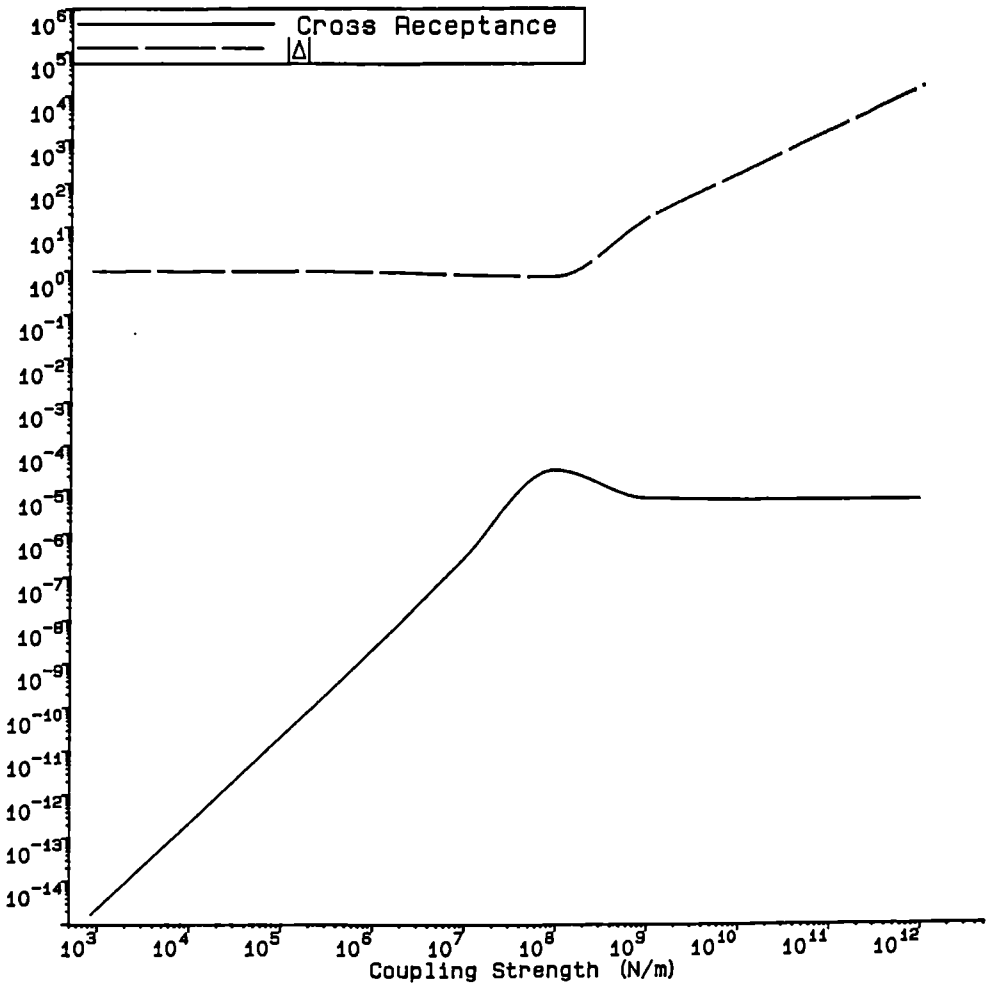

Figure 4.11 - Variation of H_{12} and Δ with coupling strength k_c at 5000 rad/s for case 14 of Table 4.2.

CHAPTER 5

Probabilistic Analysis of the Simple Example

5.1. Modifications to Include Random Parameters

SEA is concerned with the behaviour of ensemble average statistics. That is, any given deterministic system is considered to be one realisation taken from an infinite set of similar, but not identical systems. All the quantities of interest are then taken as averages across this ensemble, implying that integrations should be carried out with respect to the variables considered random; this much has been outlined in earlier chapters.

To apply this approach to the deterministic model of the previous chapter requires that random variables be identified and probability density functions ascribed to them. Simple SEA normally assumes that the sub-system natural frequencies should be handled in this way, that mode shape parameters should be ignored and that all other quantities should be considered deterministically. Some workers[22] have approximated this approach by integrating the energy flows of the deterministic model, with respect to the frequency at which the flow is taking place, over a bandwidth chosen to satisfy the various assumptions of Chapter 2. This average energy flow is not the same as given by the ensemble averaging technique in general. It is, however, very simple to apply to an otherwise deterministic model, and, as has already been noted, as the coupling strength and damping level tend to zero it converges to the ensemble average.

Clearly the most satisfactory way to generate an ensemble average response would be to specify the physical parameters of the system under study (i.e., lengths, masses etc.) in terms of probabilistic measures and create an ensemble of possible systems. Then analysing each in turn deterministically and summing their responses, the average could be formed by dividing by the number in the ensemble (i.e., a monte-carlo integration). This would map the statistics of the parameters varied into those of

natural frequencies and mode shapes in a complex but realistic fashion, an approach that is in the true spirit of SEA.

Such a process is, however, extremely time consuming and instead the usual SEA assumption is to prescribe the statistics of the natural frequencies and mode shapes directly, the frequencies being assumed evenly distributed in a given band width and the mode shapes parameters identically unity (i.e., as in section 4 of Chapter 3). This approach, which still involves monte-carlo integrations, but with simpler probability density functions, is adopted next to continue the study of the two rod model; the more rigorous approach of specifying only the statistics of physical measures of the sub-systems is reserved for a subsequent chapter. Note that either technique implies changes to the parameter values of the deterministic model, but that such changes remain unspecified if only the natural frequency statistics are given.

5.2. Comparison of Deterministic and Statistical Calculations

Before proceeding, the key limitation of *all* statistical models should be mentioned. If a particular pair of interacting sub-systems contains certain modes whose natural frequencies coincide with the frequency of interest, then anomalous results occur, distorting the ensemble averages. Clearly, very large energy flows would occur at such a frequency. The consequence is that, even if improved results are used in the main energy flow equations, there is no guarantee that the resulting relationships will be useful for the modelling of a particular system. This problem is especially severe in cases with few widely spaced modes. It is not that the *mean* energy flows calculated using SEA assumptions are fundamentally incorrect, but rather that problems occur because the mean is not a good indication of 'typical' behaviour and individual realisations may differ substantially from it at certain frequencies. It is clear that these differences tend to arise when individual modal frequencies of the sub-systems align with each other and the centre frequency. Clearly, they will be aggravated if such modes are lightly damped, and in such circumstances large responses will be inevitable. These possibilities will of course weight the mean response so that a 'typical' response at a given frequency will be below the

mean, whilst the odd rare member of the ensemble lies very far above it. When considering all frequencies in the overall bandwidth of interaction, a 'typical' member will give receptance spectra which lie below the mean at most frequencies and exceed it dramatically at a few special frequencies. The disposition of these peaks will vary from one ensemble member to the next and will be enormously large (resonant) in the rare configurations where modes of both sub-systems lie at the same frequency.

To see the previous point consider Figure 5.1, which shows the deterministic curve of $H_{12}(\omega)$ for case 13 of Table 4.2 (and Figure 4.10) together with those for $E[H_{12}(\omega)]$ resulting from using equations (3.40) and (3.47); i.e., it compares one possible ensemble member with two different forms of the average values. Notice that equations (3.40) and (3.47) give identical results here because the damping is light and the coupling weak; therefore the assumptions needed to simplify equation (3.40) to (3.47) are valid. It is of course the peaks in the deterministic curve that are of the most interest to design engineers seeking to remove resonances from frequency bands likely to be excited by external sources. In such circumstances SEA (or any other statistical model) based on uniformly probable natural frequencies is not a very helpful tool, irrespective of the accuracy of the calculations or validity of the other assumptions.

This problem of anomalous combinations has been addressed previously[41,42]. It was shown that if a 'typical' response is required in such circumstances, i.e., one that is not *'unduly affected by large contributions from rare anomalous configurations'*, then a geometric mean rather than an arithmetic mean may be more appropriate. This still does not help if a large response peak is thought likely to occur, and measures of its probable position and magnitude are sought. The idea of using geometric means as the basis for 'SEA like' analyses is not pursued further here although it is mentioned elsewhere[18].

It was noted in the previous chapter that heavy damping can assist in dealing with problems containing anomalous configurations, because then extremes of response are less likely. Figure 5.2, which is equivalent to Figure 5.1 but with a tenfold increase in damping strength, illustrates this point. Here the extreme peaks in the deterministic curve are no longer present and the averages are therefore better

measures of typical responses. Additionally, the curves for equations (3.40) and (3.47) now show significant differences, because the presence of heavy damping invalidates some of the assumptions leading to equation (3.47).

To complete this study of the two rod model, not only will the natural frequencies be considered random, but additionally the number of modes per unit of frequency (the modal density) will be allowed to vary. Both these changes give rise to variations from the parameters detailed in Table 4.1; however, the analysis is still based on incoherent forcing of sub-system 1 combined with light proportional damping and coupling of varying strength at arbitrary interior points, i.e., case 14 of Table 4.2.

5.3. Analysis of Integral Equations for Variations in Coupling Strength

Using all the assumptions leading up to equations (3.37) and (3.38), these equations will next be studied *without* assuming that Δ is unity. They are repeated here for convenience

$$E[H_{11}(\omega)] = \int_{\omega_l}^{\omega_u}\cdots\int_{\omega_l}^{\omega_u}\left[\frac{\omega^2 c_1}{m_1}\sum_{i=1}^{N_1}\left[1/|\phi_i|^2\right] + \frac{\omega k_c}{m_1^2}\mathrm{Im}\left\{\sum_{i=1}^{N_1}\left[1/\phi_i{}^2\Delta\right]\right\}\right]\frac{d\omega_{i=1}\cdots d\omega_{i=N_1}\,d\omega_{r=1}\cdots d\omega_{r=N_2}}{(\omega_u-\omega_l)^{N_1+N_2}} \tag{5.1}$$

and

$$E[H_{12}(\omega)] = \int_{\omega_l}^{\omega_u}\cdots\int_{\omega_l}^{\omega_u}\left[\frac{\omega^2 k_c^2 c_2}{m_1^2 m_2 |\Delta|^2}\sum_{i=1}^{N_1}\left[1/|\phi_i|^2\right]\sum_{r=1}^{N_2}\left[1/|\phi_r|^2\right]\right]\frac{d\omega_{i=1}\cdots d\omega_{i=N_1}\,d\omega_{r=1}\cdots d\omega_{r=N_2}}{(\omega_u-\omega_l)^{N_1+N_2}} \tag{5.2}$$

Integrals of this form are discussed in Appendix D, in which two particular cases are investigated. The first is that of individual sub-systems which both contain only one interacting mode, together with infinite coupling strength, and the second, that when either the coupling is weak or the number of interacting modes very large. In the first case (Appendix D.1), if the two sub-systems have broadly similar characteristics, equation (5.1) becomes

$$E[H_{11}(\omega)] = \frac{\omega}{2(\omega_u-\omega_l)^2\sqrt{m_1 m_2}}\left[\cos^{-1}\left[\frac{\omega_l}{\omega}\sqrt{\frac{m_1}{m_1+m_2}}\right]-\sin^{-1}\left[\frac{\omega_l}{\omega}\sqrt{\frac{m_2}{m_1+m_2}}\right]\right] \quad (5.3)$$

$$\times\left[\tan^{-1}\left[\left[\frac{\omega_u^2-\omega^2}{\omega}\right]\left[\frac{m_1+m_2}{m_1c_1+m_2c_2}\right]\right]-\tan^{-1}\left[\left[\frac{\omega_l^2-\omega^2}{\omega}\right]\left[\frac{m_1+m_2}{m_1c_1+m_2c_2}\right]\right]\right]$$

Note that if the sub-systems have markedly different masses or damping constants, this equation is not appropriate and then the two-dimensional integration discussed in the appendix must be carried out numerically. Irrespective of the sub-system characteristics equation (5.2) reduces to

$$E[H_{12}(\omega)] = \{m_2c_2/(m_1c_1+m_2c_2)\}E[H_{11}(\omega)] \quad (5.4)$$

Substitution of this expression into equation (3.7) results in the constant K_1 being infinite, as expected when assuming infinite coupling strength. Note that for identical sub-systems equation (5.4) indicates that $E[H_{12}]$ is exactly half $E[H_{11}]$, so that if only one of the (identical) sub-systems is excited they both must dissipate equal energies and therefore have identical energy levels. Substituting equation (5.4) into equations (3.1)-(3.6) reveals that the energy levels are in fact proportional to the sub-system masses, as expected.

In the second case (Appendix D.2), when either the coupling is weak or the number of interacting modes very large, equations (3.37, 5.1) and (3.38, 5.2) respectively become

$$E[H_{11}(\omega)] = (\omega^2 c_1 N_1/m_1)E[1/|\phi_i|^2] + (\omega k_c N_1/m_1^2)\mathrm{Im}\{E[1/\phi_i^2]/E[\Delta]\} \quad (5.5)$$

$$E[H_{12}(\omega)] = (\omega^2 k_c^2 c_2 N_1 N_2/m_1^2 m_2)E[1/|\phi_i|^2]E[1/|\phi_r|^2]/|E[\Delta]|^2, \quad (5.6)$$

where

$$E[\Delta] = 1 + (k_c N_1/m_1)E[1/\phi_i] + (k_c N_2/m_2)E[1/\phi_r]. \quad (5.7)$$

Here the expected values of the functions ϕ_i and ϕ_r are the same for all members of the previous summations and are simply multiplied by the number of terms in the sums. They are given by the somewhat complicated expressions already discussed and detailed in Appendix B. Notice that even these simplified forms still involve the parameter Δ which is dropped from the traditional SEA results such as equation (3.47).

No general result has been obtained for the case of moderate to strong coupling with few interacting modes. However, a parameter v may be constructed having the form

$$v = \frac{\left\{ 1/k_c + (N_1-1)\,|\,1/\phi_i\,|_{min} + (N_2-1)\,|\,1/\phi_r\,|_{min} \right\}}{\max(\,|\,1/\phi_i\,|_{max}\,,\ |\,1/\phi_r\,|_{max})} \tag{5.8}$$

where a minimum value is obtained by setting all the ω_i and ω_r to ω_u and a maximum by setting them to the frequency of interest ω. This parameter is a good measure of the range of applicability of equations (5.5) and (5.6) and measures the effect of a single mode whose natural frequency coincides with the centre frequency of interest, when compared with that of all the others, under the assumption that they all have natural frequencies on the boundary of the frequency bandwidth in use. This is, of course, the worst case situation of one mode dominating the entire response of both sub-systems. The parameter v also includes the coupling spring strength, so that the effects of individual modes are weighted by this relative coupling strength. In terms of the mathematics given in the Appendix D.2 the series expansions used converge rapidly when v is large (>>1), whilst when it is small (≤1) the analysis fails (but equations (5.3) and (5.4) apply when v is zero). This change in the behaviour of the integrals is not the same as the physical transition from 'weakly' to 'strongly' coupled behaviour of the actual sub-systems. This will be seen by contrasting it with the parameter $|\Delta|$, which has already been used to classify strong and weak coupling. (See also reference[43], in which the work in reference[40] was extended to analyze the response of strong, fluid-structure interactions, but which required high modal densities.)

5.4. Monte-Carlo Integration

Figure 5.3 shows the results of using monte-carlo integration techniques directly on equation (3.38, 5.2) at a fixed frequency of 5000 rad/s (796 Hz) with a bandwidth of 8796 rad/s (1.4 kHz). This shows variations of $E[H_{12}(\omega)]$ as the number of interacting modes and coupling strength vary, in the form of a contour plot. This figure again shows quite clearly the two regimes of 'weak' and 'strong' coupling discussed in the previous chapter. Figure 5.4 shows a similar plot that results from use of the

approximations inherent in equations (5.5) and (5.6). Because of the presence of Δ in the denominator of these expressions this figure still shows a limiting value for $E[H_{12}(\omega)]$, whatever the value of the coupling strength, a feature that is completely absent from the traditional SEA results like equation (3.47). Note that in both these plots the mode counts N_1 and N_2 have been kept equal, but similar trends are observed when they are varied independently.

The curves of $\nu = 1$ and $|\Delta| = 2$ are also included in these plots. It may be seen that $|\Delta|$ is indeed a good measure of the transition from 'weakly' to 'strongly' coupled behaviour and its formulation reveals the effect of coupling spring strength and mode count on the interaction of the sub-systems. More interesting, however, is the area of the plots for which ν is large, the lower right-hand part, indicating the region where equations (5.5) and (5.6) are valid and therefore Figures 5.3 and 5.4 are the same. This region roughly aligns with the transition between coupling strengths when the interacting sub-systems have few modes. However, when there are sufficiently many modes, ν is large whatever the level of coupling strength. These results suggest that the important parameter in assessing the applicability of SEA is not the coupling strength but the proportion any particular mode can contribute to the interaction of the overall sub-systems.

To summarize, if one mode can dominate the interaction when its natural frequency takes a particular value, then when an ensemble average is formed this event will occur and distort the average considerably. This particular ensemble member may be said to be 'anomalous'. Conversely, if there are many modes then no one mode can dominate the picture, and so an ensemble average will indicate typical behaviour. The upshot of this is that equations (5.5) and (5.6) hold for all systems where an ensemble average (and therefore SEA) is a useful measure (as indicated by ν) and break down when individual modes can dominate the response. Nonetheless, for completeness, the approach described in the next section attempts to provide an empirical method for calculating the receptances in all these circumstances.

5.5. Empirical Method for Estimating Receptances

As has been noted, no generally applicable simple expression can be given for either direct or cross-receptances in this study. However, since values for the receptances can be readily found for extremes of v, a semi-empirical method can be developed. The cross-receptances are considered first, since they are the most badly behaved functions, as might be expected.

The cross-receptance, $E[H_{12}(\omega)]$, is modelled by using equation (5.6) to give an estimated value, $E[H_{12}(\omega)]_{est}$, to which a correction factor is applied,

$$E[H_{12}(\omega)] = E[H_{12}(\omega)]_{est}\left\{1+\left\{\left.\frac{E[H_{12}(\omega)]}{E[H_{12}(\omega)]_{est}}\right|_{N_1=1=N_2,\,1/k_c=0}-1\right\}G(\mathrm{v})\right\} \tag{5.9}$$

where $G(\mathrm{v})$ is some unspecified function. Equations (5.3) and (5.4) are used to provide the expression for the exact value of $E[H_{12}(\omega)]$ at $N_1 = 1 = N_2$ and $1/k_c = 0$. (If the sub-system parameters are extreme, the numerically evaluated integral of equation (D.8) is used in place of equation (5.3).) If equation (5.9) is rearranged and an analysis carried out by using a full monte-carlo integration to calculate a series of exact values of $E[H_{12}(\omega)]$ for the example, this correction factor can be examined as a function of v. For zero or infinite v, equations (5.4) and (5.6) hold, respectively, and the function $G(\mathrm{v})$ tends to unity and zero at these limits. This suggests a representation of the function using an approximation of the form

$$G(\mathrm{v}) = e^{-p\mathrm{v}} \tag{5.10}$$

where p is some unspecified constant. A least-squares regression of the exact form of the function versus this approximation, over the range of interest, gives a value of 0.8 to the constant p, with remarkably small deviations. The data given in Figure 5.5 illustrates this analysis with some two hundred individual monte-carlo integration results shown together with the simple exponential. In this figure the monte-carlo points are divided into the following three groups:

(1) those with infinite coupling strength ($1/k_c = 0$) and with varying mode counts (N_1 and N_2),

(2) those with varying k_c, N_1 and N_2, but with N_1 kept equal to N_2,

(3) those with varying k_c and N_1, but with N_2 held fixed at an intermediate value of 10.

(Note that the value of p of 0.8 indicates that the halfway point between equations (5.4) and (5.6) occurs when v is 0.9). Substitution of the previous result into equation (5.9) gives

$$E[H_{12}(\omega)] = E[H_{12}(\omega)]_{est}\left\{1+\left\{\left.\frac{E[H_{12}(\omega)]}{E[H_{12}(\omega)]_{est}}\right|_{N_1=1=N_2,\,1/k_c=0}-1\right\}e^{-0.8v}\right\} \tag{5.11}$$

which may be used for all values of v. This equation is illustrated in Figure 5.6 by a contour plot of $E[H_{12}(\omega)]$ based on equation (5.6) with the correction applied. Since this figure was produced in one hundredth of the time taken for the exact solution shown in Figure 5.3, the agreement is rather encouraging. Of course, this analysis has been carried out for a particular example but, because of its derivation, the analysis leading to equation (5.11) should not be significantly in error in other systems involving point coupling of multi-modal systems.

A similar analysis for $E[H_{11}(\omega)]$ leads to

$$E[H_{11}(\omega)] = E[H_{11}(\omega)]_{est}\left\{1+\left\{\left.\frac{E[H_{11}(\omega)]}{E[H_{11}(\omega)]_{est}}\right|_{N_1=1=N_2,\,1/k_c=0}-1\right\}e^{-0.8v}\right\} \tag{5.12}$$

and the receptances for sub-system 2, $E[H_{22}(\omega)]$ and $E[H_{21}(\omega)]$, are again obtained by interchanging the subscripts. Notice however that, when the two sub-systems contain more than two or three modes, the expression for $E[H_{11}(\omega)]$ is dominated by the first summation in equation (3.20), which represents the uncoupled behaviour. Even when there is only one mode within a sub-system, the two summations are at most of equal magnitude, *whatever* the coupling strength, provided the sub-system masses do not differ greatly. This implies the correction factor has relatively little impact on the value of $E[H_{11}(\omega)]$; it is therefore not sensitive to the choice of the parameter p and in most cases may be safely omitted.

All these results may then be substituted into equations (3.7) and (3.8) to produce the two coefficients which can be used in the fundamental SEA result of equation (3.5) for all coupling

strengths and mode counts. Although clumsy, this method gives an expression that is exactly correct when the sub-system behaviours are not dominated by any one individual mode at one extreme, or when the coupling is infinitely strong compared with the mode count at the other (i.e. ν is infinity or zero respectively). It involves using expressions for the receptances that retain the quantity Δ and at the same time includes a correction factor to allow for the statistical simplifications adopted. It is approximately correct for all values of k_c, N_1 and N_2, the approximation being well behaved even in the transition between weak and strong coupling, at least for the case of uniform modal density and minimal mode shape coherence.

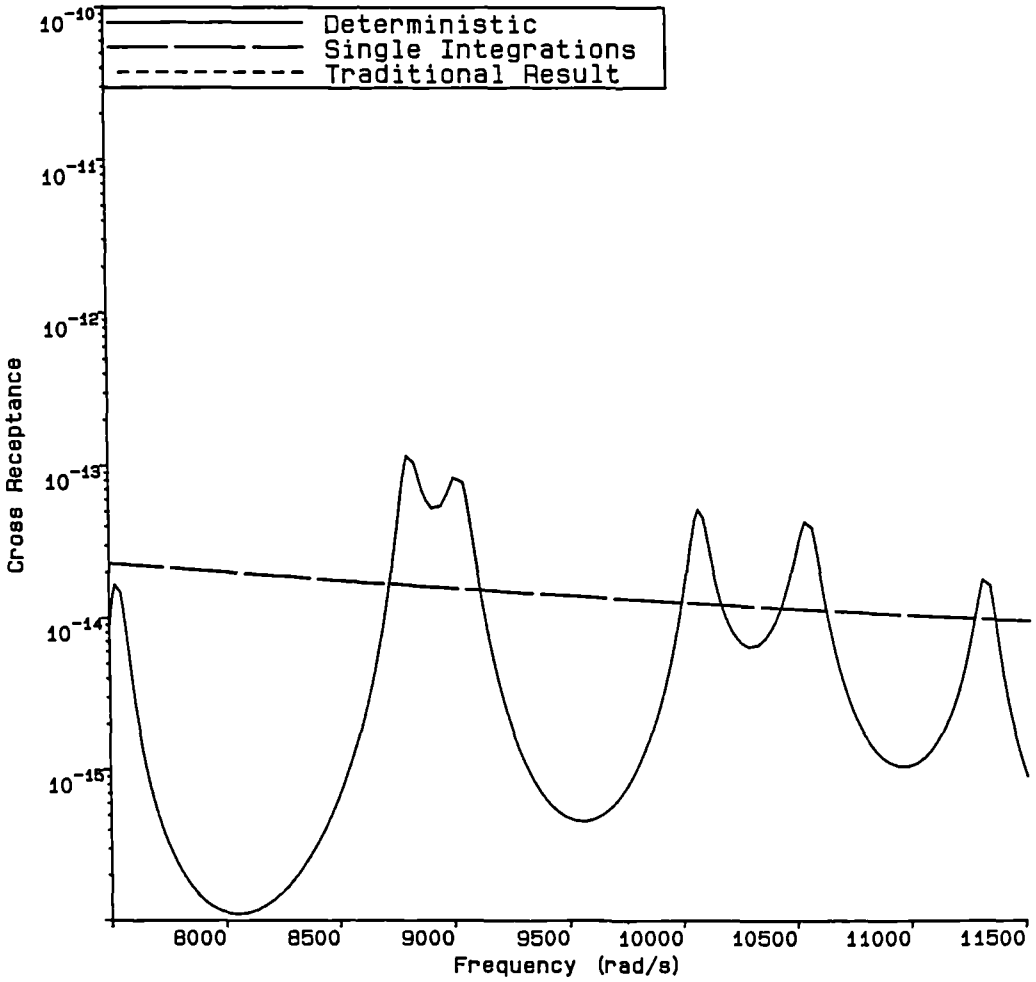

Figure 5.1 - Variation of H_{12} and $E[H_{12}]$ with frequency ω for case 13 of Table 4.2. Traditional and single integration results coincide.

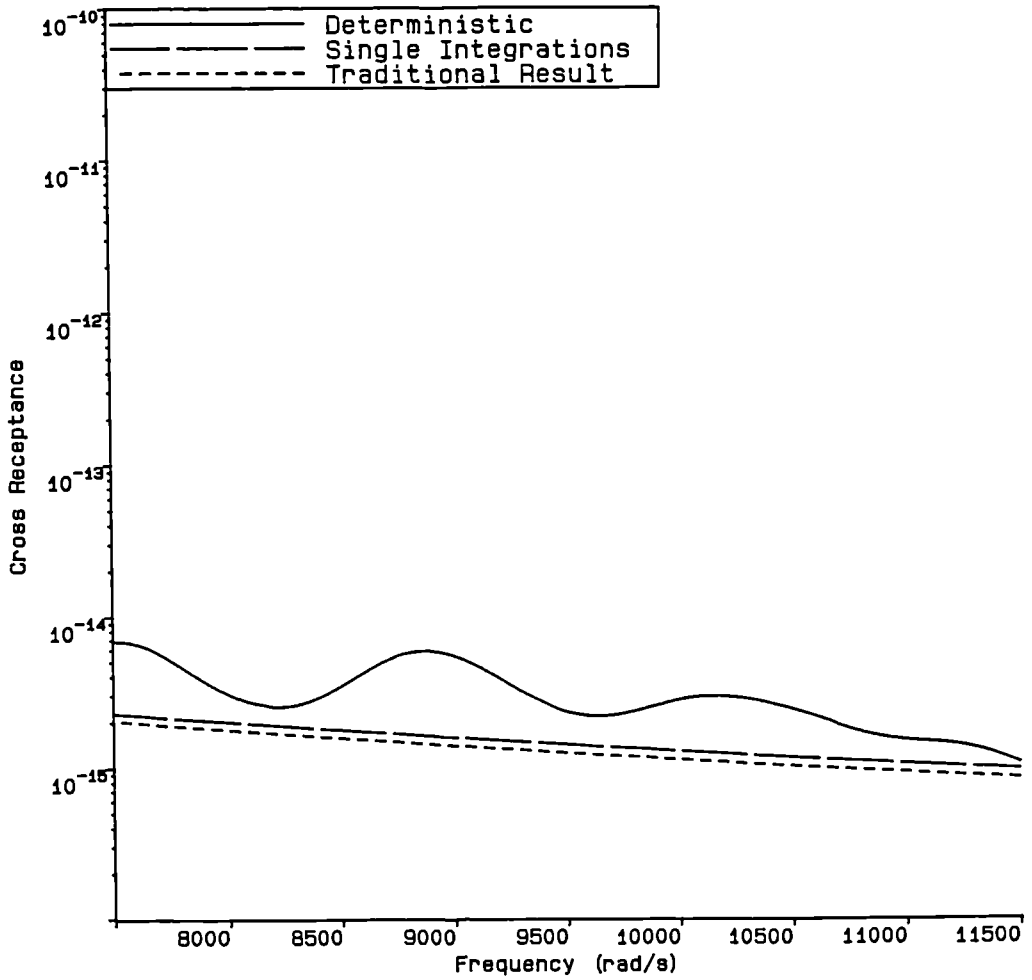

Figure 5.2 - Variation of H_{12} and $E[H_{12}]$ with frequency ω for case 13 of Table 4.2, but with tenfold increase in damping strength.

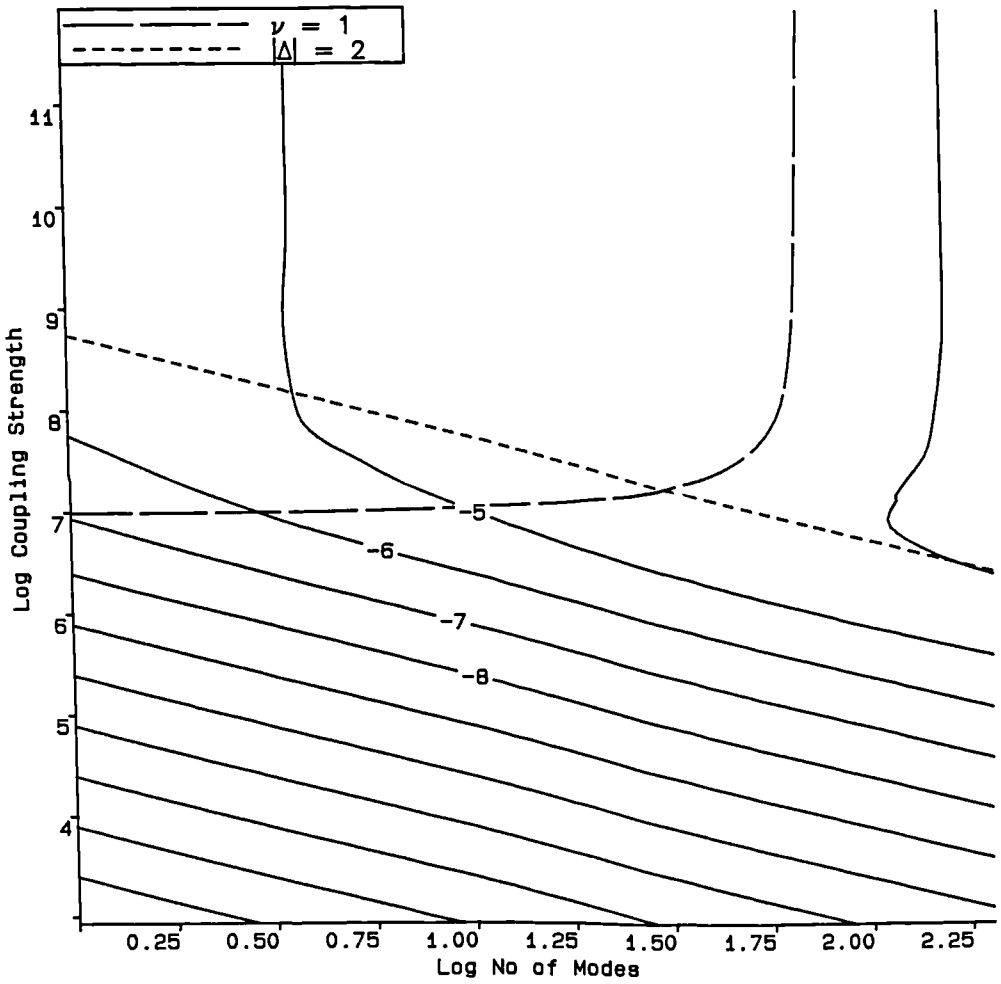

Figure 5.3 - Variation of $E[H_{12}]$ with coupling strength k_c and mode counts N_1,N_2 for case 14 of Table 4.2 calculated using monte-carlo techniques.

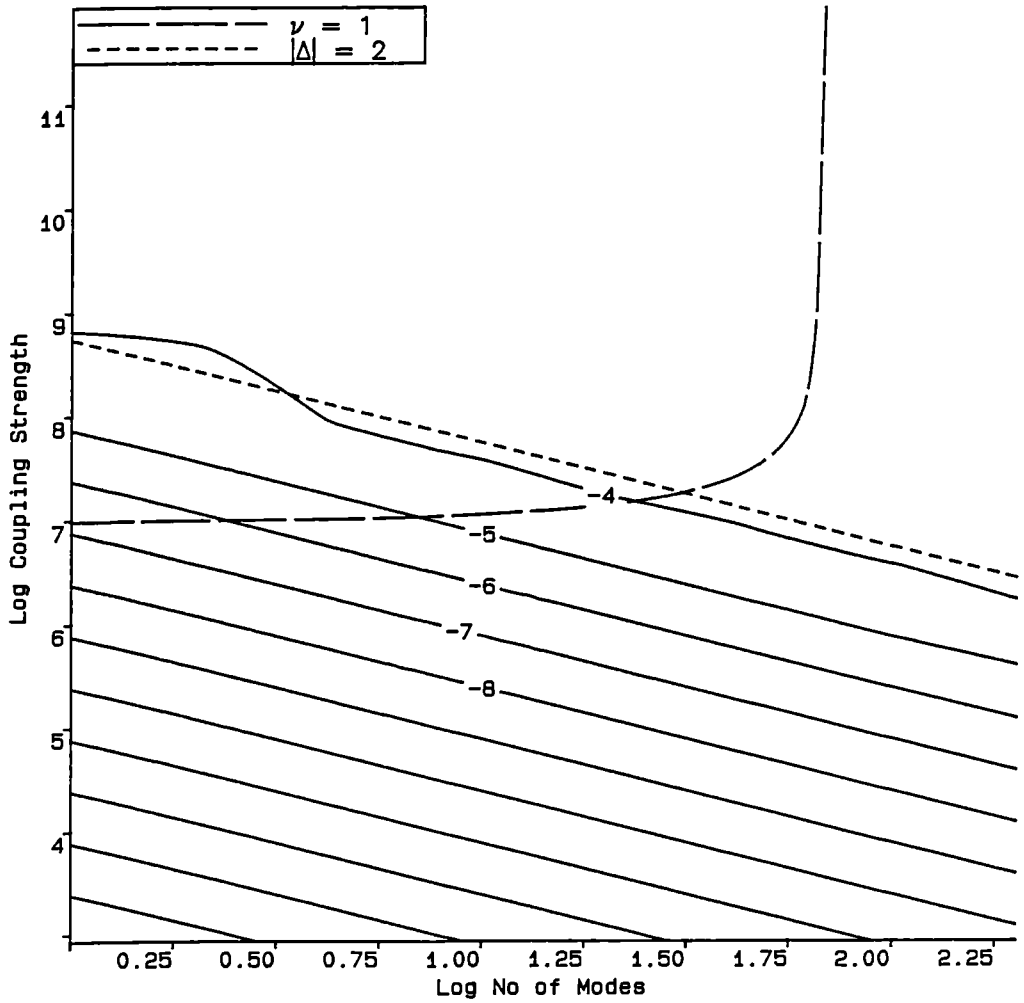

Figure 5.4 - Variation of $E[H_{12}]$ with coupling strength k_c and mode counts N_1,N_2 for case 14 of Table 4.2 calculated using the approximations inherent in equations (5.5) and (5.6).

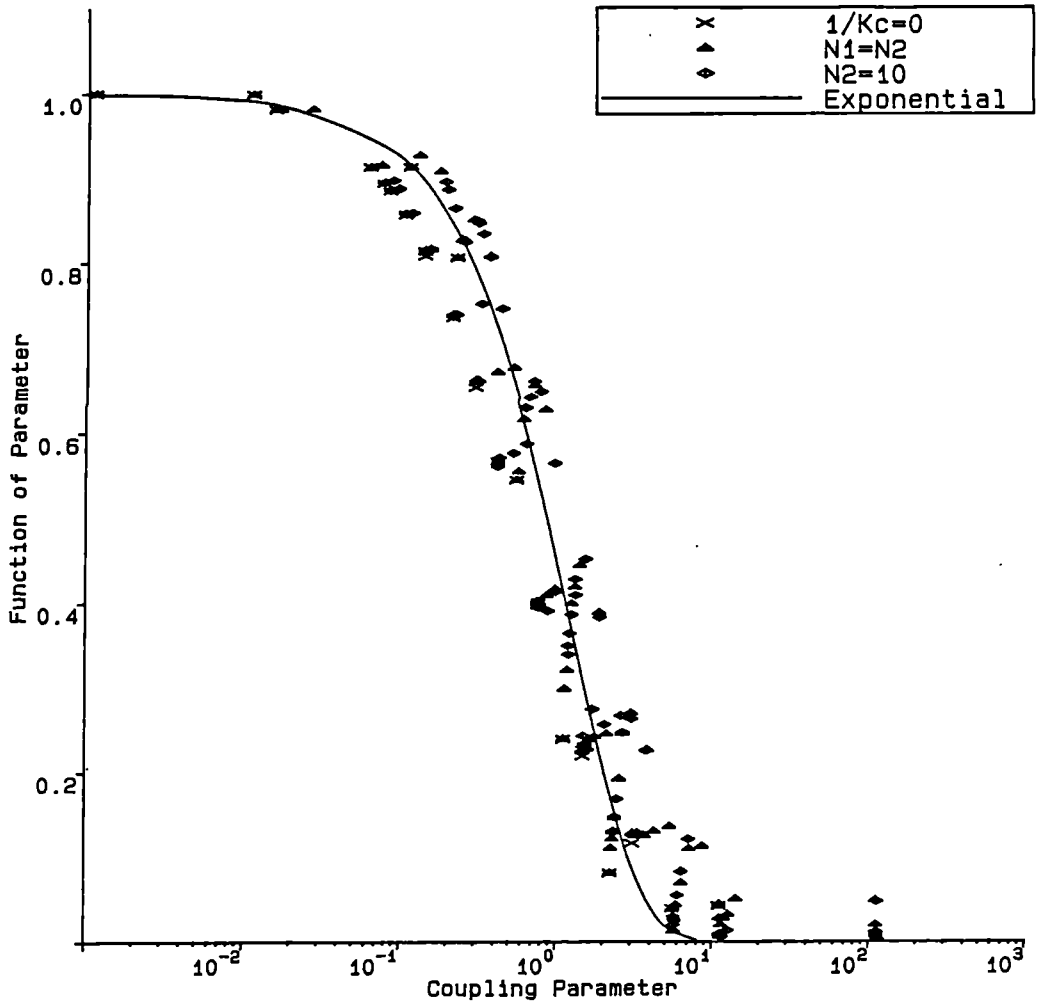

Figure 5.5 - Variation of $G(\nu)$ with coupling strength k_c and mode counts N_1,N_2 for case 14 of Table 4.2 calculated using monte-carlo techniques.

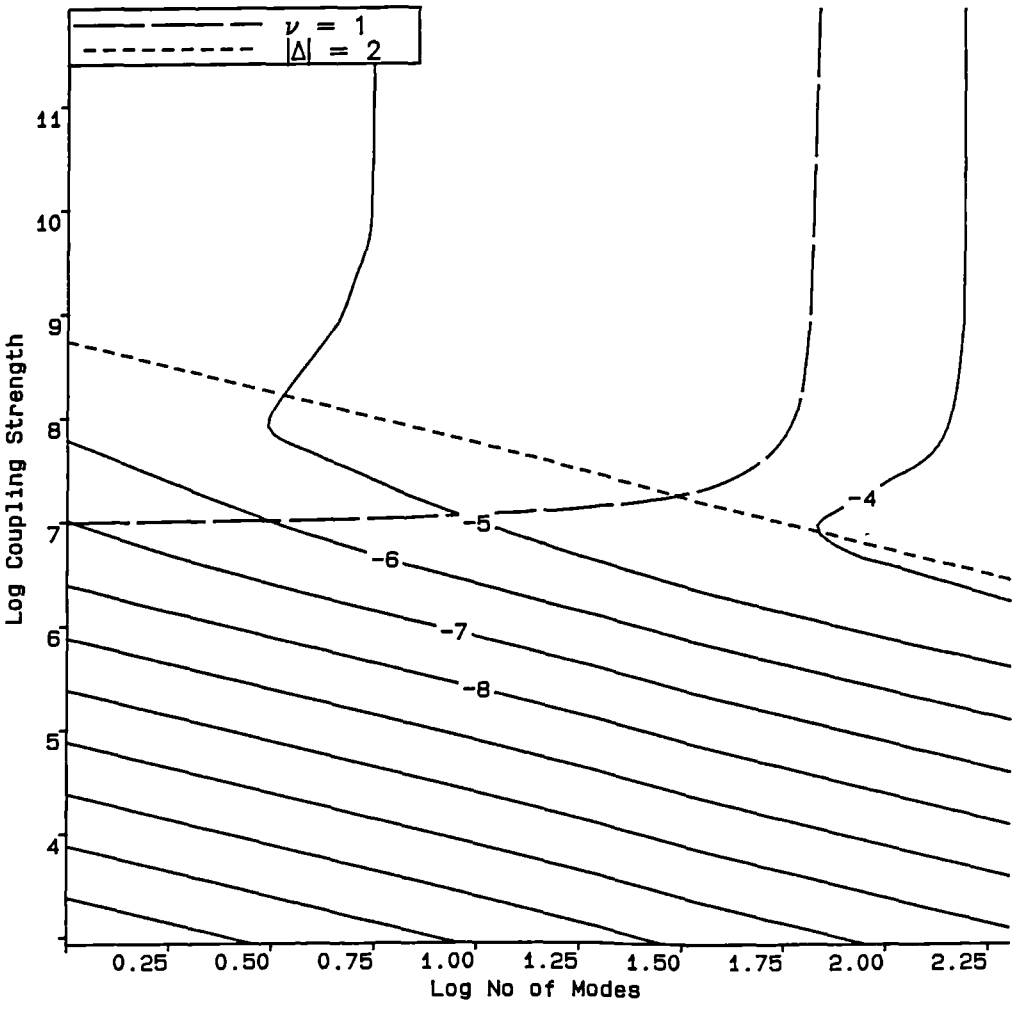

Figure 5.6 - Variation of $E[H_{12}]$ with coupling strength k_c and mode counts N_1,N_2 for case 14 of Table 4.2 calculated using the strong coupling correction.

CHAPTER 6

The Statistics of Random Systems

6.1. Probability Density Functions (PDFs) of Natural Frequencies

As has already been noted, SEA describes systems with random physical parameters by directly specifying the statistics of the sub-system natural frequencies and mode shapes. The fact that the chosen statistics are rather crude greatly simplifies the theory of SEA, but casts doubt on its ability to reflect accurately the behaviour of some problems of interest. Therefore the derivation of more realistic models will be discussed next. This will lead on to an improved method for applying SEA to one major class of engineering structures, i.e., those exhibiting some kind of geometrically periodic variation in properties.

It is possible to study deterministic systems using probabilistic tools. The probability density functions (PDFs) for deterministic parameters are just Dirac delta functions positioned at the prescribed parameter values, i.e., the probability of the parameter being other than its prescribed value is everywhere zero. Under such circumstances the ensemble average integrations, like those of section 3.4, simply collapse to the relevant deterministic results. This leads to the conclusion that sub-systems which have relatively little scatter in their parameter values should be modelled by PDFs that are not dissimilar to the Dirac delta, e.g., a Gaussian distribution with very small standard deviation. Now if a sub-system with exactly average parameters gives rise to a particular set of natural frequencies, it may seem reasonable to assume that if the deviations of the parameters from their means are slight, so also will be the deviations of the natural frequencies from those of this average sub-system. Clearly, as the deviations tend to zero, not only do the PDFs of the parameters tend to Dirac deltas, so also do those of the natural frequencies, which are just a derived function.

This is not the whole story however; although the variations in any number of physical parameters may be considered statistically independent, those of the associated natural frequencies are certainly not. It is a common experience among vibration engineers that while the first few natural frequencies of any particular structure may show predictable changes when the structure is modified, the high frequencies behave rather chaotically. Nonetheless, it is a very broad-brush approach to adopt the usual SEA procedure and model all the modes of a structure by a single uniform PDF. So, to avoid this problem, a correct application of SEA restricts its use to a range of frequencies where this model is reasonable. This requires that the range is set high enough that only the 'chaotic' modes are included. To compensate for this restriction, the first few modes may perhaps be dealt with using finite elements or some other deterministic technique. However, this leaves an intermediate frequency range where a more sophisticated approach is called for.

If some method can be proposed to predict the likely natural frequencies of a structure in this intermediate range, a non-uniform PDF could be constructed and used in SEA. It is to be expected that such a PDF would show the transition from fairly predictable natural frequencies at low frequencies to the 'chaotic' (and therefore uniformly probable distribution of) frequencies at high frequencies. Clearly the application of such PDFs to SEA may not be easy, given the great simplifications that arose in the theory of Chapters 2 and 3 upon adopting uniform frequency PDFs, but the resulting improvements in the approach should justify the effort. First however a mechanism for producing the frequency PDFs must be established. As might be expected, the greater the realism of these PDFs, the more tedious is their construction.

Leaving aside practical testing of real structures (which lies outside the scope of this thesis), at least three approaches can be visualized. First, numerical experiments might be carried out on a number of similar sub-systems to establish their natural modes. These could then be analysed to see if any underlying trends were present. Such experiments would be made in the form of a sequence of deterministic calculations. This method follows in the spirit of SEA, but is normally extremely tedious; nonetheless it offers a standard for comparison. Secondly, a finite element model could be

constructed which may then be solved repeatedly with minor modifications chosen to reflect the uncertainty in the system under study. This is essentially a sensitivity analysis and is the finite element analyst's version of repeated experiments. (It is a debatable point as to how often such sensitivity studies are actually carried out in commercial usage of F.E. models, particularly for changes in the *parameter*, as opposed to *meshing*, details).

Thirdly, and perhaps most powerfully, the structure under investigation could be studied to see if its physical properties conveyed any information regarding its likely natural frequencies. At first sight such an approach appears extremely unlikely to be workable. However, if the structure under study exhibits some underlying pattern such that it can be divided into a number of identical elements that reoccur in some geometrically periodic fashion, considerable progress may be possible. This idea leads into the study of periodic systems, which are well known to exhibit the phenomena of 'pass' and 'stop' bands, which group the natural frequencies together in a predictable way. This feature holds out the prospect of a very efficient means of constructing PDFs to describe the natural frequencies of such systems. Of course, most engineering structures are not perfectly periodic, either because of design decisions or the uncertainties inherent in manufacture. As might be expected, such deviations complicate the periodic approach but, as will be shown in subsequent chapters, they do not render it unworkable. The fact that periodic designs are central to most modern engineering structures indicates that such an approach may be of broad applicability.

6.2. Probability Density Functions of Mode Shapes

Mode shapes, and in particular their values in the region of driving or coupling points, form the other group of statistically modelled terms within SEA. Here the statistics usually adopted are extremely crude, it being assumed that ψ^2 is everywhere unity! The effect of this assumption has been explored in earlier chapters, where biases in the resulting energy flows were observed. Clearly some improvement in the modelling of this aspect would be desirable.

In principle, an exactly similar approach to that just mentioned for natural frequencies could be adopted. However, it turns out that no obvious pattern can be discerned in the resulting PDFs, even in the case of exactly periodic systems. In fact, in some cases the mode shapes of periodic structures with slight defects show extreme variations which arise from very subtle causes, a point discussed later. The only general trend observed is that the range of possible mode shape amplitudes at any given point gets larger as the higher modes are considered. It is indeed fortunate that the mode shape parameters do not play a dominant role in the various energy flow equations.

6.3. The Application of Non-Uniform PDFs in Statistical Energy Analysis

Assuming that more realistic, but non-uniform, PDFs can be constructed to model the disposition of natural frequencies and mode shapes for a sub-system, some way must be found of incorporating this information into SEA. This is very simple when carrying out full monte-carlo integrations of the complete multi-dimensional integrals like that of equation (3.36). Such integrations are performed by constructing ensembles of typical systems which are then analysed and the results averaged. If the desired PDF of natural frequency or mode shape (or any other parameter) is non-uniform, all that must be done to model these variables is that the random numbers used in the integration should be biased to conform to the given PDF. Indeed, if the chosen PDF has been constructed by solving for the natural modes of an ensemble of structures with random parameters, it is hardly more trouble to use these results directly, giving an 'exact' answer with which more limited approaches may be compared. Additionally, this 'exact' approach also correctly reproduces any statistical correlation between the mode shapes and the natural frequencies.

Most of the simplifications that occur in SEA arise from simplifying the full multi-dimensional integrals, the first step being to reduce these to the repeated products of one-dimensional integrals which are identical and so collapse to a single frequency PDF integral. If the mode shape parameters are also to be modelled by a given PDF, this becomes a double integral, i.e.

$$E[H_{12}(\omega)] = \frac{\omega^2 N_1 N_2 k_c^2 c_2}{m_1^2 m_2 E[|\Delta|^2]} \int_{-\infty}^{\infty}\int_{-\infty}^{\infty} \frac{f_{\psi_i\omega_i}\psi_i^2(a_1)d\psi_i d\omega_i}{|\phi_i|^2} \int_{-\infty}^{\infty}\int_{-\infty}^{\infty} \frac{f_{\psi_r\omega_r}\psi_r^2(a_2)d\psi_r d\omega_r}{|\phi_r|^2} \tag{6.1}$$

where $f_{\psi_i\omega_i}$ and $f_{\psi_r\omega_r}$ are the two-dimensional PDFs of mode shape at the coupling point and natural frequency for sub-systems 1 and 2, respectively. The assumption of independent mode shapes and frequencies (which is not certain) allows the integrals to be separated into the form

$$E[H_{12}(\omega)] = \frac{\omega^2 N_1 N_2 k_c^2 c_2}{m_1^2 m_2 E[|\Delta|^2]} \int_{-\infty}^{\infty} f_{\psi_i}\psi_i^2(a_1)d\psi_i \int_{-\infty}^{\infty} \frac{f_{\omega_i}d\omega_i}{|\phi_i|^2} \int_{-\infty}^{\infty} f_{\psi_r}\psi_r^2(a_2)d\psi_r \int_{-\infty}^{\infty} \frac{f_{\omega_r}d\omega_r}{|\phi_r|^2} \tag{6.2}$$

where now f_{ψ_i}, etc., are one-dimensional PDFs. When the mode shape parameters are assumed to be unity, this becomes

$$E[H_{12}(\omega)] = \frac{\omega^2 N_1 N_2 k_c^2 c_2}{m_1^2 m_2 E[|\Delta|^2]} \int_{-\infty}^{\infty} \frac{f_{\omega_i}d\omega_i}{|\phi_i|^2} \int_{-\infty}^{\infty} \frac{f_{\omega_r}d\omega_r}{|\phi_r|^2} \tag{6.3}$$

Clearly it is possible to perform any of these integrals numerically with arbitrary PDFs. However, it must be recalled that to make the simplification in the first place, the parameter Δ, which is a function of natural frequencies and mode shapes, was treated as a constant with respect to the variables of integration and so brought outside the integral (of course its mean value must also be calculated using a similar approach on equation (3.17)). In fact, the ability to do this without affecting the result was seen to be a measure of the validity of the usual SEA methods. If this step does not introduce significant inaccuracies, the use of non-uniform PDFs is remarkably easy to adopt, since numerical integrations like those of equations (6.1) to (6.3) are readily performed given the PDFs. The application to cases of strong coupling is not so straightforward, since then $|\Delta|$ is no longer sensibly constant with respect to the variable of integration. The strong coupling correction outlined in the previous chapter was developed to deal with precisely this problem. It is used with periodic structures in the example of Chapter 9.

When studying periodic and near-periodic systems, it becomes apparent that the natural frequencies tend to lie in groups, in the so called 'pass' bands. Under such circumstances it is justifiable to model the frequency PDF in a piecewise constant fashion, see Figure 6.1. Here there are two fixed levels of probability, which vary depending on whether or not a frequency lies in a 'pass' band. This kind

of PDF is of course straightforward to adopt in a numerical integration scheme, but it suggests an even simpler approach that may be worthwhile. All that this PDF indicates is that the modal density at any given frequency lies at one of two levels. Therefore it is possible to use just the traditional SEA results such as equation (3.47) with different modal densities, chosen to suit the frequency at which the calculation is performed. This technique is applied to an example discussed later. Notice that this is possible because of the very sharp fall-off with frequency separation of the ϕ parameters in the integrand and assumes that the bulk of the contribution to the integral is contained within a small range centred on ω, i.e., the summation bandwidth. Aside from the difficulty that arises at the boundary of the 'pass' bands, where there is a step change in probability density, this scheme is very useful and will be compared with the full monte-carlo and single, numerical integration methods in Chapter 9. Again, however, the mode shape information is more difficult to handle and it would seem that either it should be ignored completely, as is usual in SEA and would seem appropriate if a piecewise constant frequency PDF is being adopted, i.e., equation (6.3), or that a complete PDF should be formulated for both frequencies and mode shapes, using deterministic solutions for random parameter ensembles.

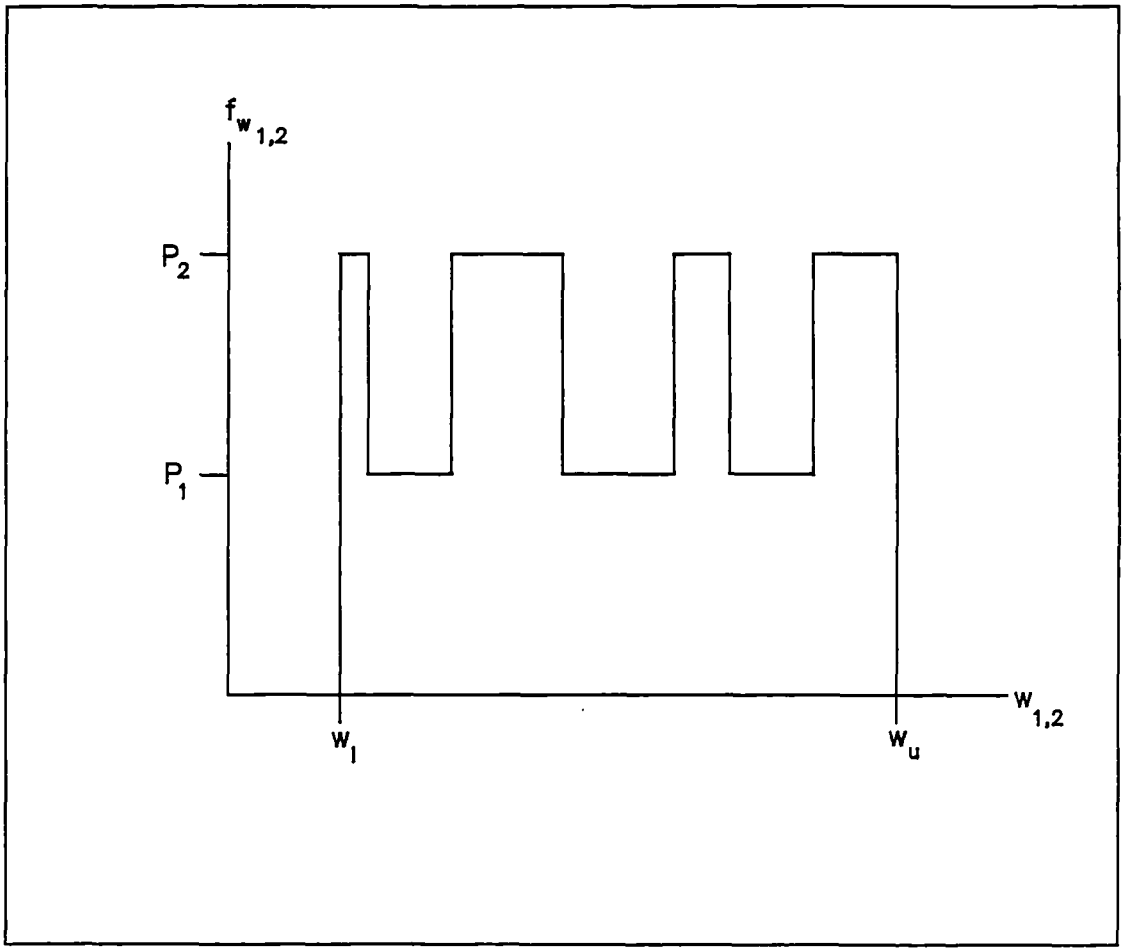

Figure 6.1 - A piece-wise constant probability density function for random natural frequencies.

CHAPTER 7

The Theory of Periodic Systems

7.1. Introduction

The previous chapter has outlined how non-uniform frequency and mode shape PDFs may be introduced into SEA. It has also mentioned that structures exhibiting a geometric variation in properties may permit the derivation of such PDFs in a straight-forward fashion. In this chapter the theory of purely periodic systems is examined and then, in the next, the effects of deviations from pure periodicity, which are implicit in SEA models, are introduced. The investigation to be discussed here adopts four commonly used approaches (i.e., wave, modal, receptance and finite element analyses); a recent review of this periodic theory is given by SenGupta[19]. The results arising from these differing approaches illustrate that it is likely to be the details of the model analysed and not the method of analysis that are crucial in dealing with periodic problems. The results of this and the following chapter are then used to apply SEA to a problem consisting of two coupled periodic sub-systems in Chapter 9.

The considerable simplifications that are possible in the study of purely periodic structures arise from application of the *Bloch* (or *Floquet*) theorem developed from considerations of the microscopic behaviour of the atoms of crystalline solids, see for example Brillouin[27] or Ziman[28]. Care is required in adapting work from this field of physics to engineering, since the effects of boundary conditions on the behaviour of periodic systems rapidly diminish when there are large numbers of sub-systems (as in the atomic model of a crystalline solid). Conversely, in most practical engineering structures the boundary conditions are an important factor in defining how a structure will behave. Additionally, most work on the atomic scale deals with lumped masses separated by (comparatively) large distances, whereas such point masses do not occur in practical structures (though they may be idealised in this manner). Finally, the effects of deviations from pure periodicity can sometimes only be seen when

studying enormous numbers of sub-systems, when the statistical properties of the defects can give rise to some subtle effects, see Anderson[44]. Such large numbers of units are common in theoretical physics, but rare in engineering. Moreover, deviations from pure periodicity are deliberately made to arise in crystalline solids by the practice of *doping*, whereby specified amounts of impurity atoms are introduced into a crystal, see for example Ziman[29]. The resulting effects are all-important when studying the behaviour of substances at an atomic level, but of little relevance to the structures encountered in engineering, where the restricted numbers of units cause more prosaic considerations to dominate.

It has already been noted that SEA assumes that the effects of mode shape coherence cancel out and thus ignores them, no distinction being made between uniform, periodic and near-periodic structures in this regard. As will be shown later, such assumptions are often erroneous when dealing with modern structural designs which have a good deal of repetition in them. In particular, the mode shapes, which are extended throughout uniform or purely periodic systems, can become localised within near-periodic systems, causing energy to be trapped within certain parts of the structure. Such areas therefore undergo much larger amplitude oscillations than the remainder. Moreover, although some modes are extremely localised, adjacent ones (in the frequency spectrum) can be fully extended. Figure 7.1 shows two mode shapes from the same 'pass' band of the simple example examined in Chapters 7 and 8, and this characteristic is clearly seen, despite the small number of repeated units in the model. Conversely, natural frequencies show no such dramatic changes in behaviour, merely migrating up and down the frequency spectrum in a fairly predictable way. This is at odds with normal SEA practice where much attention is devoted to the study of natural frequencies and their relative positions in the frequency spectrum and relatively little to the precise details of likely mode shapes. It has already been shown that mode shapes can be important when dealing with uniform structures; this is doubly so when dealing with periodic problems. Certainly a better understanding of the behaviour of periodic and near-periodic systems should be a pre-requisite to the application of statistical methods to engineering designs that exhibit such periodic characteristics.

Topologically, the simplest possible periodic structure consists of a number of identical, symmetrical sub-structures or elements coupled end-on-end in a linear chain. At first glance such a layout may seem too restrictive to be of any practical use, but the exact details of the periodic elements are to some extent irrelevant so far as the application of periodic theory is concerned. Moreover, the repeated characteristics of most engineering structures are essentially one-dimensional and almost never more than two-dimensional. These facts allow some interesting real structures to be considered in a simple fashion and useful results can be obtained from such elementary models (e.g., a taut string, rotating shaft or the axially vibrating rods considered earlier). It is recalled that the results presented in earlier chapters require details only of the undamped natural frequencies and mode shapes of the uncoupled sub-systems. Therefore this and the following chapters will be restricted to the discussion of mono-coupled structures in the absence of damping. A typical idealised system is illustrated in Figure 7.2. The figure shows a system of axially vibrating rods of varying mass densities and stiffnesses coupled end-on-end, sliding in frictionless bearings. This system exhibits a periodic variation in properties, and it may be seen that a single element is symmetric and consists of three sub-elements of varying properties. The exact choice of periodic element is made to simplify the subsequent analysis, but is also affected by the overall end conditions of the system (notice that here the end pieces are half the length of their equivalent interior sections). The behaviour of systems that cannot be broken into a complete number of repeated elements (such as the case when the end pieces are the same length as the equivalent interior ones) must be dealt with as deviations from pure periodicity; such deviations are considered in the next chapter.

7.2. Analysis of Periodic Systems

The behaviour of periodic systems has been of interest for many years and an extensive historical survey is given by Brillouin[27]. The fundamental result is known as the *Bloch* (or *Floquet*) theorem, which Ziman[28] states as

" *For any wave-function/state function that satisfies the Schrodinger equation (or its classical or quantal equivalent) there exists a vector* **k** *such that translation by a lattice vector* **l** *is equivalent to multiplying by the phase factor* $e^{i\mathbf{k}.\mathbf{l}}$ "

In other words, if one moves through a periodic structure, the motions at a fixed position within each repeated element making up the structure, differ only by a constant phase factor. The whole exponent of this factor can be shown to be purely imaginary for free vibrations of structures consisting of symmetric elements, leading to the conclusion that, over large ranges, the mean amplitude of vibration at the points considered does not alter. Consequently, the analysis of such problems collapses to that of finding the relevant phase factor and solving for the behaviour of a *single* element; a potentially massive simplification. The behaviour of asymmetric elements is slightly more complex but leads to essentially similar results.

Since the vibrations of undamped structures may be considered in terms of wave equations, this result is directly applicable to structural mechanics, see for example Coulson[45].

7.3. Wave Analysis

Following traditional theory, see for example Bishop and Johnson[3], the equation of motion of an axially vibrating rod is

$$AE\frac{\partial^2 y}{\partial x^2} = \rho\frac{\partial^2 y}{\partial t^2} \tag{7.1}$$

where AE is the product of cross-sectional area and Young's modulus and ρ the mass per unit length, both assumed unvarying with respect to x within each portion of the rod; y is the longitudinal deflection from equilibrium at the point x and time t. Assuming solutions that vary harmonically in time such that

$$y(x,t) = y(x)e^{-i\omega t} \tag{7.2}$$

equation (7.1) becomes

$$\frac{d^2y}{dx^2} + \lambda^2 y = 0 \tag{7.3}$$

where $\lambda^2 = \omega^2 \rho / AE$. If the properties of the rod vary with position, such that over a region A of length l_A they are constant but different from those pertaining over a region B of length l_B, the constant λ will differ, indicated by subscripts, λ_A and λ_B, respectively. Equations (7.1-7.3) then hold in a piece-wise fashion and if the regions A and B alternate the rod exhibits a periodic fluctuation in properties. The resulting equation of motion is sometimes referred to as *Hill's Equation*, although traditionally in *Hill's Equation* the periodic fluctuation is in time rather than space. Following Brillouin[27] (article 44), a *D'Alembert* wave solution may then be used in each portion and the continuity of force and displacement at the boundaries between adjacent sections of the rod used to eliminate the unknown quantities.

Initially assume that the rod is of infinite length and that the origin of x lies at the right-hand end of a piece of rod with properties A. It follows that a solution of the form

$$y = C_1 e^{i\lambda_A x} + C_2 e^{-i\lambda_A x} \tag{7.4}$$

holds in the piece to the left of the origin, A whilst one of the form

$$y = C_3 e^{i\lambda_B x} + C_4 e^{-i\lambda_B x} \tag{7.5}$$

holds in the adjacent piece to the right, B (note that complex exponentials are used here to indicate the harmonically varying displacements). This problem is amenable to a periodic solution and therefore the displacements in the various periodic elements can be related in terms of a *Floquet exponential* that relates two elements, M units apart. That is

$$y(x) = e^{M\mu d} y(x - Md) \tag{7.6}$$

where $d = l_A + l_B$, which is the length of the periodic element, and $M-1$ is the number of units between the elements considered. Here μd is the phase factor governing the relationship between the successive units, and this is determined through the application of suitable boundary conditions. This type of analysis provides an explanation of how the variable μ varies with frequency ω. Applying the continuity conditions of displacement and force at $x = 0$ gives

$$C_1 + C_2 = C_3 + C_4 \tag{7.7}$$

and

$$(C_1-C_2)(AE_A/AE_B)\lambda_A = (C_3-C_4)\lambda_B \tag{7.8}$$

respectively, whilst at $x = l_B$ the equivalent relationships are

$$C_1 e^{\mu d - i\lambda_A l_A} + C_2 e^{\mu d + i\lambda_A l_A} = C_3 e^{i\lambda_B l_B} + C_4 e^{-i\lambda_B l_B} \tag{7.9}$$

and

$$C_1(AE_A/AE_B)\lambda_A e^{\mu d - i\lambda_A l_A} - C_2(AE_A/AE_B)\lambda_A e^{\mu d + i\lambda_A l_A} = C_3\lambda_B e^{i\lambda_B l_B} - C_4\lambda_B e^{-i\lambda_B l_B} \tag{7.10}$$

These four equations may be written in matrix form

$$\begin{bmatrix} 1 & 1 & 1 & 1 \\ (AE_A/AE_B)\lambda_A & -(AE_A/AE_B)\lambda_A & \lambda_B & -\lambda_B \\ e^{\mu d - i\lambda_A l_A} & e^{\mu d + i\lambda_A l_A} & e^{i\lambda_B l_B} & e^{-i\lambda_B l_B} \\ (AE_A/AE_B)\lambda_A e^{\mu d - i\lambda_A l_A} & -(AE_A/AE_B)\lambda_A e^{\mu d + i\lambda_A l_A} & \lambda_B e^{i\lambda_B l_B} & -\lambda_B e^{-i\lambda_B l_B} \end{bmatrix} \begin{Bmatrix} C_1 \\ C_2 \\ -C_3 \\ -C_4 \end{Bmatrix} = \begin{Bmatrix} 0 \\ 0 \\ 0 \\ 0 \end{Bmatrix} \tag{7.11}$$

and clearly for this equation to be non-trivial the determinant of the matrix must be zero. The expansion of this determinant is somewhat lengthy, but Brillouin[27] shows that it yields an equation for the unknown constant μ in the *Floquet exponential* which satisfies the expression

$$\cosh(\mu d) = \cos(\lambda_A l_A)\cos(\lambda_B l_B) - \frac{1}{2}\left\{\frac{\lambda_A}{\lambda_B} + \frac{\lambda_B}{\lambda_A}\right\}\sin(\lambda_A l_A)\sin(\lambda_B l_B) \tag{7.12}$$

Figure 7.3 shows a typical graph of $\cosh(\mu d)$ versus radian frequency ω, which relates to the example that is discussed in some detail later on. It is noted that μ is wholly real only when the right-hand side of this equation is greater than unity, since $\cosh(\mu d)$ has a minimum value of unity for all real arguments. In fact, for $\cosh(\mu d)$ less than minus one the imaginary part of μd is always π, whereas in the range $-1<\cosh(\mu d)<1$, μd is purely imaginary.

These variations in μ between complex and real are well known and give rise to the presence of *pass* and *stop* bands within the frequency spectrum for the structure, see Mead[30]. If a wave with characteristic frequency ω is travelling along the rod and ω lies in a 'pass' band, then μ is purely imaginary, the *Floquet exponential* merely causes a phase shift, and the wave will travel unattenuated from element to element with jumps in phase at the boundaries of elements. Note that an element or periodic unit consists of two *sub-elements* here, one of type *A* and the other of type *B*. Conversely, if the wave has a frequency ω lying in a 'stop' band, then μd will be either entirely real or have an ima-

ginary part that is a multiple of π, and it will either grow or decay exponentially at the sub-system boundaries. Ziman[28] has shown that boundary condition considerations would ensure against the presence of waves growing without limit for a real structure.

It is interesting to note from Figure 7.3 that, since $\cosh(\mu d)$ shows a beating characteristic in the frequency domain (being the sum of harmonics of different functions of ω), the widths of successive 'pass' bands fluctuate in a similar beating fashion. This particular phenomenon does *not* arise when a similar analysis is carried out for a rod with periodically spaced point masses instead of the varying mass densities used in this example. If the mass density per unit length of the heavy sections of the rod is allowed to increase without limit at the same time as the length of these heavy sections tends to zero, such that a fixed finite mass is maintained within the section, then the solution given here tends to that for point masses. This causes the period of the fluctuation in 'pass' band widths to tend to infinity, so that the fluctuations disappear, leaving a sequence of ever narrowing bands, such as described by Hodges and Woodhouse[46]. This difference *may* explain some of the experimental results presented by those authors who, because of their chosen mathematical model of point masses, were unable to conceive the previous reasoning.

The positions of the 'stop' and 'pass' bands in the frequency domain give no formal indication of where the natural frequencies will lie, although it is noted in passing that if a natural frequency occurs in a 'stop' band, then it is to be expected that the corresponding mode shape will have unusual characteristics, as will be discussed later. To fix the natural frequencies for any particular problem requires suitable boundary conditions to be specified. The simplest conditions, and those first used for crystals, are known as cyclic or *Born-von Karman* boundary conditions[47]. This model assumes that the ends of the linear system of periodic units are joined together in a loop, forcing continuity to exist between the first and last sub-elements of the system. This device allows the density and disposition of natural frequencies to be examined and gives an indication of how a more practical solution might behave. Specifically, this forces the initially chosen *Floquet exponential* of equation (7.6) to repeat after exactly one cycle of the system. If there are M periodic units in the complete cycle, this gives

$$e^{M\mu d} = 1 \tag{7.13}$$

implying that μ is purely imaginary with values

$$\mu = \frac{2i\pi s}{Md} \tag{7.14}$$

where s is any integer. Clearly, only a reduced range need be considered, causing μ to lie in the range $-i\pi/d < \mu \leq i\pi/d$, which means that s can be restricted to lie in the range $-M/2 < s \leq M/2$. This gives rise to exactly M evenly spaced values of μ, all of which are complex and therefore lie in the 'pass' bands (ignoring the trivial problem of whether M is odd or even). The corresponding natural frequencies, ω_i etc., are found by mapping these values of μ through the relationship of equation (7.12), as already discussed and shown in Figure 7.3.

7.4. Modal Analysis

The preceding analysis takes no account of the behaviour of individual periodic units in isolation, and a more elegant solution is found if the eigenvalues of these units are used as the basis of solution. To illustrate this, the approach proposed by Lin[32] and Faulkner and Hong[33] is adopted, and the transfer matrix of a single periodic unit constructed. This transfer matrix relates the coupling forces and displacements in successive periodic units and is based on the direct and cross-receptances of the individual elements, α_{11}, α_{12}, etc. Let subscripts L_k and R_k denote quantities at the left and right-hand ends of the *kth* periodic element, respectively. Then y_{L_k} and y_{R_k} are the displacements and F_{L_k} and F_{R_k} the forces at the ends of the *kth* element. The receptances are then defined by (see for example Bishop and Johnson[3])

$$\begin{Bmatrix} y_L \\ y_R \end{Bmatrix}_k = \begin{bmatrix} \alpha_{11} & \alpha_{12} \\ \alpha_{21} & \alpha_{22} \end{bmatrix}_k \begin{Bmatrix} F_L \\ F_R \end{Bmatrix}_k \tag{7.15}$$

whilst the continuity conditions require that

$$\begin{Bmatrix} y_L \\ F_L \end{Bmatrix}_k = \begin{Bmatrix} y_R \\ -F_R \end{Bmatrix}_{k+1} \tag{7.16}$$

For the conservative element under discussion, $\alpha_{12} = \alpha_{21}$, and using this fact the two previous equations may be rearranged to yield the transfer matrix $[T]_k$, giving

$$[T]_k = \begin{bmatrix} \dfrac{\alpha_{22}}{\alpha_{12}} & \alpha_{12} - \dfrac{\alpha_{11}\alpha_{22}}{\alpha_{12}} \\ \dfrac{-1}{\alpha_{12}} & \dfrac{\alpha_{11}}{\alpha_{12}} \end{bmatrix}_k \tag{7.17}$$

The matrix $[T]_k$ completely defines the behaviour of an isolated periodic element, and it is the eigenvalues of this matrix that are used in the following analysis. They may be derived from the characteristic determinant as

$$\Xi_{k_1}, \Xi_{k_2} = \frac{\alpha_{11}+\alpha_{22}}{2\alpha_{12}} \pm \sqrt{\left[\frac{\alpha_{11}+\alpha_{22}}{2\alpha_{12}}\right]^2 - 1} \tag{7.18}$$

where Ξ_{k_1}, Ξ_{k_2} are associated with the positive and negative solutions, respectively. Making the substitution

$$\cosh(\mu d) = \frac{\alpha_{11}+\alpha_{22}}{2\alpha_{12}} \tag{7.19}$$

the eigenvalues Ξ_{k_1} and Ξ_{k_2} become $e^{\mu d_k}$ and $e^{-\mu d_k}$, respectively, and these are the *Floquet exponentials* used previously. In the present context the eigenvectors $\{X\}_k$ of the transfer matrix $[T]_k$ may be expressed in the form

$$\left\{X_1\right\}_k = \begin{Bmatrix} \alpha_{11} - \alpha_{12} e^{\mu d} \\ 1 \end{Bmatrix}_k \tag{7.20}$$

and

$$\left\{X_2\right\}_k = \begin{Bmatrix} \alpha_{11} - \alpha_{12} e^{-\mu d} \\ 1 \end{Bmatrix}_k \tag{7.21}$$

Notice that equation (7.19) allows the function $\cosh(\mu d)$ to be constructed (and therefore the 'pass' bands to be found) for *any* mono-coupled periodic element whose receptances are known. These receptances can readily be related to the behaviour of an isolated element, since α_{11}/α_{12} is given by the force required at the right-hand end of the element to generate unit reaction at the fixed left-hand end, i.e.

$$\frac{\alpha_{11}}{\alpha_{12}} = -F_r\Big|_{F_L=1, y_L=0} \tag{7.22}$$

Also α_{22}/α_{12} is given by the displacement required at the right-hand end to generate unit amplitude

vibrations at the other, when it is free, i.e.

$$\frac{\alpha_{22}}{\alpha_{12}} = -y_r\Big|_{F_L=0, y_L=1} \tag{7.23}$$

These quantities may usually be calculated for any element of interest; moreover the relationships are well behaved even at the element natural frequencies.

Because of the fundamental properties of eigenvectors, any other vector describing the motion of the periodic unit can be described in terms of these two orthogonal vectors. Suppose a vector $\{Z\}_k$ describes a wave that exists in the *kth* element, then this vector can be represented by

$$\left\{Z\right\}_k = z_{1_k}\left\{X_1\right\}_k + z_{2_k}\left\{X_2\right\}_k \tag{7.24}$$

The vector existing in the adjacent $(k+1)th$ element is derived by applying the transfer matrix $[T]_k$ to this expression, yielding

$$\left\{Z\right\}_{k+1} = [T]_k\left\{Z\right\}_k = [T]_k\left\{z_{1_k}\left\{X_1\right\}_k + z_{2_k}\left\{X_2\right\}_k\right\} \tag{7.25}$$

Substitution of the previously derived eigenvalues gives

$$\left\{Z\right\}_{k+1} = z_{1_k}e^{\mu d_k}\left\{X_1\right\}_k + z_{2_k}e^{-\mu d_k}\left\{X_2\right\}_k \tag{7.26}$$

and it is observed that the constituent parts of the initial vector are caused to grow and decay in the expected way, factored by the relevant *Floquet exponential.*

Inserting the desired boundary conditions, these results may be readily used to determine the natural frequencies of the whole system. Consider for example a system of M periodic elements with free-free end boundary conditions, e.g., $F_{L_1} = 0$ and $F_{R_M} = 0$. Comparison of the eigenvectors given in equations (7.20) and (7.21) with equation (7.24) leads to the derived boundary condition at the left-hand end of the first unit, viz

$$z_{1_1} + z_{2_1} = 0 \tag{7.27}$$

Then the direct receptance of the whole system at its right-hand end, which is the ratio of the displace-

ment over the force at the right-hand end of the last unit, becomes

$$\frac{y_{R_M}}{F_{R_M}} = -\frac{y_{L_{M+1}}}{F_{L_{M+1}}} = -\frac{z_{1_1} e^{M\mu d}\left[\alpha_{11} - \alpha_{12} e^{\mu d}\right] + z_{2_1} e^{-M\mu d}\left[\alpha_{11} - \alpha_{12} e^{-\mu d}\right]}{z_{1_1} e^{M\mu d} + z_{2_1} e^{-M\mu d}} \tag{7.28}$$

$$= -\alpha_{11} + \frac{\alpha_{12}\sinh([M+1]\mu d)}{\sinh(M\mu d)}$$

$$= -\alpha_{11} + \alpha_{12}\left\{\cosh(\mu d) + \frac{\cosh(M\mu d)\sinh(\mu d)}{\sinh(M\mu d)}\right\}$$

This result is similar to that given by Mead[30] as his equation (22a) (although his equation is for the direct receptance of the extreme left-hand end). It is noted that this ratio is *always* entirely real since the imaginary parts cancel. When the ratio tends to infinity a resonance exists, and the frequency is a natural frequency of the entire system. The natural frequencies are found when either α_{11} or α_{12} tends to infinity (resonances of the individual periodic units) or when $\sinh(M\mu d)/\sinh(\mu d)$ tends to zero. These conditions, as Mead[30] notes, arise in the 'stop' bands (or at their boundaries if the periodic units are symmetric, when $\alpha_{11} = \alpha_{22}$) for the individual element natural frequencies, or wholly within the 'pass' bands for the overall system resonances. Similar analyses can be performed for the left-hand end system direct receptance or the overall system cross-receptance; all three functions show singularities at the same frequencies, of course.

Faulkner and Hong[33] continued this analysis by forming the transfer matrix for a sequence of identical periodic units, gaining results for both symmetric and asymmetric periodic units. For the case of M symmetric units, all of type k, where $(\alpha_{11})_k = (\alpha_{22})_k$, the analysis proceeds by rewriting $[T]_k$ as

$$[T]_k = \begin{bmatrix} \cosh(\mu d) & D\sinh(\mu d) \\ \frac{1}{D}\sinh(\mu d) & \cosh(\mu d) \end{bmatrix}_k \tag{7.29}$$

where $D_k = -(\alpha_{12})_k \sinh(\mu d_k)$ and all parameters within the matrix have the same subscript as the matrix. By successive application to the M identical elements, it follows that the repeated products of $[T]_k$ collapse, because the D_k terms all cancel, irrespective of other elements in the formulation, giving

$$[T]_k^M = \begin{bmatrix} \cosh(M\mu d) & D\sinh(M\mu d) \\ \frac{1}{D}\sinh(M\mu d) & \cosh(M\mu d) \end{bmatrix}_k \tag{7.30}$$

The fact that the repeated product of the transfer matrix collapses in this way is the *essence* of periodic theory. Notice that the ratio of the upper-left over the lower-left terms of this matrix gives the direct receptance of the system again, and that this is indeed the same as that given in equation (7.28) because the expression for $\cosh(\mu d)$, given as equation (7.19), collapses to α_{11}/α_{12} for symmetric units.

7.5. Receptance Analysis

It is possible, and also often computationally simpler, to calculate the response of a finite linear assembly of periodic units solely in terms of the direct and cross-receptances of their (uniform) constituent sub-elements. This approach, which ignores the underlying periodicity of the whole system, permits a check calculation to be performed for any problem and additionally allows for systems with deviations from pure periodicity to be handled with little added complexity. The application of receptance theory is well established, see for example Bishop and Johnson[3], and so only the final results of a traditional analysis are given here.

Previously the subscript k has been used to refer to the particular periodic units or elements; now let the subscript l refer to the individual, constituent sub-elements, counting continuously from one end, with the left-hand end of the left most element being station zero. That is, if there are three parts to each periodic unit, then l will increment three times as fast as k. Clearly any vibration of the overall rod system will be made up of sinusoidal variations in space (with possible discontinuities in slope at the junctions, counted by the subscripts l), all varying harmonically in time with frequency ω. This happens because all the individual sub-elements in the system are uniform and have mode shapes that are, individually, purely sinusoidal. To define completely the free vibrations of the system merely requires knowledge of the amplitudes and phases of the spatially varying cosine waves on each sub-element, the individual wave-lengths being fixed by the parameters of the particular section (i.e., the local wave speeds). Defining Y_l to be the amplitude of the cosine wave within the *lth* sub-element and

ε_l to be the phase angle at the right-hand end of the section; it may be seen that the displacement within the *lth* sub-element, in terms of a local x (i.e. x_l) is given by

$$y(x_l,t) = Y_l \cos(\lambda_l[x_l - l_l] + \varepsilon_l) e^{-i\omega t} \tag{7.31}$$

and again l_l is the section length and λ_l defines the local wave speed. Following Bishop and Johnson[3], and after some algebraic manipulations (see Borland[48]), the continuity conditions of force and displacement allow the phases and amplitudes of adjacent sections to be linked by

$$\tan(\lambda_{l+1} l_{l+1} - \varepsilon_{l+1}) = -\sqrt{\frac{\rho_l AE_l}{\rho_{l+1} AE_{l+1}}} \tan(\varepsilon_l) \tag{7.32}$$

and

$$\left[\frac{Y_{l+1}}{Y_l}\right]^2 = 1 + \left[\frac{\rho_l AE_l - \rho_{l+1} AE_{l+1}}{\rho_{l+1} AE_{l+1}}\right] \sin^2(\varepsilon_l) \tag{7.33}$$

where ρ and AE are as defined in equation (7.1). These relationships show the effect of phase at the boundaries of sections and indicate that it is possible for the amplitude of the displacement cosine function to be unchanged at a boundary, and also that the maximum change is simply the square root of the ratio of ρ and AE. The sectional end forces are recovered from these expressions as the products of the end 'slopes' and the parameter AE, i.e.

$$F_{L_l} = AE_l \left.\frac{\partial y}{\partial x_l}\right|_{x_l=0} \tag{7.34}$$

$$F_{R_l} = AE_l \left.\frac{\partial y}{\partial x_l}\right|_{x_l=l_l} \tag{7.35}$$

The boundary conditions for a free-free system require these forces to be zero at the extreme ends, i.e., $F_{L_1} = 0 = F_{R_M}$. Thus the natural frequencies may be determined by inserting a zero force at one end and calculating along the system, seeking frequencies where a zero force occurs at the other. An alternative is to look for frequencies that give rise to a total phase shift of an integer multiple of π. These expressions may be readily encoded into a computer program, and it is then a simple root searching problem to establish the natural frequencies, the mode shapes being recovered by back substitution. Problems are usually encountered with this scheme only if insufficient care is taken in setting up the

principal values of the arc-tangent function used to calculate the phases. It has the marked advantage of not requiring complex arithmetic. Moreover, since it will work for any system, periodic or not, it is rather more flexible than schemes based solely on periodic theory.

7.6. Finite Element Analysis

The final approach discussed here makes use of finite elements (F.E.), see for example Meirovitch[4] or Zienkiewicz[5]. Again the method is well known and only brief details will be given. Finite element methods are basically discretization procedures which use approximations to the actual deformed shape within each element. The key to their accuracy (compared with exact, classical solutions) lies in the ability of the approximating shape functions to adopt the correct deformations. Clearly, the simplest methods for improving accuracy are either to increase the capabilities of the individual elements or to use more elements. It is possible to modify the F.E. method to take account of the underlying periodicity inherent in a structure, see Orris and Petyt[49], but most users of F.E. codes probably wish to use normal modelling techniques and standard commercial programs. Here the aim is to demonstrate that normal F.E. techniques *can* calculate the behaviour of periodic structures *and* also predict the effects of discontinuities. Therefore elements with a simple, linear shape function have been used together with discretizations that reflect normal practice in engineering. The examples have been analysed with the commercially available PAFEC[50] suite of programs (with element type 34400), and the results of the other approaches can be compared with those produced from one of the most commonly adopted techniques of vibrations analysis.

7.7. An Example of Ten Periodic Units

To form the basis for comparison of the various methods outlined above, the axially vibrating rod example of Figure 7.3 is used. In its purely periodic form it consists of ten periodic units, assembled end-on-end with free-free boundary conditions at the extremities. As has already been noted, each unit is made up of three sub-elements, i.e. a long, low mass density section, a short, heavy section and another similar long, light section. Following Bishop and Johnson[3] and using β and γ for the

receptances of the long and short sub-elements respectively, the overall direct and cross-receptances for this form of periodic unit, α_{11} and α_{12}, become

$$\alpha_{11} = \beta_{11}+\beta_{12}-2(\beta_{11}+\beta_{12})\left\{\frac{\beta_{11}+\beta_{12}+\gamma_{11}}{(\beta_{11}+\beta_{12}+\gamma_{11})^2-\gamma_{12}^2}\right\} \tag{7.36}$$

and

$$\alpha_{12} = \frac{2\beta_{12}(\beta_{11}+\beta_{12})\gamma_{12}}{(\beta_{11}+\beta_{12}+\gamma_{11})^2-\gamma_{12}^2} \tag{7.37}$$

where for systems obeying equation (7.1)

$$\beta_{11} = \frac{-\cos(\lambda l)}{AE\lambda\sin(\lambda l)} = \gamma_{11} \tag{7.38}$$

$$\beta_{12} = \frac{-1}{AE\lambda\sin(\lambda l)} = \gamma_{12} \tag{7.39}$$

(For completeness, it is noted that if a sub-element length tends to zero as its density goes to infinity a point mass results. Under these circumstances, both the direct and cross-receptances tend to $-1/\rho l\omega^2$, where the quantity ρl is the size of the mass.) The parameters associated with the components are shown in Table 7.1. The subsequent variations in μd are illustrated by Figure 7.3, and it is seen that the first eleven 'pass' bands lie in the frequency range from zero to ten radians per second, representing a complete cycle in the fluctuations of 'pass' band widths. This system has been chosen since the alternation of long, light portions with short, heavy sections is reminiscent of the stiffened plate structures common in engineering design. It should be noted, however, that plate and beam *bending* problems are *not* mono-coupled problems, since they do not follow equation (7.1), being fourth order in nature; it is only the *axial* vibrations of such structures that follow the equation used here. It is considered that the introduction of more complex equations is not justified by the present work, since the aim has been

PARAMETERS USED IN THE EXAMPLES OF CHAPTERS 7 & 8				
Parameter	Left Hand End	Centre	Right Hand End	Units
Mass density per unit length (ρ)	1.0	100.0	1.0	kg/m
Rigidity (AE)	π^{-2}	π^{-2}	π^{-2}	N
Sub-element length (l)	0.5	0.01	0.5	m

Table 7.1

to give a qualitative understanding of the phenomena involved. Moreover as Mead and Markus[51] have noted, the *transmission* of energy around vibrating structures can arise largely through the medium of axial vibrations with the coupled transverse vibrations being the *resultant* observed phenomenon, or the mechanism by which the structure is excited. Symmetric units have been used since these simplify the analysis without loss of generality, however it must be stated that the model adopted here has been chosen primarily to simplify the subsequent analysis.

Figure 7.4a illustrates the magnitude of the cross-receptance for the whole system (i.e., ignoring signs) as a function of frequency and also the variation of the real part of μ. The latter is zero in the 'pass' bands, the first 'pass' band starting at zero frequency, since this free-free system is of course capable of rigid-body motions. The very low values of cross-receptance that are found in the 'stop' bands arise because of the extreme attenuation that takes place at these frequencies, making it very difficult to cause one end to move by forcing the other. Notice that this overall cross-receptance relates the forces and motions at the ends of this single, undamped system of vibrating rods. It should not be confused with the cross-receptance H_{12}, which relates two, damped sub-systems, used in earlier chapters. The receptance for the frequency range of the second 'pass' band is illustrated in Figure 7.4b, which shows a detail from Figure 7.4a.

As has been noted by Hodges and Woodhouse[46], the mode shapes in the first 'pass' band are not very illuminating, since in these modes the long, light sections deform linearly and the classical 'masses on a massless string' responses result. Figure 7.5, which shows *axial* deflections as transverse for clarity, gives the mode shapes and corresponding natural frequencies that are predicted by the first three (classical) methods outlined above. These are for the second 'pass' band, lying between 0.990 and 1.289 radians per second (all three methods give identical results), c.f. Figure 7.4b. The F.E. analysis gives essentially similar results but with some loss of accuracy when compared with the other methods, as expected given the approximations implicit in the approach, see Figure 7.6. It is noted that the modes possess a satisfying symmetry and progression and extend throughout the structure in such a way that, if the system were vibrating at any frequency, all parts of the system would undergo

significant motion (excepting the nodes of the various modes). This behaviour will be contrasted with that arising when deviations from pure periodicity are introduced.

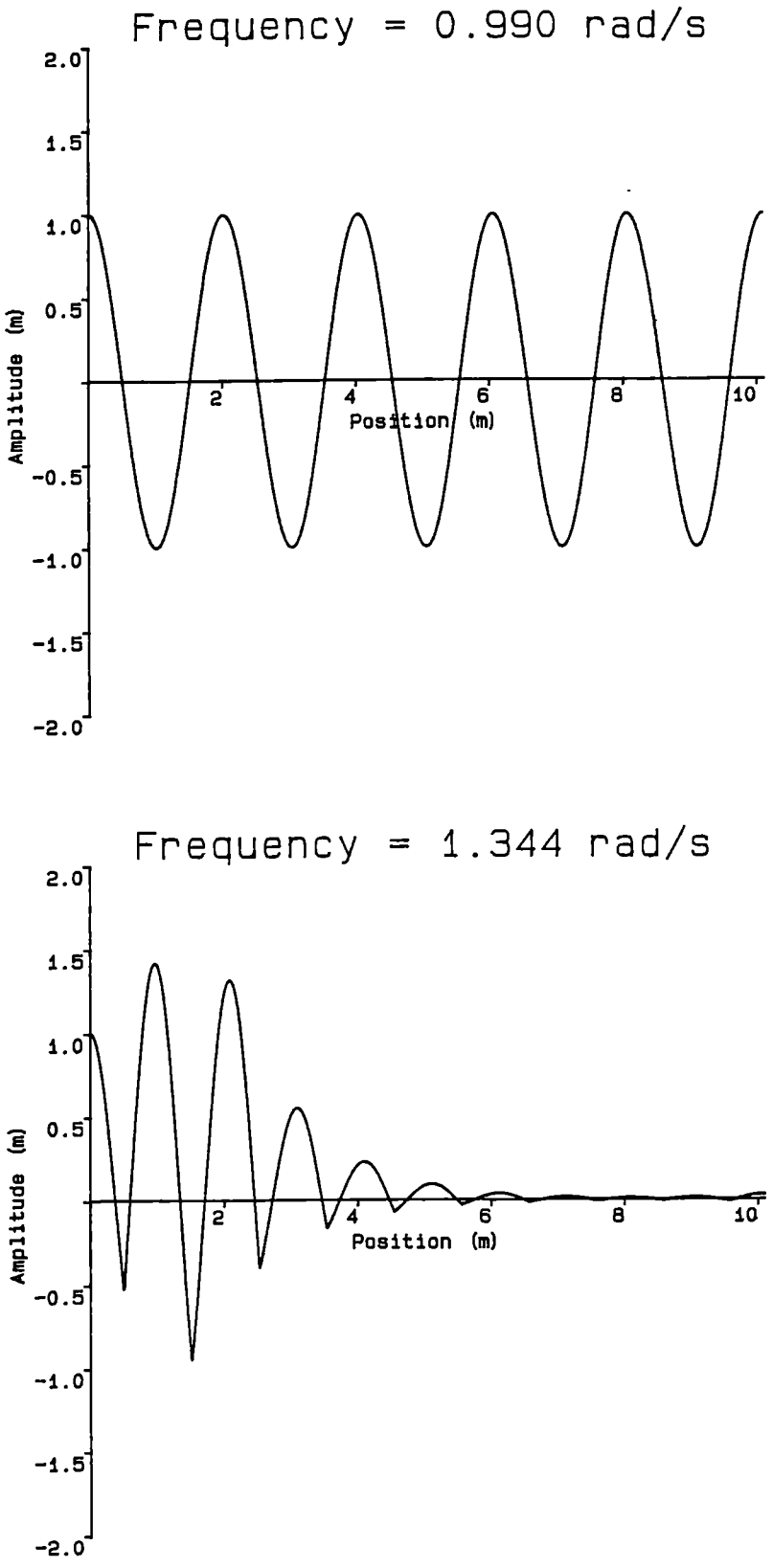

Figure 7.1 - Two mode shapes from the second pass band of the example examined, taken from Figure 8.2.

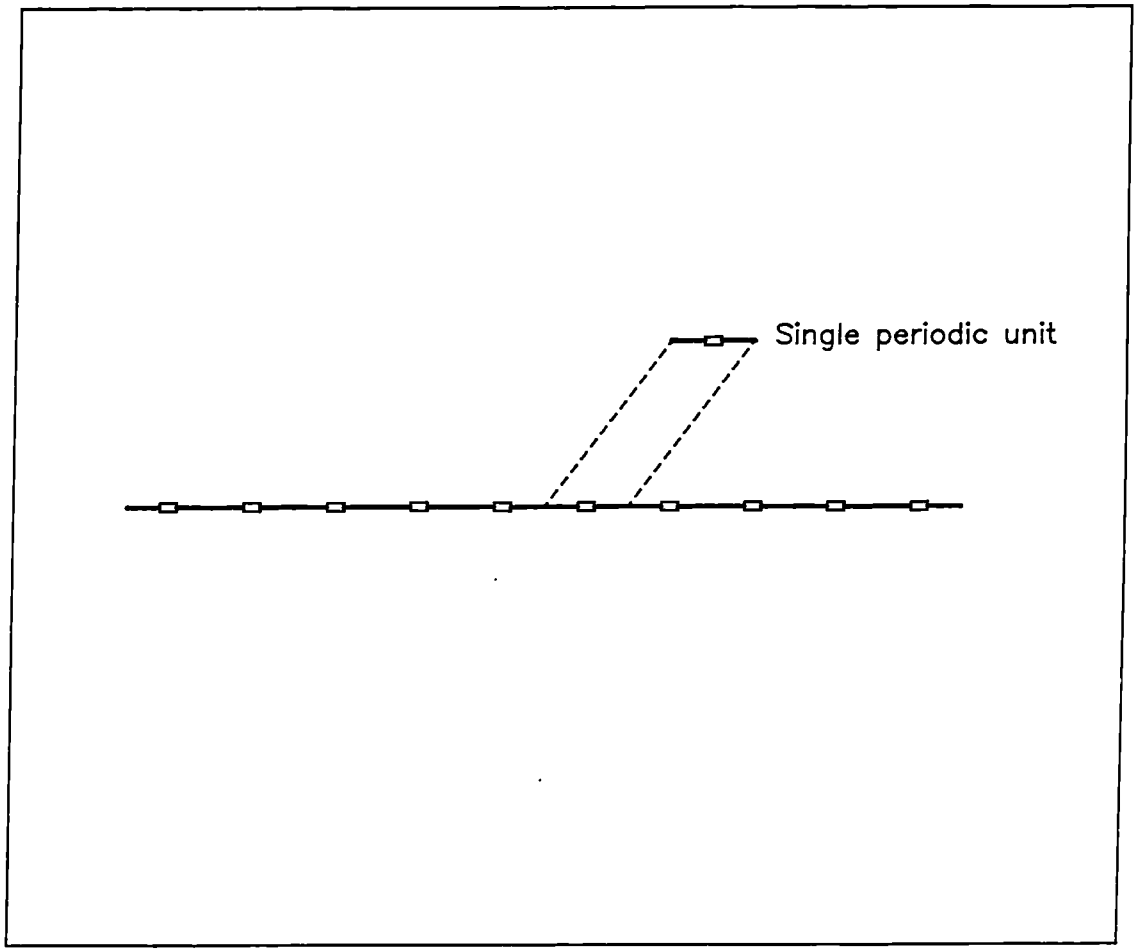

Figure 7.2 - A periodic system of axially vibrating, undamped rods showing a single periodic element.

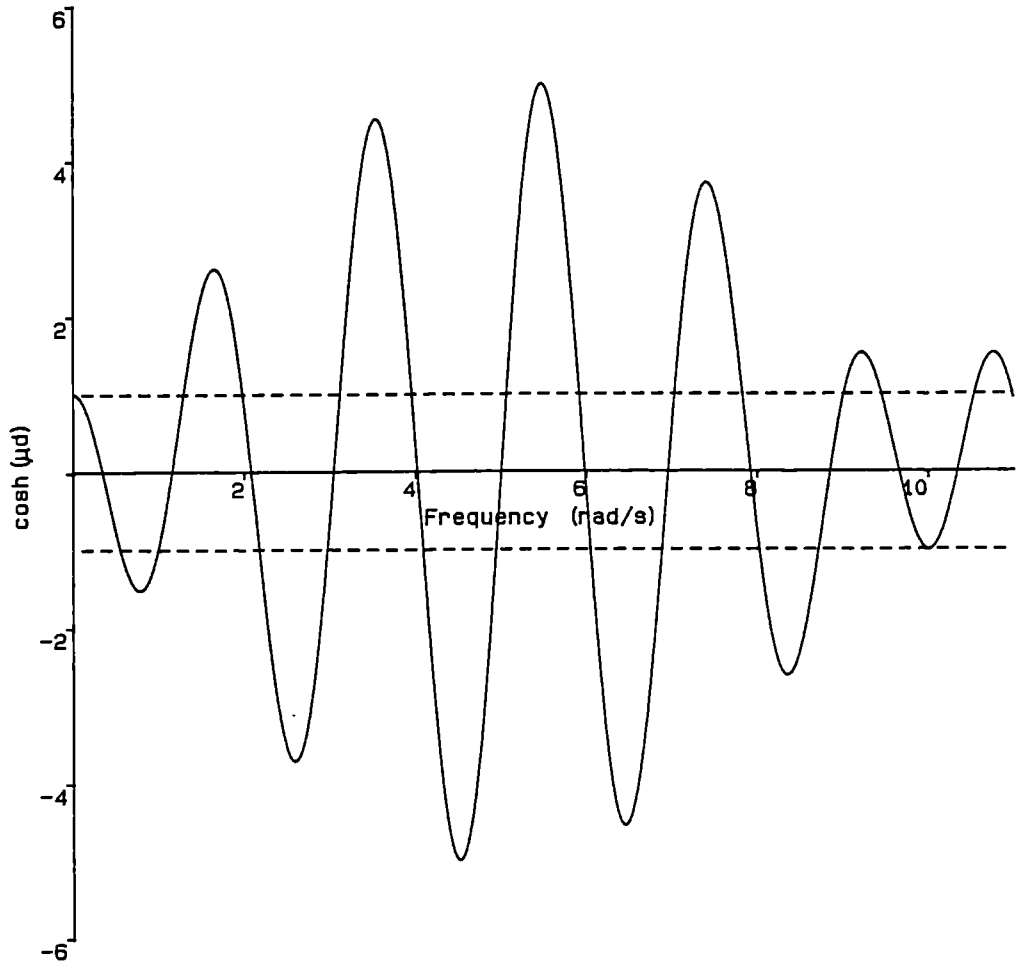

Figure 7.3 - Graph of cosh(μd) versus radian frequency ω.

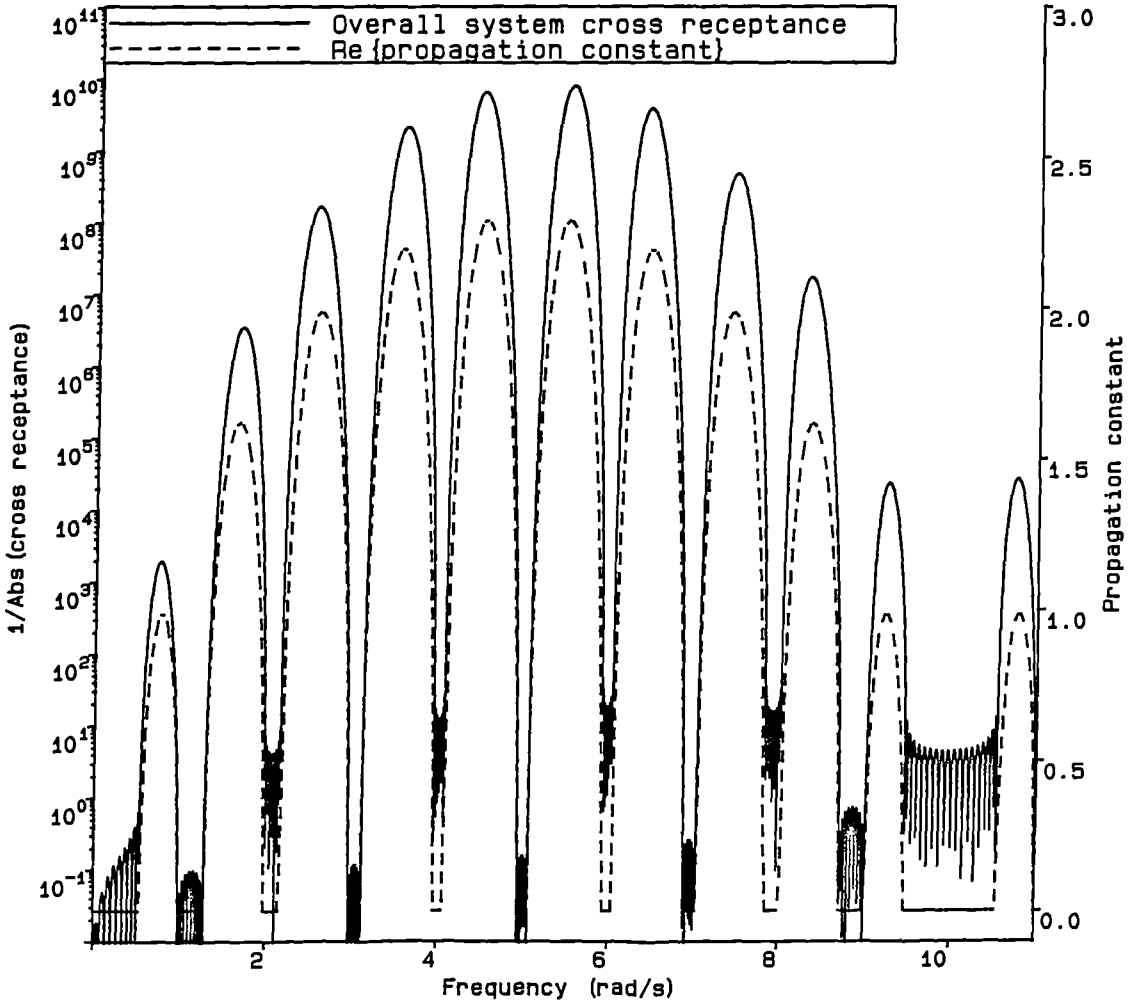

Figure 7.4a - Graph of the overall cross receptance and real part of μ versus radian frequency ω.

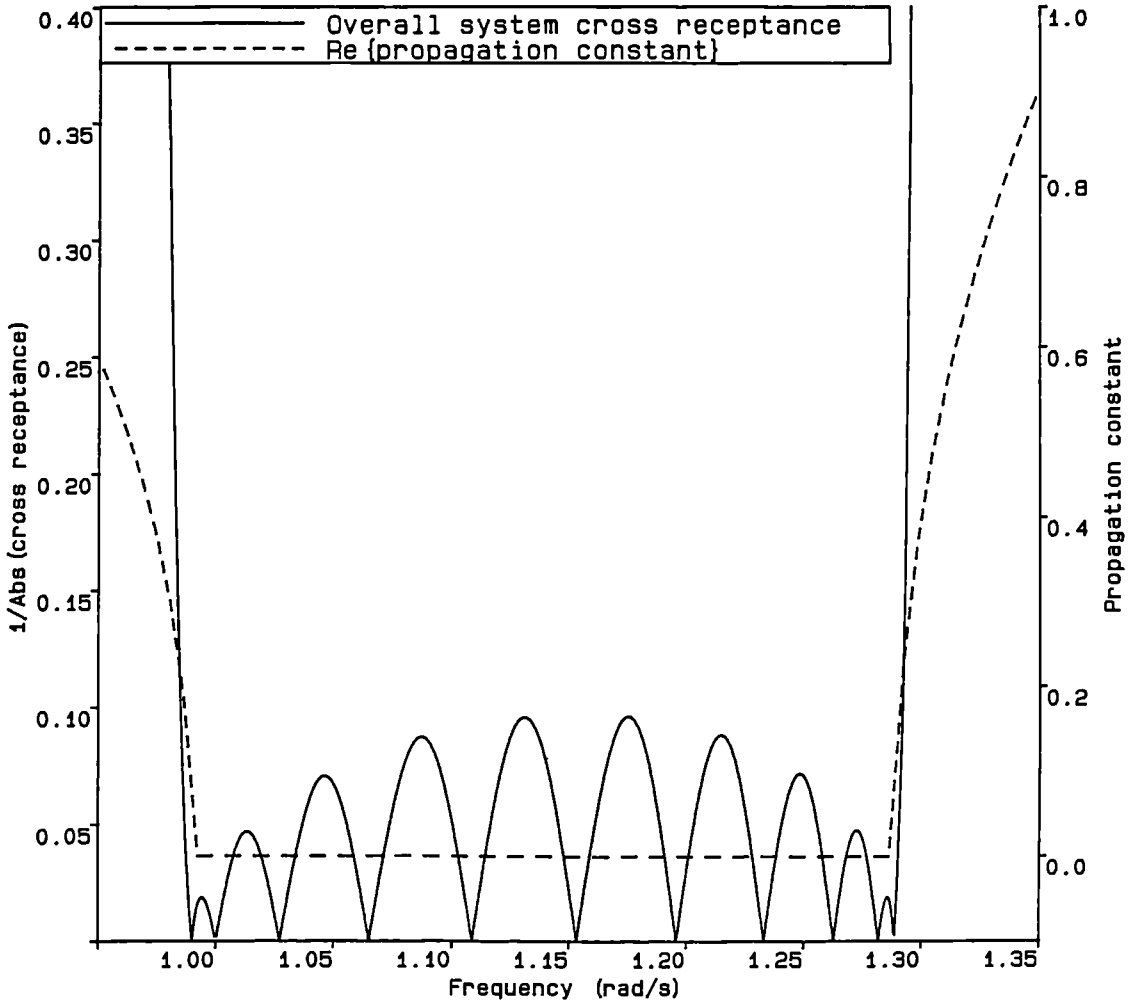

Figure 7.4b - A detail from Figure (7.4a), the graph of overall cross receptance and real part of μ versus radian frequency ω.

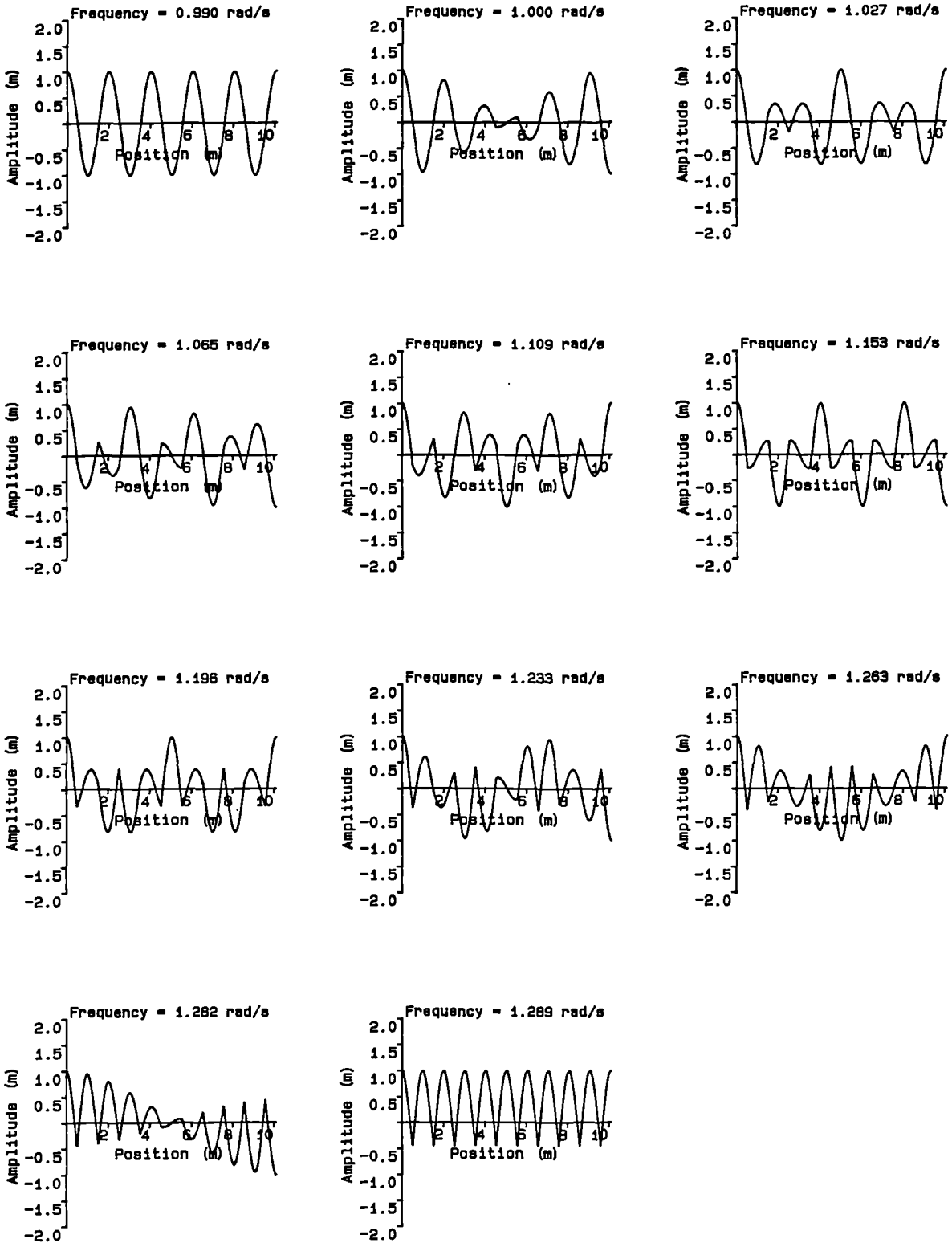

Figure 7.5 - Mode shapes and natural frequencies ω_i for modes in the second pass band, calculated using receptance theory (axial deflections shown transverse for clarity). Wave and modal theories give identical results.

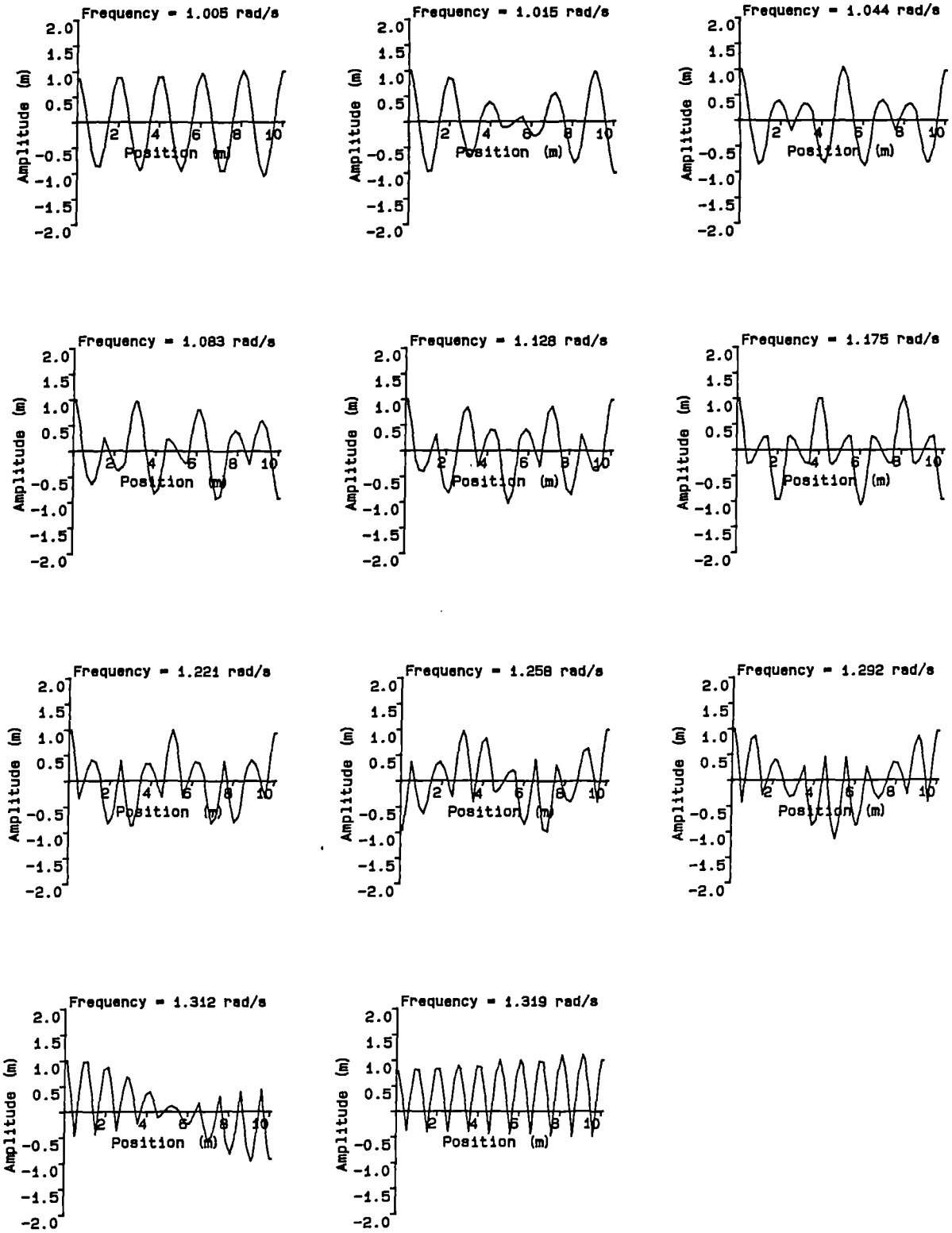

Figure 7.6 - Mode shapes and natural frequencies ω_i for modes in the second pass band, calculated using F.E. methods (axial deflections shown transverse for clarity).

CHAPTER 8

Near-Periodic Systems

8.1. Analysis of Periodic Systems with Discontinuities

Practical structures are of course, never purely periodic. Sometimes departures from perfect periodicity are made deliberately and the differences are then likely to be large and infrequent, on other occasions deviations arise due to the inevitable errors inherent in the manufacturing process, and the differences are then usually small, but random. Often, both types of discontinuity occur at once in a design. Since SEA is concerned with the behaviour of systems with random parameters, the effects of changes from pure periodicity are central to any application of periodic theory to the method. Here the example of the previous chapter is modified in a variety of ways, and the resulting effects studied to see if the essential nature of 'stop' and 'pass' bands is preserved in such cases. If it is not, then application of the theories described in the previous chapter will be much more difficult. It transpires that this is not the case, at least as far as natural frequencies are concerned. However, mode shapes are again found to be more awkward to deal with.

8.2. Single Defects

The simplest defect that can arise in an otherwise periodic system is the single discontinuity. The effects of such changes are easily calculated, and give rise to changes in the behaviour of the system that are not unexpected when due consideration is given to the nature of purely periodic systems, for example see Ziman[29] , article 8.7. If one element of a system of symmetric elements is distorted, its natural frequencies will change in a predictable fashion. Since the boundaries of the 'pass' bands for such an element lie at its natural frequencies, this will give rise to a structure that has a section with non-standard 'pass' bands. Now, as the natural frequencies for the whole system will occur within both the standard and non-standard 'pass' bands, the possibility of modes lying outside the

predominant standard 'pass' bands arises. These modes, which are associated with the resonance of the modified element, will rapidly decay in the periodic portion of the system, since they lie in the 'stop' bands for these portions. The outcome is mode shapes that are sharply localized in the vicinity of the defect, with amplitudes decreasing exponentially away from it.

By way of example, consider the previous ten unit periodic system of light and heavy elements and make one element (the second from the left, say) have a centre section with half the previous mass density per unit length. Clearly, the natural frequencies of this particular element will tend to rise, causing the boundaries of the 'pass' bands to migrate upwards. For the second 'pass' band this gives rise to the overall cross-receptance shown in Figure 8.1, where both the standard value of μ and that pertaining in the non-standard element, μ', are also indicated, c.f. Figure 7.4b. As may be seen, there is now a single natural frequency lying in the 'stop' band of most of the system. The mode shapes for this revised system are given in Figure 8.2 together with their changed natural frequencies, ω_i', c.f. Figure 7.5. As expected, all the modes extend throughout the structure, except for that where the natural frequency lies in the 'stop' band. These results have been calculated using the receptance theory outlined above, but entirely similar results are recovered from a F.E. study, see Figure 8.3. It would seem that such a feature *is* recoverable using standard techniques.

The effects on other groups of modes are similar; whenever a mode lies in the 'stop' band of the bulk of the structure, that mode is exponentially localized: all that the magnitude of the defect affects is the rapidity of the localization. This exponential relationship becomes clear when the absolute magnitudes of the standing waves present within a portion of the system (the Y_l's of equation (7.31)) are plotted on logarithmic scales, see Figure 8.4.

When the higher 'pass' bands are examined it is found that, since the fundamental repetition of the widths of the bands have differing periods, the modes lie in all manner of combinations of 'pass' and 'stop' bands. Nonetheless, the same phenomenon is observed concerning the localizations of modes. In these higher bands the traditional F.E. analysis of course breaks down unless increasingly many elements are included in the discretization: this is the fundamental limitation of the F.E.

approach.

One class of exceptions to this rule concerning localization of modes lying in 'stop' bands is however apparent. When a system is constructed such that at its extreme ends, incomplete periodic elements occur, it may be argued that no defects are present. However, these incomplete elements cause modes to lie within the 'stop' bands for the system. Even so, these modes have finite amplitudes at the extremes and are thus not strictly localized. In solid state physics such modes are known as *surface modes*. All of this reinforces the view that, although natural frequencies may usually be predicted from a knowledge of the 'pass' and 'stop' bands, mode shapes are highly varied.

The theories based on purely periodic systems may not be readily applied to the modified example. However, by considering it as a collection of end-coupled periodic systems, some progress can be made. Consider the product

$$[T]_1^{M_1}.[T]_2^{M_2} \tag{8.1}$$

which describes the overall transfer matrix of a system consisting of M_1 elements of type 1 coupled to M_2 elements of type 2. This matrix becomes, for symmetric elements throughout

$$\frac{(D_1+D_2)}{2D_2}\begin{bmatrix} \cosh(M_1\mu d_1+M_2\mu d_2) & D_2\sinh(M_1\mu d_1+M_2\mu d_2) \\ \frac{1}{D_1}\sinh(M_1\mu d_1+M_2\mu d_2) & \frac{D_2}{D_1}\cosh(M_1\mu d_1+M_2\mu d_2) \end{bmatrix} \tag{8.2}$$

$$-\frac{(D_1-D_2)}{2D_2}\begin{bmatrix} \cosh(M_1\mu d_1-M_2\mu d_2) & -D_2\sinh(M_1\mu d_1-M_2\mu d_2) \\ \frac{1}{D_1}\sinh(M_1\mu d_1-M_2\mu d_2) & \frac{-D_2}{D_1}\cosh(M_1\mu d_1-M_2\mu d_2) \end{bmatrix}$$

Notice that the two matrices represent average and differential terms. Again the ratio of the upper and lower-left terms of the sum of the matrices forms the overall system direct receptance, and it may be used to establish the natural frequencies of the system. This process can be carried out *ad infinitum* with one transfer matrix power per group of similar periodic units. It has been carried out for four differing groups but this process is algebraically unwieldy and is not reproduced here. Setting the subscripts 1-4 to indicate the four groups of periodic elements, containing M_1, M_2, M_3 and M_4 elements respectively, and using ζ_1, $\zeta_2 \cdots$ to indicate the product $M_1\mu d_1$, $M_2\mu d_2 \cdots$ etc., the final overall

transfer matrix becomes

$$\frac{(D_1+D_2)(D_2+D_3)(D_3+D_4)}{8D_2D_3D_4}\begin{bmatrix}\cosh(\zeta_1+\zeta_2+\zeta_3+\zeta_4) & D_4\cosh(\zeta_1+\zeta_2+\zeta_3+\zeta_4)\\ \frac{1}{D_1}\sinh(\zeta_1+\zeta_2+\zeta_3+\zeta_4) & \frac{D_4}{D_1}\sinh(\zeta_1+\zeta_2+\zeta_3+\zeta_4)\end{bmatrix} \tag{8.3}$$

$$-\frac{(D_1-D_2)(-D_2+D_3)(D_3+D_4)}{8D_2D_3D_4}\begin{bmatrix}\cosh(\zeta_1-\zeta_2+\zeta_3+\zeta_4) & D_4\cosh(\zeta_1-\zeta_2+\zeta_3+\zeta_4)\\ \frac{1}{D_1}\sinh(\zeta_1-\zeta_2+\zeta_3+\zeta_4) & \frac{D_4}{D_1}\sinh(\zeta_1-\zeta_2+\zeta_3+\zeta_4)\end{bmatrix}$$

$$-\frac{(D_1+D_2)(D_2-D_3)(-D_3+D_4)}{8D_2D_3D_4}\begin{bmatrix}\cosh(\zeta_1+\zeta_2-\zeta_3+\zeta_4) & D_4\cosh(\zeta_1+\zeta_2-\zeta_3+\zeta_4)\\ \frac{1}{D_1}\sinh(\zeta_1+\zeta_2-\zeta_3+\zeta_4) & \frac{D_4}{D_1}\sinh(\zeta_1+\zeta_2-\zeta_3+\zeta_4)\end{bmatrix}$$

$$-\frac{(D_1+D_2)(D_2+D_3)(D_3-D_4)}{8D_2D_3D_4}\begin{bmatrix}\cosh(\zeta_1+\zeta_2+\zeta_3-\zeta_4) & D_4\cosh(\zeta_1+\zeta_2+\zeta_3-\zeta_4)\\ \frac{1}{D_1}\sinh(\zeta_1+\zeta_2+\zeta_3-\zeta_4) & \frac{D_4}{D_1}\sinh(\zeta_1+\zeta_2+\zeta_3-\zeta_4)\end{bmatrix}$$

$$+\frac{(D_1-D_2)(-D_2-D_3)(-D_3+D_4)}{8D_2D_3D_4}\begin{bmatrix}\cosh(\zeta_1-\zeta_2-\zeta_3+\zeta_4) & D_4\cosh(\zeta_1-\zeta_2-\zeta_3+\zeta_4)\\ \frac{1}{D_1}\sinh(\zeta_1-\zeta_2-\zeta_3+\zeta_4) & \frac{D_4}{D_1}\sinh(\zeta_1-\zeta_2-\zeta_3+\zeta_4)\end{bmatrix}$$

$$+\frac{(D_1-D_2)(-D_2+D_3)(D_3-D_4)}{8D_2D_3D_4}\begin{bmatrix}\cosh(\zeta_1-\zeta_2+\zeta_3-\zeta_4) & D_4\cosh(\zeta_1-\zeta_2+\zeta_3-\zeta_4)\\ \frac{1}{D_1}\sinh(\zeta_1-\zeta_2+\zeta_3-\zeta_4) & \frac{D_4}{D_1}\sinh(\zeta_1-\zeta_2+\zeta_3-\zeta_4)\end{bmatrix}$$

$$+\frac{(D_1+D_2)(D_2-D_3)(-D_3-D_4)}{8D_2D_3D_4}\begin{bmatrix}\cosh(\zeta_1+\zeta_2-\zeta_3-\zeta_4) & D_4\cosh(\zeta_1+\zeta_2-\zeta_3-\zeta_4)\\ \frac{1}{D_1}\sinh(\zeta_1+\zeta_2-\zeta_3-\zeta_4) & \frac{D_4}{D_1}\sinh(\zeta_1+\zeta_2-\zeta_3-\zeta_4)\end{bmatrix}$$

$$-\frac{(D_1-D_2)(-D_2-D_3)(-D_3-D_4)}{8D_2D_3D_4}\begin{bmatrix}\cosh(\zeta_1-\zeta_2-\zeta_3-\zeta_4) & D_4\cosh(\zeta_1-\zeta_2-\zeta_3-\zeta_4)\\ \frac{1}{D_1}\sinh(\zeta_1-\zeta_2-\zeta_3-\zeta_4) & \frac{D_4}{D_1}\sinh(\zeta_1-\zeta_2-\zeta_3-\zeta_4)\end{bmatrix}$$

The distinct pattern of average and differential terms that is apparent in this result allows for a simple nested loop computer implementation, which may be readily used to describe the behaviour of a wide range of systems. It recovers the results given by Mead and Lee[34] for point masses and springs, but now has been extended to a more general approach giving greater insight than is possible using the

pure receptance methods outlined in that work. However, it is probably no faster computationally.

8.3. Random Small Defects

Random defects give rise to a more subtle form of localization than that caused by a single, bold modification. These effects have been extensively studied by physicists, but have only recently aroused interest in structural engineers[46, 52, 53]. This interest stems from the fact that, although physically a structure is intended to be periodic, in reality the practices of construction will introduce random small defects. The fundamental property of all disordered linear chains is often known as *Anderson Localization*[44, 54]. The phenomenon has been studied for one, two and three-dimensional problems, but usually for systems with very many constituents. Briefly the phenomenon of *Anderson Localization* may be stated as, (see Ziman[29]),

> " *the eigenfunctions are localized even in a spectral region where the Bloch functions of a regular chain of each of the constituents would be extended* "

In other words, localization *can* arise when the natural frequency occurs in such a position as to lie in the 'pass' band for *all* elements. The arguments underlying this effect are somewhat subtle, but essentially depend on the probability of being able to predict the behaviour at one end of a long chain, given details of the other. When the system is purely periodic this is simple, but when random defects are introduced, the probability of being able to do this becomes vanishingly small, see Borland[48]. The consequence is that waves are unable to travel throughout the system, implying that the modes must be localized. As Ziman[29] goes on to note, the strength of the localization in one dimension that arises because of this property is rather weak and is often only noticed over extremely large numbers of sub-systems. Moreover, it is only the average amplitude of motion that decays, and quite large fluctuations about this trend may be observed: this contrasts with the situation outlined previously for just one disorder. Because the large numbers of sub-systems required do not usually arise in the structures of interest to vibration engineers, this feature may seem to be of academic interest only. Of course if transmission between the ends of a structure with some tens of periodic units is of interest, a small

transmission loss at each element may well product up to a substantial effect. (Some likely candidates are satellites, towed-array sonars or the legs of offshore jack-up structures, where hundreds of periodic units may be present.)

To illustrate the effects of random small defects on engineering problems, the previous example of ten periodic elements is used, but with the heavy, centre sections of the units taken to have masses that are normally distributed about the previous value of 100.0 kg/m with a standard deviation of 10.0 kg/m, all other parameters being kept constant. The cross-receptance for this system is given in Figure 8.5, and the associated mode shapes and natural frequencies are displayed in Figure 8.6. No clear pattern emerges, and certainly the rapid exponential localization caused by a single well chosen defect is absent.

To see the effects of *Anderson Localization* requires significantly greater numbers of periodic units. If the previous example is extended to include 250 periodic units, again with random masses, the desired effect is achieved. This is illustrated in Figure 8.7a, which shows the amplitude of the waves within each sub-element, (Y_i) as well as the actual mode shape. Here the fluctuations and localization become apparent, but the fall off with distance is much less severe than for the case of the single large defect, c.f. Figure 8.4, mode shape for 1.3444 rad/s. This result is not dissimilar to that given by Borland[48].

It is noted in passing that *all* modes of this much longer, randomized system should localize according to accepted understanding of the phenomenon, see Ziman[29]. At least one mode has been discovered for this system which does not appear to behave in this way, see Figure 8.7b. The reason for this occurrence is not fully understood and is the subject of further studies. One tentative explanation is possible: this model still uses purely symmetric sub-systems and the heavy sections within these are virtually point masses. Moreover, it is *only* these heavy sections that are random. Clearly for the case of random point masses periodically spaced there will always be a mode where the masses remain stationary and only the intervening sections vibrate. In this degenerate case the system reverts to purely periodic behaviour. The system used here perhaps shows sufficient similarity to this degenerate

case that the mode illustrated will localize only when an even larger number of units is included.

It is interesting to recall that in the previous chapter the use of point masses was cited as a limitation in the analysis used by Hodges and Woodhouse[46], and yet here this model is used to explain the unexpected behaviour of a long randomized system. Clearly, the use of such idealizations is not straight-forward and can lead to unforeseen consequences.

8.4. Combined Forms of Defect

It is perhaps reasonable to expect that the effect of random defects on structures with few periodic units would be to lessen the consequences of any large, distinct discontinuities. This expectation arises because the very precise mistuning produced by the single defect in an otherwise exact structure would be lost (in electrical terms the 'Q' of the filter would be degraded). This is apparently not the case, however: if the defects of the previous two models, using ten periodic units, are combined (i.e., one element significantly different and the others with small fluctuations), no significant changes arise compared with the case of just the distinct single defect, see Figure 8.8, c.f. Figure 8.2. This perhaps surprising result indicates that the use of deliberate defects to modify the behaviour of a structure should be possible *despite* the presence of other small random errors.

This result invites inquiry as to how large the random defects need to become before they will swamp the distinct individual modification. Other workers note that the two regimes outlined do not have a sharp division; rather the one blends into the other as the number of sub-systems and the randomness of the deviations increase, see Ziman[29]. It is thought that this blending may perhaps have a distinct division when considering two and three-dimensional systems, but this is a topic of current research in the field of crystalline physics and is perhaps also of less relevance to engineering structures, where the periodic patterns of interest tend to lie in a single direction.

8.5. Summary of Periodic Theory

Chapters 7 and 8 have discussed some of the methods of periodic theory as they apply to the vibrations of simple one-dimensional, undamped engineering structures. This approach has shown that the natural frequencies of such systems tend to lie in groups defined by the 'pass' bands of the individual elements. This is clearly very relevant information when carrying out SEA on structures of periodic nature and to ignore it would seem unwise. Conversely, the behaviour of the modes of periodic structures is orderly only provided that defects are not introduced. Since all engineering structures must contain some imperfections, and also because SEA is built on the assumption of ensembles of similar, but not identical, systems, the effects of defects must be accepted when undertaking SEA. However, the changes that arise in mode shapes because of these defects vary from the slight to the dramatic, and it is clear that simple tools for predicting their probability density functions do not exist. These various ideas are discussed further during the study of a final example in Chapter 9.

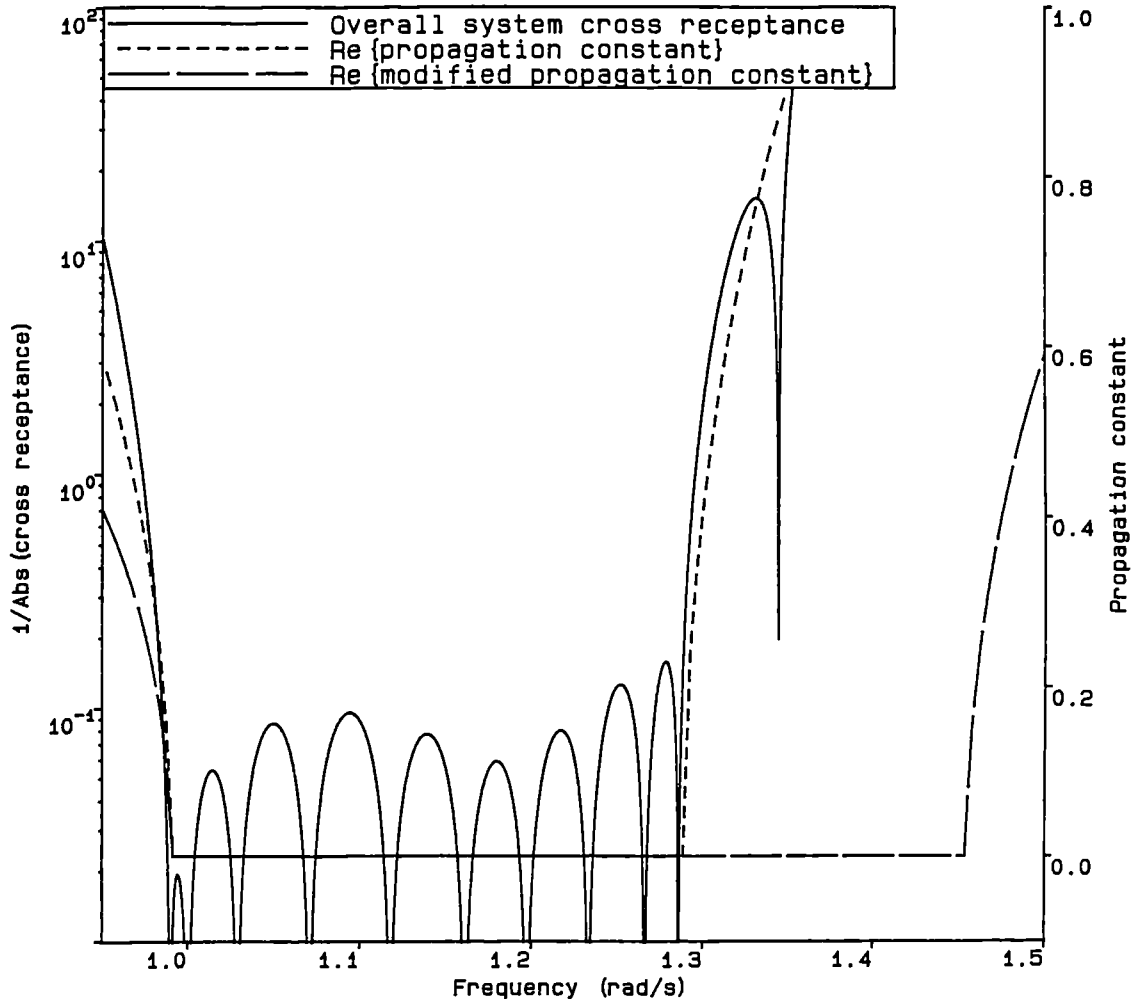

Figure 8.1 - Graph of the overall cross receptance and real parts of μ and μ' versus radian frequency ω for the system with one light element.

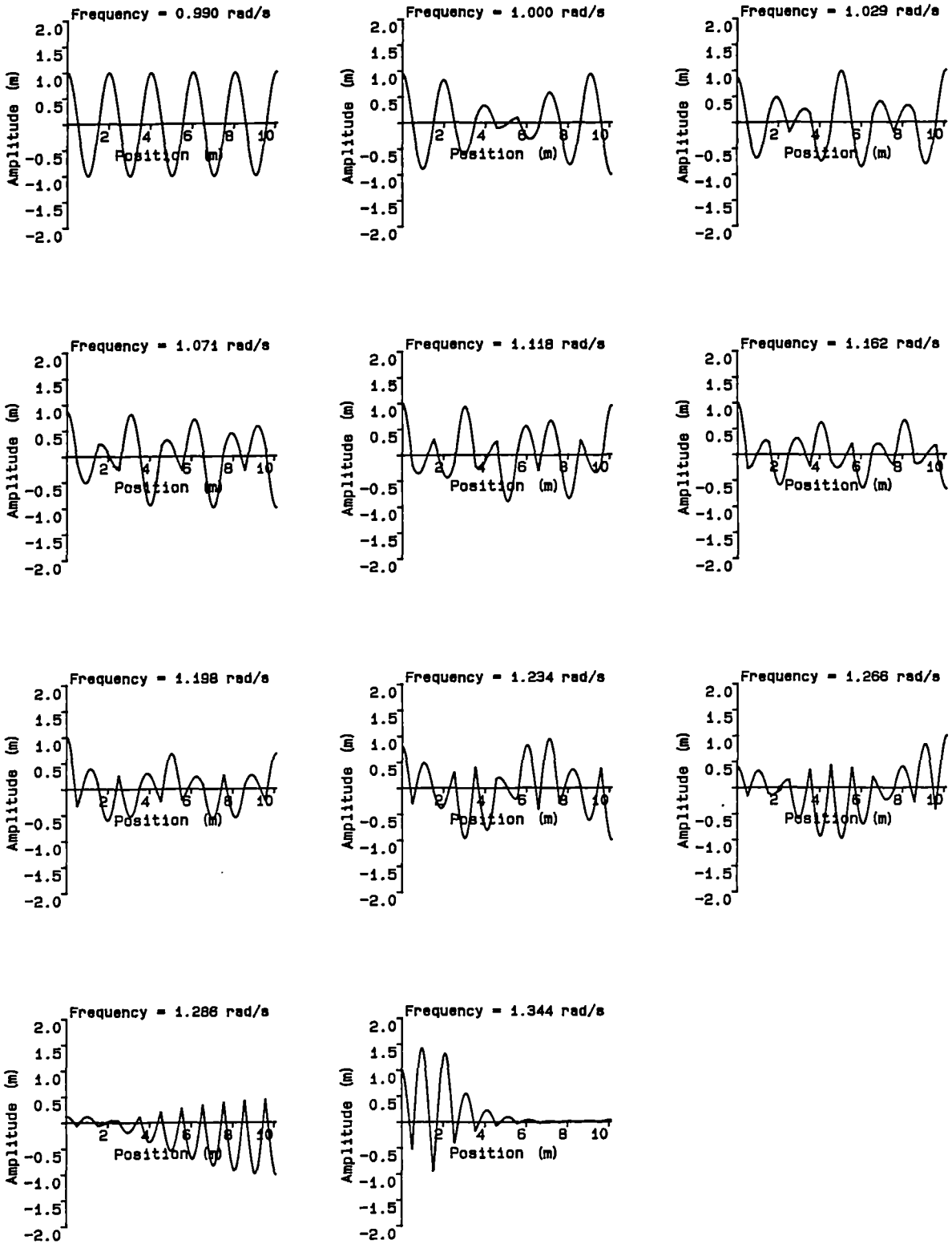

Figure 8.2 - Mode shapes and natural frequencies ω_i' for modes in the second 'pass' band, calculated using receptance theory, for the system with one light element (axial deflections shown transverse for clarity).

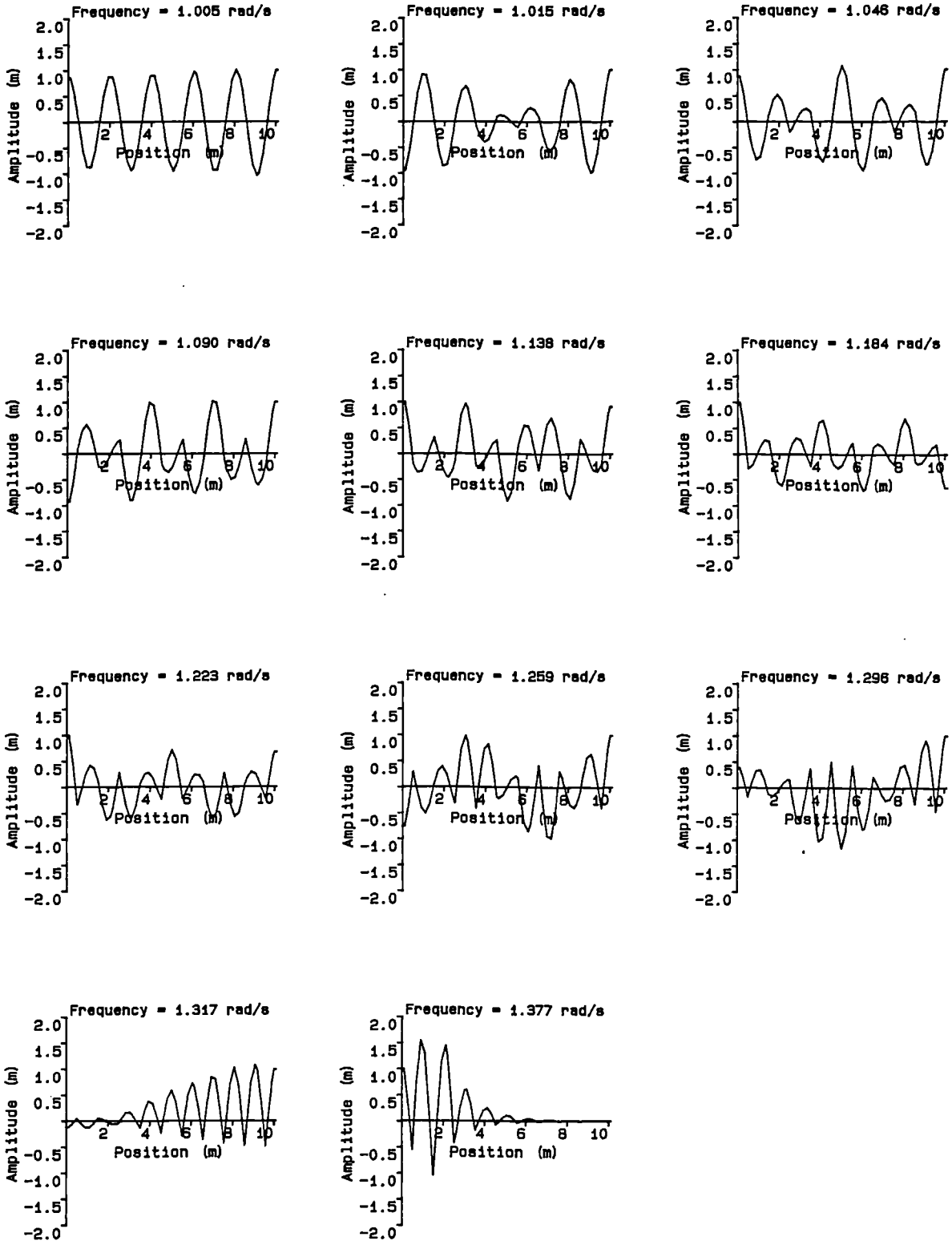

Figure 8.3 - Mode shapes and natural frequencies ω_i' for modes in the second 'pass' band, calculated using F.E. methods, for the system with one light element (axial deflections shown transverse for clarity).

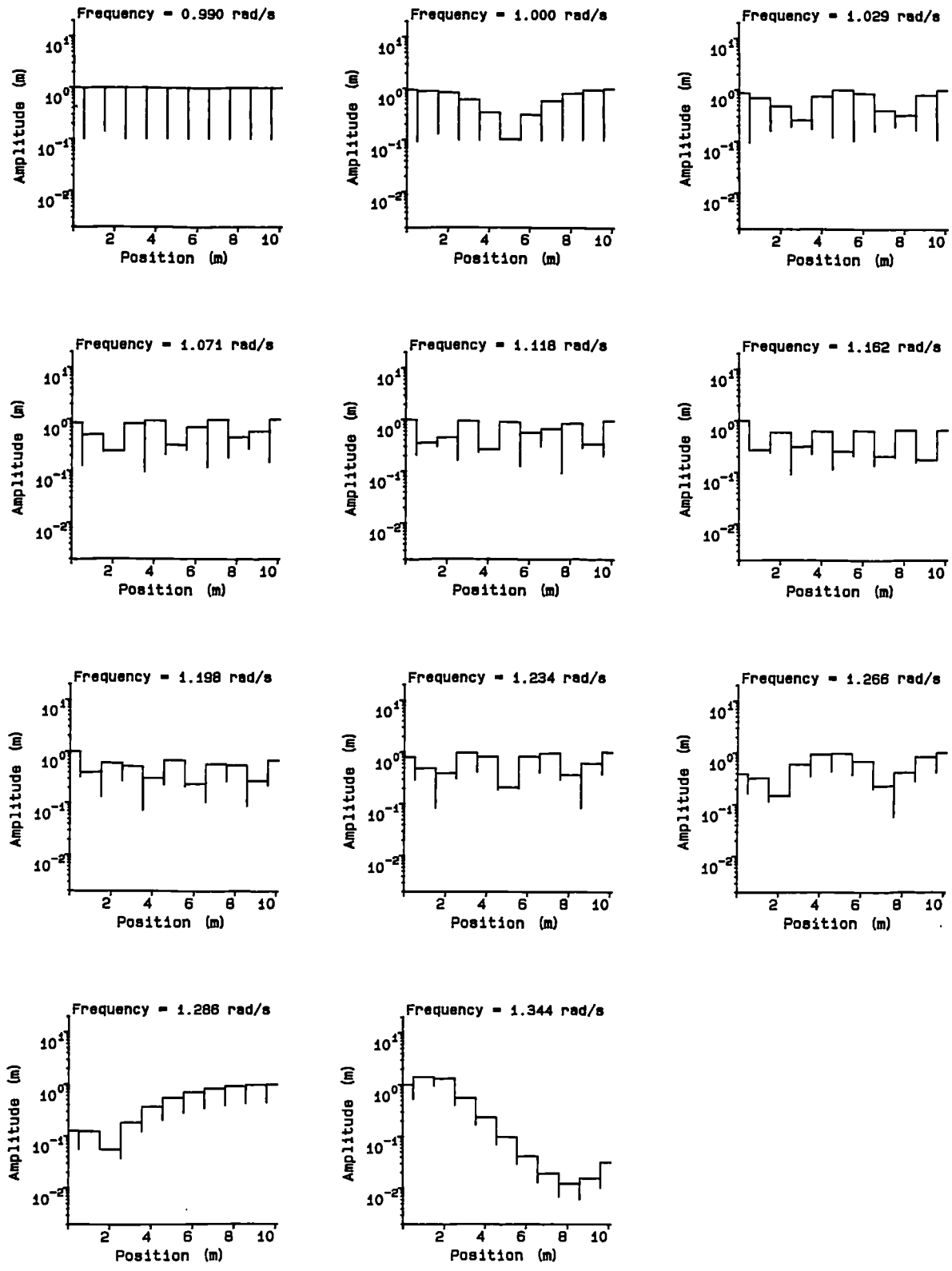

Figure 8.4 - Amplitudes of standing waves Y_i and natural frequencies ω_i' for modes in the second 'pass' band, calculated using receptance theory, for the system with one light element.

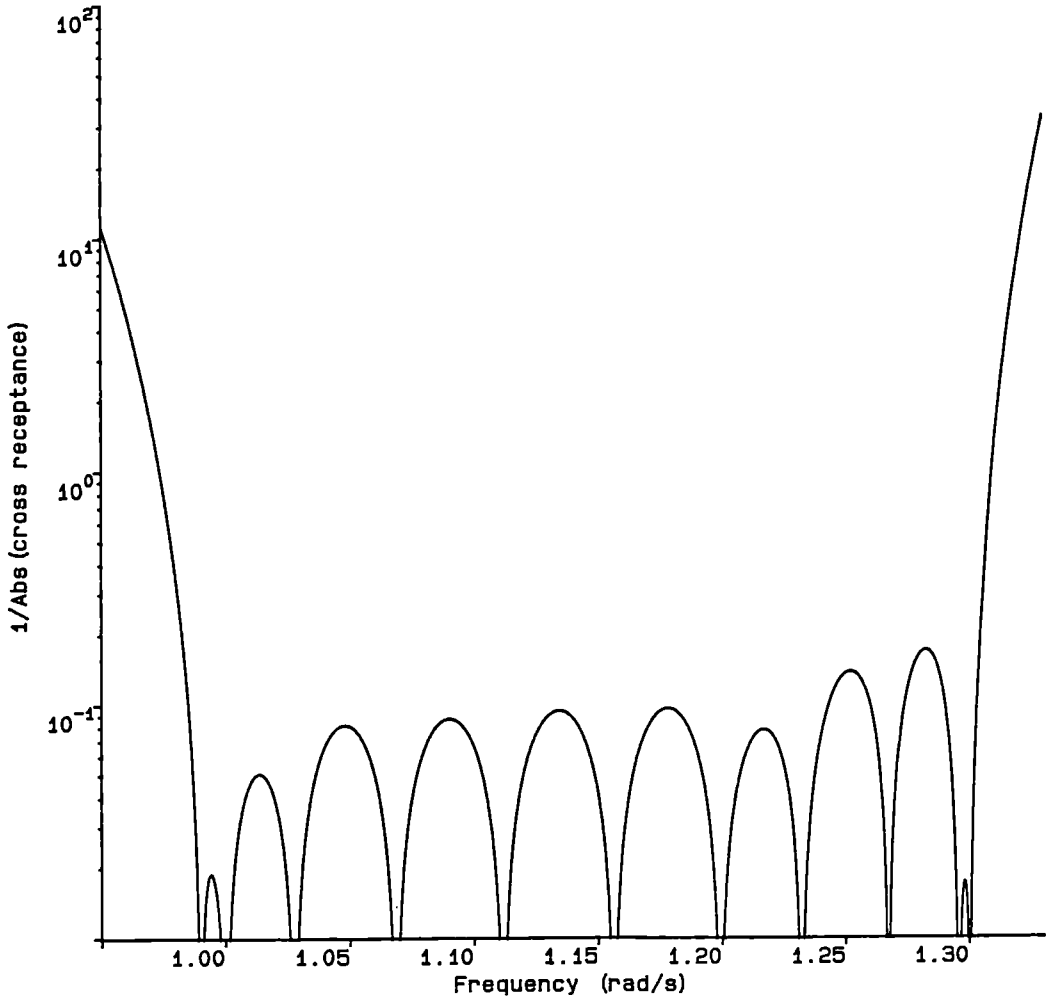

Figure 8.5 - Graph of the overall cross receptance versus radian frequency ω for the system with random masses.

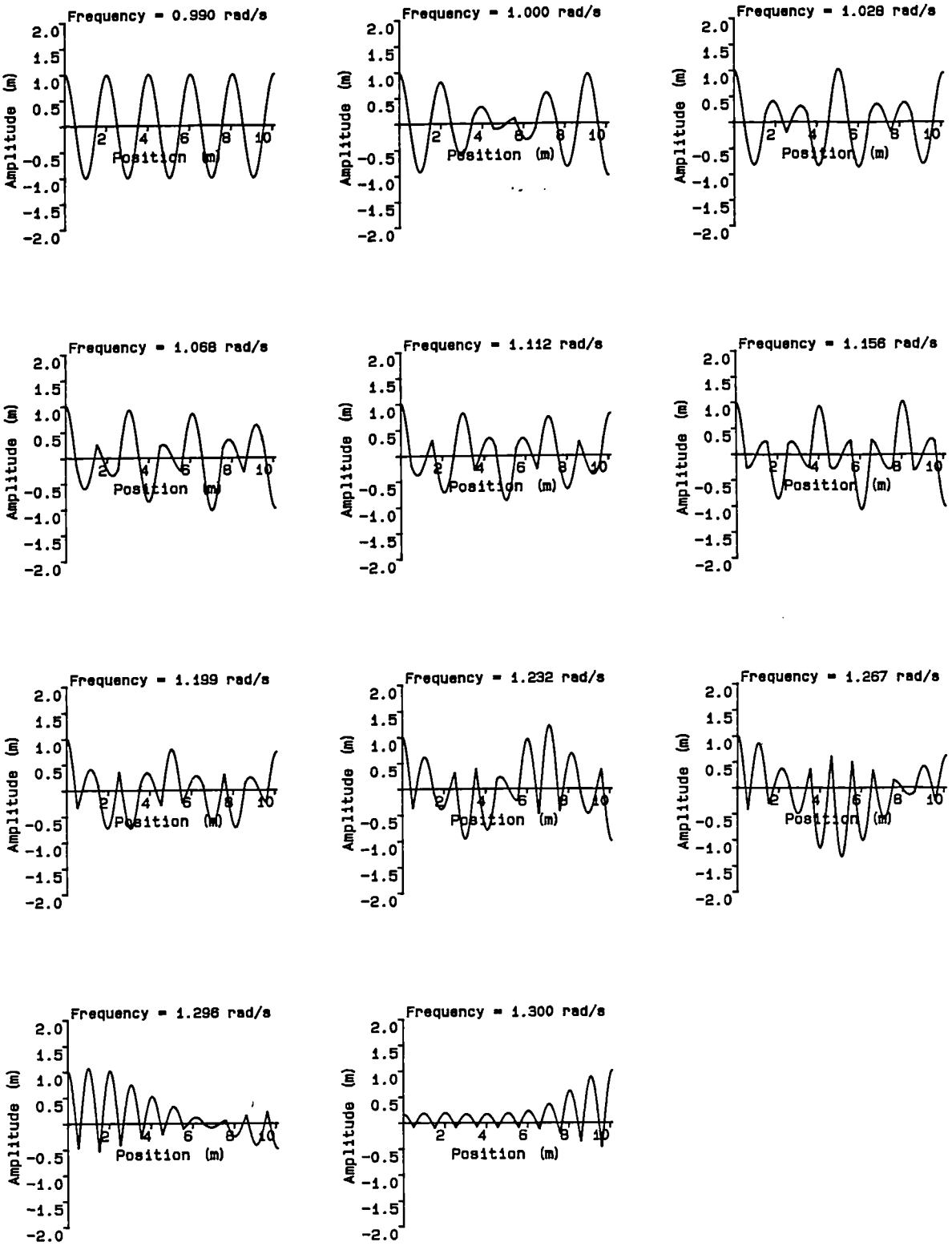

Figure 8.6 - Mode shapes and natural frequencies ω_i' for modes in the second 'pass' band, calculated using receptance theory, for the system with random masses (axial deflections shown transverse for clarity).

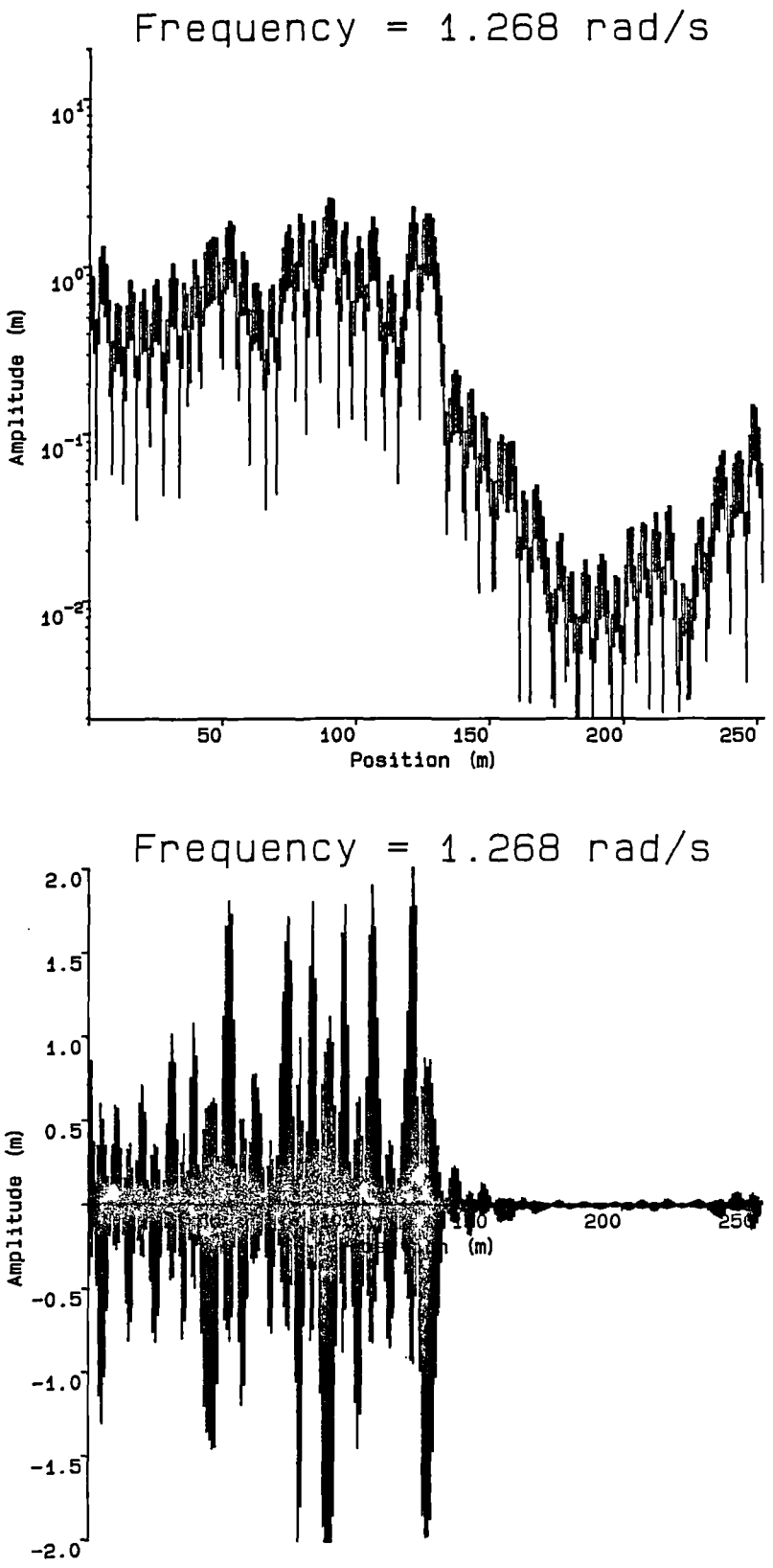

Figure 8.7a - Amplitude of the standing wave Y_i (upper), mode shape and natural frequency ω_i' (lower), for one mode of a system with 250 periodic units and random masses, calculated using receptance theory (axial deflections shown transverse for clarity).

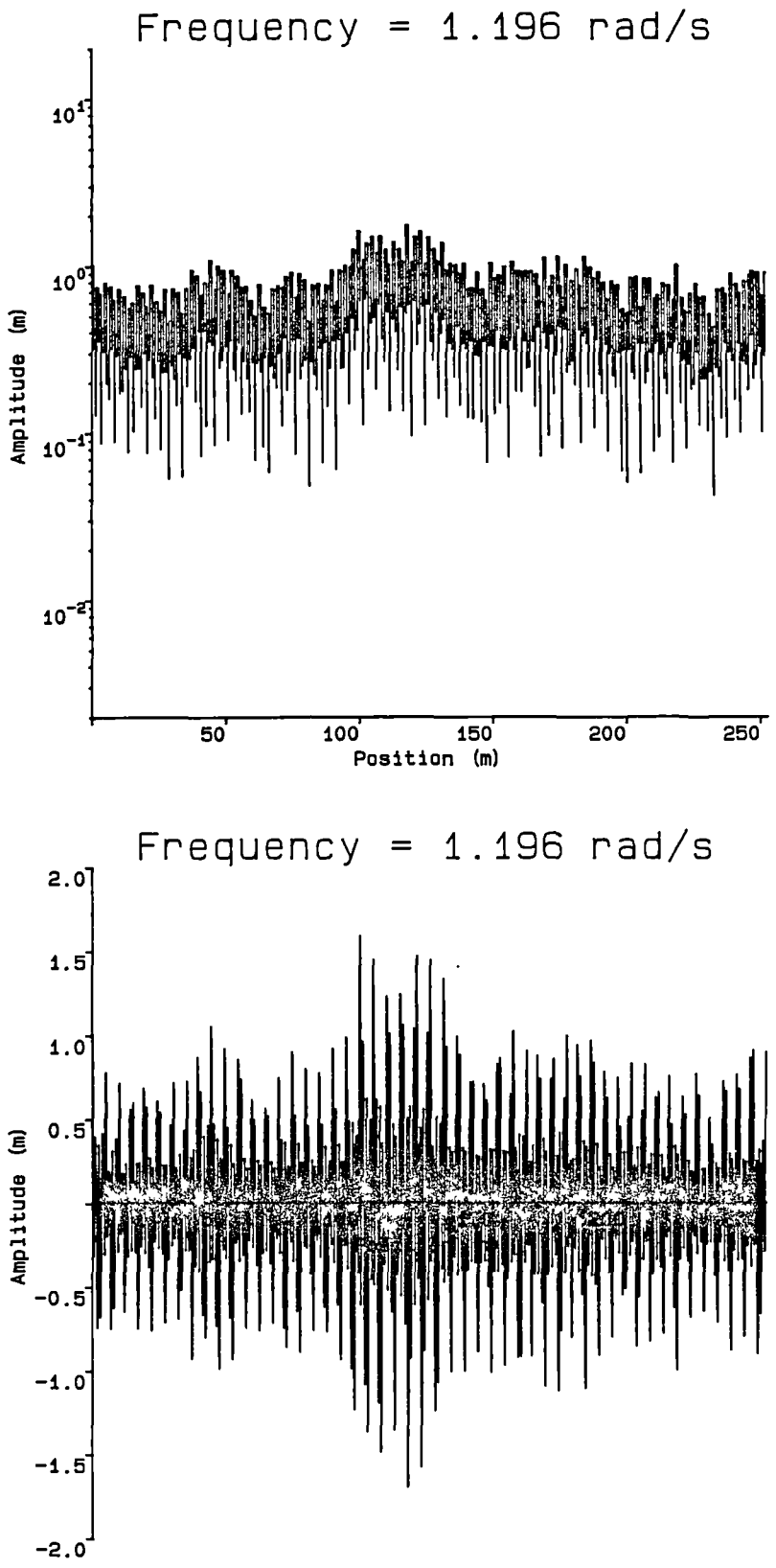

Figure 8.7b - Amplitude of the standing wave Y_i (upper), mode shape and natural frequency ω_i' (lower), for a mode of a system with 250 periodic units and random masses, that does not localize, calculated using receptance theory (axial deflections shown transverse for clarity).

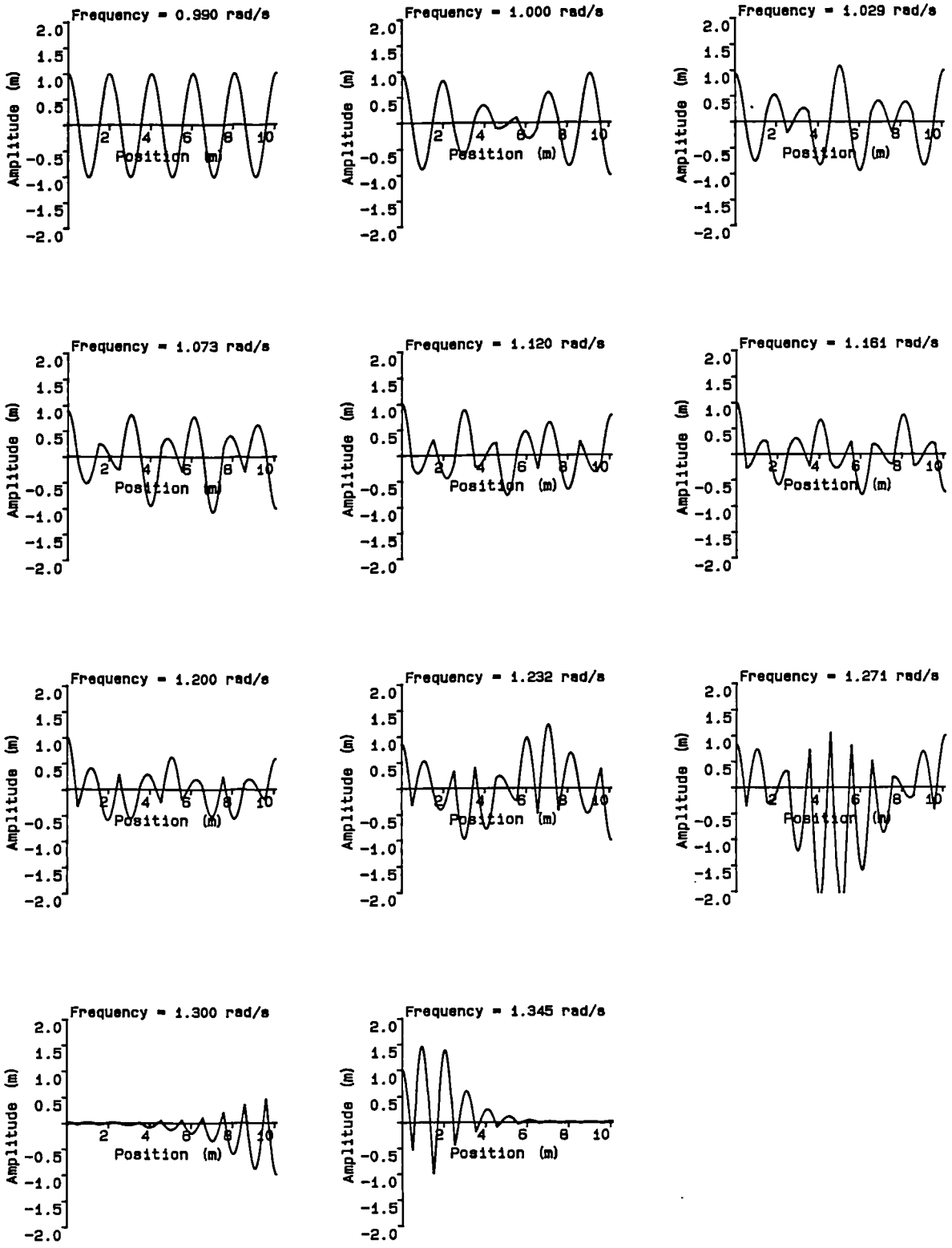

Figure 8.8 - Mode shapes and natural frequencies ω_i' for modes in the second 'pass' band, calculated using receptance theory, for the system with one light element and random masses (axial deflections shown transverse for clarity).

CHAPTER 9

Statistical Energy Analysis of a Periodic Example

9.1. The Example

The final example to be discussed in this work is illustrated in Figure 9.1, which shows part of the structure of a ship. The details of the various elements making up this example are given in Table 9.1 and are typical of a modern warship. Clearly the example chosen is highly idealised, there being no major discontinuities in the steel work, which is also assumed flat. However, to study even this model using the techniques discussed in the previous chapters, *additional simplifications are necessary*.

As has already been mentioned, the flow of energy around structures of the type considered here tends to arise because of axial vibrations, these being observed when they couple to transverse vibrations in any given location. Additionally, the tools developed so far are valid only for mono-coupled transfers of energy. Therefore the hull-bulkhead model is further idealised as two, point-spring coupled, axially vibrating, free-free rods, but now with periodic fluctuations in parameters, see Table 9.2 and Figure 9.2, c.f. Tables 4.1, 7.1 and Figures 4.1, 7.2. Notice that the stiffeners perpendicular to the direction of vibration have been modelled as point masses, and those parallel to it included in the cross-section of the rod portions, the resulting periodic unit consisting of a rod sub-element (A) with a

DETAILS OF THE EXAMPLE SHIP STRUCTURE			
Parameter	Hull	Bulkhead	Units
Plate thickness	10	6	mm
Vertical stiffener type	7	6	see BS4 part 1, 1962
Horizontal stiffener type	2	n/a	see BS4 part 1, 1962
Young's modulus	207	207	GPa
Density	7820	7820	kg/m^3

Table 9.1

point mass (B) at one end (i.e., an unsymmetric element). The junction between these two *perpendicular* sub-systems is represented by a pair of point masses located at the extreme ends of the sub-systems, where they meet together with a linear spring coupling two arbitrarily positioned points within the final rod sub-elements. The point masses simulate the contribution of the transverse inertia of one sub-system (which is ignored in the axially vibrating model of that sub-system) to the longitudinal inertia of the other. The masses are chosen to be similar to those representing the other vertical stiffeners for consistency and convenience. The arbitrary positions of the coupling points take account of the importance of transverse vibration to the coupling mechanism. This mechanism is unlikely to be dominated by the strong modal coherence found at the free ends of the axial models used here. The consequences of moving these points to the extreme ends of the sub-systems are illustrated later. The limitations imposed by using point masses on 'pass' band widths, noted in Chapter 7, only arise above 15 kHz here and are therefore safely ignored. Finally, the damping constants, which are for a proportional damping model, are chosen to give light damping which rises to only 20% of critical at 10 kHz. Again only one sub-system (the hull) will be forced, and the average cross-receptance $E[H_{12}(\omega)]$ studied, so as to clarify the various results.

AXIALLY VIBRATING ROD PARAMETERS FOR THE SHIP STRUCTURE			
Parameter	Sub-system 1 Hull	Sub-system 2 Bulkhead	Units
Rod mass density per unit length (ρ_A)	46.53	23.46	kg/m
Rod length (l_A)	1	0.5	m
Rod rigidity (AE_A)	1.231	0.621	GN
Point masses ($\rho_B l_B$)	17.7	12.5	kg
Element length ($d=l_A+l_B$)	1	0.5	m
Element damping (c_1, c_2)	500	500	s^{-1}
No. of elements per sub-system	11	16	-
Summation band-width	2	2	kHz

Table 9.2

9.2. Application of Periodic Theory

Before applying statistical models to the hull/bulkhead problem, periodic theory will be used to analyse the uncoupled, perfectly periodic, individual sub-systems. First the 'pass' and 'stop' bands of the two sub-systems are found by constructing the functions $\cosh(\mu d)$ from the element receptances (see equations (7.19), (7.22), (7.23), (7.38) and (7.39)) and establishing the frequency ranges where they lie in the range ± 1; see Figure 9.3 where

$$\cosh(\mu d) = \cos(\omega l_A \sqrt{\rho_A / A E_A}) - \frac{\omega^2 \rho_B l_B}{2\omega \sqrt{m_A A E_A}} \sin(\omega l_A \sqrt{\rho_A / A E_A}) \tag{9.1}$$

c.f. equation (7.12). Notice that, as expected, a sequence of narrowing 'pass' bands is observed and additionally that these bands overlap at various frequencies, specifically from 0 to 1.9 kHz, 2.6 to 2.8 kHz, 5.1 to 6.1 kHz and 10.3 to 10.9 kHz. Clearly, in these frequency ranges large energy flows between the two sub-systems are more probable, given the likelihood of co-incident natural frequencies.

If the overall cross-receptance curves of the uncoupled sub-systems are plotted, Figure 9.4, this overlap is again visible, and now the actual natural frequencies for the perfectly periodic sub-systems may also be seen, there being eleven modes per 'pass' band of the hull and sixteen for the bulkhead. This is as expected, given the number of repeated periodic units in each. The mode shapes from the second 'pass' band of the hull are illustrated in Figure 9.5 c.f. Figure 7.5, and notice that the displacements are again *axial* and have merely been shown as transverse for clarity.

9.3. Random Parameters

To produce an ensemble of random hull/bulkhead models, the mass densities of *all* sub-elements in *both* sub-systems are randomized so that they have normal distributions whose means align with the values in Table 9.2 and with standard deviations of 10% of these. The natural frequencies and modes of one possible realisation for the hull second 'pass' band are illustrated in Figure 9.6, c.f. Figure 8.6

If some 500 different realisations are produced and analysed for *all* their respective modes in the frequency range 0-12 kHz, Figures 9.7 and 9.8 result. These histograms, which contain approximately 25,000 different eigensolutions, show the numbers of natural frequencies occurring in each 80 Hz division of the frequency spectrum in Figure 9.7 and the variation in ψ^2 at the coupling point (lying at arbitrary positions within the end sub-elements of the sub-systems) in Figure 9.8. Figure 9.7 clearly shows the presence of the 'stop' and 'pass' bands seen in Figures 9.3 and 9.4. Additionally, it shows that the natural frequencies of the first 'pass' band are not chaotic, tending to occur at similar frequencies for all members of the ensemble. At higher frequencies the banding slowly breaks down, reverting towards a uniform distribution. These features are as expected and have already been discussed in Chapter 6. What is particularly interesting is that standard deviations of 10% do not cause this breakdown to be significant below 10 kHz. In the range 2-10 kHz the PDF model proposed in Chapter 6 and illustrated in Figure 6.1 would appear to be valid. Below this, deterministic methods would seem to be more appropriate. This is very interesting, given that traditional SEA methods cannot cope with such banding and also that most of the vibrational problems that occur in such ships arise in the range 100 Hz to 10 kHz, see for example Kinns[55].

Figure 9.8 illustrates very strikingly the difficulties to be overcome in predicting the ψ^2 term in the coupling summations. The large majority of modes have rather small values of ψ^2 at the chosen coupling point($<0.1\ m^2$). These are balanced at the other extreme by a few rare modes whose ψ^2 amplitudes at this point are occasionally as high as $15\ m^2$. In fact the extreme values found for the ensemble used here were $27.5\ m^2$ and $55.5\ m^2$ for the hull and bulkhead, respectively. Then there is a rather more common group whose values lie in the range $0.1\ m^2$ to $2.0\ m^2$. Against this it must be recalled that traditional SEA assumes this parameter is unity for all modes. The problem is made more complex by the fact that the extremes of ψ^2 (both small and large) are made worse by the squaring required to form the parameter, and also that the extremes become increasingly unpredictable as the higher natural frequencies are encountered. This of course implies that a joint PDF of ω_n and ψ should be adopted if variations of mode shape parameters are to be used at all. The only conclusion that can

be reached from these mode shape results is that SEA is most likely to overestimate the coupling parameters and that if underestimates do occur, these are unlikely to be in error by more than a factor of two (although factors as high as 50 are conceivable).

To make use of the natural frequency results shown in Figure 9.7, probability density functions must be constructed. This is achieved by scaling the area under the histograms to unity and adopting continuous functions in place of the discrete histograms, see Figure 9.9. (Figure 9.10 shows the equivalent PDFs for the coupling point mode shapes, but with logarithmic scales that reveal more clearly the extent of the high amplitude tail in the PDFs.) These curves may be used to generate sequences of random numbers with the desired probability distributions, provided the natural frequencies and mode shape functions are assumed independent. To overcome the requirement of statistical independence, the individual results used to construct Figures 9.7 to 9.10 may be used directly in the SEA monte-carlo calculations, where they correctly model the cross-correlation between natural frequencies and mode shapes. As such, they form the basis for an 'exact' answer against which other approaches can be measured.

9.4. Statistical Energy Analysis (Weak Coupling)

To begin the SEA of the system illustrated in Figure 9.2, the traditional formulation, equation (3.47), is adopted and the variation of $E[H_{12}]$ plotted over a range of frequencies at low coupling strength, i.e., case 1 of Table 9.3, see Figure 9.11. This figure also shows the results of evaluating the multi-dimensional integrals, such as the one given in equation (3.36) (but with fixed k_c), using the ensemble of solutions discussed in the previous section. (Notice that the frequency range of this graph is reduced compared with that used in the previous figures, since provision must be made for the summation bandwidth, both above and below the frequency of calculation.) Although SEA correctly predicts the overall trends observed in the 'exact' solution, there are large discrepancies in many frequency sub-ranges. When it is noted that Figure 9.11 is plotted on logarithmic scales, these discrepancies appear even more significant. The fluctuations in the 'exact' curve are, of course, due to the non-

uniform distribution of natural frequencies and mode shapes of the near-periodic sub-systems used.

To make use of the 'pass' and 'stop' band information gained from studying the propagation constant μ, illustrated in Figure 9.3, PDFs of the form discussed in Chapter 6 are adopted for the natural frequencies, see Figure 9.12. Here the ratio of 'pass' band to 'stop' band probability is arbitrarily taken to be nine, which gives reasonable agreement with the parameter standard deviations of 10% of their means. When such piece-wise constant PDFs are used to generate random numbers for the natural frequencies, and additionally the mode shape parameters ψ^2 are assumed equal to unity, the full monte-carlo integrals of Chapter 3 give the results shown in Figure 9.13. This figure also includes the 'exact' and traditional curves from Figure 9.11. Clearly an improvement over traditional SEA has been achieved, which reproduces the increased flows of energy that occur when 'pass' bands overlap. Note that the large dips that occur in the 'exact' curve are accentuated by the logarithmic scales used in the figures. In fact, all that these dips indicate is that over some frequency ranges very few modes contribute to the energy flow between the sub-systems. These dips are very much less important than the peaks in the curve, which represent high energy flows. Moreover, they are very sensitive to the randomization scheme adopted, whereas the peaks are not. Similar remarks apply to the piece-wise constant PDF curve where it is the ratio of 'pass' to 'stop' band probability that governs the depths of the dips.

PARAMETERS USED IN THE EXAMPLES OF CHAPTER 9						
Case No.	Coupling Position		Coupling Strength	ν Sub-system		Coupling Type
	x_1, m	x_2, m	GN/m	1	2	
1	0.2727	0.0909	0.1	10.3	120	weak
2	0.0	0.0	0.1	10.3	120	weak
3	0.2727	0.0909	1	1.29	12.4	intermediate
4	0.2727	0.0909	10	0.39	1.62	intermediate
5	0.2727	0.0909	100	0.30	0.54	strong

Table 9.3

The monte-carlo integrations are rather tedious to perform, and so the approximate frequency PDFs of Figure 9.12 are next used in the simplified equations of Chapters 3 and 6. That is, equation (6.3) is integrated numerically. Figure 9.14 illustrates this approach, together with that resulting from assuming that the frequency PDFs are uniform, but with varying modal densities, depending on whether the frequency of interest lies in a 'pass' band or not. Both results are very similar, differing only in the transition between the 'pass' and 'stop' bands. More importantly, they are also similar to that achieved using the full monte-carlo technique, but with the approximate PDFs. This is as expected for this lightly coupled example. They therefore show reasonable correspondence to the behaviour of the 'exact' solution. Notice that, since the 'pass' bands overlap between 2.6 and 2.8 kHz, an increased energy flow is predicted in this frequency range, which does not in fact occur. This may be explained by studying Figure 9.9 which shows that the random natural frequencies do not *often* overlap in this rather narrow region, despite the overlapping 'pass' bands of the *perfectly* periodic sub-systems. Again the depths of the dips in these two curves depend on the chosen probability ratios.

If the extreme ends of the sub-systems are used as the coupling points, case 2 of Table 9.3, the agreement between the 'exact' monte-carlo results and the other methods worsens, see Figure 9.15. The fall-off with frequency in the 'exact' curve arises because of coupling point modal coherence at the masses on the free-ends of the rods. At high frequencies the modes of the sub-systems tend to nodes at these masses, with consequent small values of ψ^2. Removing the masses does not avoid this problem since the coherence prevails, but instead the the ends become anti-nodes and the resulting energy flows then lie above, rather than below, the predicted levels. Again the difficulties of dealing with mode shape coherence, which underlies these variations, is apparent.

9.5. Statistical Energy Analysis (Strong Coupling)

If the coupling strength between the two sub-systems of Figure 9.2 is increased from the level of the previous section, the transition from weak to strong coupling is encountered. Cases 3-5 of Table 9.3 represent this transition, with equi-partition of energy being fully reached for case 5. The effects of

these changes on $E[H_{12}]$ are illustrated in Figure 9.16, where the calculations have been performed using the full monte-carlo method with the 'exact' ensemble of natural frequencies and mode shapes. As the coupling strength rises so does the energy flow, at least to start with. Eventually, however, a limiting value is reached. As has already been illustrated in Chapters 4 and 5, this phenomenon is not modelled well by the traditional SEA approach and an alternative formulation including a correction factor was derived to deal with it. The effects on case 5 of Table 9.3, arising from the adoption of the various periodic formulations and also this correction factor, are considered next.

First the idealised periodic frequency PDFs can be used directly in the full monte-carlo methods, there being no difficulties arising due to presence of strong coupling. Figure 9.17 results, which also repeats the 'exact' curve for case 5 shown in Figure 9.16, together with that given by the traditional SEA formulations. Here variations from the 'exact' curve again arise only from the differences in the PDFs of Figure 9.9 and those of 9.12, and also because the mode shape parameters have been dropped.

The usual SEA method is considerably in error here since it cannot model the limiting value of cross-receptance that occurs with this level of coupling; this fundamental limitation has already been noted in Chapters 4 and 5. Simplifying the multi-dimensional integrals to single integrals like that of equation (6.3) is not strictly valid here, this being the reason for the derivation of a strong coupling correction factor in Chapter 5. Figure 9.18 shows the results obtained by performing these individual integrals, both with and without the strong coupling correction. Significant improvements over traditional SEA are obtained in both cases. These are achieved without recourse to the monte-carlo techniques required to produce Figure 9.17. The results obtained with the strong coupling correction are most encouraging.

Finally the traditional SEA result of equation (3.47) can be used with varying modal densities, both with and without the strong coupling correction, see Figure 9.19. Notice that to employ the strong coupling correction here a revised formulation for $E[H_{12}(\omega)]$ is necessary since Δ is not assumed equal to unity in the derivation of the factor, i.e., equations (5.6) and (5.7) are used in place of equation (3.40). This final approach is very simple to apply and gives very good agreement with the 'exact'

results.

This completes the study of this periodic problem. Five approaches have been used.

(i) First, the 'exact' relationships have been solved for an ensemble of random structures by finding the modal solutions for each realisation in turn, and then averaging the resulting energy flows using monte-carlo integration techniques.

(ii) Secondly, the traditional SEA formulation of equation (3.47) has been shown to give approximately correct trends, providing the coupling is weak. It does not model the limiting value of cross-receptance reached for strongly coupled sub-systems, instead predicting ever increasing cross-receptances with coupling strength.

(iii) Next, approximate frequency PDFs have been constructed, based on the propagation constants of perfectly periodic sub-systems and their 'pass' bands. These were used to provide random natural frequency sequences for the monte-carlo integrations and reveal the differences due to modal coherence and also scatter from the precisely banded model. This method correctly models variations in coupling strength.

(iv) Fourthly, the approximate frequency PDFs have been integrated directly after the multi-dimensional integrals have been simplified. This approach is computationally much simpler, but is strictly valid only for weakly coupled sub-systems. However, when applied to strongly coupled problems the results are not grossly in error and the strong coupling correction of Chapter 5 gives additional, worthwhile, improvements in accuracy.

(v) Finally, the original formulation of equation (3.40) has been used but with varying modal densities $N_1/(\omega_u-\omega_l)$, $N_2/(\omega_u-\omega_l)$ modified to suit the presence of 'pass' and 'stop' bands. This models the behaviour of periodic systems very well, but is significantly in error for strongly coupled sub-systems. However, the strong coupling correction and revised formulation of equations (5.6) and (5.7) give an extremely simple method for dealing with strongly coupled periodic structures. Its only weakness lies in the difficulty of predicting the effects of mode shape coher-

ence at the coupling and driving points. If such coherence is slight, the results are extremely encouraging.

This last method combines both robustness and ease of application and represents a new, recommended, approach for everyday practitioners of SEA.

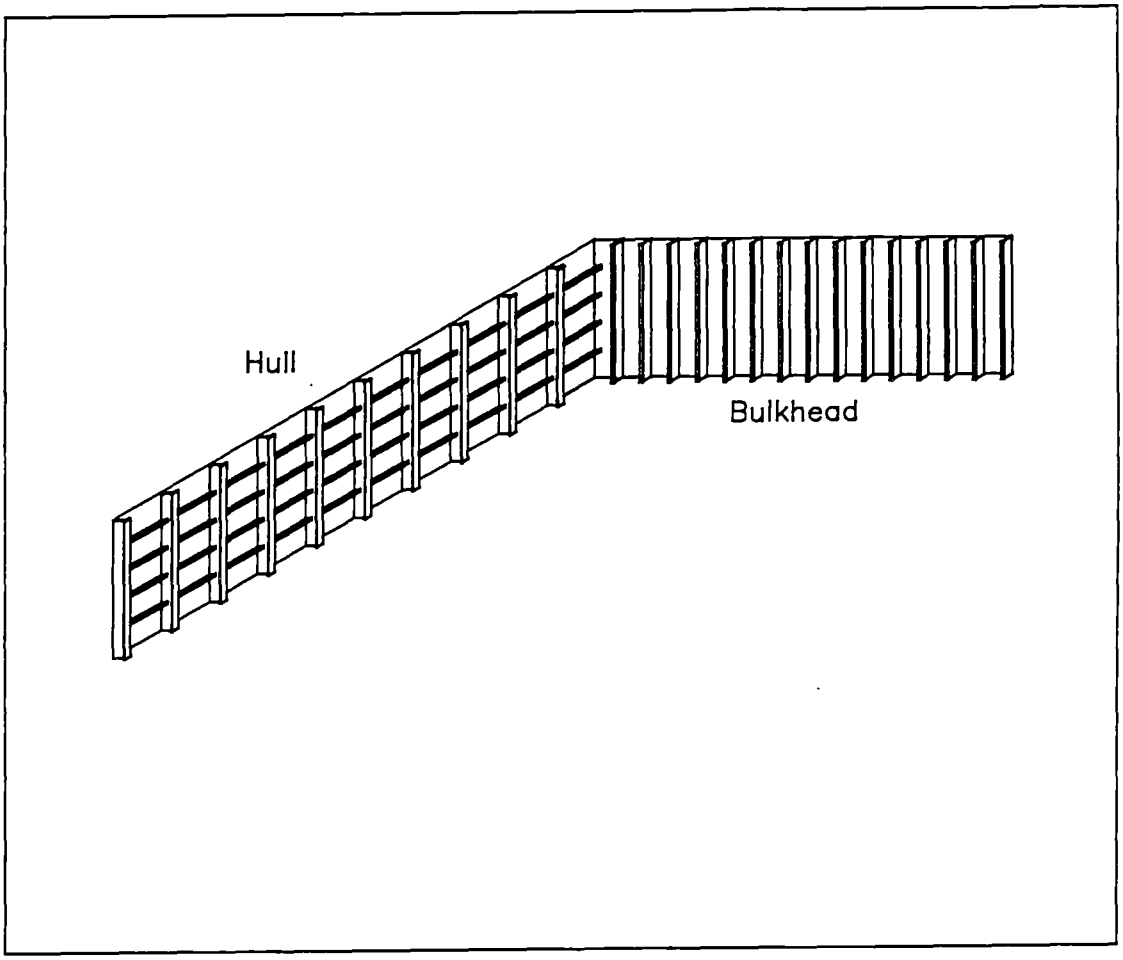

Figure 9.1 - An idealised portion of a ship's structure.

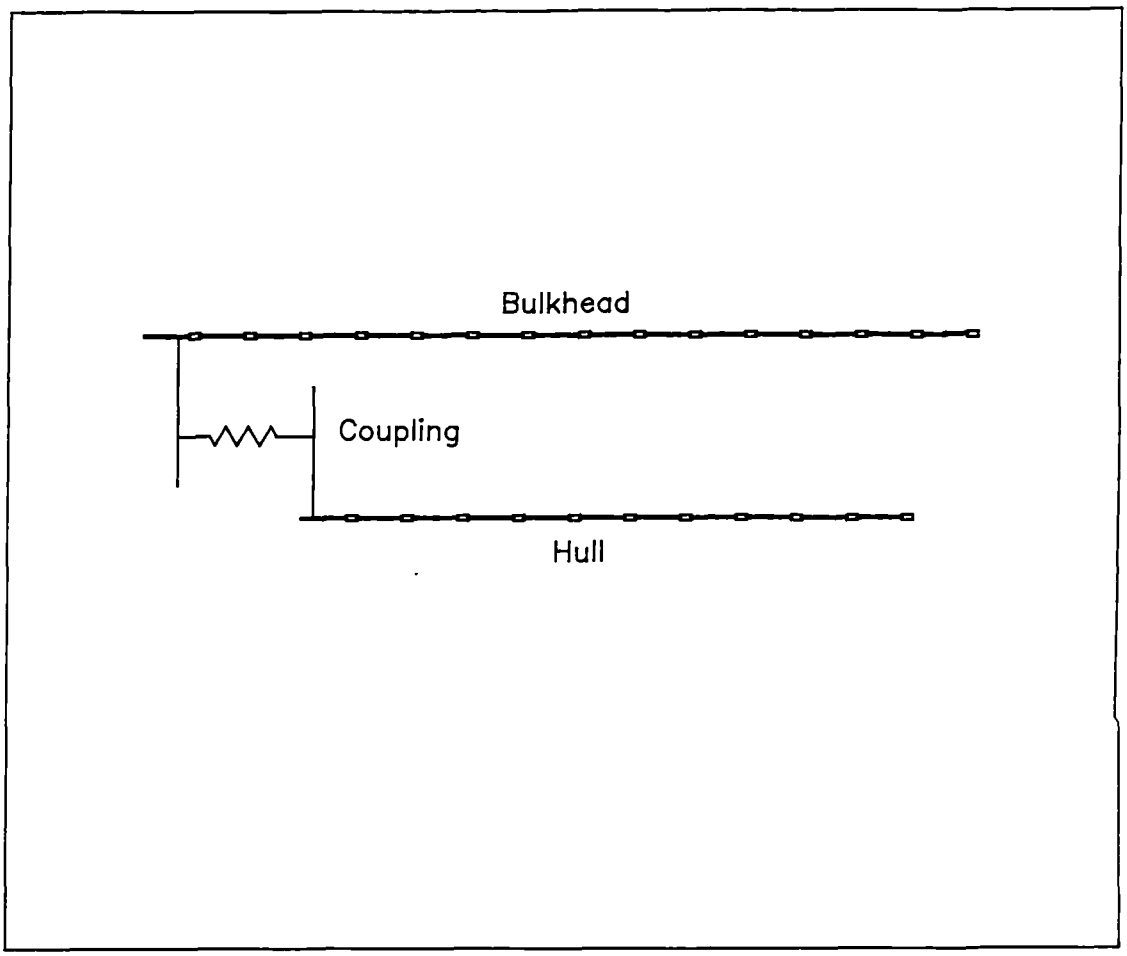

Figure 9.2 - Periodic, axially vibrating rod model of the problem illustrated in Figure 9.1.

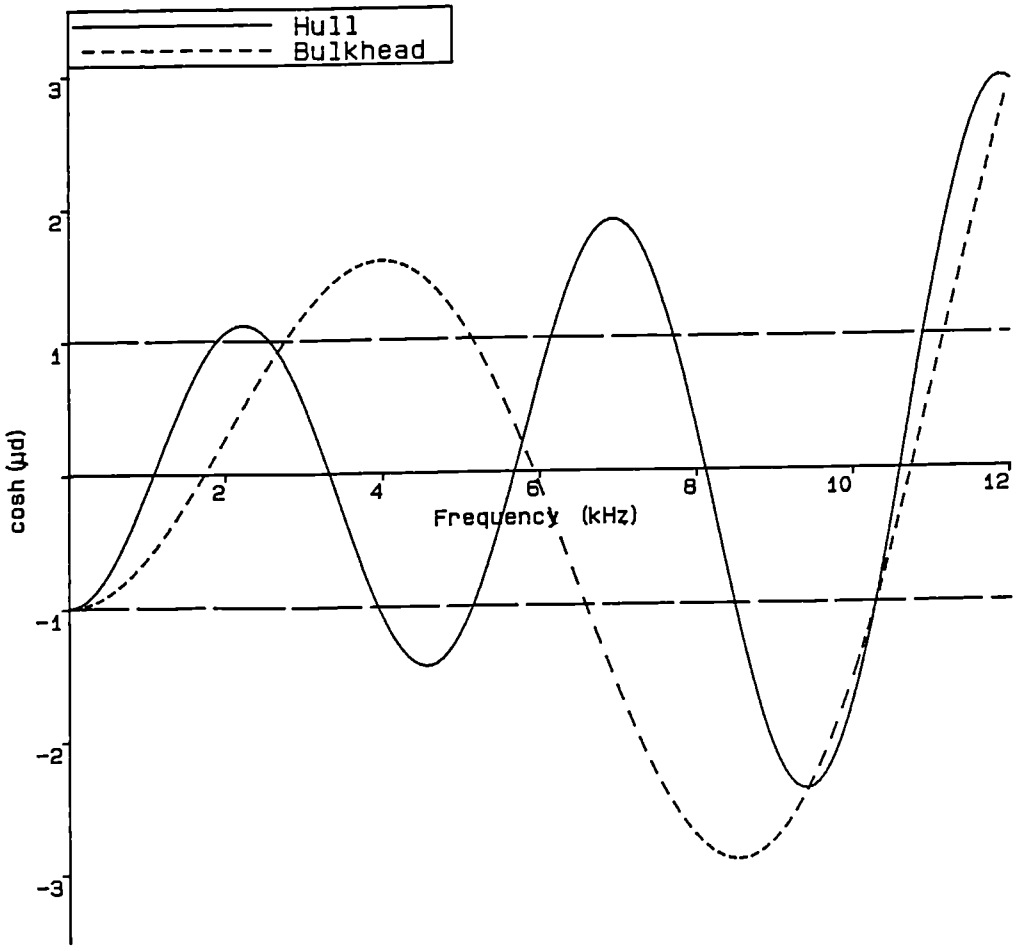

Figure 9.3 - Graph of cosh(μd) versus frequency ω for the hull and bulkhead.

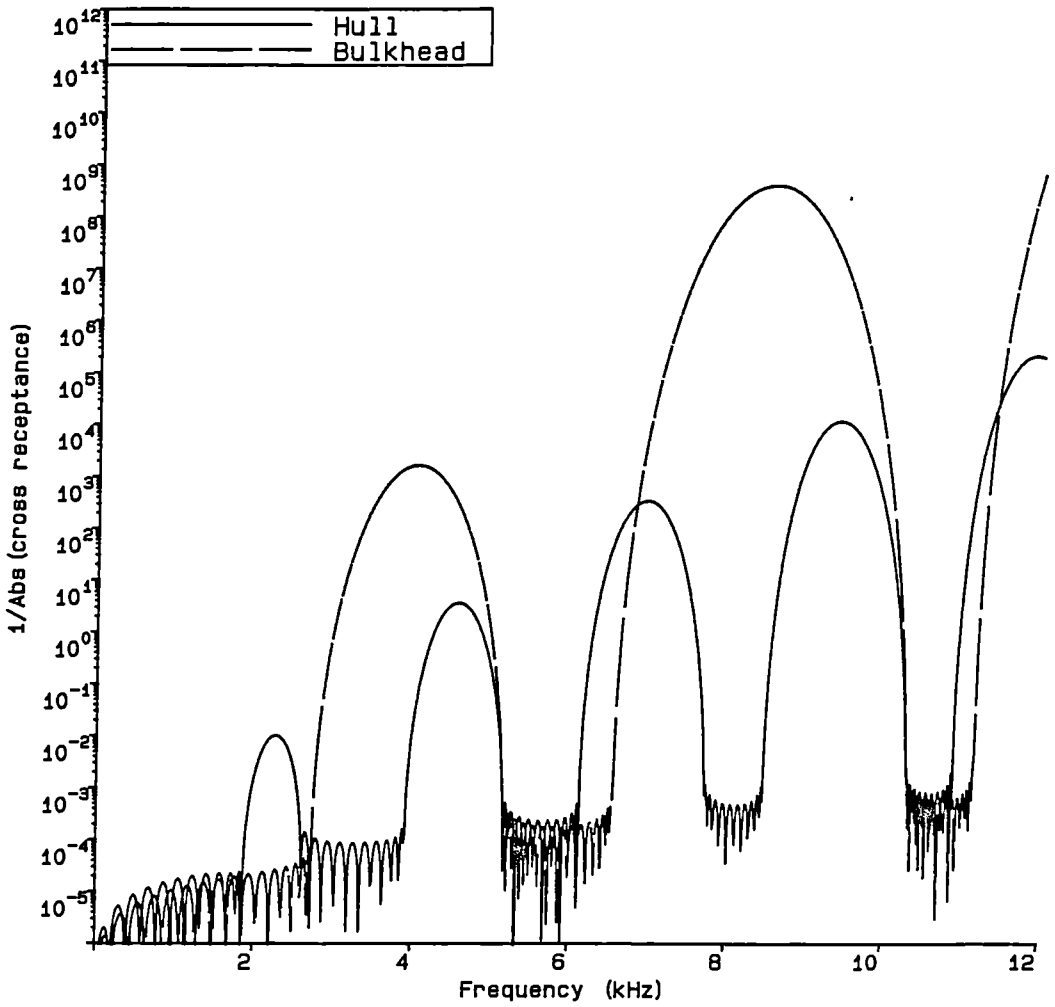

Figure 9.4 - Graph of the uncoupled cross receptances of the hull and bulkhead versus frequency ω.

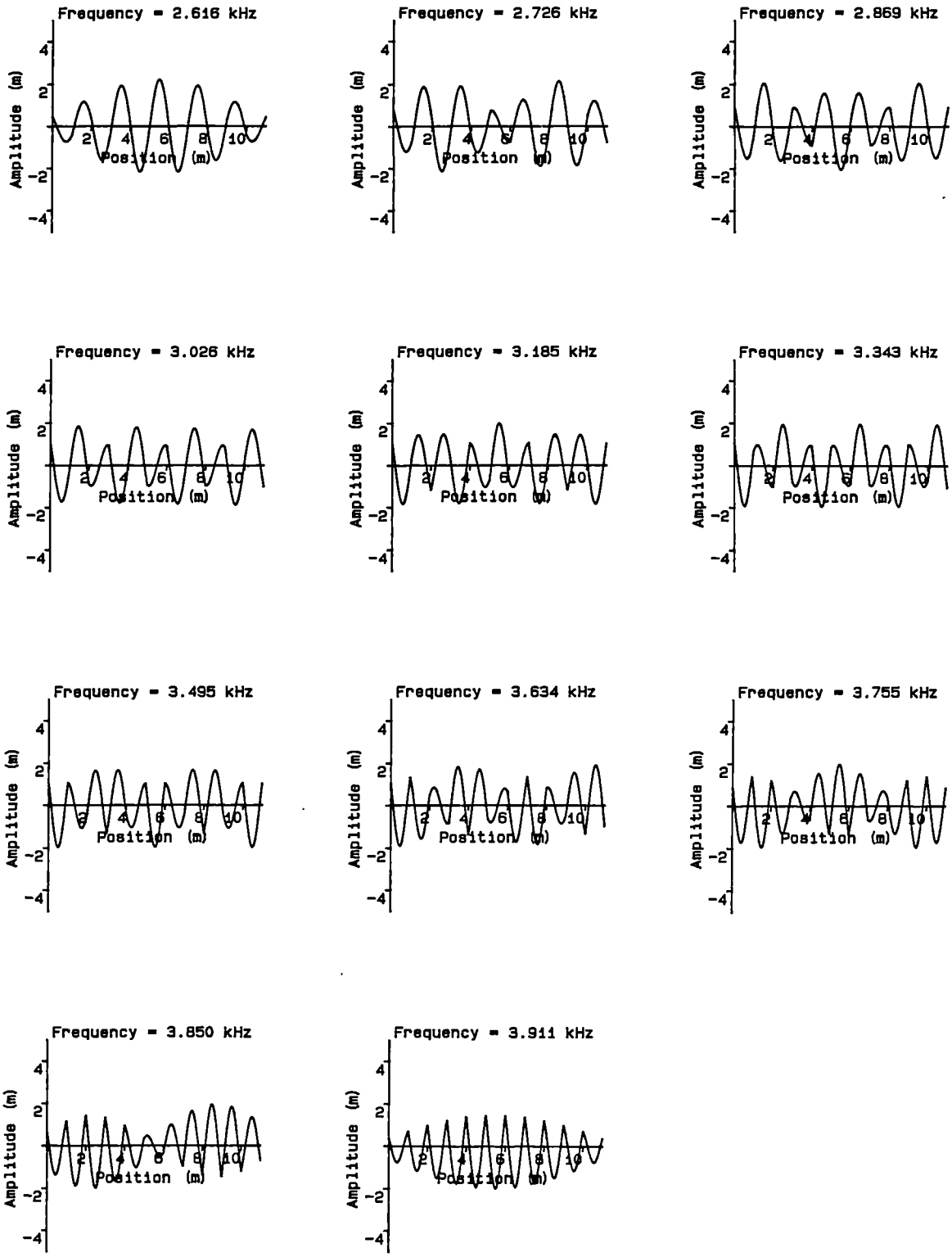

Figure 9.5 - Mode shapes and natural frequencies ω_i for hull modes in the second pass band, calculated using receptance theory (axial deflections shown transverse for clarity). Wave and modal theories give identical results.

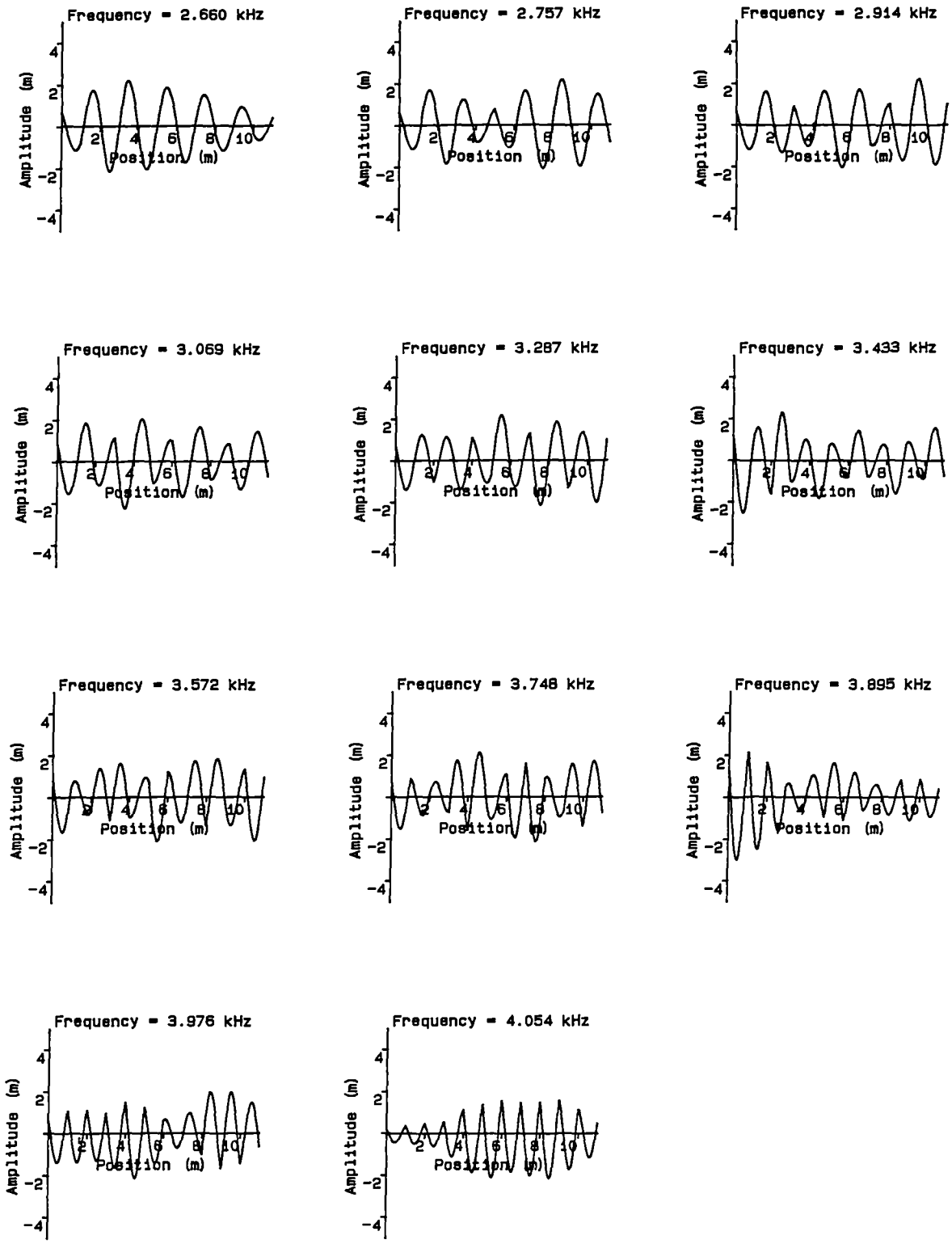

Figure 9.6 - Mode shapes and natural frequencies ω_i' for hull modes in the second pass band, calculated using receptance theory, for the system with random masses (axial deflections shown transverse for clarity).

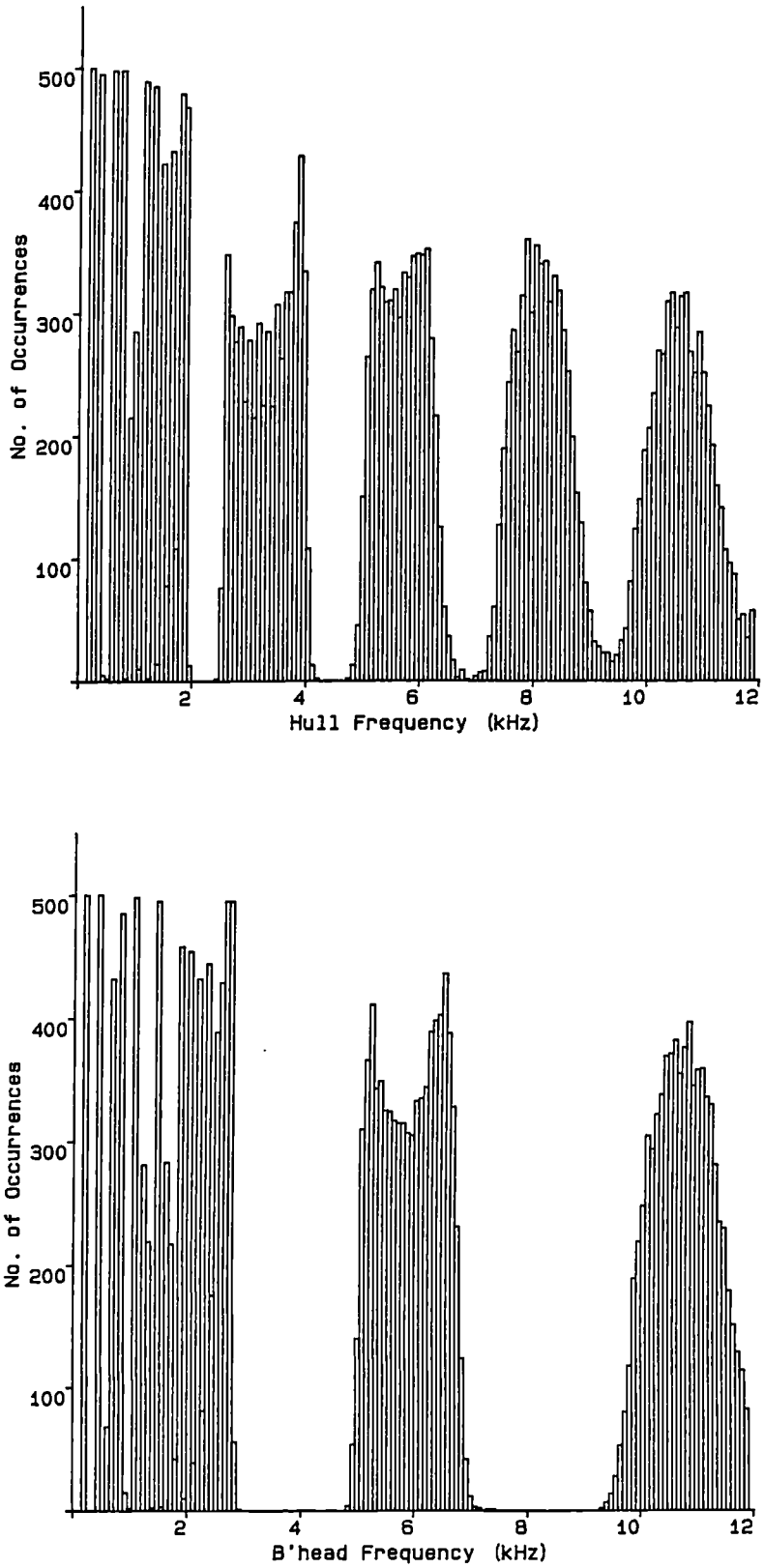

Figure 9.7 - Histograms of random natural frequency occurrences ω_i' for the hull and bulkhead.

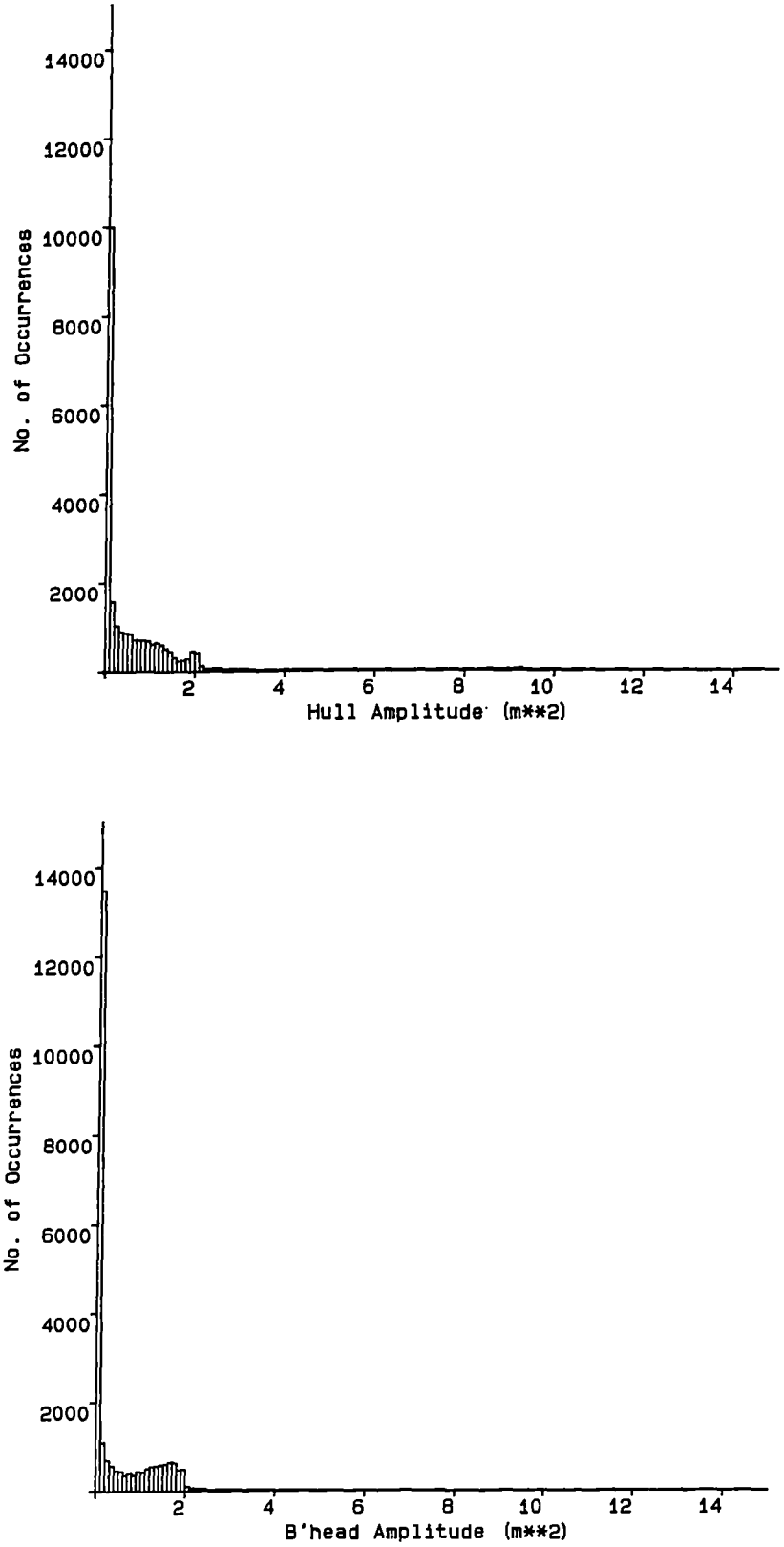

Figure 9.8 - Histograms of random mode shape parameter occurrences $\psi_i'^2$ at the coupling point for the hull and bulkhead (m**2 equivalent to m^2).

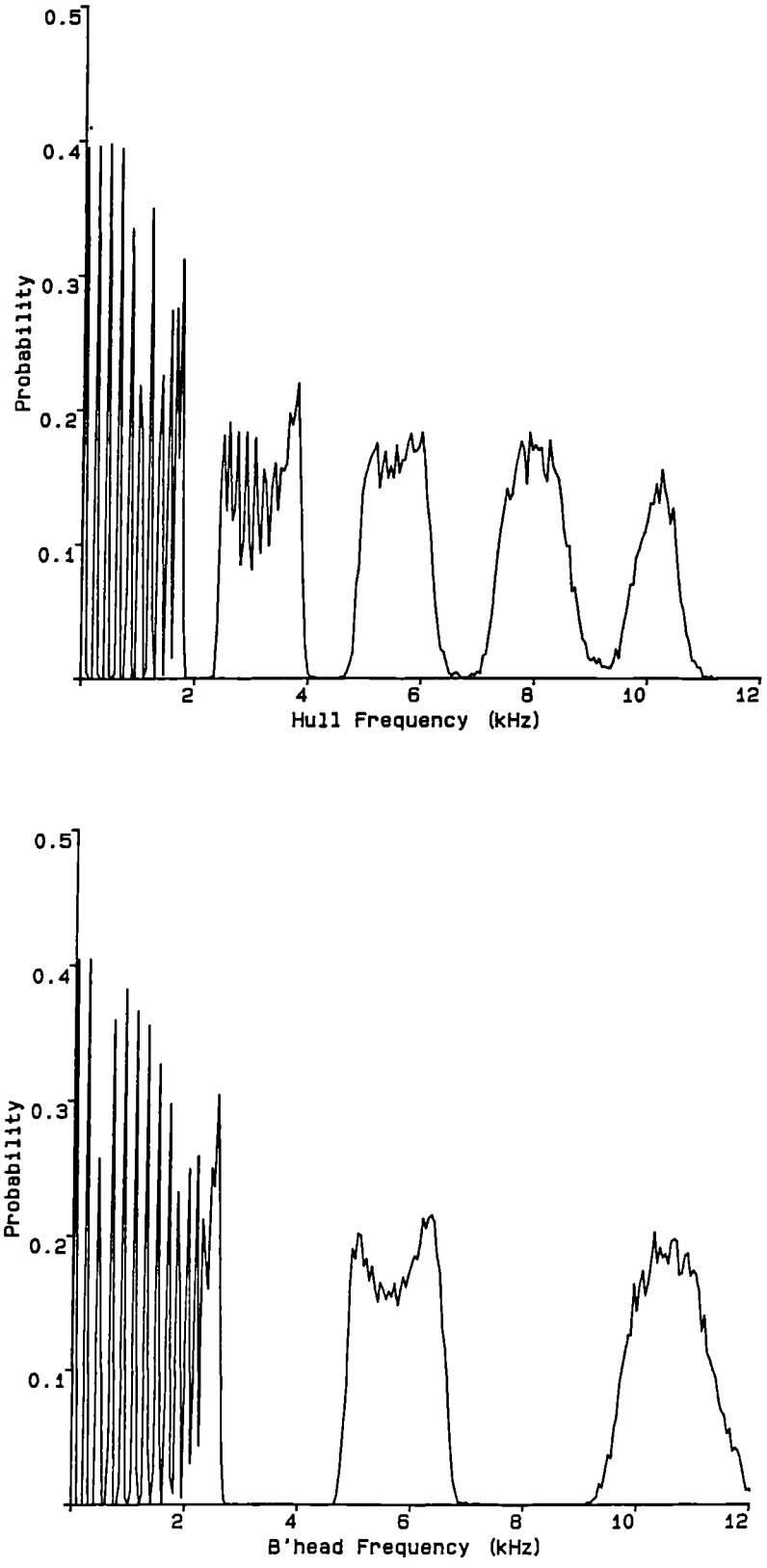

Figure 9.9 - Probability density functions of random natural frequency occurrences ω_i' for the hull and bulkhead.

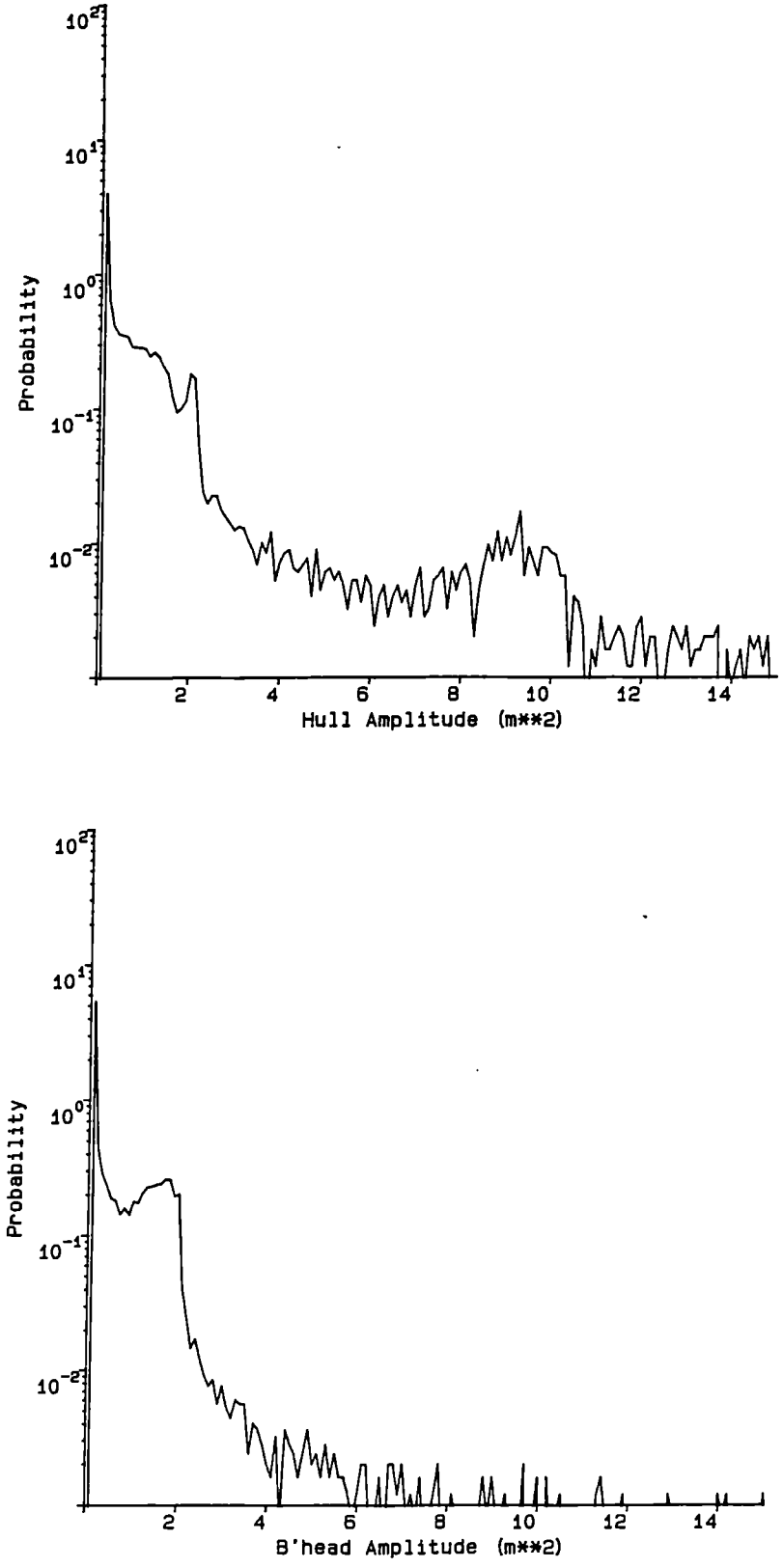

Figure 9.10 - Probability density functions of random mode shape parameter occurrences $\psi_i'^2$ at the coupling point for the hull and bulkhead (m**2 equivalent to m^2).

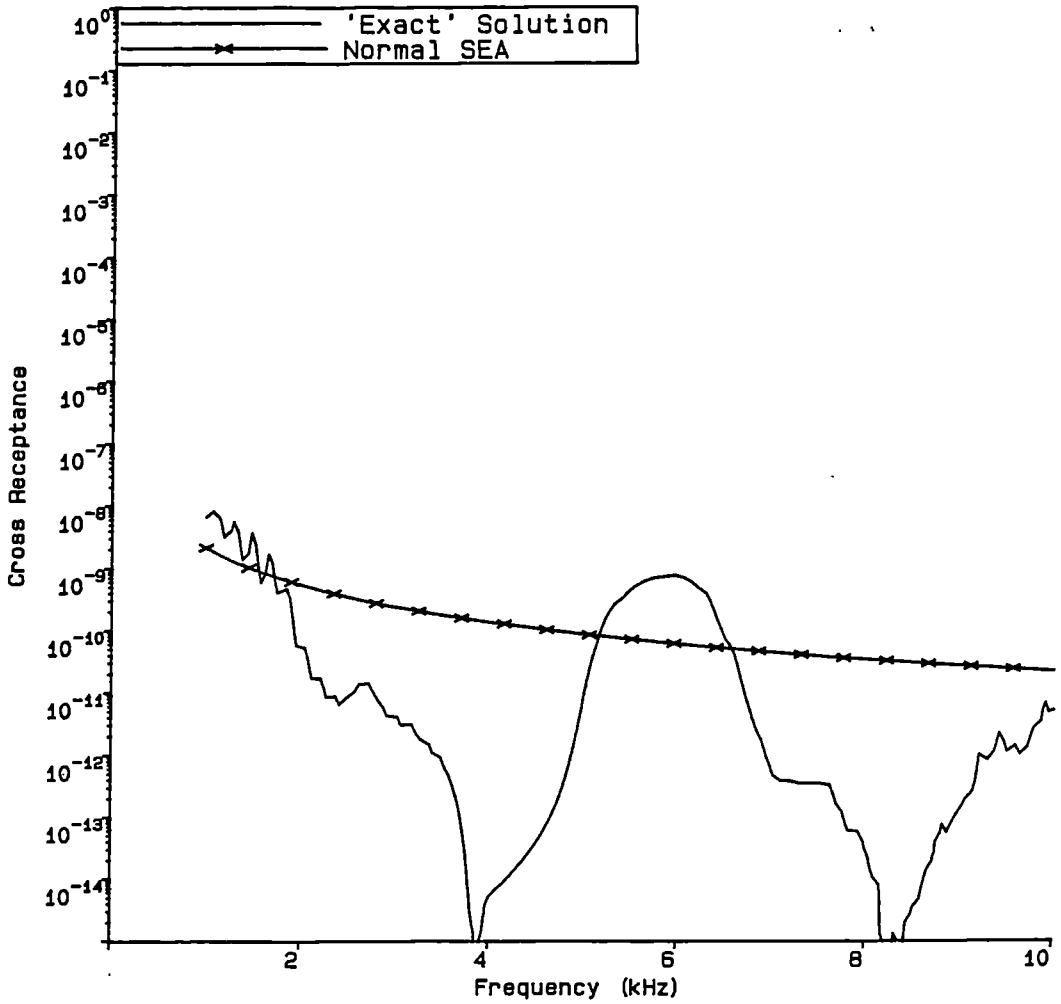

Figure 9.11 - Variation of $E[H_{12}]$ with frequency ω for case 1 of Table 9.3 calculated using 'exact' monte-carlo and traditional SEA techniques.

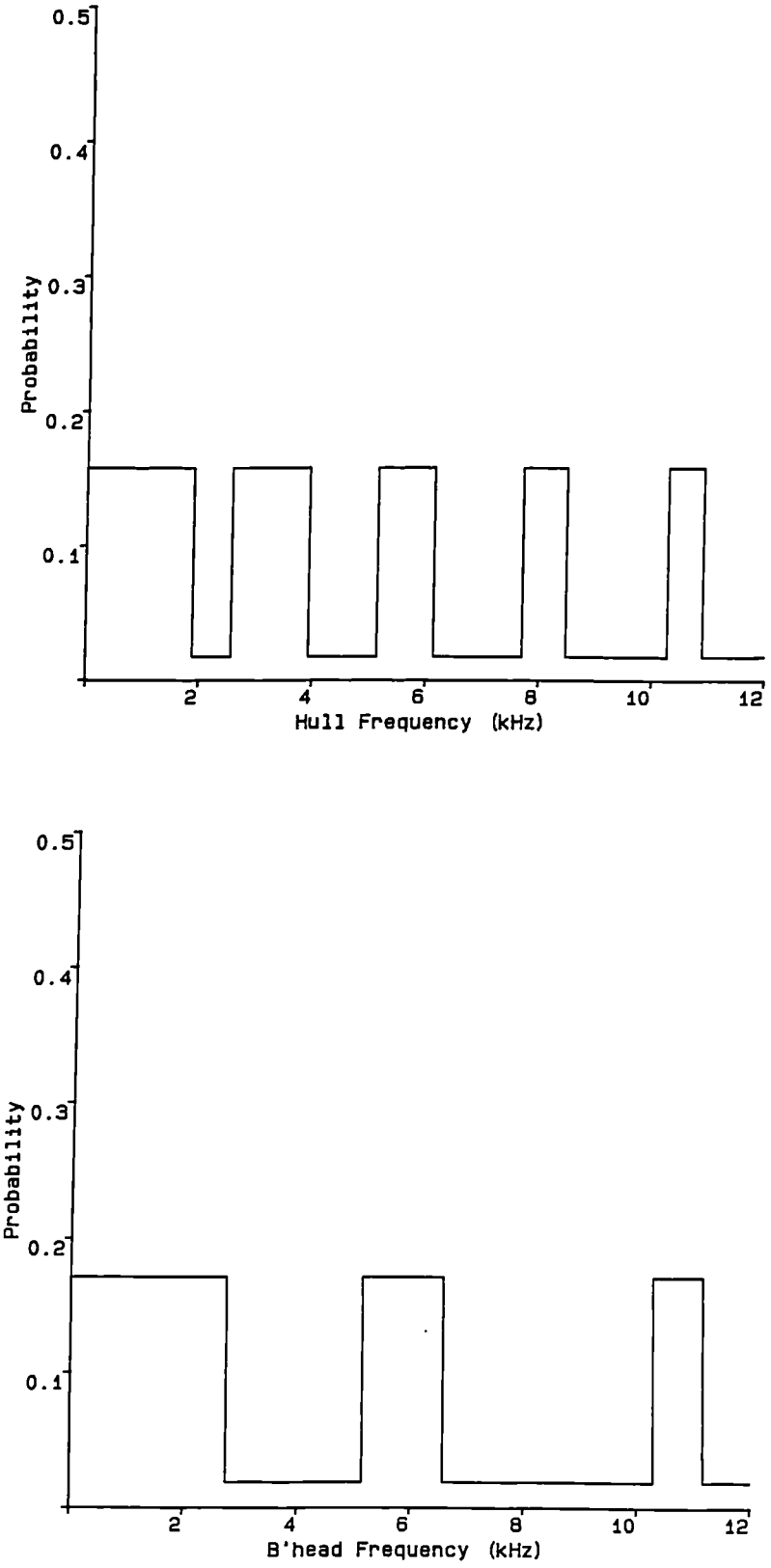

Figure 9.12 - Piece-wise constant probability density functions for random natural frequencies based on the pass bands derived from Figure 9.3.

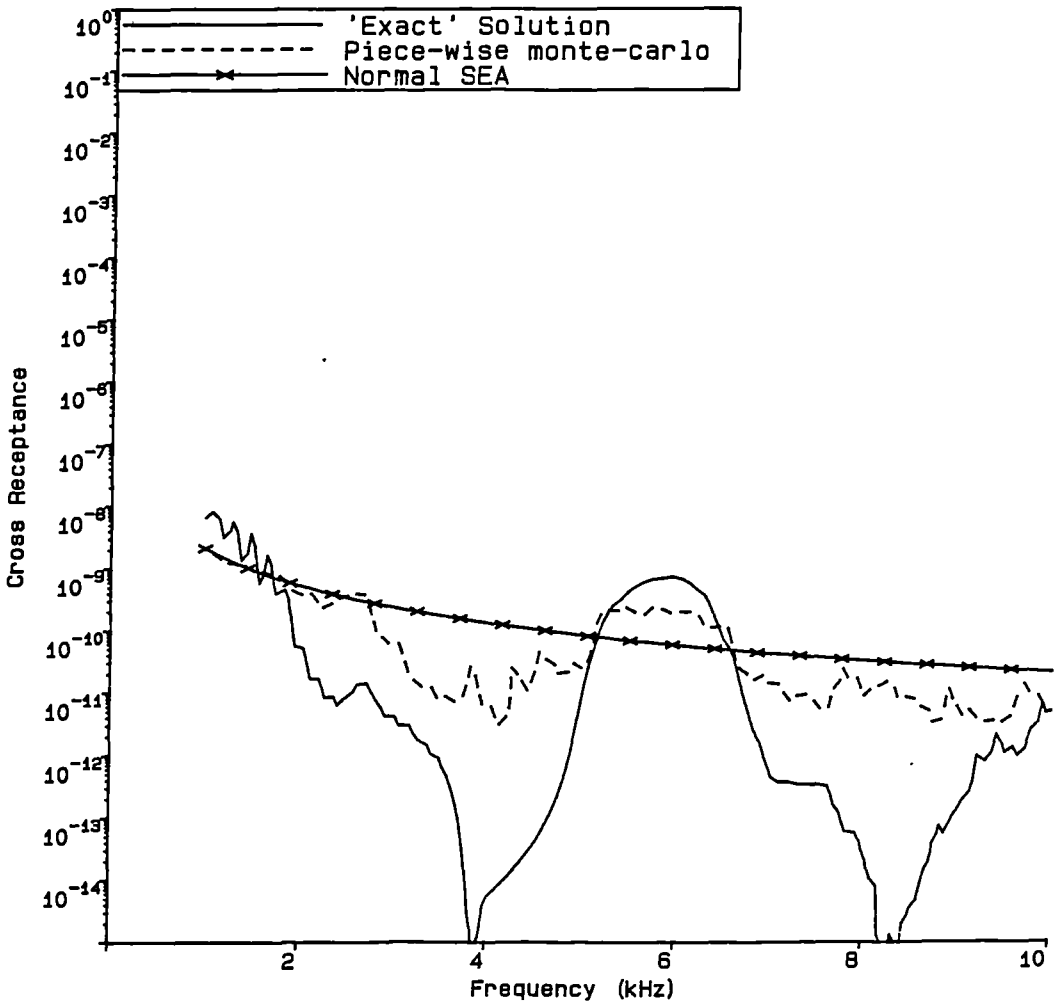

Figure 9.13 - Variation of $E[H_{12}]$ with frequency ω for case 1 of Table 9.3 calculated using 'exact' monte-carlo and traditional SEA techniques together with a calculation adopting piece-wise constant probability density functions like that of Figure 9.12.

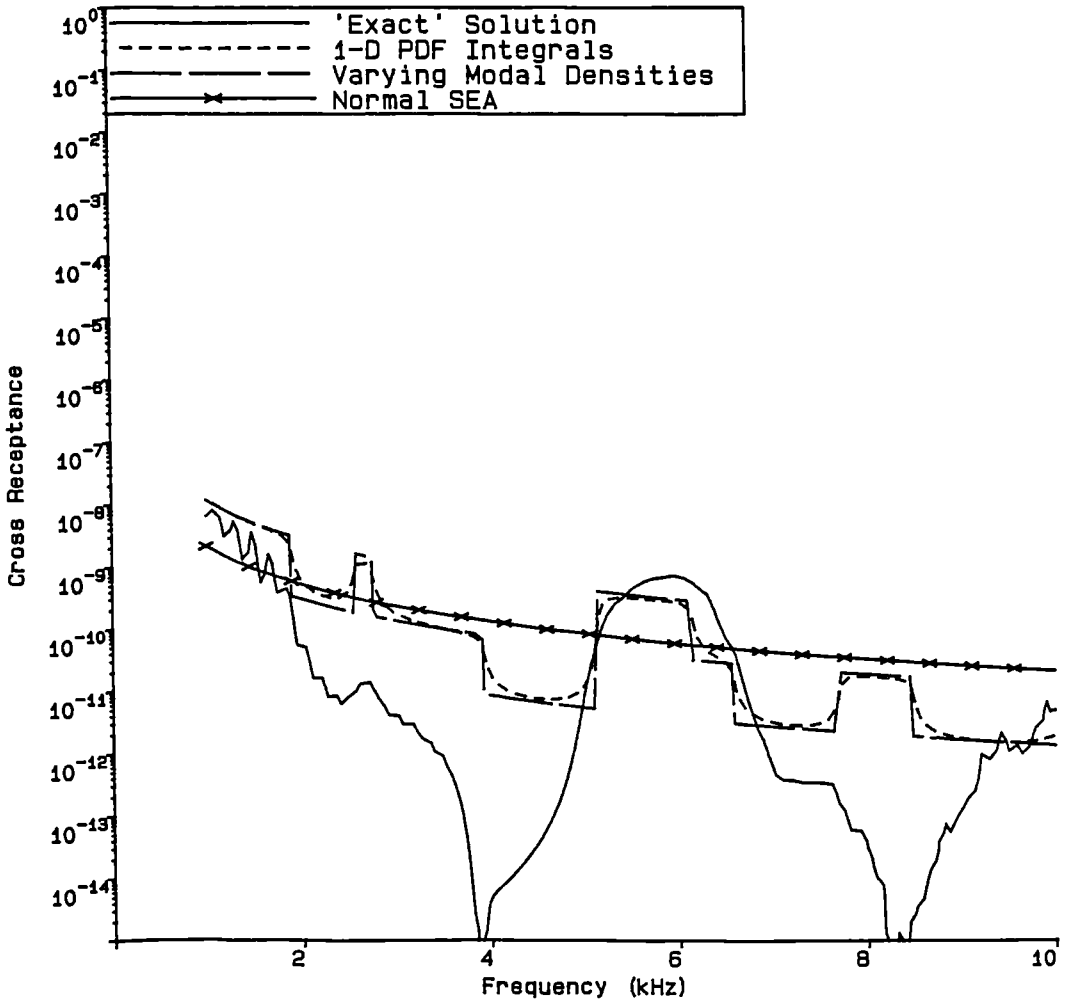

Figure 9.14 - Variation of $E[H_{12}]$ with frequency ω for case 1 of Table 9.3 calculated by integrating the simplified results of equation (3.38) and a calculation adopting a piece-wise constant modal density together with the 'exact' and traditional results.

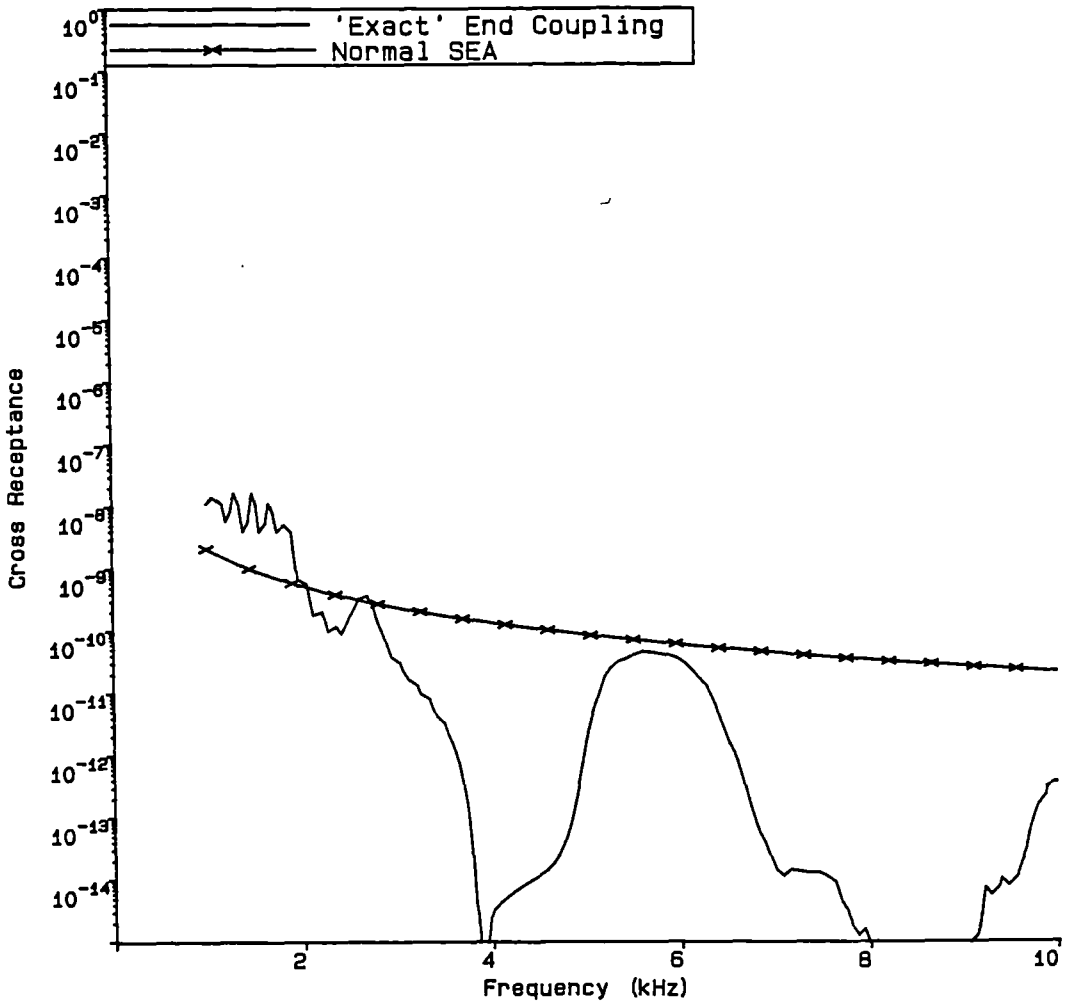

Figure 9.15 - Variation of $E[H_{12}]$ with frequency ω for case 2 of Table 9.3 calculated using 'exact' monte-carlo and traditional SEA techniques.

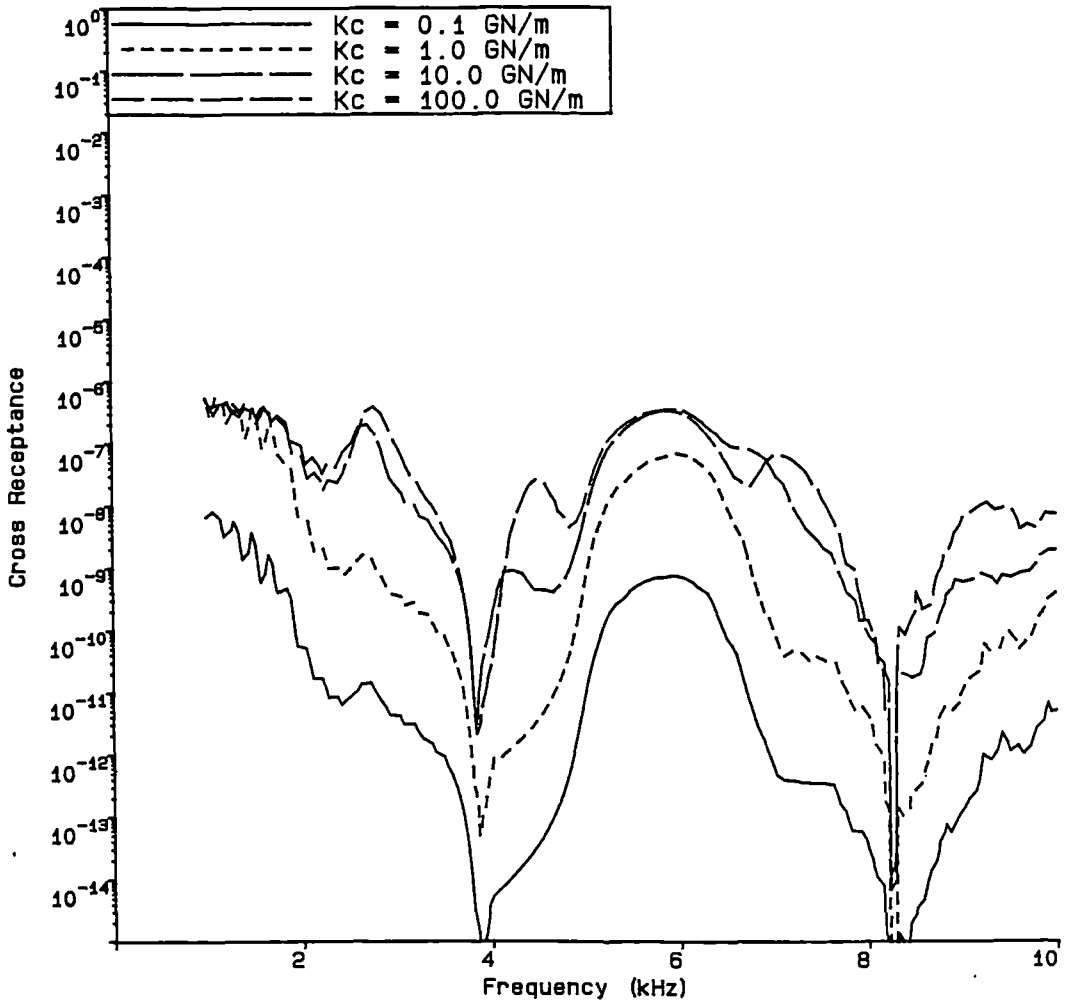

Figure 9.16 - Variation of $E[H_{12}]$ with frequency ω for cases 1 and 3 to 5 of Table 9.3 calculated using 'exact' monte-carlo techniques (Kc equivalent to k_c).

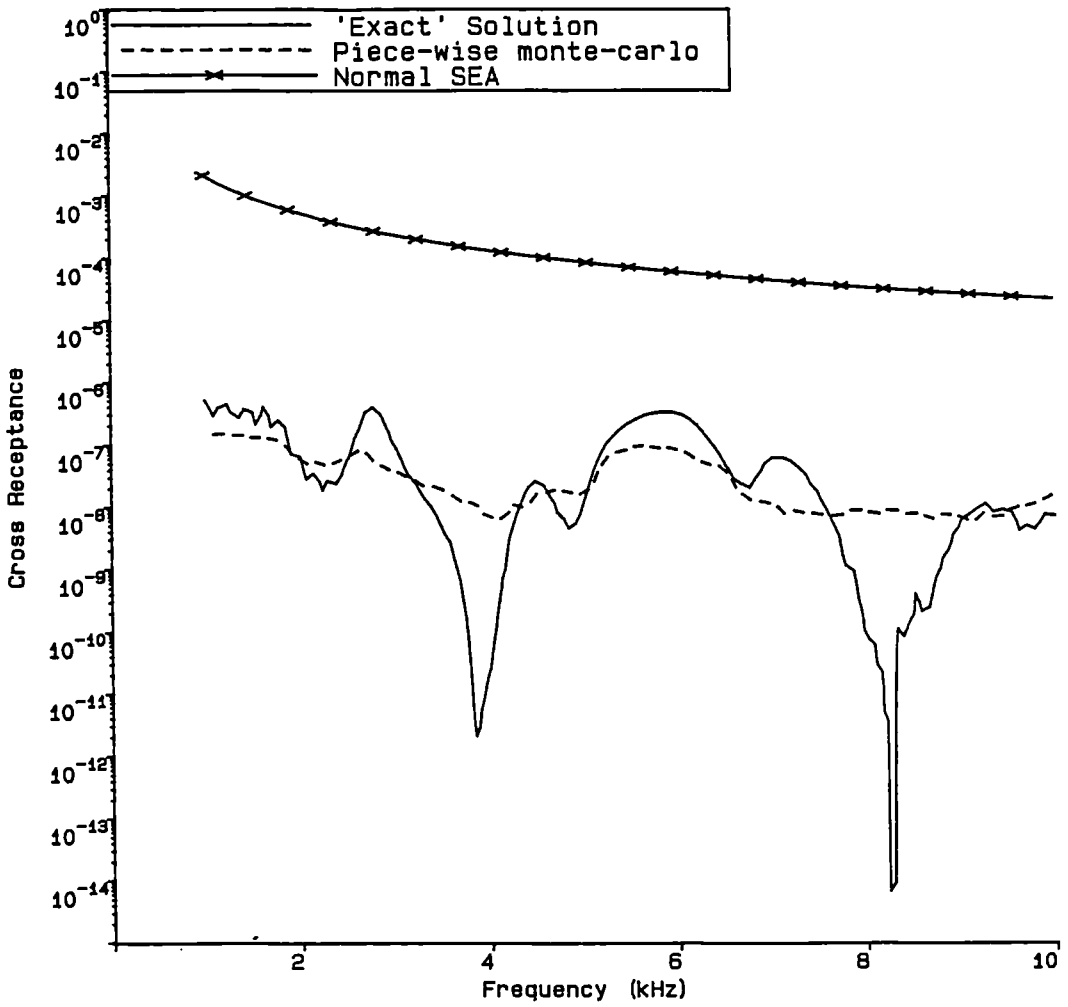

Figure 9.17 - Variation of $E[H_{12}]$ with frequency ω for case 5 of Table 9.3 calculated using 'exact' monte-carlo and traditional SEA techniques together with a calculation adopting piece-wise constant probability density functions like that of Figure 9.12.

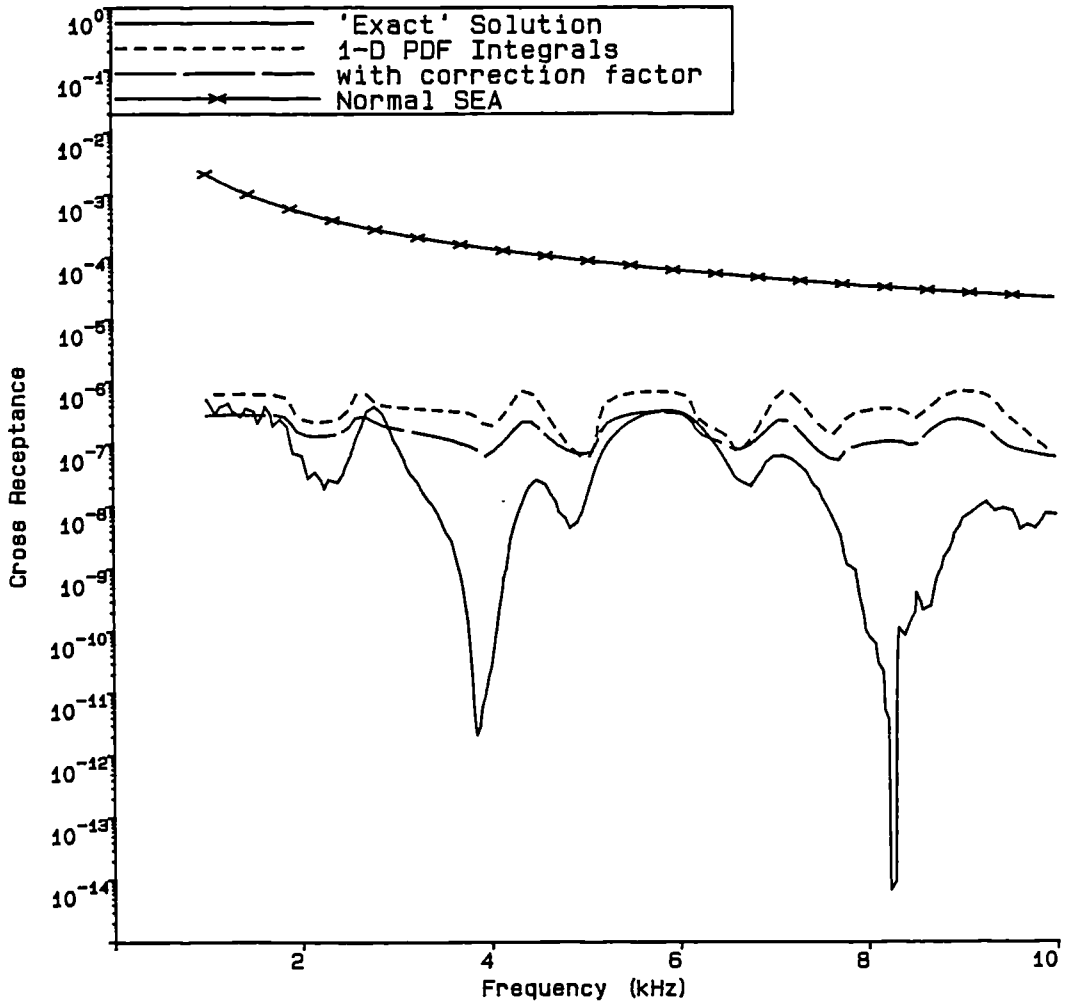

Figure 9.18 - Variation of $E[H_{12}]$ with frequency ω for case 5 of Table 9.3 calculated by integrating the simplified results of equation (3.38) both with and without the strong coupling correction together with the 'exact' and traditional results.

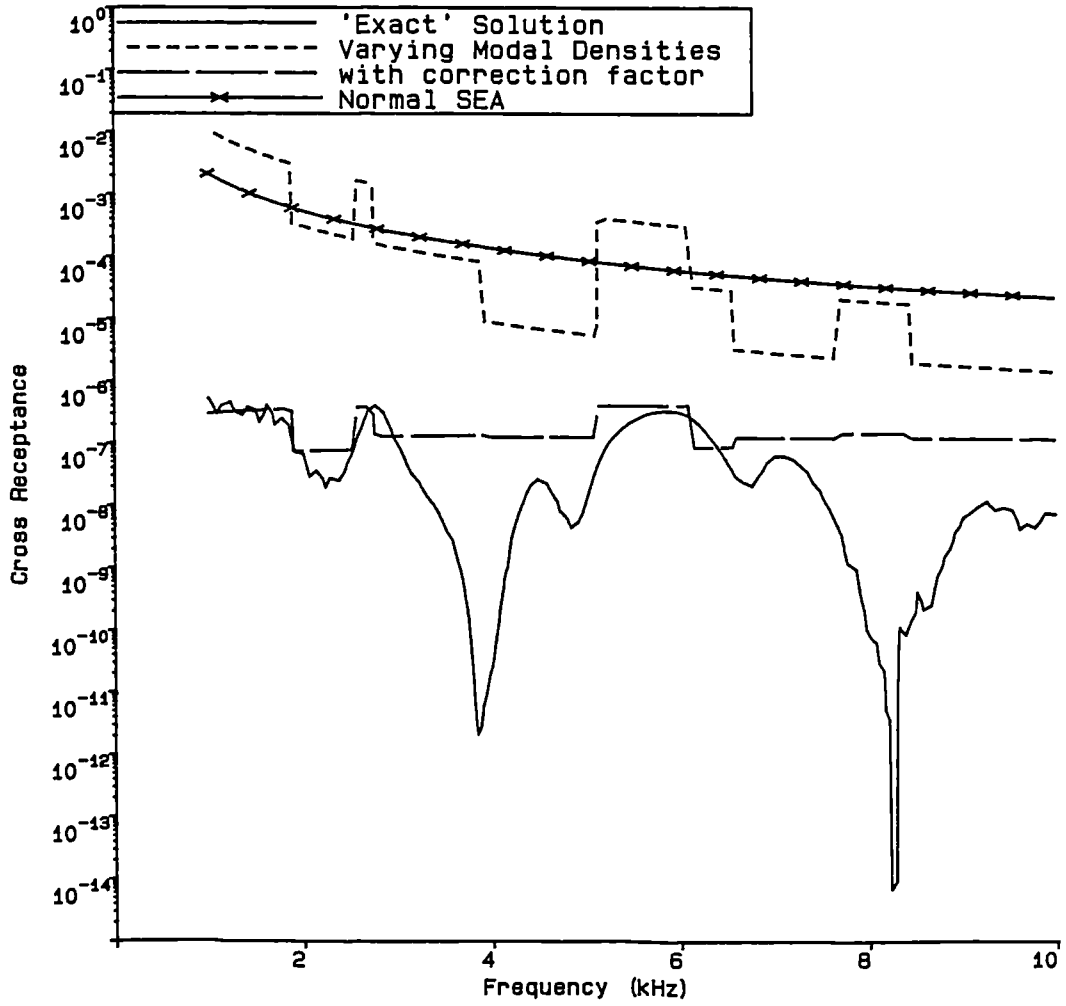

Figure 9.19 - Variation of $E[H_{12}]$ with frequency ω for case 5 of Table 9.3 calculated by assuming a piece-wise constant modal density both with and without the strong coupling correction together with the 'exact' and traditional results.

CHAPTER 10

Conclusions

10.1. Scientific Conclusions

The earlier chapters of this work have reviewed statistical energy analysis in some detail, especially as applied to just two multi-modal sub-systems. The principal assumptions underlying the accepted theories in this field are listed at the end of Chapter 2, and a number of aspects from this list have been investigated, covering damping, coupling and forcing models. Underlying these discussions has been the development of exact analytical solutions, which have been used as a basis for comparison when adopting more straight-forward approaches. In particular, assumptions (iv) to (x) of the list in section 2.4 have been assessed in the light of a number of examples, and the following observations may be made :-

assumption (iv)

Strong coupling between multi-modal sub-systems *can* be correctly modelled using SEA.

assumption (v)

Damping must remain proportional for the correct application of SEA.

assumption (vi)

Adopting expansions in the uncoupled modes of the sub-systems avoids any difficulties associated with the statistics of the individual modes.

assumption (vii)

Mode shapes of the uncoupled sub-systems at the coupling and driving points *do* have a significant bearing on the results of SEA calculations, although such effects remain difficult to understand in some cases.

assumption (viii)

Non-uniform natural frequency PDFs can be successfully incorporated into SEA.

assumption (ix)

No restrictions are necessary on the summations bandwidths used in SEA, provided that the various modal summations converge within the bandwidths adopted.

assumption (x)

Although damping must remain proportional for the correct application of SEA, *any* level of damping can be accommodated.

Additionally, the effects of low modal density have been studied, and it is reaffirmed that SEA can give a poor indication of the responses of systems with few, widely spaced modes.

This work has shown that SEA is a potentially powerful tool, but when applied to typical engineering problems which exhibit heavy damping, strong coupling between sub-systems or grouped natural frequencies, more sophisticated formulations are required than SEA usually adopts. These formulations are not as elegant as those originally proposed, but they are not impossibly complex.

Throughout this work difficulties associated with predicting the mode shapes of random systems have been encountered. These have not been overcome although some results have been obtained which place bounds on their effects. Fortunately these problems do not appear to render SEA unusable although they do indicate that substantial variations of behaviour between apparently similar structures should be expected.

10.2. Recommendations for Practitioners

The studies carried out have led to the following three main recommendations for practitioners of SEA:

(i) First, check to see if the damping present in the system under study can realistically be considered as either light or proportional (so that modal cross-coupling can be discounted). Heavy

proportional damping can be catered for by using more involved expressions for the various energy flow proportionality constants discussed in Chapter 3. Significant inter-modal coupling cannot be dealt with using SEA as normally conceived.

(ii) Secondly, construct the function v of Chapter 5 to see whether the original formulations of SEA can be expected to hold regarding coupling strength. If it transpires that the coupling strength is too great for this, either adopt the revised formulations and correction factor outlined in Chapter 5 or reconfigure the divisions between sub-systems to avoid the problem. The results of the usual analysis are likely to be orders-of-magnitude in error if such steps are not taken.

(iii) Thirdly, if the structures under investigation show some underlying pattern, do not ignore this feature. It is most probable that the natural frequency statistics of such structures do not show the completely even spread of frequencies required by traditional SEA. At the very least, a number of different modal densities should be used for successive frequency ranges. The work carried out here shows that significant improvements can be gained by such an approach. Moreover, it has been shown that the theory of periodic structures may be able to yield estimates for the frequency points at which modal densities change, if not their absolute values.

The combination of more sophisticated damping formulations, a strong coupling correction and periodic theory based modal density curves constitutes a significant improvement in the modelling of pairs of multi-modal sub-systems. Since SEA for multiple sub-systems, and more complex coupling, is based on the results for these simple problems, adopting such ideas for these broader categories of problems can be recommended, if traditional SEA methods give unacceptable results.

10.3. Further Work

This work has identified a number of areas that warrant further study. Foremost amongst these appears to be the whole problem of coupling mechanisms and modal coherence in the region of the coupling between sub-systems. A brief excursion into the theory of nearly periodic structures has indicated that such studies may be extremely difficult. As Lyon[16] has noted, perhaps the best method is to

conduct practical experiments on various coupling types. The theoretical work carried out here may be of use to guide the conduct of such experiments. If nothing else, it indicates that practical experiments should *not* be restricted to highly idealised, perfectly periodic samples.

Perhaps the greatest limitation in this theoretical approach lies in its adoption of mono-coupled sub-systems. Clearly, real structures are more complex, and although difficult, some attempt should be made to investigate the changes necessary to accommodate such systems.

Finally, mention must be made of the whole subject of validation of the work done here. Some form of experimental verification would be very worthwhile; however, since a number of different approaches have been used at each stage of development, gross errors in the theory presented can perhaps be discounted.

APPENDIX A

Derivation of Modal Summation Results

A.1. Multi-Modal Systems

The differential equations of motion describing coupled, multi-modal sub-systems are

$$\{\Lambda_1+r_1(x_1)\mathrm{d}/\mathrm{d}t+\rho_1(x_1)\mathrm{d}^2/\mathrm{d}t^2\}y_1(x_1,t)=P_1(x_1,t), \tag{A.1}$$

$$\{\Lambda_2+r_2(x_2)\mathrm{d}/\mathrm{d}t+\rho_2(x_2)\mathrm{d}^2/\mathrm{d}t^2\}y_2(x_2,t)=P_2(x_2,t) \tag{A.2}$$

where Λ_1 is a linear spatial differential operator on sub-system 1, $r_1(x_1)$ is the damping constant of sub-system 1, $\rho_1(x_1)$ is the mass density per unit length of sub-system 1, and $P_1(x_1,t)$ is a forcing function on sub-system 1 which may be a function of $y_2(x_2,t)$; and similarly for sub-system 2 but with the subscripts reversed, 2 for 1. Both the damping and mass densities are allowed to vary with the positions within the sub-systems x_1 and x_2, subject to assumption (v) of Chapter 2, which requires that

$$r_1(x_1)=c_1\rho_1(x_1) \tag{A.3}$$

and

$$r_2(x_2)=c_2\rho_2(x_2) \tag{A.4}$$

i.e., proportional damping within the sub-systems. The forcing functions P, are assumed to contain the coupling forces resulting from the connection between the two sub-systems. If this is a point spring coupling at $x_1=a_1$ and $x_2=a_2$, with a spring of strength k_c, the forcing function becomes

$$P_1(x_1,t)=F_1(x_1,t)+k_c\{y_2(a_2,t)-y_1(a_1,t)\}\delta(x_1-a_1) \tag{A.5}$$

where $F_1(x_1,t)$ is the external driving force on sub-system 1, which may vary with position as well as time and similarly for sub-system two, but with the subscripts altered. This problem is classically solved by using modal analysis. An expansion in the eigenfunctions of the uncoupled ($k_c=0$) sub-systems $\psi_i(x_1)$ and $\psi_r(x_2)$ is made, and this produces equations of the form

$$\{\Lambda_1-\rho_1(x_1)\omega_i^2\}\psi_i(x_1)=0 \tag{A.6}$$

where the ω_i are the natural frequencies of the modes of system 1. These eigenfunctions may be normalized so that

$$\int\psi_i(x_1)\psi_j(x_1)\rho_1(x_1)dx_1=m_1\delta_{ij} \tag{A.7}$$

Next define the modal components of the driving forces,$L_i(t)$ as

$$L_i(t)=\int\psi_i(x_1)F_1(x_1,t)dx_1 \tag{A.8}$$

so that the external driving force on sub-system 1 is given by

$$F_1(x_1,t)=\frac{\rho_1(x_1)}{m_1}\sum_{i=1}^{\infty}\psi_i(x_1)L_i(t) \tag{A.9}$$

Also define the modal components of the coupling forces, $V_i(t)$ as

$$V_i(t)=\int k_c\psi_i(x_1)\{y_2(a_2,t)-y_1(a_1,t)\}\delta(x_1-a_1)dx_1 \tag{A.10}$$

$$=k_c\psi_i(a_1)\{y_2(a_2,t)-y_1(a_1,t)\}$$

so that

$$k_c\{y_2(a_2,t)-y_1(a_1,t)\}\delta(x_1-a_1)=\rho_1(x_1)/m_1\sum_{i=1}^{\infty}V_i(t)\psi_i(x_1) \tag{A.11}$$

Substituting these expressions into equation (A.1) yields

$$\rho_1(x_1)\left\{\ddot{y}_1(x_1,t)+r_1(x_1)\dot{y}_1(x_1,t)/\rho_1(x_1)+1/\rho_1(x_1)\Lambda_1 y_1(x_1,t)\right\} \tag{A.12}$$

$$=\rho_1(x_1)/m_1\sum_{i=1}^{\infty}\psi_i(x_1)\{L_i(t)-V_i(t)\}$$

and an expansion of $y_1(x_1,t)$ in terms of its eigenvectors with weightings, $W_i(t)$, i.e.,

$$y_1(x_1,t)=\sum_{i=1}^{\infty}\psi_i(x_1)W_i(t) \tag{A.13}$$

gives

$$\rho_1(x_1)\sum_{i=1}^{\infty}\psi_i(x_1)\left\{\ddot{W}_i(t)+r_1(x_1)\dot{W}_i(t)/\rho_1(x_1)+\omega_i^2W_i(t)\right\} \tag{A.14}$$

$$=\rho_1(x_1)/m_1\sum_{i=1}^{\infty}\psi_i(x_1)\{L_i(t)-V_i(t)\}$$

Provided r_1/ρ_1 is independent of x_1 the damping is *proportional*, so that multiplying equation (A.14)

by $\psi_j(x_1)$ and integrating with respect to x_1 gives

$$\ddot{W}_j(t)+c_1\dot{W}_j(t)+\omega_j^2 W_j(t) = \{L_j(t)-V_j(t)\}/m_1 \tag{A.15}$$

where now

$$V_j(t) = k_c\psi_j(a_1)\left\{\sum_{r=1}^{\infty}\psi_r(a_2)W_r(t)-\sum_{i=1}^{\infty}\psi_i(a_1)W_i(t)\right\} \tag{A.16}$$

which shows the action of the coupling spring in coupling together all modes of both sub-systems (except those whose modal functions are zero at the coupling point). The analysis now proceeds in the frequency domain by taking the Fourier transforms of the modal equations in W to obtain

$$m_1\phi_j(\omega)W_j(\omega) = L_j(\omega)-k_c\psi_j(a_1)\left\{\sum_{r=1}^{\infty}\psi_r(a_2)W_r(\omega)-\sum_{i=1}^{\infty}\psi_i(a_1)W_i(\omega)\right\} \tag{A.17}$$

where

$$\phi_j(\omega)=\{\omega_j^2-\omega^2+\sqrt{-1}\,c_1\omega\} \tag{A.18}$$

and

$$W_j(\omega) = 1/2\pi\int_{-T/2}^{+T/2} W_j(t)e^{-i\omega t}dt \tag{A.19}$$

in the limit as $T\to\infty$. In this last equation the random processes are truncated over the range $-T/2<t<T/2$ so that the Fourier transforms, $W_j(\omega)$ etc., exist; see for example Price and Bishop[56]. Notice that an alternative definition of ϕ is

$$\phi_j(\omega)=\{\omega_j^2-\omega^2+\sqrt{-1}\,\omega_j\eta_1\omega\} \tag{A.20}$$

where now η_1 is a constant damping ratio for all the modes of sub-system 1, but this implies that damping increases with natural frequency, which does *not* meet the normal SEA assumption and so is not used within SEA. Continuing with the main analysis, next multiply equation (A.17) by $\psi_j(a_1)/m_1\phi_j(\omega)$ and sum over all the j of sub-system 1 to get

$$\sum_{j=1}^{\infty}\psi_j(a_1)W_j(\omega) = \sum_{j=1}^{\infty}\frac{\psi_j(a_1)L_j(\omega)}{m_1\phi_j(\omega)} \tag{A.21}$$

$$+\sum_{j=1}^{\infty}\frac{k_c\psi_j^2(a_1)}{m_1\phi_j(\omega)}\left[\sum_{r=1}^{\infty}\psi_r(a_2)W_r(\omega)-\sum_{i=1}^{\infty}\psi_i(a_1)W_i(\omega)\right]$$

and

$$\sum_{s=1}^{\infty}\psi_s(a_2)W_s(\omega)=\sum_{s=1}^{\infty}\frac{\psi_s(a_2)L_s(\omega)}{m_2\phi_s(\omega)} \tag{A.22}$$

$$+\sum_{s=1}^{\infty}\frac{k_c{\psi_s}^2(a_2)}{m_2\phi_s(\omega)}\left[\sum_{i=1}^{\infty}\psi_i(a_1)W_i(\omega)-\sum_{r=1}^{\infty}\psi_r(a_2)W_r(\omega)\right]$$

Let

$$\Delta=1+\sum_{i=1}^{\infty}\frac{k_c{\psi_i}^2(a_1)}{m_1\phi_i(\omega)}+\sum_{r=1}^{\infty}\frac{k_c{\psi_r}^2(a_2)}{m_2\phi_r(\omega)} \tag{A.23}$$

and noting that the sums over i and j are similar as are those over r and s, these simultaneous equations for the various summations may be solved to give

$$\sum_{j=1}^{\infty}\psi_j(a_1)W_j(\omega)-\sum_{j=1}^{\infty}\frac{\psi_j(a_1)L_j(\omega)}{m_1\phi_j(\omega)}=\sum_{j=1}^{\infty}\frac{k_c{\psi_j}^2(a_1)}{m_1\phi_j(\omega)} \tag{A.24}$$

$$\times\left[\sum_{r=1}^{\infty}\frac{\psi_r(a_2)L_r(\omega)}{m_2\phi_r(\omega)}-\sum_{i=1}^{\infty}\frac{\psi_i(a_1)L_i(\omega)}{m_1\phi_i(\omega)}\right]/\Delta$$

and

$$\sum_{s=1}^{\infty}\psi_s(a_2)W_s(\omega)-\sum_{s=1}^{\infty}\frac{\psi_s(a_2)L_s(\omega)}{m_2\phi_s(\omega)}=\sum_{s=1}^{\infty}\frac{k_c{\psi_s}^2(a_2)}{m_2\phi_s(\omega)} \tag{A.25}$$

$$\times\left[\sum_{i=1}^{\infty}\frac{\psi_i(a_1)L_i(\omega)}{m_1\phi_i(\omega)}-\sum_{r=1}^{\infty}\frac{\psi_r(a_2)L_r(\omega)}{m_2\phi_r(\omega)}\right]/\Delta$$

By way of example the *jth* term from the summations on the left-hand side gives

$$\psi_j(a_1)W_j(\omega)-\frac{\psi_j(a_1)L_j(\omega)}{m_1\phi_j(\omega)}=\frac{k_c{\psi_j}^2(a_1)}{m_1\phi_j(\omega)} \tag{A.26}$$

$$\times\left[\sum_{r=1}^{\infty}\frac{\psi_r(a_2)L_r(\omega)}{m_2\phi_r(\omega)}-\sum_{i=1}^{\infty}\frac{\psi_i(a_1)L_i(\omega)}{m_1\phi_i(\omega)}\right]/\Delta$$

or, after a slight rearrangement

$$\phi_j(a_1)W_j(\omega)-L_j(\omega)/m_1=k_c\psi_j(a_1)/m_1 \tag{A.27}$$

$$\times\left[\sum_{r=1}^{\infty}\frac{\psi_r(a_2)L_r(\omega)}{m_2\phi_r(\omega)}-\sum_{i=1}^{\infty}\frac{\psi_i(a_1)L_i(\omega)}{m_1\phi_i(\omega)}\right]/\Delta$$

Here the term on the right-hand side represents the coupling force between the two sub-systems on the *jth* mode of sub-system 1 as compared with $L_j(\omega)$, which is the external force acting on that mode. It may be written as $\kappa_j(\omega)$, defined as

$$\kappa_j(\omega) = k_c \psi_j(a_1) \left[\sum_{r=1}^{\infty} \frac{\psi_r(a_2) L_r(\omega)}{m_2 \phi_r(\omega)} - \sum_{i=1}^{\infty} \frac{\psi_i(a_1) L_i(\omega)}{m_1 \phi_i(\omega)} \right] / \Delta \tag{A.28}$$

leading to

$$W_j(\omega) = \{L_j(\omega) + \kappa_j(\omega)\} / m_1 \phi_j(a_1) \tag{A.29}$$

Equation (A.29) is the fundamental result of Davies' work[21] and allows a form of modal analysis to be applied. It is based on an expansion of the modes of the *uncoupled* sub-systems but applies for *all* coupling strengths.

A.2. Long Term Averages

SEA is concerned with long term energy flows which are calculated from the products of various time varying functions (such as forces and velocities). Therefore attention is focused on cross-correlation functions such as $\langle \dot{y}_1 y_1 \rangle$ which, for the ergodic processes considered here, are the same as ensemble averages $E[\dot{y}_1 y_1]$. In the frequency domain the Fourier transforms of such functions are the spectral density functions such as $S_{\dot{y}_1 y_1}$, defined as

$$S_{\dot{y}_1 y_1}(\omega) = \underset{T \to \infty}{limit} \left\{ \dot{y}_1^{\,*}(\omega) y_1(\omega) 2\pi / T \right\} \tag{A.30}$$

where again the random processes are truncated over the range $-T/2 < t < T/2$ so that the Fourier transforms, $\dot{y}_1(\omega)$ etc., exist. Using this definition, the expected values become, for example

$$E[\dot{y}_1 y_1] = \int_{-\infty}^{\infty} S_{\dot{y}_1 y_1}(\omega) d\omega \tag{A.31}$$

where it is noted that a two sided spectrum defined for both positive and negative frequencies is used. Combining the results of the previous section with these definitions all the parameters of interest may be formed in terms of frequency spectra and the Fourier transforms of the various responses.

A.3. Coupling Power

Concentrating on the equations that apply to sub-system 1, the energy flowing from sub-system 2 into sub-system 1 at any instant, $\Pi_{21}(t)$, is simply the product of the force in the coupling spring and the velocity at the point of coupling on sub-system 1, i.e.

$$\Pi_{21}(t) = \dot{y}_1(a_1,t) \times k_c\{y_2(a_2,t) - y_1(a_1,t)\} \tag{A.32}$$

$$= k_c\dot{y}_1(a_1,t)y_2(a_2,t) - k_c\dot{y}_1(a_1,t)y_1(a_1,t)$$

The ensemble average of this energy is

$$E[\Pi_{21}(t)] = E[\Pi_{21}] = k_c E[\dot{y}_1(a_1,t)y_2(a_2,t)] - k_c E[\dot{y}_1(a_1,t)y_1(a_1,t)] \tag{A.33}$$

but, as has already been noted in Chapter 2, $E[\dot{y}_1(a_1,t)y_1(a_1,t)] = 0$, so that

$$E[\Pi_{21}] = k_c E[\dot{y}_1(a_1,t)y_2(a_2,t)] \tag{A.34}$$

Next, inserting the modal expansions for the displacement functions gives

$$E[\Pi_{21}] = k_c \sum_{i=1}^{\infty}\sum_{r=1}^{\infty} \psi_i(a_1)\psi_r(a_2)E[\dot{W}_i(t)W_r(t)] \tag{A.35}$$

but $E[\dot{W}_i(t)W_r(t)]$ may be replaced by its spectral density and $E[\Pi_{21}]$ by its Fourier transform, so that

$$\Pi_{21}(\omega) = k_c \sum_{i=1}^{\infty}\sum_{r=1}^{\infty} \psi_i(a_1)\psi_r(a_2)S_{\dot{W}_i W_r}(\omega) \tag{A.36}$$

Further the time differential on W_i in the spectral density can be replaced by $-\sqrt{-1}\,\omega$ so that

$$\Pi_{21}(\omega) = -\sqrt{-1}\,\omega k_c \sum_{i=1}^{\infty}\sum_{r=1}^{\infty} \psi_i(a_1)\psi_r(a_2)S_{W_i W_r}(\omega) \tag{A.37}$$

which is equivalent to equation (13) in Davies' paper[21]. Next the spectral density of the derived process $S_{W_i W_r}(\omega)$ is replaced by the Fourier transforms of the input processes factored by the relevant frequency response functions, i.e.

$$S_{W_i W_r}(\omega) = \lim_{T\to\infty}\left\{ W_i^*(\omega)W_r(\omega)\right\}\frac{2\pi}{T} \tag{A.38}$$

$$= \lim_{T\to\infty}\left\{ \frac{\{L_i(\omega)+\kappa_i(\omega)\}^*\{L_r(\omega)+\kappa_r(\omega)\}}{\{m_1\phi_i(a_1)\}^*\{m_2\phi_r(a_2)\}}\right\}\frac{2\pi}{T}$$

giving

$$\Pi_{21}(\omega) = -\sqrt{-1}\,\omega k_c \sum_{i=1}^{\infty}\sum_{r=1}^{\infty}\left\{ \psi_i(a_1)\psi_r(a_2)\right. \tag{A.39}$$

$$\left.\lim_{T\to\infty}\left\{ \frac{\{L_i(\omega)+\kappa_i(\omega)\}^*\{L_r(\omega)+\kappa_r(\omega)\}}{\{m_1\phi_i(a_1)\}^*\{m_2\phi_r(a_2)\}}\right\}\frac{2\pi}{T}\right\}$$

where it is recalled that the quantities $\kappa_i(\omega)$ etc. are themselves summations of Fourier transforms divided by Δ which is also formed from such summations. Multiplying out these various terms and

replacing

$$\lim_{T\to\infty}\left\{L_j^*(\omega)L_s(\omega)2\pi/T\right\}$$

by $S_{js}(\omega)$ etc. gives the desired energy flow in terms of the modal components of the *external* driving forces, i.e.

$$\Pi_{21}(\omega)=\frac{-\sqrt{-1}\,\omega k_c}{m_1m_2}\sum_{i=1}^{\infty}\sum_{r=1}^{\infty}\left[\frac{\psi_i(a_1)\psi_r(a_2)S_{ir}}{\phi_i^*(\omega)\phi_r(\omega)}\right] \tag{A.40}$$

$$-\frac{\sqrt{-1}\,\omega k_c}{\Delta^*}\sum_{i=1}^{\infty}\frac{k_c\psi_i^2(a_1)}{m_1\phi_i^*(\omega)}\sum_{r=1}^{\infty}\left[\frac{\psi_r(a_2)}{m_2\phi_r(\omega)}\left\{\sum_{s=1}^{\infty}\frac{\psi_s(a_2)S_{sr}(\omega)}{m_2\phi_s^*(\omega)}-\sum_{j=1}^{\infty}\frac{\psi_j(a_1)S_{jr}(\omega)}{m_1\phi_j^*(\omega)}\right\}\right]$$

$$-\frac{\sqrt{-1}\,\omega k_c}{\Delta}\sum_{r=1}^{\infty}\frac{k_c\psi_r^2(a_2)}{m_2\phi_r(\omega)}\sum_{i=1}^{\infty}\left[\frac{\psi_i(a_1)}{m_1\phi_i^*(\omega)}\left\{-\sum_{r=1}^{\infty}\frac{\psi_r(a_2)S_{ir}(\omega)}{m_2\phi_r(\omega)}+\sum_{j=1}^{\infty}\frac{\psi_j(a_1)S_{ij}(\omega)}{m_1\phi_j(\omega)}\right\}\right]$$

$$-\frac{\sqrt{-1}\,\omega k_c}{|\Delta|^2}\sum_{i=1}^{\infty}\frac{k_c\psi_i^2(a_1)}{m_1\phi_i^*(\omega)}\sum_{r=1}^{\infty}\frac{k_c\psi_r^2(a_2)}{m_2\phi_r(\omega)}\left[-\sum_{i=1}^{\infty}\sum_{j=1}^{\infty}\frac{\psi_i(a_1)\psi_j(a_1)S_{ij}(\omega)}{m_1^2\phi_i^*(\omega)\phi_j(\omega)}\right.$$

$$-\sum_{r=1}^{\infty}\sum_{s=1}^{\infty}\frac{\psi_r(a_2)\psi_s(a_2)S_{sr}(\omega)}{m_2^2\phi_r(\omega)\phi_s^*(\omega)}$$

$$\left.+\sum_{i=1}^{\infty}\sum_{r=1}^{\infty}\left\{\frac{\psi_i(a_1)\psi_r(a_2)S_{ir}(\omega)}{m_1m_2\phi_i^*(\omega)\phi_r(\omega)}+\frac{\psi_i(a_1)\psi_r(a_2)S_{ri}(\omega)}{m_1m_2\phi_i(\omega)\phi_r^*(\omega)}\right\}\right]$$

Now this rather complex expression includes various cross-spectral densities relating the modal components of the external driving forces on sub-system 1 and those on sub-system 2, i.e. $S_{ir}(\omega)$. If the driving forces are statistically independent, assumption (ii) of Chapter 2, then so are their modal components, so that these terms are all zero, leaving only the cross-spectra relating the various *modes* of *one* sub-system, i.e.

$$\Pi_{21}(\omega)=-\sqrt{-1}\,\omega k_c\left[\frac{\sum_{i=1}^{\infty}\frac{k_c\psi_i^2(a_1)}{m_1\phi_i^*(\omega)}}{\Delta^*}-\frac{\sum_{i=1}^{\infty}\frac{k_c\psi_i^2(a_1)}{m_1\phi_i^*(\omega)}\sum_{r=1}^{\infty}\frac{k_c\psi_r^2(a_2)}{m_2\phi_r(\omega)}}{|\Delta|^2}\right] \tag{A.41}$$

$$\times\sum_{r=1}^{\infty}\sum_{s=1}^{\infty}\frac{\psi_r(a_2)\psi_s(a_2)S_{sr}(\omega)}{m_2^2\phi_r(\omega)\phi_s^*(\omega)}$$

$$-\sqrt{-1}\,\omega k_c\left[\frac{\sum_{r=1}^{\infty}\frac{k_c\psi_r^2(a_2)}{m_2\phi_r(\omega)}}{\Delta}-\frac{\sum_{i=1}^{\infty}\frac{k_c\psi_i^2(a_1)}{m_1\phi_i^*(\omega)}\sum_{r=1}^{\infty}\frac{k_c\psi_r^2(a_2)}{m_2\phi_r(\omega)}}{|\Delta|^2}\right]$$

$$\times\sum_{i=1}^{\infty}\sum_{j=1}^{\infty}\frac{\psi_i(a_1)\psi_j(a_1)S_{ij}(\omega)}{m_1^2\phi_i^*(\omega)\phi_j(\omega)}$$

This may be further simplified by recalling the formula for Δ, equation (A.23), which leads to

$$\Pi_{21}(\omega)=-\sqrt{-1}\,\omega k_c\left[\frac{\sum_{i=1}^{\infty}\frac{k_c\psi_i^2(a_1)}{m_1\phi_i^*(\omega)}+\left|\sum_{i=1}^{\infty}\frac{k_c\psi_i^2(a_1)}{m_1\phi_i(\omega)}\right|^2}{|\Delta|^2}\right] \tag{A.42}$$

$$\times\sum_{r=1}^{\infty}\sum_{s=1}^{\infty}\frac{\psi_r(a_2)\psi_s(a_2)S_{rs}(\omega)}{m_2^2\phi_r^*(\omega)\phi_s(\omega)}$$

$$-\sqrt{-1}\,\omega k_c\left[\frac{\sum_{r=1}^{\infty}\frac{k_c\psi_r^2(a_2)}{m_2\phi_r(\omega)}+\left|\sum_{r=1}^{\infty}\frac{k_c\psi_r^2(a_2)}{m_2\phi_r(\omega)}\right|^2}{|\Delta|^2}\right]$$

$$\times\sum_{i=1}^{\infty}\sum_{j=1}^{\infty}\frac{\psi_i(a_1)\psi_j(a_1)S_{ij}(\omega)}{m_1^2\phi_i^*(\omega)\phi_j(\omega)}$$

To proceed from this point, it is noted that the spectrum $\Pi_{21}(\omega)$ is defined over the range $-\infty$ to ∞. Therefore, when assessing the energy flowing within a given range of frequencies, contributions from both the positive and negative frequency ranges must be considered. The consequence of this is that only the even components of $\Pi_{21}(\omega)$ need be considered, which allows a further simplification. Clearly ϕ has even real parts and odd imaginary ones, also cross-spectra have even real and odd imaginary parts. This means that both $\sum_{i=1}^{\infty}\frac{k_c\psi_i^2(a_1)}{m_1\phi_i(\omega)}$ and $S_{ij}/\phi_i^*(\omega)\phi_j(\omega)$ have even real parts and odd imaginary ones, so that a simplified expression for the power spectrum becomes

$$\Pi_{21}(\omega)=\mathrm{Im}\left\{-\omega k_c\left[\frac{\sum_{i=1}^{\infty}\frac{k_c\psi_i^2(a_1)}{m_1\phi_i^*(\omega)}+\left|\sum_{i=1}^{\infty}\frac{k_c\psi_i^2(a_1)}{m_1\phi_i(\omega)}\right|^2}{|\Delta|^2}\right]\right\} \tag{A.43}$$

$$\times\,\mathrm{Re}\left\{\sum_{r=1}^{\infty}\sum_{s=1}^{\infty}\frac{\psi_r(a_2)\psi_s(a_2)S_{rs}(\omega)}{m_2^2\phi_r^*(\omega)\phi_s(\omega)}\right\}$$

$$+\mathrm{Im}\left\{-\omega k_c\left[\frac{\sum_{r=1}^{\infty}\frac{k_c\psi_r^2(a_2)}{m_2\phi_r(\omega)}+\left|\sum_{r=1}^{\infty}\frac{k_c\psi_r^2(a_2)}{m_2\phi_r(\omega)}\right|^2}{|\Delta|^2}\right]\right\}$$

$$\times\mathrm{Re}\left\{\sum_{i=1}^{\infty}\sum_{j=1}^{\infty}\frac{\psi_i(a_1)\psi_j(a_1)S_{ij}(\omega)}{m_1^2\phi_i^*(\omega)\phi_j(\omega)}\right\}$$

or

$$\Pi_{21}(\omega)=\frac{\omega k_c}{|\Delta|^2}\mathrm{Im}\left\{\sum_{i=1}^{\infty}\frac{k_c\psi_i^2(a_1)}{m_1\phi_i(\omega)}\right\}\sum_{r=1}^{\infty}\sum_{s=1}^{\infty}\mathrm{Re}\left\{\frac{\psi_r(a_2)\psi_s(a_2)S_{rs}(\omega)}{m_2^2\phi_r^*(\omega)\phi_s(\omega)}\right\} \tag{A.44}$$

$$-\frac{\omega k_c}{|\Delta|^2}\mathrm{Im}\left\{\sum_{r=1}^{\infty}\frac{k_c\psi_r^2(a_2)}{m_2\phi_r(\omega)}\right\}\sum_{i=1}^{\infty}\sum_{j=1}^{\infty}\mathrm{Re}\left\{\frac{\psi_i(a_1)\psi_j(a_1)S_{ij}(\omega)}{m_1^2\phi_i^*(\omega)\phi_j(\omega)}\right\}$$

which is equivalent to equation (14) of Davies' paper[21]. Finally reversing the various subscripts and noting that $\mathrm{Im}\{\phi_i(\omega)\}$ is ωc_1 etc., the expression given in Chapter 3, equation (3.16), is recovered. That is,

$$\Pi_{12}(\omega)=\frac{\omega^2k_c^2c_2}{m_1^2m_2|\Delta|^2}\sum_{r=1}^{\infty}\left[\frac{\psi_r^2(a_2)}{|\phi_r|^2}\right]\sum_{i=1}^{\infty}\sum_{j=1}^{\infty}\left[\mathrm{Re}\{S_{ij}(\omega)\}\frac{\psi_i(a_1)\psi_j(a_1)\mathrm{Re}\{\phi_i\phi_j^*\}}{|\phi_i|^2|\phi_j|^2}\right] \tag{A.45}$$

$$-\frac{\omega^2k_c^2c_1}{m_1m_2^2|\Delta|^2}\sum_{i=1}^{\infty}\left[\frac{\psi_i(a_1)^2}{|\phi_i|^2}\right]\sum_{r=1}^{\infty}\sum_{s=1}^{\infty}\left[\mathrm{Re}\{S_{rs}(\omega)\}\frac{\psi_r(a_2)\psi_s(a_2)\mathrm{Re}\{\phi_r\phi_s^*\}}{|\phi_r|^2|\phi_s|^2}\right]$$

where $\phi(\omega)$ is written as ϕ for clarity, and $\mathrm{Re}\{S_{ij}(\omega)\}$ etc., are in fact *co-spectra* here.

A.4. Input Power

Continuing with the equations that apply to sub-system 1, the energy flowing into sub-system 1 from external driving at any instant, $\Pi_{1_{IN}}(t)$, is simply the product of the force applied and the velocity at the point of application integrated over the sub-system, i.e.

$$\Pi_{1_{IN}}(t)=\int_1\dot{y}_1(x_1,t)F_1(x_1,t)\mathrm{d}x_1 \tag{A.46}$$

The ensemble average of this is

$$E[\Pi_{1_{IN}}(t)]=E[\Pi_{1_{IN}}]=\int_1E[\dot{y}_1(x_1,t)F_1(x_1,t)]\mathrm{d}x_1 \tag{A.47}$$

Next, inserting the modal expansions and moving terms that do not vary with position from within the

integral gives

$$E[\Pi_{1_{IN}}] = \sum_{i=1}^{\infty}\sum_{j=1}^{\infty}\left[E[\dot{W}_i(t)L_j(t)]\int_1 \frac{\psi_i(x_1)\psi_j(x_1)\rho_1(x_1)dx_1}{m_1}\right] \tag{A.48}$$

Because of the normalisation scheme adopted, the integral collapses to δ_{ij} leaving

$$E[\Pi_{1_{IN}}] = \sum_{i=1}^{\infty} E[\dot{W}_i(t)L_i(t)] \tag{A.49}$$

Now taking spectral densities and Fourier transforms as before gives

$$\Pi_{1_{IN}}(\omega) = \sum_{i=1}^{\infty} S_{\dot{W}_i}(\omega) \tag{A.50}$$

where $S_{\dot{W}_i}$ is the cross-spectral density of the modal response velocity and the modal driving force. The time differential can again be dropped in favour of $-\sqrt{-1}\,\omega$, i.e.

$$\Pi_{1_{IN}}(\omega) = -\sqrt{-1}\,\omega\sum_{i=1}^{\infty} S_{W_i}(\omega) \tag{A.51}$$

where

$$S_{W_i}(\omega) = \underset{T\to\infty}{limit}\left\{W_i^*(\omega)L_i(\omega)\right\}\frac{2\pi}{T} \tag{A.52}$$

The substitution of $W_i(\omega)$ using equation (A.29) gives

$$\Pi_{1_{IN}}(\omega) = -\sqrt{-1}\,\omega\sum_{i=1}^{\infty}\left[\underset{T\to\infty}{limit}\left\{\frac{\{L_i(\omega)+\kappa_i(\omega)\}^*}{\{m_1\phi_i(a_1)\}^*}L_i(\omega)\right\}\frac{2\pi}{T}\right] \tag{A.53}$$

so that multiplying out the various terms gives

$$\Pi_{1_{IN}}(\omega) = -\sqrt{-1}\,\omega\sum_{i=1}^{\infty}\frac{S_{ii}(\omega)}{m_1\phi_i^*(\omega)} - \frac{\sqrt{-1}\,\omega k_c}{\Delta^*}\sum_{i=1}^{\infty}\sum_{r=1}^{\infty}\left[\frac{\psi_i(a_1)\psi_r(a_2)S_{ir}(\omega)}{m_1 m_2\phi_i^*(\omega)\phi_r^*(\omega)}\right] \tag{A.54}$$

$$+\frac{\sqrt{-1}\,\omega k_c}{\Delta^*}\sum_{i=1}^{\infty}\sum_{j=1}^{\infty}\left[\frac{\psi_i(a_1)\psi_j(a_1)S_{ij}(\omega)}{m_1^2\phi_i^*(\omega)\phi_j^*(\omega)}\right]$$

Again, assuming that the modal driving components on sub-systems 1 and 2 are independent allows the second of these summations to be dropped leaving

$$\Pi_{1_{IN}}(\omega) = -\sqrt{-1}\,\omega\sum_{i=1}^{\infty}\frac{S_{ii}(\omega)}{m_1\phi_i^*(\omega)} + \frac{\sqrt{-1}\,\omega k_c}{\Delta^*}\sum_{i=1}^{\infty}\sum_{j=1}^{\infty}\left[\frac{\psi_i(a_1)\psi_j(a_1)S_{ij}(\omega)}{m_1^2\phi_i^*(\omega)\phi_j^*(\omega)}\right] \tag{A.55}$$

Next taking the even component, since the spectra are defined from $-\infty$ to ∞ gives

$$\Pi_{1_{IN}}(\omega)=\frac{\omega^2 c_1}{m_1}\sum_{i=1}^{\infty}\frac{S_{ii}(\omega)}{|\phi_i|^2}+\frac{\omega k_c}{m_1^2}\mathrm{Im}\left\{\sum_{i=1}^{\infty}\sum_{j=1}^{\infty}\frac{S_{ij}(\omega)\psi_i(a_1)\psi_j(a_1)}{\phi_i\phi_j\Delta}\right\} \tag{A.56}$$

where $\phi(\omega)$ is written as ϕ for clarity, and it has been noted that $\mathrm{Im}\{\phi_i(\omega)\}$ is just ωc_1 etc. This is, in fact, equation (3.20). Also it is assumed that only the real, even parts of the cross-spectral densities are used.

A.5. Dissipated Power

Continuing again with the equations that apply to sub-system 1, the energy dissipated by damping within sub-system 1 at any instant, $\Pi_{1_{DISS}}(t)$, is the product of the viscous damping force and the velocity at the point of application integrated over the sub-system, i.e.

$$\Pi_{1_{DISS}}(t)=\int_1 \dot{y}_1(x_1,t)r_1(x_1)\dot{y}_1(x_1,t)\mathrm{d}x_1 \tag{A.57}$$

The ensemble average of this is

$$E[\Pi_{1_{DISS}}(t)]=E[\Pi_{1_{DISS}}]=\int_1 E[\dot{y}_1^2(x_1,t)]r_1(x_1)\mathrm{d}x_1 \tag{A.58}$$

Next, inserting the modal expansions for $\dot{y}_1(t)$ and moving terms that do not vary with position from within the integral gives

$$E[\Pi_{1_{DISS}}]=\sum_{i=1}^{\infty}\sum_{j=1}^{\infty}\left[E[\dot{W}_i(t)\dot{W}_j(t)]\int_1\psi_i(x_1)\psi_j(x_1)r_1(x_1)\mathrm{d}x_1\right] \tag{A.59}$$

Because of the normalisation scheme adopted and the fact that damping is assumed proportional the integral collapses to $m_1 c_1 \delta_{ij}$ leaving

$$E[\Pi_{1_{DISS}}]=m_1 c_1\sum_{i=1}^{\infty}E[\dot{W}_i(t)\dot{W}_i(t)] \tag{A.60}$$

Now taking spectral densities and Fourier transforms as before gives

$$\Pi_{1_{DISS}}(\omega)=m_1 c_1\sum_{i=1}^{\infty}S_{\dot{W}_i\dot{W}_i} \tag{A.61}$$

where $S_{\dot{W}_i\dot{W}_i}$ is the direct spectral density of the modal response velocity. The time differentials can again be dropped in favour of $-\sqrt{-1}\,\omega$, i.e.

$$\Pi_{1_{DISS}}(\omega) = m_1 c_1 \omega^2 \sum_{i=1}^{\infty} S_{W_i W_i} \tag{A.62}$$

where

$$S_{W_i W_i}(\omega) = \underset{T\to\infty}{limit} \left\{ W_i^*(\omega) W_i(\omega) \right\} \frac{2\pi}{T} \tag{A.63}$$

Now substituting for $W_i(\omega)$ using equation (A.29) gives

$$\Pi_{1_{DISS}}(\omega) = m_1 c_1 \omega^2 \sum_{i=1}^{\infty} \left[\underset{T\to\infty}{limit} \left\{ \frac{\{L_i(\omega)+\kappa_i(\omega)\}^* \{L_i(\omega)+\kappa_i(\omega)\}}{\{m_1\phi_i(a_1)\}^* \{m_1\phi_i(a_1)\}} \right\} \frac{2\pi}{T} \right] \tag{A.64}$$

so that multiplying out the various terms gives

$$\Pi_{1_{DISS}}(\omega) = \frac{c_1\omega^2}{m_1} \sum_{i=1}^{\infty} \frac{S_{ii}}{|\phi_i(\omega)|^2} \tag{A.65}$$

$$+ \frac{c_1\omega^2 k_c}{m_1\Delta} \sum_{i=1}^{\infty} \left[\frac{\psi_i(a_1)}{|\phi_i(\omega)|^2} \left\{ \sum_{r=1}^{\infty} \frac{\psi_r(a_2) S_{ir}(\omega)}{m_2\phi_r(\omega)} - \sum_{j=1}^{\infty} \frac{\psi_j(a_1) S_{ij}(\omega)}{m_1\phi_j(\omega)} \right\} \right]$$

$$+ \frac{c_1\omega^2 k_c}{m_1\Delta^*} \sum_{i=1}^{\infty} \left[\frac{\psi_i(a_1)}{|\phi_i(\omega)|^2} \left\{ \sum_{r=1}^{\infty} \frac{\psi_r(a_2) S_{ri}(\omega)}{m_2\phi_r^*(\omega)} - \sum_{j=1}^{\infty} \frac{\psi_j(a_1) S_{ji}(\omega)}{m_1\phi_j^*(\omega)} \right\} \right]$$

$$+ \frac{c_1\omega^2 k_c^2}{m_1 |\Delta|^2} \sum_{i=1}^{\infty} \left[\frac{\psi_i^2(a_1)}{|\phi_i(\omega)|^2} \right] \times \left[\sum_{i=1}^{\infty}\sum_{j=1}^{\infty} \frac{\psi_i(a_1)\psi_j(a_1) S_{ij}(\omega)}{m_1^2 \phi_i^*(\omega)\phi_j(\omega)} \right.$$

$$\left. + \sum_{r=1}^{\infty}\sum_{s=1}^{\infty} \frac{\psi_r(a_2)\psi_s(a_2) S_{rs}(\omega)}{m_2^2 \phi_r^*(\omega)\phi_s(\omega)} \right.$$

$$\left. - \sum_{i=1}^{\infty}\sum_{r=1}^{\infty} \left\{ \frac{\psi_i(a_1)\psi_r(a_2) S_{ir}(\omega)}{m_1 m_2 \phi_i^*(\omega)\phi_r(\omega)} + \frac{\psi_i(a_1)\psi_r(a_2) S_{ri}(\omega)}{m_1 m_2 \phi_i(\omega)\phi_r^*(\omega)} \right\} \right]$$

Again, assuming that the modal driving components on sub-systems 1 and 2 are independent allows a number of these summations to be dropped, leaving

$$\Pi_{1_{DISS}}(\omega) = \frac{c_1\omega^2}{m_1} \sum_{i=1}^{\infty} \frac{S_{ii}}{|\phi_i(\omega)|^2} \tag{A.66}$$

$$- \frac{c_1\omega^2 k_c}{m_1^2} \sum_{i=1}^{\infty}\sum_{j=1}^{\infty} \frac{\psi_i(a_1)\psi_j(a_1)}{|\phi_i(\omega)|^2} \left\{ \frac{S_{ij}(\omega)}{\phi_j(\omega)\Delta} + \frac{S_{ji}(\omega)}{\phi_j^*(\omega)\Delta^*} \right\}$$

$$+ \frac{c_1\omega^2 k_c^2}{m_1 |\Delta|^2} \sum_{i=1}^{\infty} \left[\frac{\psi_i^2(a_1)}{|\phi_i(\omega)|^2} \right] \times \left[\sum_{i=1}^{\infty}\sum_{j=1}^{\infty} \frac{\psi_i(a_1)\psi_j(a_1) S_{ij}(\omega)}{m_1^2 \phi_i^*(\omega)\phi_j(\omega)} \right.$$

$$+\sum_{r=1}^{\infty}\sum_{s=1}^{\infty}\frac{\psi_r(a_2)\psi_s(a_2)S_{rs}(\omega)}{m_2^2\phi_r^*(\omega)\phi_s(\omega)}\Bigg]$$

but $S_{ji}(\omega) = S_{ij}^*(\omega)$ so that this equation reduces to

$$\Pi_{1_{DISS}}(\omega) = \frac{c_1\omega^2}{m_1}\sum_{i=1}^{\infty}\frac{S_{ii}}{|\phi_i(\omega)|^2} \tag{A.67}$$

$$-\frac{2c_1\omega^2k_c}{m_1^2}\sum_{i=1}^{\infty}\sum_{j=1}^{\infty}\frac{\psi_i(a_1)\psi_j(a_1)}{|\phi_i(\omega)|^2}\mathrm{Re}\left\{\frac{S_{ij}(\omega)}{\phi_j(\omega)\Delta}\right\}$$

$$+\frac{c_1\omega^2k_c^2}{m_1|\Delta|^2}\sum_{i=1}^{\infty}\left[\frac{\psi_i^2(a_1)}{|\phi_i(\omega)|^2}\right]\times\left[\sum_{i=1}^{\infty}\sum_{j=1}^{\infty}\frac{\psi_i(a_1)\psi_j(a_1)S_{ij}(\omega)}{m_1^2\phi_i^*(\omega)\phi_j(\omega)}\right.$$

$$\left.+\sum_{r=1}^{\infty}\sum_{s=1}^{\infty}\frac{\psi_r(a_2)\psi_s(a_2)S_{rs}(\omega)}{m_2^2\phi_r^*(\omega)\phi_s(\omega)}\right]$$

Again taking only the even component, since the spectra are defined from $-\infty$ to ∞, finally gives

$$\Pi_{1_{DISS}}(\omega) = \frac{c_1\omega^2}{m_1}\sum_{i=1}^{\infty}\frac{S_{ii}}{|\phi_i|^2} \tag{A.68}$$

$$-\frac{2c_1\omega^2k_c}{m_1^2}\sum_{i=1}^{\infty}\sum_{j=1}^{\infty}\frac{\psi_i(a_1)\psi_j(a_1)}{|\phi_i|^2}\mathrm{Re}\left\{\frac{S_{ij}(\omega)}{\phi_j\Delta}\right\}$$

$$+\frac{c_1\omega^2k_c^2}{m_1|\Delta|^2}\sum_{i=1}^{\infty}\left[\frac{\psi_i^2(a_1)}{|\phi_i|^2}\right]\times\left[\sum_{i=1}^{\infty}\sum_{j=1}^{\infty}\frac{\psi_i(a_1)\psi_j(a_1)}{m_1^2}\mathrm{Re}\left\{\frac{S_{ij}(\omega)}{\phi_i^*\phi_j}\right\}\right.$$

$$\left.+\sum_{r=1}^{\infty}\sum_{s=1}^{\infty}\frac{\psi_r(a_2)\psi_s(a_2)}{m_2^2}\mathrm{Re}\left\{\frac{S_{rs}(\omega)}{\phi_r^*\phi_s}\right\}\right]$$

where again $\phi(\omega)$ is written as ϕ for clarity.

A.6. Energy Levels

The final parameter of interest on sub-system 1 is the energy level, which is taken to be twice the kinetic energy. The instantaneous kinetic energy, $KE_1(t)$, is given by $\delta m_1\dot{y}_1(x_1,t)/2$ integrated over the sub-system, i.e.

$$KE_1(t) = 1/2\int_1\dot{y}_1^2(x_1,t)\rho_1(x_1)dx_1 \tag{A.69}$$

so that

$$E_1(t) = \int_1 \dot{y}_1^2(x_1,t)\rho_1(x_1)dx_1 \tag{A.70}$$

Comparing this result to equation (A.57), it is clear that it is simply related to the dissipated power since the damping is assumed proportional, i.e. $r_1(x_1) = c_1\rho_1(x_1)$. This relationship leads to

$$E_1(t) = \Pi_{1_{DISS}}(t)/c_1 \tag{A.71}$$

so that using equation (A.68) gives

$$\begin{aligned} E_1(\omega) = {} & \frac{\omega^2}{m_1}\sum_{i=1}^{\infty}\frac{S_{ii}}{|\phi_i(\omega)|^2} \\ & - \frac{2\omega^2 k_c}{m_1^2}\sum_{i=1}^{\infty}\sum_{j=1}^{\infty}\frac{\psi_i(a_1)\psi_j(a_1)}{|\phi_i(\omega)|^2}\mathrm{Re}\left\{\frac{S_{ij}(\omega)}{\phi_j(\omega)\Delta}\right\} \\ & + \frac{\omega^2 k_c}{m_1|\Delta|^2}\sum_{i=1}^{\infty}\left[\frac{\psi_i^2(a_1)}{|\phi_i(\omega)|^2}\right]\times\left[\sum_{i=1}^{\infty}\sum_{j=1}^{\infty}\frac{\psi_i(a_1)\psi_j(a_1)}{m_1^2}\mathrm{Re}\left\{\frac{S_{ij}(\omega)}{\phi_i^*(\omega)\phi_j(\omega)}\right\}\right. \\ & \left. + \sum_{r=1}^{\infty}\sum_{s=1}^{\infty}\frac{\psi_r(a_2)\psi_s(a_2)}{m_2^2}\mathrm{Re}\left\{\frac{S_{rs}(\omega)}{\phi_r^*(\omega)\phi_s(\omega)}\right\}\right] \end{aligned} \tag{A.72}$$

A.7. Relationship between Coupling, Input and Dissipated Powers

To verify that the proceeding analysis is consistent with the law of conservation of energy consider $E[\Pi_{1_{IN}}] - E[\Pi_{1_{DISS}}] - E[\Pi_{12}]$ which should of course be zero. Using the results of the preceding sections, this quantity is

$$\begin{aligned} E[\Pi_{1_{IN}}] - E[\Pi_{1_{DISS}}] - E[\Pi_{12}] = {} & \left[\frac{\omega^2 c_1}{m_1}\sum_{i=1}^{\infty}\frac{S_{ii}(\omega)}{|\phi_i(\omega)|^2}\right. \\ & \left. + \frac{\omega k_c}{m_1^2}\mathrm{Im}\left\{\sum_{i=1}^{\infty}\sum_{j=1}^{\infty}\frac{S_{ij}(\omega)\psi_i(a_1)\psi_j(a_1)}{\phi_i(\omega)\phi_j(\omega)\Delta}\right\}\right] \\ & - \left[\frac{c_1\omega^2}{m_1}\sum_{i=1}^{\infty}\frac{S_{ii}}{|\phi_i(\omega)|^2} - \frac{2c_1\omega^2 k_c}{m_1^2}\sum_{i=1}^{\infty}\sum_{j=1}^{\infty}\frac{\psi_i(a_1)\psi_j(a_1)}{|\phi_i(\omega)|^2}\mathrm{Re}\left\{\frac{S_{ij}(\omega)}{\phi_j(\omega)\Delta}\right\}\right. \\ & + \frac{c_1\omega^2 k_c^2}{m_1|\Delta|^2}\sum_{i=1}^{\infty}\left[\frac{\psi_i^2(a_1)}{|\phi_i(\omega)|^2}\right]\left[\sum_{i=1}^{\infty}\sum_{j=1}^{\infty}\frac{\psi_i(a_1)\psi_j(a_1)}{m_1^2}\mathrm{Re}\left\{\frac{S_{ij}(\omega)}{\phi_i^*(\omega)\phi_j(\omega)}\right\}\right. \\ & \left.\left. + \sum_{r=1}^{\infty}\sum_{s=1}^{\infty}\frac{\psi_r(a_2)\psi_s(a_2)}{m_2^2}\mathrm{Re}\left\{\frac{S_{rs}(\omega)}{\phi_r^*(\omega)\phi_s(\omega)}\right\}\right]\right] \end{aligned} \tag{A.73}$$

$$- \left[\frac{\omega^2 k_c^2 c_2}{m_1^2 m_2 |\Delta|^2} \sum_{r=1}^{\infty} \left[\frac{\psi_r{}^2(a_2)}{|\phi_r|^2} \right] \sum_{i=1}^{\infty}\sum_{j=1}^{\infty} \left[\mathrm{Re}\{S_{ij}(\omega)\} \frac{\psi_i(a_1)\psi_j(a_1)\mathrm{Re}\{\phi_i\phi_j{}^*\}}{|\phi_i|^2|\phi_j|^2} \right] \right.$$

$$\left. - \frac{\omega^2 k_c^2 c_1}{m_1 m_2^2 |\Delta|^2} \sum_{i=1}^{\infty} \left[\frac{\psi_i(a_1)^2}{|\phi_i|^2} \right] \sum_{r=1}^{\infty}\sum_{s=1}^{\infty} \left[\mathrm{Re}\{S_{rs}(\omega)\} \frac{\psi_r(a_2)\psi_s(a_2)\mathrm{Re}\{\phi_r\phi_s{}^*\}}{|\phi_r|^2|\phi_s|^2} \right] \right]$$

Cancelling various terms leaves

$$E[\Pi_{1_{IN}}] - E[\Pi_{1_{DISS}}] - E[\Pi_{12}] = \frac{\omega k_c}{m_1^2} \mathrm{Im} \left\{ \sum_{i=1}^{\infty}\sum_{j=1}^{\infty} \frac{S_{ij}(\omega)\psi_i(a_1)\psi_j(a_1)}{\phi_i(\omega)\phi_j(\omega)\Delta} \right\} \tag{A.74}$$

$$+ \frac{2c_1\omega^2 k_c}{m_1^2} \sum_{i=1}^{\infty}\sum_{j=1}^{\infty} \frac{\psi_i(a_1)\psi_j(a_1)}{|\phi_i(\omega)|^2} \mathrm{Re} \left\{ \frac{S_{ij}(\omega)}{\phi_j(\omega)\Delta} \right\}$$

$$- \frac{\omega^2 k_c^2 c_1}{m_1^3 |\Delta|^2} \sum_{i=1}^{\infty} \left[\frac{\psi_i{}^2(a_1)}{|\phi_i|^2} \right] \sum_{i=1}^{\infty}\sum_{j=1}^{\infty} \left[\mathrm{Re}\{S_{ij}(\omega)\} \frac{\psi_i(a_1)\psi_j(a_1)\mathrm{Re}\{\phi_i\phi_j{}^*\}}{|\phi_i|^2|\phi_j|^2} \right]$$

$$- \frac{\omega^2 k_c^2 c_2}{m_1^2 m_2 |\Delta|^2} \sum_{r=1}^{\infty} \left[\frac{\psi_r{}^2(a_2)}{|\phi_r|^2} \right] \sum_{i=1}^{\infty}\sum_{j=1}^{\infty} \left[\mathrm{Re}\{S_{ij}(\omega)\} \frac{\psi_i(a_1)\psi_j(a_1)\mathrm{Re}\{\phi_i\phi_j{}^*\}}{|\phi_i|^2|\phi_j|^2} \right]$$

The last two terms here can be combined by recalling the formulation for Δ, equation (A.23), giving

$$E[\Pi_{1_{IN}}] - E[\Pi_{1_{DISS}}] - E[\Pi_{12}] = \frac{\omega k_c}{m_1^2} \mathrm{Im} \left\{ \sum_{i=1}^{\infty}\sum_{j=1}^{\infty} \frac{S_{ij}(\omega)\psi_i(a_1)\psi_j(a_1)}{\phi_i(\omega)\phi_j(\omega)\Delta} \right\} \tag{A.75}$$

$$+ \frac{2c_1\omega^2 k_c}{m_1^2} \sum_{i=1}^{\infty}\sum_{j=1}^{\infty} \frac{\psi_i(a_1)\psi_j(a_1)}{|\phi_i(\omega)|^2} \mathrm{Re} \left\{ \frac{S_{ij}(\omega)}{\phi_j(\omega)\Delta} \right\}$$

$$+ \frac{\omega k_c \mathrm{Im}\{\Delta\}}{m_1^2 |\Delta|^2} \sum_{i=1}^{\infty}\sum_{j=1}^{\infty} \left[\mathrm{Re}\{S_{ij}(\omega)\} \frac{\psi_i(a_1)\psi_j(a_1)\mathrm{Re}\{\phi_i\phi_j{}^*\}}{|\phi_i|^2|\phi_j|^2} \right]$$

All these summations are over the same ranges and can be combined to give

$$E[\Pi_{1_{IN}}] - E[\Pi_{1_{DISS}}] - E[\Pi_{12}] = \frac{\omega k_c}{m_1^2 |\Delta|^2} \sum_{i=1}^{\infty}\sum_{j=1}^{\infty} \left[\left\{ \frac{\psi_i(a_1)\psi_j(a_1)}{|\phi_i(\omega)|^2|\phi_j(\omega)|^2} \right\} \right. \tag{A.76}$$

$$\left. \times \left\{ \mathrm{Im}\{S_{ij}(\omega)\phi_i^*(\omega)\phi_j^*(\omega)\Delta^*\} + 2\mathrm{Im}\{\phi_i(\omega)\}\mathrm{Re}\{S_{ij}(\omega)\phi_j^*(\omega)\Delta^*\} + \mathrm{Im}\{\Delta\}\mathrm{Re}\{S_{ij}(\omega)\phi_i(\omega)\phi_j^*(\omega)\} \right\} \right]$$

where it has been noted that $c_1\omega/|\phi_i(\omega)|^2 = \mathrm{Im}\{-1/\phi_i(\omega)\}$. Multiplying out these various real and imaginary quantities and cancelling gives

$$E[\Pi_{1_{IN}}] - E[\Pi_{1_{DISS}}] - E[\Pi_{12}] = \frac{\omega k_c}{m_1^2 |\Delta|^2} \sum_{i=1}^{\infty}\sum_{j=1}^{\infty} \left[\left\{ \frac{\psi_i(a_1)\psi_j(a_1)}{|\phi_i(\omega)|^2|\phi_j(\omega)|^2} \right\} \right. \tag{A.77}$$

$$\times \operatorname{Re}\{\Delta\}\left[\operatorname{Im}\{S_{ij}(\omega)\}\operatorname{Re}\{\phi_i(\omega)\phi_j^*(\omega)\}\operatorname{Re}\{S_{ij}(\omega)\}\operatorname{Im}\{\phi_i(\omega)\phi_j^*(\omega)\}\right]\Bigg]$$

Now since the quantities $\operatorname{Im}\{S_{ij}(\omega)\}\operatorname{Re}\{\phi_i(\omega)\phi_j^*(\omega)\}$ are all odd here they make no contribution to the overall energy flows integrated across all frequencies leaving

$$E[\Pi_{1_{IN}}] - E[\Pi_{1_{DISS}}] - E[\Pi_{12}] = \frac{\omega k_c}{m_1^2 |\Delta|^2} \sum_{i=1}^{\infty}\sum_{j=1}^{\infty}\left\{\left\{\frac{\psi_i(a_1)\psi_j(a_1)}{|\phi_i(\omega)|^2 |\phi_j(\omega)|^2}\right\}\right. \tag{A.78}$$

$$\left.\times \operatorname{Re}\{\Delta\}\operatorname{Re}\{S_{ij}(\omega)\}\operatorname{Im}\{\phi_i(\omega)\phi_j^*(\omega)\}\right]$$

Now for every term $\operatorname{Im}\{\phi_i(\omega)\phi_j^*(\omega)\}$ in the double summation there is a term $\operatorname{Im}\{\phi_i^*(\omega)\phi_j(\omega)\}$ so since $\operatorname{Re}\{S_{ij}(\omega)\} = \operatorname{Re}\{S_{ji}(\omega)\}$, this double summation is identically zero, proving the desired result.

APPENDIX B

Derivation of Expected Values of Modal Functions

The mean values of three types of modal functions are required for the various expressions used in Chapters 3 and 5. These are

$$E[1/\phi_i(\omega)] = \int_{\omega_l}^{\omega_u} \frac{du}{(\omega_u-\omega_l)\{u^2-\omega^2+\sqrt{-1}\,c_1\omega\}} \tag{B.1}$$

$$E[1/\phi_i^2(\omega)] = \int_{\omega_l}^{\omega_u} \frac{du}{(\omega_u-\omega_l)\{u^2-\omega^2+\sqrt{-1}\,c_1\omega\}^2} \tag{B.2}$$

and

$$E[1/|\phi_i(\omega)|^2] = \int_{\omega_l}^{\omega_u} \frac{du}{(\omega_u-\omega_l)\{(u^2-\omega^2)^2+c_1^2\omega^2\}} \tag{B.3}$$

These integrals are somewhat tedious but by making substitutions of the form

$$\Omega_u = \frac{\omega}{\xi} + \frac{\omega_u-\omega_l}{2\xi} \tag{B.4}$$

$$\Omega_l = \frac{\omega}{\xi} - \frac{\omega_u-\omega_l}{2\xi} \tag{B.5}$$

and

$$v = u/\xi \tag{B.6}$$

where $\xi^2 = \omega^2-\sqrt{-1}\,c_1\omega$ and it is assumed that ω is midway between ω_u and ω_l, they may be simplified to give respectively

$$E[1/\phi_i(\omega)] = \frac{1}{\xi(\omega_u-\omega_l)} \int_{\Omega_l}^{\Omega_u} \frac{dv}{(v^2-1)} \tag{B.7}$$

$$E[1/\phi_i^2(\omega)] = \frac{1}{\xi^3(\omega_u-\omega_l)} \int_{\Omega_l}^{\Omega_u} \frac{dv}{(v^2-1)^2} \tag{B.8}$$

and

$$E[1/|\phi_i(\omega)|^2] = \frac{1}{c_1\omega\xi(\omega_u-\omega_l)}\mathrm{Im}\left\{\int_{\Omega_l}^{\Omega_u}\frac{dv}{(v^2-1)}\right\} \tag{B.9}$$

These are of standard form, although the variables of integration are now complex. They yield

$$E[1/\phi_i(\omega)] = \frac{\ln\left\{\dfrac{(\Omega_u-1)(\Omega_l+1)}{(\Omega_u+1)(\Omega_l-1)}\right\}}{2\xi(\omega_u-\omega_l)} \tag{B.10}$$

$$E[1/\phi_i^2(\omega)] = \frac{\dfrac{\Omega_u}{1-\Omega_u^2} - \dfrac{\Omega_l}{1-\Omega_l^2} - \dfrac{1}{2}\ln\left\{\dfrac{(\Omega_u-1)(\Omega_l+1)}{(\Omega_u+1)(\Omega_l-1)}\right\}}{2\xi^3(\omega_u-\omega_l)} \tag{B.11}$$

and

$$E[1/|\phi_i(\omega)|^2] = -\frac{\mathrm{Im}\left\{\dfrac{1}{\xi}\ln\left\{\dfrac{(\Omega_u-1)(\Omega_l+1)}{(\Omega_u+1)(\Omega_l-1)}\right\}\right\}}{2c_1\omega(\omega_u-\omega_l)} \tag{B.12}$$

When the subscripts are interchanged (i.e. 1 for 2 etc.) the relevant terms for the other sub-system are obtained.

If it is assumed that the frequency bandwidths are narrow and the damping light, i.e.

$$\omega, \omega_i, \omega_r \gg \omega_u-\omega_l \gg c_1, c_2 \tag{B.13}$$

then

$$\xi \to \omega, \tag{B.14}$$

$$\ln\left\{\frac{(\Omega_u-1)(\Omega_l+1)}{(\Omega_u+1)(\Omega_l-1)}\right\} \to -\frac{(\omega_u-\omega_l)}{\omega} - \sqrt{-1}\,\pi \tag{B.15}$$

and

$$\frac{\Omega_u}{1-\Omega_u^2} - \frac{\Omega_l}{1-\Omega_l^2} \to -\frac{2\omega}{(\omega_u-\omega_l)} + \frac{4\sqrt{-1}\,c_1}{\omega} \tag{B.16}$$

so that the previous results simplify considerably giving finally

$$E[1/\phi_i(\omega)] = -\left\{\frac{1}{4\omega^2} + \frac{\sqrt{-1}\,\pi}{2\omega(\omega_u-\omega_l)}\right\} \tag{B.17}$$

$$E[1/\phi_i^2(\omega)] = -\left\{\frac{1}{\omega^2(\omega_u-\omega_l)^2} - \frac{\sqrt{-1}\,\pi}{4\omega^3(\omega_u-\omega_l)}\right\} \tag{B.18}$$

and

$$E[1/|\phi_i(\omega)|^2] = \frac{\pi}{2\omega^2 c_1(\omega_u-\omega_l)} \tag{B.19}$$

APPENDIX C

Green's Function Solution for Coupled Rods

If $g_i(a_i,b_i,\omega)$ is the Green's function relating the displacement on sub-system i at position $x_i = a_i$, to a unit harmonic force of form $e^{i\omega t}$ applied at the point $x_i = b_i$ also on sub-system i, it is possible to construct all the parameters of interest for the sub-system. For the case of two, point spring coupled, axially vibrating rods, the displacements become

$$y_1(x_1,t) = k_c\{y_2(a_2,t)-y_1(a_1,t)\}g_1(x_1,a_1,\omega) \tag{C.1}$$

$$+\int_1 F_1(u_1,t)g_1(x_1,u_1,\omega)du_1$$

and

$$y_2(x_2,t) = k_c\{y_1(a_1,t)-y_2(a_2,t)\}g_2(x_2,a_2,\omega) \tag{C.2}$$

$$+\int_2 F_2(u_2,t)g_2(x_2,u_2,\omega)du_2$$

where u_1 and u_2 are dummy variables of integration, the integrations being carried over the sub-systems to establish the contributions to motion at any given point from forces applied anywhere within the sub-systems. If the forces are constrained to act at single points on the sub-systems, $x_1 = b_1$ and $x_2 = b_2$, these equations become

$$y_1(x_1,t) = k_c\{y_2(a_2,t)-y_1(a_1,t)\}g_1(x_1,a_1,\omega) + F_1(t)g_1(x_1,b_1,\omega) \tag{C.3}$$

and

$$y_2(x_2,t) = k_c\{y_1(a_1,t)-y_2(a_2,t)\}g_2(x_2,a_2,\omega) + F_2(t)g_2(x_2,b_2,\omega) \tag{C.4}$$

These results can be evaluated at the coupling and driving points to give

$$y_1(a_1,t) = k_c\{y_2(a_2,t)-y_1(a_1,t)\}g_1(a_1,a_1,\omega) + F_1(t)g_1(a_1,b_1,\omega) \tag{C.5}$$

$$y_2(a_2,t) = k_c\{y_1(a_1,t)-y_2(a_2,t)\}g_2(a_2,a_2,\omega) + F_2(t)g_2(a_2,b_2,\omega) \tag{C.6}$$

$$y_1(b_1,t) = k_c\{y_2(a_2,t)-y_1(a_1,t)\}g_1(b_1,a_1,\omega) + F_1(t)g_1(b_1,b_1,\omega) \tag{C.7}$$

and

$$y_2(b_2,t) = k_c\{y_1(a_1,t)-y_2(a_2,t)\}g_2(b_2,a_2,\omega) + F_2(t)g_2(b_2,b_2,\omega) \tag{C.8}$$

These four equations in the four unknowns $y_1(a_1,t)$ etc. can be solved to give

$$y_1(a_1,t) = \Big[F_1(t)g_1(a_1,b_1,\omega) \tag{C.9}$$

$$+ k_c \Big\{ F_1(t)g_1(a_1,b_1,\omega)g_2(a_2,a_2,\omega)+F_2(t)g_2(a_2,b_2,\omega)g_1(a_1,a_1,\omega) \Big\} \Big] / \bar{\Delta}$$

$$y_2(a_2,t) = \Big[F_2(t)g_2(a_2,b_2,\omega) \tag{C.10}$$

$$+ k_c \Big\{ F_1(t)g_1(a_1,b_1,\omega)g_2(a_2,a_2,\omega)+F_2(t)g_2(a_2,b_2,\omega)g_1(a_1,a_1,\omega) \Big\} \Big] / \bar{\Delta}$$

$$y_1(b_1,t) = F_1(t)g_1(b_1,b_1,\omega) \tag{C.11}$$

$$+ k_c \Big\{ F_2(t)g_2(a_2,b_2,\omega)-F_1(t)g_1(a_1,b_1,\omega) \Big\} g_1(b_1,a_1,t) / \bar{\Delta}$$

and

$$y_2(b_2,t) = F_2(t)g_2(b_2,b_2,\omega) \tag{C.12}$$

$$+ k_c \Big\{ F_1(t)g_1(a_1,b_1,\omega)-F_2(t)g_2(a_2,b_2,\omega) \Big\} g_2(b_2,a_2,t) / \bar{\Delta}$$

where $\bar{\Delta}$ is related to Δ and is given by

$$\bar{\Delta} = 1 + k_c g_1(a_1,a_1,\omega) + k_c g_2(a_2,a_2,\omega) \tag{C.13}$$

These results may be used to calculate the desired energy flows and levels in a fashion entirely similar to that followed in Appendix A. Assuming that the driving forces on the two sub-systems are statistically independent, and keeping just the even portions of the response spectra as in Appendix A, the coupling and input energy flows are found to be

$$\Pi_{12}(\omega) = -\omega k_c^2 S_{F_1F_1} \mid g_1(a_1,b_1,\omega)/\bar{\Delta} \mid^2 \mathrm{Im}\{g_2(a_2,a_2,\omega)\} \tag{C.14}$$

$$+ \omega k_c^2 S_{F_2F_2} \mid g_2(a_2,b_2,\omega)/\bar{\Delta} \mid^2 \mathrm{Im}\{g_1(a_1,a_1,\omega)\}$$

$$\Pi_{1_{IN}}(\omega) = -\omega S_{F_1F_1} \mathrm{Im} \Big\{ g_1(b_1,b_1,\omega) - k_c\{g_1(a_1,b_1,\omega)g_1(b_1,a_1,\omega)\}/\bar{\Delta} \Big\} \tag{C.15}$$

These results bear great similarities to the results of Appendix A, but with summations across modes

replaced by Green's functions.

To calculate the energy lost by dissipation a damping model must be assumed; here it is taken to consist of four point dampers, with damping constants c_1 on sub-system 1 and c_2 on sub-system 2. These take the form of dashpots mounted on the extreme ends of the rods, i.e. at $x_1 = 0, l_1$ and $x_2 = 0, l_2$. This leads to

$$\Pi_{1_{DISS}}(\omega) = \omega^2 c_1 S_{F_1F_1} \tag{C.16}$$

$$\times \left\{ \left| g_1(0,b_1,\omega) - k_c g_1(a_1,b_1,\omega) g_1(0,a_1,\omega)/\bar{\Delta} \right|^2 \right.$$

$$\left. + \left| g_1(l_1,b_1,\omega) - k_c g_1(a_1,b_1,\omega) g_1(l_1,a_1,\omega)/\bar{\Delta} \right|^2 \right\}$$

$$+ \omega^2 k_c^2 c_1 S_{F_2F_2} \left\{ \left| g_2(a_2,b_2,\omega) g_1(0,a_1,\omega)/\bar{\Delta} \right|^2 \right.$$

$$\left. + \left| g_2(a_2,b_2,\omega) g_1(l_1,a_1,\omega)/\bar{\Delta} \right|^2 \right\}$$

Finally, to calculate the energy levels of the sub-systems, which are again assumed to be twice the kinetic energies, requires integrals of the displacement velocities across the sub-systems, i.e.

$$E_1(\omega) = \omega^2 m_1 \int_1 \left\{ S_{F_1F_1} \left| g_1(x_1,b_1,\omega) - k_c g_1(a_1,b_1,\omega) g_1(x_1,a_1,\omega)/\bar{\Delta} \right|^2 \right. \tag{C.17}$$

$$\left. + k_c^2 S_{F_2F_2} \left| g_2(a_2,b_2,\omega) g_1(x_1,a_1,\omega)/\bar{\Delta} \right|^2 \right\} dx_1$$

The equivalent results for sub-system 2 are once more obtained by interchanging the subscripts 1 for 2 etc.

The required Green's function used in all these results, i.e. for axially vibrating rods supported at their ends by viscous dampers, is given by Remington and Manning[22] as

$$g_1(a_1,b_1,\omega) = \frac{e^{\pm i\omega(a_1-b_1)\sqrt{m_1/AE_1}} + \chi_1 \cos(\omega a_1 \sqrt{m_1/AE_1}) + \chi_2 \sin(\omega a_1 \sqrt{m_1/AE_1})}{2\sqrt{-1}\,\omega\sqrt{m_1 AE_1}} \tag{C.18}$$

where the plus sign is for $a_1 < b_1$ and the minus sign for $a_1 > b_1$, and where

$$\chi_1 = -\frac{1}{\chi_d}\left[\frac{c_1}{\sqrt{m_1 AE_1}} - 1\right]\left[e^{-i\omega(l_1-b_1)\sqrt{m_1/AE_1}}\right. \tag{C.19}$$

$$\left. + \cos(\omega l_1\sqrt{m_1/AE_1})e^{-i\omega b_1\sqrt{m_1/AE_1}} + \frac{\sqrt{-1}\,c_1}{\sqrt{m_1 AE_1}}\sin(\omega l_1\sqrt{m_1/AE_1})e^{-i\omega b_1\sqrt{m_1/AE_1}}\right]$$

and

$$\chi_2 = -\frac{1}{\chi_d}\left[\frac{c_1}{\sqrt{m_1 AE_1}} - 1\right]\left[\frac{\sqrt{-1}\,c_1}{\sqrt{m_1 AE_1}}e^{-i\omega(l_1-b_1)\sqrt{m_1/AE_1}}\right. \tag{C.20}$$

$$\left. - \frac{\sqrt{-1}\,c_1}{\sqrt{m_1 AE_1}}\cos(\omega l_1\sqrt{m_1/AE_1})e^{-i\omega b_1\sqrt{m_1/AE_1}} + \sin(\omega l_1\sqrt{m_1/AE_1})e^{-i\omega b_1\sqrt{m_1/AE_1}}\right]$$

with

$$\chi_d = \frac{2c_1}{\sqrt{m_1 AE_1}}\cos(\omega l_1\sqrt{m_1/AE_1}) + \sqrt{-1}\left[\frac{c_1^2}{m_1 AE_1} + 1\right]\sin(\omega l_1\sqrt{m_1/AE_1}) \tag{C.21}$$

APPENDIX D

Multi-Dimensional Integrals

D.1. Infinite Coupling Strength, Two Modes

When two sub-systems both contain only a single oscillator ($N_1 = 1 = N_2$) and the coupling spring between them is infinitely strong ($1/k_c = 0$) it follows that

$$E[H_{11}(\omega)] = \int_{\omega_l}^{\omega_u}\int_{\omega_l}^{\omega_u} \left[\frac{\omega^2 c_1}{m_1 |\phi_i(\omega)|^2} \right. \tag{D.1}$$

$$\left. + \frac{\omega}{m_1^2} \mathrm{Im}\left\{ 1/\phi_i^2(\omega) \left\{ \frac{1}{m_1 \phi_i(\omega)} + \frac{1}{m_2 \phi_r(\omega)} \right\} \right\} \right] \frac{d\omega_i d\omega_r}{(\omega_u - \omega_l)^2}$$

and since $\mathrm{Im}\{\phi_i(\omega)\}$ is ωc_1, this reduces to

$$E[H_{11}(\omega)] = \frac{\omega^2 (m_1 c_1 + m_2 c_2)}{(\omega_u - \omega_l)^2} \int_{\omega_l}^{\omega_u}\int_{\omega_l}^{\omega_u} \frac{d\omega_i d\omega_r}{|\, m_1 \phi_i(\omega) + m_2 \phi_r(\omega) \,|^2} \tag{D.2}$$

Similarly the cross-receptance is given by

$$E[H_{12}(\omega)] = \int_{\omega_l}^{\omega_u}\int_{\omega_l}^{\omega_u} \left[\frac{\omega^2 c_2}{m_1^2 m_2 |\phi_i(\omega)|^2 |\phi_r(\omega)|^2} \right] \tag{D.3}$$

$$\times \left[\frac{1}{|\, 1/m_1 \phi_i(\omega) + 1/m_2 \phi_r(\omega) \,|^2} \right] \frac{d\omega_i d\omega_r}{(\omega_u - \omega_l)^2}$$

$$= \frac{\omega^2 m_2 c_2}{(\omega_u - \omega_l)^2} \int_{\omega_l}^{\omega_u}\int_{\omega_l}^{\omega_u} \frac{d\omega_i d\omega_r}{|\, m_1 \phi_i(\omega) + m_2 \phi_r(\omega) \,|^2} \tag{D.4}$$

Equations (D.2) and (D.4) correspond with the result given in equation (5.4), i.e.

$$E[H_{12}(\omega)] = \{m_2 c_2/(m_1 c_1 + m_2 c_2)\} E[H_{11}(\omega)] \tag{D.5}$$

Both involve elliptic integrals in ω_i and ω_r. To proceed with equation (D.2), simplification of the integrand is obtained by letting

$$R^2 = m_1\omega_i^2 + m_2\omega_r^2 \tag{D.6}$$

and

$$\theta = \tan^{-1}(\{\omega_r/\omega_i\}\sqrt{m_2/m_1}) \tag{D.7}$$

although complications in the limits of integration now arise. After integration with respect to θ this substitution yields

$$\begin{aligned} E[H_{12}(\omega)] = & \int_{\omega_l\sqrt{m_1+m_2}}^{\sqrt{\omega_l^2 m_1+\omega_u^2 m_2}} RQ(R)\cos^{-1}\left[\frac{\omega_l\sqrt{m_1}}{R}\right]dR \\ & - \int_{\omega_l\sqrt{m_1+m_2}}^{\sqrt{\omega_l^2 m_2+\omega_u^2 m_1}} RQ(R)\sin^{-1}\left[\frac{\omega_l\sqrt{m_2}}{R}\right]dR \\ & + \int_{\sqrt{\omega_l^2 m_1+\omega_u^2 m_2}}^{\omega_u\sqrt{m_1+m_2}} RQ(R)\sin^{-1}\left[\frac{\omega_u\sqrt{m_2}}{R}\right]dR \\ & - \int_{\sqrt{\omega_l^2 m_2+\omega_u^2 m_1}}^{\omega_u\sqrt{m_1+m_2}} RQ(R)\cos^{-1}\left[\frac{\omega_u\sqrt{m_1}}{R}\right]dR \end{aligned} \tag{D.8}$$

where

$$Q(R) = \frac{\omega^2 m_2 c_2}{\sqrt{m_1 m_2}\,(\omega_u-\omega_l)^2(\{R^2-\omega^2(m_1+m_2)\}^2 + \{m_1 c_1\omega+m_1 c_1\omega\}^2)} \tag{D.9}$$

However, the major contribution to the integral equation (D.2) occurs when

$$R^2 = \omega^2(m_1+m_2) \tag{D.10}$$

and the variable limits of the integration may be approximated by the constant limits of

$$\omega_l\sqrt{m_1+m_2} < R < \omega_u\sqrt{m_1+m_2} \tag{D.11}$$

and

$$\sin^{-1}\left(\frac{\omega_l}{\omega}\sqrt{\frac{m_2}{m_1+m_2}}\right) < \theta < \cos^{-1}\left(\frac{\omega_l}{\omega}\sqrt{\frac{m_1}{m_1+m_2}}\right) \tag{D.12}$$

The solution given in Chapter 5 in equation (5.3), i.e.

$$E[H_{11}(\omega)] = \frac{\omega}{2(\omega_u-\omega_l)^2\sqrt{m_1 m_2}}\left[\cos^{-1}\left[\frac{\omega_l}{\omega}\sqrt{\frac{m_1}{m_1+m_2}}\right] - \sin^{-1}\left[\frac{\omega_l}{\omega}\sqrt{\frac{m_2}{m_1+m_2}}\right]\right] \tag{D.13}$$

$$\times\left[\tan^{-1}\left[\left[\frac{\omega_u^2-\omega^2}{\omega}\right]\left[\frac{m_1+m_2}{m_1c_1+m_2c_2}\right]\right]-\tan^{-1}\left[\left[\frac{\omega_l^2-\omega^2}{\omega}\right]\left[\frac{m_1+m_2}{m_1c_1+m_2c_2}\right]\right]\right.$$

is obtained by adopting this approximation and using these constant limits. It is adequately accurate provided the two oscillators are not heavily damped and do not have grossly different masses. In any case, since equation (D.8) is a one-dimensional integral it may readily be evaluated numerically in place of this approximation.

D.2. Many Weakly Coupled Modes

When there are many modes within each sub-system and the coupling is weak the relevant integrals occurring in equations (5.1) and (5.2) may be greatly simplified. Consider initially the general class of integrals described by

$$I=\int_{\omega_l}^{\omega_u}\cdots\int\frac{\sum_{i=1}^{N_1}q_1(u_i)\sum_{r=1}^{N_2}q_2(v_r)\mathrm{d}u_{i=1}\cdots\mathrm{d}u_{i=N_1}\mathrm{d}v_{r=1}\cdots\mathrm{d}v_{r=N_2}}{\left|\frac{1}{k_c}+\sum_{i=1}^{N_1}q_3(u_i)+\sum_{r=1}^{N_2}q_4(v_r)\right|^2(\omega_u-\omega_l)^{N_1+N_2}} \tag{D.14}$$

for four unspecified functions of the many variables of integration $q_1(u_i)$, $q_2(v_r)$, $q_3(u_i)$ and $q_4(v_r)$. Additionally define the expected values of these functions as

$$E[q_1(u_i)]=\int_{\omega_l}^{\omega_u}\frac{q_1(u_i)\mathrm{d}u_i}{\omega_u-\omega_l}=\sigma_1 \tag{D.15}$$

$$E[q_2(v_r)]=\int_{\omega_l}^{\omega_u}\frac{q_2(v_r)\mathrm{d}v_r}{\omega_u-\omega_l}=\sigma_2 \tag{D.16}$$

$$E[q_3(u_i)]=\int_{\omega_l}^{\omega_u}\frac{q_3(u_i)\mathrm{d}u_i}{\omega_u-\omega_l}=\sigma_3 \tag{D.17}$$

$$E[q_4(v_r)]=\int_{\omega_l}^{\omega_u}\frac{q_4(v_r)\mathrm{d}v_r}{\omega_u-\omega_l}=\sigma_4 \tag{D.18}$$

where the expected values are of course the same for all the i,r. Next the denominator of equation (D.14) is expanded in a series about $q_3(u_1)$ to give

$$I = \int\int_{\omega_l}^{\omega_u} \cdots \int\int \left[q_1(u_1) + \sum_{i=2}^{N_1} q_1(u_i) \right] \left[\sum_{r=1}^{N_2} q_2(v_r) \right] \tag{D.19}$$

$$\times \left| 1 - \frac{q_3(u_1)}{\frac{1}{k_c} + \sum_{i=2}^{N_1} q_3(u_i) + \sum_{r=1}^{N_2} q_4(v_r)} \right|^2$$

$$\times \frac{du_{i=1} \cdots du_{i=N_1} dv_{r=1} \cdots dv_{r=N_2}}{\left| \frac{1}{k_c} + \sum_{i=2}^{N_1} q_3(u_i) + \sum_{r=1}^{N_2} q_4(v_r) \right|^2 (\omega_u - \omega_l)^{N_1+N_2}}$$

This is valid if $|q_3(u_1)|$ is very much less than

$$\left| \frac{1}{k_c} + \sum_{i=2}^{N_1} q_3(u_i) + \sum_{r=1}^{N_2} q_4(v_r) \right|$$

throughout the range of integration. Multiplying out this expression and integrating the individual terms, but assuming the higher order terms of the form

$$\frac{q_1(u_1) q_2(v_1)}{\left| \frac{1}{k_c} + \sum_{i=2}^{N_1} q_3(u_i) + \sum_{r=1}^{N_2} q_4(v_r) \right|^2}$$

provide negligible contributions and can be ignored, it follows that, in this first order theory,

$$I = \int\int_{\omega_l}^{\omega_u} \cdots \int\int \left[\sigma_1 + \sum_{i=2}^{N_1} q_1(u_i) \right] \left[\sum_{r=1}^{N_2} q_2(v_r) \right] \tag{D.20}$$

$$\times \left| 1 - \frac{\sigma_3}{\frac{1}{k_c} + \sum_{i=2}^{N_1} q_3(u_i) + \sum_{r=1}^{N_2} q_4(v_r)} \right|^2$$

$$\times \frac{du_{i=2} \cdots du_{i=N_1} dv_{r=1} \cdots dv_{r=N_2}}{\left| \frac{1}{k_c} + \sum_{i=2}^{N_1} q_3(u_i) + \sum_{r=1}^{N_2} q_4(v_r) \right|^2 (\omega_u - \omega_l)^{N_1+N_2-1}}$$

which may be reconstructed to give

$$I = \int\int_{\omega_l}^{\omega_u} \cdots \int\int \frac{\left[\sigma_1 + \sum_{i=2}^{N_1} q_1(u_i) \right] \left[\sum_{r=1}^{N_2} q_2(v_r) du_{i=2} \cdots du_{i=N_1} dv_{r=1} \cdots dv_{r=N_2} \right.}{\left| \sigma_3 + \frac{1}{k_c} + \sum_{i=2}^{N_1} q_3(u_i) + \sum_{r=1}^{N_2} q_4(v_r) \right|^2 (\omega_u - \omega_l)^{N_1+N_2-1}} \tag{D.21}$$

It can be seen that this procedure allows the multiple integral in equation (D.14) to be replaced by ensemble means of the relevant terms in the integrand, provided higher order contributions are

assumed negligible. This process is performed on all terms in both u_i and v_r to give

$$I = \frac{N_1\sigma_1 N_2\sigma_2}{|1/k_c + N_1\sigma_3 + N_2\sigma_4|^2} \tag{D.22}$$

provided that

$$\begin{aligned} |q_3(u_i)| &\ll \left| \frac{1}{k_c} + \sum_{i=2}^{N_1} q_3(u_i) + \sum_{r=1}^{N_2} q_4(v_r) \right| , \\ &\ll \left| \sigma_3 + \frac{1}{k_c} + \sum_{i=3}^{N_1} q_3(u_i) + \sum_{r=1}^{N_2} q_4(v_r) \right| , \\ &\ll \left| 2\sigma_3 + \frac{1}{k_c} + \sum_{i=4}^{N_1} q_3(u_i) + \sum_{r=1}^{N_2} q_4(v_r) \right| , \cdots , \\ &\ll \left| (N_1-1)\sigma_3 + \frac{1}{k_c} + \sum_{r=1}^{N_2} q_4(v_r) \right| \end{aligned} \tag{D.23}$$

for all $q_3(u_i)$ in the range $\omega_l < q_3(u_i) < \omega_u$, and that

$$\begin{aligned} |q_4(v_r)| &\ll \left| N_1\sigma_3 + \frac{1}{k_c} + \sum_{r=2}^{N_2} q_4(v_r) \right| , \\ &\ll \left| N_1\sigma_3 + \sigma_4 + \frac{1}{k_c} + \sum_{r=3}^{N_2} q_4(v_r) \right| , \\ &\ll \left| N_1\sigma_3 + 2\sigma_4 + \frac{1}{k_c} + \sum_{r=4}^{N_2} q_4(v_r) \right| , \cdots , \\ &\ll |N_1\sigma_3 + (N_2-1)\sigma_4 + 1/k_c| \end{aligned} \tag{D.24}$$

for all $q_4(v_r)$ in the range $\omega_l < q_4(v_r) < \omega_u$. These two equations are always satisfied if

$$|q_3(u_i)|_{\max} \ll 1/k_c + (N_1-1)|q_3(u_i)|_{\min} + N_2|q_4(v_r)|_{\min} \tag{D.25}$$

and

$$|q_4(v_r)|_{\max} \ll 1/k_c + N_1|q_3(u_i)|_{\min} + (N_2-1)|q_4(v_r)|_{\min} \tag{D.26}$$

It is these requirements which must be satisfied if the normal SEA approach is to hold, i.e. many modes and weak coupling.

Although this analysis is directed towards integrals of the type contained in equation (5.2) a similar process is applicable to equation (5.1) and the same constraints may be shown to be relevant. Therefore, all that is required to evaluate the multi-dimensional integrals of equations (5.1) and (5.2)

are the mean values of the individual functions in the summations, σ_1 etc. These have already been discussed in Appendix B.

It has been shown that this analysis is applicable to sub-systems involving many modes and weak coupling. The assumptions made are implicit in the normal SEA approach, but it is instructive to examine such fundamentals in this manner since it allows a calculation to be performed which reveals whether there are sufficient modes, or weak enough coupling for the method to hold in the situation under consideration. The parameter ν, discussed in Chapter 5, provides one means of attempting to combine the requirements of equations (D.25) and (D.26) into a single expression, such that when ν is large the first order analysis given here may be confidently expected to hold. That the parameter is a useful measure of this behaviour is borne out by the examples presented in Chapters 5 and 9.

NOMENCLATURE

General conventions

(1) A system consists of two or more connected sub-systems between which energy flows. Each sub-system may consist of a number of elements or units which are often periodically repeated. The elements are made up of a number of sub-elements which are individually of uniform properties.

(2) Subscript 1 implies sub-system 1 and subscript 2 sub-system 2. Subscript *i, j* implies a mode of sub-system 1 and subscript *r, s* implies a mode of sub-system 2. Subscript 12 implies energy flow from sub-system 1 to 2, subscript 1_{DISS} implies energy dissipated by sub-system 1 and subscript 1_{IN} implies energy flowing into sub-system 1. Sub-subscript *TOTAL* implies the total energy flow between all modes of both sub-systems.

(3) Subscript *k* implies the *kth* element of a periodic sub-system and subscript *l* the *lth* sub-element counting continuously along a sub-system. Subscript *L* implies the left-hand end of a periodic element and subscript *R* the right-hand end. Subscript *A* implies properties within the sub-element *A* and subscript *B* those within the sub-element *B*. ' indicates an element with revised properties.

(4) $E[]$ implies an ensemble average whereas angle brackets <> imply a long term, time average.

(5) Re{} and Im{} imply the real and imaginary parts of a function whereas * implies the complex conjugate and | | the magnitude.

(6) Superscript *i* in an exponential term implies the square root of −1.

(7) Single and double over-dots imply the first and second differentials with respect to time and (t) indicates functions that vary with time.

List of symbols

Symbols not included in the list below are only used at specific places and are explained where they occur.

a Position of the coupling point within a sub-system.

b Position of the driving point within a sub-system under point forcing.

c The damping factor of a sub-system or the dashpot constants for sub-systems with point damping.

d The total length of a periodic element.

$f_{uv}(u,v)$

A two-dimensional probability function of u and v.

g A Green's function relating displacement at a given point to harmonic forcing at any other.

h_{12} The cross-coupling energy flow constant of proportionality.

k_c The coupling spring strength between two sub-systems.

k The spring strength for a simple mass, spring, damper sub-system.

l The length of a sub-system, or of a sub-element within a periodic element.

m The total mass of a sub-system.

p The exponential coupling strength correction factor constant.

q An unspecified function.

r The damping constant of a sub-system.

s An arbitrary integer.

t Time.

u A dummy variable.

v A dummy variable.

x The position within a sub-system.

y The deflection from equilibrium within a sub-system.

z Constants in the make up of a travelling wave.

AE The product of cross-sectional area and Young's modulus for an axially vibrating rod segment.

C A constant in the periodic solutions.

D A constant in the transfer matrix $[T]$.

E The total energy within a sub-system (usually twice kinetic).

F An external force acting on a sub-system.

G The correction factor for strong coupling.

H A sub-system receptance.

I An integral.

K A constant in the energy flow equations.

KE The kinetic energy within a sub-system.

L The modal components of the driving force.

M The number of periodic elements or units repeated in a sub-system.

N The number of modes interacting from a sub-system.

P The combined driving force acting on a sub-system (including both external and coupling forces).

PE The potential energy within a sub-system.

Q A function in an elliptic integral.

R The radius term in an elliptic integral.

$S_{F_1F_1}$ The frequency spectrum of the force F on sub-system 1.

S_{ij} The cross-frequency spectrum of the *ith* and *jth* modal force components on sub-system 1.

S_{rs} The cross-frequency spectrum of the *rth* and *sth* modal force components on sub-system 2.

$[T]$ The transfer matrix of an element within a periodic sub-system.

V The modal components of the coupling force.

W The modal weighting factors in the expansion of the deflected shape y.

X The eigenvectors of the transfer matrix $[T]$.

Y The amplitude constant associated with the standing wave on a sub-element within a periodic sub-system.

Z A vector describing an arbitrary wave travelling along a periodic sub-system.

α The receptances of an element within a periodic sub-system.

β The receptances of a sub-element within one element of a periodic sub-system.

γ The receptances of another sub-element within one element of a periodic sub-system.

δ The Dirac delta function.

ε The right-hand end phase constant associated with the standing wave on a sub-element within a periodic sub-system.

ζ The product $M\mu d_1$ etc. in the transfer matrix expansion for periodic units of various kinds.

$\eta_{1,2}$ The critical damping ratio of sub-systems 1 or 2.

η_{12} The coupling loss factor.

θ The angular term in an elliptic integral.

κ The coupling force acting on a given mode of a sub-system.

λ The local wave speed within a sub-element of a periodic sub-system,

μ The propagation constant within a periodic sub-system.

ν The relative coupling strength measure.

ξ A substitution variable in the expected value integrations.

ρ The mass density of a sub-system or sub-element per unit length.

σ The mean or expected value of some unspecified function.

ϕ_i The receptance of an individual mode, $\omega_i^2-\omega^2+\sqrt{-1}\,c_1\omega$.

χ Constants in the Green's function formulation.

$\psi_i(x_1)$

The mode shape of the *ith* mode as a function of position x_1 on sub-system 1.

$\psi_i(a_1)$

The mode shape of the *ith* mode at the *coupling* point a_1 on sub-system 1.

$\psi_i(b_1)$

The mode shape of the *ith* mode at the *driving* point b_1 on sub-system 1.

ω The frequency of interest at which energy flows and levels are calculated.

$\omega_{1,2}$ and $\omega_{i,j,r,s}$

The natural frequencies of sub-systems 1 or 2.

ω_l The lower limit frequency at which natural frequencies contribute to the energy flow summations, defining the lower limit of the summation band width.

ω_u The upper limit frequency at which natural frequencies contribute to the energy flow summations, defining the upper limit of the summation band width.

Δ The denominator function of the coupling strength, see equation (3.17).

$\bar{\Delta}$ The denominator function of the coupling strength in the Green's function solution, see equation (C.13).

Λ The spatial differential operator defining the type of sub-system.

Ξ An eigenvalue of a periodic element transfer matrix.

Π An energy flow.

Ω A substitution variable in the expected value integrations.

REFERENCES

1. Lord Rayleigh, *The Theory of Sound*, Macmillan, London (1894).

2. R. E. D. Bishop, G. M. L. Gladwell, and S. Michaelson, *The Matrix Analysis of Vibration*, Cambridge University Press (1965).

3. R. E. D. Bishop and D. C. Johnson, *The Mechanics of Vibration*, Cambridge University Press (1979).

4. L. Meirovitch, *Elements of Vibration Analysis*, McGraw-Hill (1975).

5. O. C. Zienkiewicz, *The Finite Element Method (3rd edition)*, McGraw Hill (1977).

6. R. H. Lyon and G. Maidanik, "Power Flow between Linearly Coupled Oscillators," *J. Acoust. Soc. Am.* **34**(5) pp. 623-639 (1962).

7. P. W. Smith, Jr., "Responses and Radiation of Structural Modes Excited by Sound," *J. Acoust. Soc. Am.* **34**(5) pp. 640-647 (1962).

8. E. Eichler, "Thermal Circuit Approach to Vibrations in Coupled Systems and the Noise Reduction of a Rectangular Box," *J. Acoust. Soc. Am.* **37**(6) pp. 995-1007 (1963).

9. E. E. Ungar, "Statistical Energy Analysis of Vibrating Systems," *Trans. ASME J. Eng. Ind.*, pp. 626-632 (1967).

10. D. E. Newland, "Calculation of Power Flow Between Coupled Oscillators," *J. Sound Vib.* **3**(3) pp. 262-276 (1966).

11. T. D. Scharton and R. H. Lyon, "Power Flow and Energy Sharing in Random Vibration.," *J. Acoust. Soc. Am.* **43**(6) pp. 1332-1343 (1968).

12. R. H. Lyon and T. D. Scharton, "Vibrational Energy Transmission in a Three Element Structure," *J. Acoust. Soc. Am.* **38**(2) pp. 253-261 (1965).

13. W. Gersch, "Average Power and Power Exchange in Oscillators," *J. Acoust. Soc. Am.* **46**(5) pp. 1180-1185 (1969).

14. J. L. Zeman and J. L. Bogdanoff, "A Comment on Complex Structural Response to Random Vibration," *AIAA* **7** pp. 1225-1231 (1969).

15. R. H. Lyon, "What Good is Statistical Energy Analysis, Anyway ?," *Shock and Vibration Digest* 3(6) pp. 2-10 (1970).

16. R. H. Lyon, *Statistical Energy Analysis of Dynamical Systems : Theory and Applications*, MIT Press (1975).

17. F. J. Fahy, "Statistical Energy Analysis - A Critical Review," *Shock and Vibration Digest* **6** pp. 14-33 (1974).

18. C. H. Hodges and J. Woodhouse, "Theories of noise and vibration transmission in complex structures," *Reports on Progress in Physics*, (49) pp. 107-170 (1986).

19. G. SenGupta, "Vibration of Periodic Structures," *Shock and Vibration Digest* **12** pp. 17-31 (1980).

20. H. G. Davies, "Exact Solutions for the Response of some Coupled Multimodal Systems," *J. Acoust. Soc. Am.* **51**(1) pp. 387-392 (1972).

21. H. G. Davies, "Power Flow between Two Coupled Beams.," *J. Acoust. Soc. Am.* **51**(1) pp. 393-401 (1972).

22. P. J. Remington and J. E. Manning, "Comparison of Statistical Energy Analysis power flow predictions with an 'exact' calculation," *J. Acoust. Soc. Am.* **57**(2) pp. 374-379 (1975).

23. A. J. Keane and W. G. Price, "An appraisal of the fundamentals of Statistical Energy Analysis," in *Proceedings of the International Conference on Vibration Problems in Engineering*, , Xi'an (1986).

24. K. L. Chandiramani, "Some simple models describing transition from weak to strong coupling in statistical energy analysis," *J. Acoust. Soc. Am.* **63**(4) pp. 1081-1083 (1978).

25. P. W. Smith, Jr., "Statistical models of coupled dynamical systems and the transition from weak to strong coupling," *J. Acoust. Soc. Am.* **65**(3) pp. 695-698 (1979).

26. A. J. Keane and W. G. Price, "Statistical Energy Analysis of Strongly Coupled Systems," *J. Sound Vib.* **117**(2) pp. 363-386 (1987).

27. L. Brillouin, *Wave Propagation in Periodic Structures,* Dover Publications, Inc. (1953).

28. J. M. Ziman, *Principles of the Theory of Solids,* Cambridge University Press (1972).

29. J. M. Ziman, *Models of Disorder,* Cambridge University Press (1979).

30. D. J. Mead, "Wave Propagation and Natural Modes in Periodic Systems: I. Mono-Coupled Systems," *J. Sound Vib.* **40**(1) pp. 1-18 (1975).

31. D. J. Mead, "Wave Propagation and Natural Modes in Periodic Systems: II. Multi-Coupled Systems, with and without Damping," *J. Sound Vib.* **40**(1) pp. 19-39 (1975).

32. Y. K. Lin, "Random Vibration of Periodic and Almost Periodic Structures," *Mech. Today* **3** pp. 93-124 Pergamon Press, (1976).

33. M. G. Faulkner and D. P. Hong, "Free Vibrations of a Mono-Coupled Periodic System," *J. Sound Vib.* **99**(1) pp. 29-42 (1985).

34. D. J. Mead and S.M Lee, "Receptance Methods and the Dynamics of Disordered One-Dimensional Lattices," *J. Sound Vib.* **92**(3) pp. 427-445 (1984).

35. A. J. Keane and W. G. Price, "On the Vibrations of Periodic and Near Periodic Structures," *J. Sound Vib.*, (To be published).

36. D. E. Newland, *An Introduction to Random Vibrations and Spectral Analysis (2nd edition),* Longman (1975).

37. J. Woodhouse, "An approach to the theoretical background of statistical energy analysis applied to structural vibration," *J. Acoust. Soc. Am.* **69**(6) pp. 1695-1709 (1981).

38. Y. K. Lin, *Probabilistic Theory of Structural Dynamics*, McGraw-Hill (1967).

39. E. Skudrzyk, *Simple and Complex Vibratory Systems*, Pennsylvania State University Press (1968).

40. H. G. Davies, "Random vibration of distributed systems strongly coupled at discrete points," *J. Acoust. Soc. Am.* **54**(2) pp. 507-515 (1973).

41. C. H. Hodges, "Confinement of vibration by one-dimensional disorder: theory of ensemble averaging," TOP/14/81/1, Topexpress Ltd., Cambridge UK (1981).

42. J. Woodhouse, "Confinement of vibration by one-dimensional disorder: a numerical experiment on different ensemble averages," TOP/14/81/2, Topexpress Ltd., Cambridge, U.K. (1981).

43. C. Gulizia and A. J. Price, "Power flow between strongly coupled oscillators," *J. Acoust. Soc. Am.* **61**(6) pp. 1511-1515 (1977).

44. P. W. Anderson, "Absence of diffusion in certain random lattices," *Physical Review* **109** pp. 1492-1505 (1958).

45. C. A. Coulson, *Waves*, Oliver and Boyd (1961).

46. C. H. Hodges and J. Woodhouse, "Vibration isolation from irregularity in a nearly periodic structure: Theory and measurements," *J. Acoust. Soc. Am.* **74**(3) pp. 894-905 (1983).

47. M. Born and T. von Karman, "Uber Schwingungen in Raumgittern," *Physikalische Zeitschrift* **13** pp. 297-309 (1912).

48. R. E. Borland, "The nature of the electronic states in disordered one-dimensional systems," *Proc. Roy. Soc.* **A274** pp. 529-545 (1963).

49. R. M. Orris and M. Petyt, "A Finite Element Study of Harmonic Wave Propagation in Periodic Structures," *J. Sound Vib.* **33**(2) pp. 223-236 (1974).

50. PAFEC, *PAFEC 75 Data Preparation,* PAFEC Ltd., U.K. (1978).

51. D. J. Mead and S. Markus, "Coupled Flexural-longitudinal Wave Motion in a Periodic Beam," *J. Sound Vib.* **90**(1) pp. 1-24 (1983).

52. C. H. Hodges, "Confinement of Vibration by Structural Irregularity," *J. Sound Vib.* **82** pp. 411-424 (1982).

53. C. Pierre and E. H. Dowell, "Localization of Vibrations by Structural Irregularity," *J. Sound Vib.* **114**(3) pp. 549-564 (1987).

54. N. F. Mott and P. W. Anderson, "Nobel Lectures in Physics for 1977," *Rev. Mod. Phys.* **50** pp. 191-208 (1978).

55. R. Kinns, "Isolation of vibration from diesel generators," *The Naval Architect,* pp. E283-E284 (1987).

56. W. G. Price and R. E. D. Bishop, *Probabilistic Theory of Ship Dynamics,* Chapman and Hall (1974).

Acknowledgements

I gratefully acknowledge the guidance, advice and encouragement of Prof. W.G. Price, my supervisor at Brunel University who suggested this topic in the first place and was also responsible for my re-entering academia.

Also Dr. J. Woodhouse at Cambridge University who entertained us and lent support during the early days as did Dr. F. Fahy at the Institute of Sound and Vibration Research, Southampton University. Various colleagues at Brunel University, particularly Dr. B. Coburn and Prof. A.J. Reynolds, have shown interest and support, including attendance at two lectures during this work. Their forbearance is acknowledged as is that of Mrs. O. Rolph who carried out the typing.

Finally, none of this would have been possible without the support, encouragement and cajoling of my wife, whose patience never failed.